Investigations of LST and WCFT using complexity as a probe

Gaurav Katoch

A Dissertation Submitted to

Indian Institute of Technology Hyderabad

In Partial Fulfillment of the Requirements for

The Degree of Doctor of Philosophy

भारतीय प्रौद्योगिकी संस्थान हैदराबाद
Indian Institute of Technology Hyderabad

Department of Physics
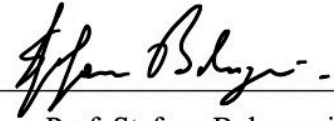
February, 2023

Declaration

I declare that this written submission represents my ideas in my own words, and where ideas or words of others have been included, I have adequately cited and referenced the original sources. I also declare that I have adhered to all principles of academic honesty and integrity and have not misrepresented or fabricated or falsified any idea/data/fact/source in my submission. I understand that any violation of the above will be a cause for disciplinary action by the Institute and can also evoke penal action from the sources that have thus not been properly cited, or from whom proper permission has not been taken when needed.

....
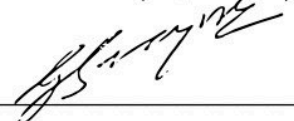Gaurav Katoch
(PH16RESCH11003)

Approval Sheet

This thesis entitled "Investigations of LST and WCFT using complexity as a probe" by Gaurav Katoch is approved for the degree of Doctor of Philosophy from IIT Hyderabad.

Prof. Stefano Bolognesi

Professor of Physics. Univ. of Pisa

(Examiner 1)

Prof. Gautam Sengupta

Professor of Physics, IIT Kanpur

(Examiner 2)

Dr. Anurag Tripathi
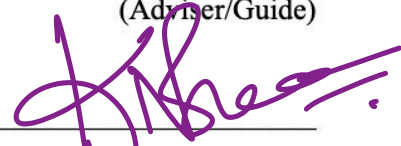
Associate Professor of Physics, IIT Hyderabad

(Internal Examiner)

Dr. Shubho R. Roy, IIT Hyderabad

Assistant Professor of Physics, IIT Hyderabad

(Adviser/Guide)

Dr. Kaushik Nayak

Associate Professor of Electrical Engineering, IIT Hyderabad

(Chairman)

Acknowledgements

raised me from an infant to this day with tireless dedication and love. I know that no amount of words can do justice to the toils she endured in raising me and it wouldn't be an overstatement on my part to say that I would've been nothing without her.

Dedication

This work is dedicated to my grandmother **Smt. Kamla Devi Mandyal** to whom I owe a lot more than I can possibly express for the hardships she gracefully endured in the way for me to pursue my aspirations. She is the person that I picture as my *home*.

Abstract

AdS/CFT, or more broadly speaking gauge/gravity duality has revolutionized our understanding of strongly coupled quantum field theories. For a large class of field theories, calculations which were once considered beyond reach due to breakdown of coupling constant perturbation theory are now routinely being done by first mapping the field theory to its gravity dual (often constructed from the "*bottom up*" without even the need for knowledge of any details of string theory), and then solving (numerically in most cases) the classical gravity-matter system, i.e. Einstein field equations coupled to classical matter fields. This so called "*holographic approach*" of solving strongly coupled (gauge) fields theories have extended the use of gravitational methods (GR/SUGRA) to the fields of condensed matter physics. and QCD.

However, the impact of AdS/CFT (gauge/gravity) has been far more deep and revealing than merely providing a classical geometrical computational tool for strongly coupled field theory phenomena. Thinking about how field theory codes various phenomena on the gravity side, such as emergence of a quasilocal bulk spacetime local observables propagating on it, spatial connectivity of the bulk geometry, event horizons and gravitational singularities etc., has led to the recognition and importance of various concepts from the quantum information and computation (QIC) literature which capture aspects of quantum field theories not captured by traditional observables such as correlation functions of local operators or Wilson loops. Information geometry/information metrics, Von-Neumann and Renyi Entropy, Mutual Information, Tensor networks Computational Complexity, Fidelity susceptibility, Quantum error correcting codes are only to name a few. This has become a highly productive enterprise leading to insights which might even solve the information paradox. Combining insights from holographic gravity duals, from integrability or supersymmetry based arguments, from lattice based approaches and perturbative approaches, we have explored the landscape of local quantum field theories rather comprehensively. Chapter 1 of this thesis gives a short review of AdS/CFT correspondence as to how it arises together with its important ingredients viz. AdS background and the boundary conformal field theory.

In this thesis we employ the notion of holographic complexity to navigate the lesser chartered territories like timelike singularities, non-local and lorentz violating field theories and warped CFT's. In places we have leveraged the holographic tools to define the boundary gauge theory using the bulk description. thereby studied the characteristics of the boundary gauge theory by quantifying their complexity. The complexity is defined holographically by Susskind's complexity volume and complexity action conjectures. Both of the conjectures of CV and CA as they came to be known, comes handy when characterizing the universal features of quantum complexity of the boundary field theory. Quantum complexity has emerged to be a crucial property of field theories capable of capturing physical phenomena which cannot be easily captured by more traditional field theory probes such as correlation function of local operators, and is touted to play a major role in holographic bulk reconstruction. We also compare and contrast the outcomes of both prescriptions to the extent that they appear as a viable tool in capturing the formerly obscure content of boundary field theory. In chapter 2 of the thesis, we introduce the notion of holographic quantum complexity and present the reasoning for its introduction as a viable tool.

Combining insights from complementary approaches such as holography, integrability or supersymmetry based arguments, lattice based approaches and perturbative approaches, we have explored the landscape of local quantum field theories rather comprehensively. However, the landscape of nonlocal quantum field theories is still mostly unexplored. We are optimistic that holography will be as productive in demystifying properties of nonlocal quantum field theories such as

the LST as it has been for enhancing our understanding of strongly coupled regimes of local field theories. Another fact is that holography beyond the traditional asymptotically AdS setting is also little explored. Our hope is that studying set ups such as the LST will help us get an handle on nonperturbative quantum gravity beyond pure AdS asymptotics to flat asymptotics.

In chapter 3 we present the study of string theory in the background that interpolates between AdS_3 in the IR to flat spacetime with a linear dilaton in the UV. The boundary dual theory interpolates between a CFT_2 in the IR to a certain two-dimensional Little String Theory (LST) in the UV. In particular, we study *computational complexity* of such a theory through the lens of holography and investigate the signature of non-locality in the short distance behavior of complexity. When the cutoff UV scale is much smaller than the non-locality (Hagedorn) scale, we find exotic quadratic and logarithmic divergences (for both volume and action complexity) which are not expected in a local quantum field theory. We also generalize our computation to include the effects of finite temperature. Up to second order in finite temperature correction, we do not any find newer exotic UV-divergences compared to the zero temperature case.

Thereafter, chapter 4 is the generalization of our work presented in previous chapter where we exploited holography to compute the complexity characteristics of Little String Theory (LST), a nonlocal, non-gravitational field theory which is connected via RG flow to local 2d CFT in the IR by an integrable irrelevant ($T\overline{T}$) deformation. In this work, we look at the LST obtained by further deforming the 2d CFT by Lorentz violating irrelevant $J\overline{T}$ and $T\overline{J}$ deformations, in an effort to capture the novel signatures of Lorentz violation (on top of nonlocality) on quantum complexity. It turns out that for this system the nonlocality and Lorentz violation effects are inextricably intertwined in the divergence structure of the quantum complexity. In anticipation of the fact that the dual field theory is lorentz violating, we compute the volume complexity in two different lorentz frames and the comparison is drawn between the results. These new results are consistent with our previous work, and null warped AdS_3 is treated as special case of interest.

In chapter 5 we investigate $WCFT_2$s using *circuit complexity* as a tool. Warped conformal field theories in two dimensions are exotic nonlocal, Lorentz violating field theories characterized by Virasoro-Kac-Moody symmetries and have attracted a lot of attention as candidate boundary duals to warped AdS_3 spacetimes, thereby expanding the scope of holography beyond asymptotically AdS spacetimes. First we compute the holographic volume complexity (CV) which displays a linear UV divergence structure, more akin to that of a local CFT_2 and has a very complicated dependence on the Virasoro central charge c and the $U(1)$ Kac-Moody level parameter k. Next we consider circuit complexity based on Virasoro-Kac-Moody symmetry gates where the complexity functional is the geometric (group) action on coadjoint orbits of the Virasoro-Kac-Moody group. We consider a special solution to extremization equations for which complexity scales linearly with "time". In the semiclassical limit (large c, k, while c/k remains finite and small) both the holographic volume complexity and circuit complexity scales with k.

In the final chapter 6, we turn our attention towards the quantum complexity of CFT/quantum gravity states which are dual to bulk geometries containing a naked timelike singularity. The appearance of naked timelike singularities in semiclassical limit are allowed in string theory, particularly in the context of holography, so long as they satisfy the "Gubser criterion" - only those naked timelike singularities are admissible which arise in the extremal limits of geometries containing cloaked singularities. In this work, we formulate an analogous criterion for the appearance of naked timelike singularities based on holographic complexity. We study three specific cases of naked timelike singularities, namely the negative mass Schwarzschild-AdS spacetime, the timelike Kasner-AdS and Einstein-dilaton system. The first two cases are outright ruled out by the Gubser criterion while the third case is more subtle - according to the Gubser criterion the singularity

switches from forbidden to admissible as the parameter δ is dialed in the range $[0, 1]$ across the transition point at $\delta = 1/\sqrt{3}$. We probe all three geometries using two holographic complexity prescriptions, namely CA and CV. We propose a simple criterion that if the holographic complexity of a geometry with naked timelike singularities is less than that of empty AdS, then that singularity cannot arise in the semiclassical limit of a UV-complete theory of quantum gravity. Our study strongly suggests that action complexity (CA) is a sensitive tool to investigate of timelike singularities being perfectly consistent with the Gubser criterion in all cases. On the other hand, volume complexity (CV) turns out to be not a reliable tool to probe timelike singularities.

Contents

List of Figures

List of Tables

Chapter 1

Overview of Holography

1.1 Quest for Quantum Gravity

"Behind it all is an idea so simple, so beautiful, that when we grasp it- in a decade, a century, or a millenium- we will all say to each other, how could it have been otherwise? How could we have been so stupid?"

- John A. Wheeler

Stephen Hawking in his pop-sci bestseller, *A Brief History of Time* has quoted that, *"But ever since the dawn of civilization, people have not been content to see events as unconnected and inexplicable. They have craved an understanding of the underlying order in the world.".* Since time immemorial, humankind has always been fascinated by the mystery the night sky holds as is evident from prehistoric paintings, ancient architecture, and writings. Humanity's insatiable quest to know it all has partially satiated in the early 20th century with the advent of the theory of relativity at the hands of Albert Einstein, which has become the *"go to book"* when it comes to finding answers to the questions pertaining to the large scale structure of spacetime. On the other hand, in the regime of the small, the reductionist approach of inquiry has borne wonderful fruits and has proven a successful and powerful approach to investigation since the time of Democritus in ancient Greece. Quantum Mechanics (QM) assumes the role to be the rightful heir of this course of inquiry of nature and is contemporary to relativistic mechanics. It is obvious that with two chief theories in place governing both regimes of the large and the small, nature has presented us with the unusual phenomenon which required us to borrow and look for the fusion of the methods from both paradigms. And hence in the thirties, with the labors of Dirac, Heisenberg, Pauli, Jordan, and many others gave birth to Relativistic Quantum Mechanics (RQM) or later dubbed with further conceptual developments as Quantum Field Theory (QFT). Which as the name suggests, incorporates both the (special) relativity theory and quantum mechanics nicely into a single framework that works nicely in each other's company. It has so far been credited with being the most successful scientific theory explaining the phenomena from the territory of atomic scale down to the subnuclear scale. To put it in perspective in Feynman's words, the predicting power of RQM is *"equivalent of measuring the distance from Los Angeles to New York, to within the thickness of the human hair."* It sounded like an overstatement those times to which

Feynman was referring but the precision available today is more than 600 times better - equivalent to measuring the distance from the Earth to the Moon to within the width of the human hair.

Everybody was happy with the way physics was going in the day until Hawking came into the picture with his path-breaking work and professed that black holes are the playground not only of general relativity but also the hotbed of quantum mechanics. Hawking's study has brought general relativity and quantum mechanics in the crosshairs of each other. Seems like, in the black holes, quantum mechanics and relativity coexists but in separate rooms with no chance of coexisting in the harmony with each other's company. If one tries to put them together, one runs into the bizarre phenomenon and logical inconsistencies like the information paradox. So it seems that the marriage of quantum mechanics with general relativity, unlike that with special relativity has so far always ended in a violent divorce.

It is not only to fulfill the empirical need but for the logical consistency of the enterprise, the offspring of quantum mechanics and general relativity now unanimously dubbed as Quantum Gravity (QG) has conceptually been sought after the successful completion of the standard model. Among the four fundamental forces of nature known to exist today, viz. electromagnetism, the weak force, and the strong force have all been quantized, *i.e.* they had been cast successfully into the quantum mechanical framework. It is only the theory of gravity manifesting itself in the form of curved spacetime that has been standing alone from this quantum mechanical association with the other forces. And the venture to put together the two has the reputation to be dubbed the *"holy grail"* of modern physics. As we entered the 21st century and are celebrating the centenaries of the inauguration of two of mankind's most colossal intellectual milestones, the ultimate laws governing the origin of the universe are still shrouded in mystery. And this mysteriously appears to be the plot of a cryptic design that the usual elusive playgrounds of quantum gravity are always hidden from the inquiring eye as if nature is intentionally trying to keep the secrets locked away. These obscure habitats like the Planck scale physics inaccessible by any conceivable accelerator, singularities cloaked behind the black hole horizon, and the initial singularity at the birth of space and time only dictate that for the time being, the physicists have only to resort to the theoretical considerations based upon gendanken experiments, symmetry principles and mathematical consistencies if they ever intend to make any fruitful progress. In light of all of this, the black hole information paradox is not only a stumbling block but the harbinger of progress whose resolution is promising to reward humankind with the invitation to the uncharted territory of quantum gravity, which for the time being bears resemblance to the distant mirage. To sum it all up, Hawking taking a jibe at Einstein's contrarian perception of quantum mechanics has declared that, *"Consideration of particle emission from black holes would seem to suggest that God not only plays dice but also sometimes throws them where they cannot be seen."*. This brings us back to conclude by quoting the master once again- *"Today we still yearn to know why we are here and where we come from. Humanity's deepest desire for knowledge is justification enough for our continuing quest. And our goal is nothing less than a complete description of the universe we live in."*

1.2 Holographic Principle

Black holes effectively behave as thermodynamic systems in quantum gravity having a finite temperature [1] and entropy [2]. Black holes are not only the simplest gravitational objects with no room for variation at all, but have proven to be the perfect theoretical laboratories to study quantum gravity. They can do so by making the Planck scale phenomenon accessible to the low

energy physics. The first great breakthrough in this direction was the formulation of the black hole entropy (BH entropy) relation by Bekenstein [2] and Hawking [1]

$$S_{BH} = \frac{\mathcal{A}_{\mathcal{BH}}}{4G_N} \; .$$

which indicates that somehow the relevant degrees of freedom are encoded in its event horizon instead of the bulk with the density of no more than one bit per unit Planck area. This all seems contrary at the face of the conventional thermodynamic systems where degrees of freedom reside in the *bulk* of the system as indicated by the entropy scaling extensively with its volume. This observation was later dubbed *the holographic principle* by t'Hooft [3] and Susskind [4] who propounded that this property qualifies to be the signature of quantum gravity at work. For supermassive black holes like the one at the center of the Milky Way, this amounts to packing an enormous entropy $\sim 10^{88}$ - a whopping large number - million times the total entropy of all the baryonic matter in the observable universe. The Bekenstein Hawking formula serves as an upper bound for the maximum entropy that can fit inside a region of the space bounded by the area of the black hole horizon. To see this, assume the contrary where we have some matter bounded inside some area and we throw in some extra matter and thereby increasing the entropy but also simultaneously forming a black hole. Consequently, we are led to the Bekenstein bound which asserts that there cannot be more than one degree of freedom per unit Planck area residing at the horizon.

To strengthen the claim of the holographic principle, we will provide the counting argument and start by estimating the number of degrees of freedom participating in the dynamics on both sides of the duality. Since entropy counts the number of such degrees of freedom (henceforth, *dof*), in the light of the holographic principle we expect the entropy computed using both descriptions to come the same. The entropy is an extensive quantity in QFT therefore it scales linearly with the spatial volume containing the degrees of freedom. Now for the validity of the holographic principle, it is essential that the entropy thus computed must be a sub-extensive quantity *i.e.* scaling linearly only with the area in the bulk description.

Consider a *d*-dimensional QFT living in the lattice of linear size l with each cell having a lattice spacing of ϵ. Here, l plays the role of the IR cutoff and in order to regulate the counting, it is necessary to identify ϵ as a short-distance cutoff. If ρ governs the number of dof per lattice site, then the total number of dof in the CFT is

$$n_{QFT} = \rho \left(\frac{l}{\epsilon}\right)^{d-1} \; .$$

Now let us compute the number of participating dof according to the bulk description. On the bulk side of the duality, the number of dof are governed by the BH entropy formula

Consequently, the number of dof governing the bulk dynamics scales as

$$\begin{aligned}
n_{AdS} &= \frac{1}{4}\frac{L^{d-1}}{G_N}\left(\frac{l}{\epsilon}\right)^{d-1} , \\
&= \frac{1}{4}\left(\frac{L}{l_p}\right)^{d-1}\left(\frac{l}{\epsilon}\right)^{d-1} ,
\end{aligned}$$

where we used $G_N \sim l_p^{d-1}$. Classical Einstein gravity limit is applicable when AdS curvature is very large in Planck units i.e.$(L/l_p)^{d-1} \gg 1$.

The whole upshot of this counting argument is the holographic principle which in its most generality is stated as the information contained in the quantum gravity theory can also be encoded in the field theory living in one lower dimensional spacetime, given that we identify

$$\rho = \frac{1}{4} \frac{L^{d-1}}{G_N} \ .$$

Now G_N plays the role of the coupling constant in the Einstein-Hilbert action of gravity

$$S_{EH} \sim \frac{1}{G_N} \int \sqrt{g} R + ... \ ,$$

Hence the above argument implies that we have a classical gravity description dominated by the saddle point if the dual QFT has the large number of dof. This also explains Bekenstein and Hawking's remarkable observation by suggesting that in the case of black holes, all the gravitational dof's are localized on the horizon therefore, the entropy of black holes scales with the horizon area instead of the bulk volume. Another observation that serves as a recurring theme in the holographic duality is the *UV/IR duality*. UV/IR duality states that in a holographic description, the UV cutoff of the QFT acts as the IR cutoff of the bulk gravity and the IR cutoff of the boundary description acts as the UV cutoff in the bulk. In other words, probing long distance scales in the bulk is equivalent to probing short distances in the boundary and vice versa. Therefore one can associate the region close to the boundary with the UV physics living at the boundary and the region close to the interior in the bulk with the IR regime of the boundary field theory. This equality of the dof on both sides substantiates the conjecture that both theories are like the two sides of a same coin. As a result of this, the bulk dynamics can also be alternatively, described using the boundary description.

The discovery of AdS/CFT correspondence in 1997 [5] has brought the holographic principle to the center stage in superstring theory. However, one might object as to the relevance of studying the exotic spacetime viz. the AdS spacetime while our spacetime is actually de Sitter. The answer is that by attacking the problem of quantum gravity in relatively favourable AdS spacetime, we hope to learn more about the general features of the quantum gravity like the information paradox in our own spacetime, which has proven to be a bit more challenging due to its global features (like the lack of timelike and null asymptotic region, etc.). The rest of the chapter is devoted to elucidating this interesting and fruitful paradigm of quantum gravity.

1.3   Major ingredients of AdS/CFT duality

The paradigm of AdS/CFT Duality [5, 6, 7, 8] or more generally *Gauge-Gravity Duality* [9], emerged from the superstring theory, which is regarded as the prime candidate of the unified theory, bringing all the known forces under a single umbrella. The most striking feature of AdS/CFT is its holographic nature, which relates $(d+1)$-dimensional gravitational theory to d-dimensional quantum field theory/gauge theory. To be specific, the gravitational theory has to be formulated in the Anti-de Sitter (AdS) spacetimes and the quantum field theory is a very specific kind of gauge theory, which lives at the conformal boundary of the AdS spacetime. Gauge theories, in general, describe the interactions viz. the electromagnetic, weak force, and the strong force except for gravity. At the first glance, both theories look different, even the dimensionality of spacetime in

which they operate is different, but AdS/CFT duality establishes a close equivalence or duality between the two.

In what follows, we will present Maldacena's decoupling argument for AdS/CFT correspondence and try to gain some intuition as to why the holography works but we will first set the stage by introducing the main characters - AdS spacetime and Conformal Field Theory.

1.3.1 Anti de Sitter spacetime

Anti-de Sitter spacetime in $(d+1)$- dimensions, (AdS_{d+1}) is an exact solution to the Einstein field equations which arises as the solution of the equations of motion to the following Einstein-Hilbert action with negative cosmological constant

$$S = \frac{1}{16\pi G_N} \int d^{d+1}x (R - 2\Lambda) .$$

It admits the maximum number of Killing vectors (i.e. $(d+1)(d+2)/2$ in number) and hence is maximally symmetric spacetime with constant negative curvature. Therefore the following relation holds between the curvature tensor and the metric

$$R_{\mu\nu\rho\sigma} = \frac{-1}{L^2}(g_{\mu\rho}g_{\nu\sigma} - g_{\mu\sigma}g_{\nu\rho}) ,$$

where L sets the curvature scale. And constant negative scalar curvature is given by

$$R = -\frac{d(d+1)}{L^2} ,$$

together with the cosmological constant

$$\Lambda = -\frac{d(d-1)}{2L^2} .$$
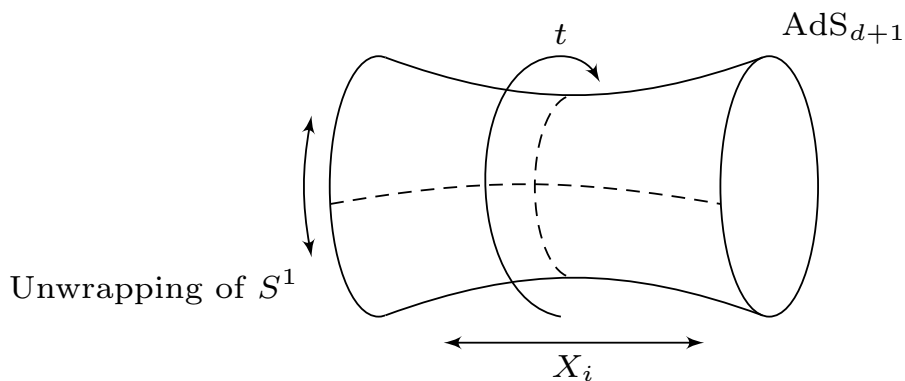
Figure 1.1: Global AdS_{d+1} realized as lorentzian hyperboloid.

AdS_{d+1} space can be realized as a lorentzian hyperboloid having the global topology of $S^1 \times \mathbb{R}^d$[10]

$$-X_0^2 - X_{d+1}^2 + \sum_{i=1}^{d} X_i^2 = -L^2 ,$$

19

embedded in $(d + 2)$ dimensional ambient space. By construction, the *isometry group $SO(d, 2)$*[1] is manifest therefore it can be thought of as a homogeneous space of the same group manifold. It is evident that the spacetime admits the pathological closed timelike curve (CTC) and thus violates causality. To restore causality, one unwraps the time direction and works instead with its simply connected *universal covering space* which we recognize as the familiar lorentzian AdS_{d+1} spacetime.

The symmetry generators $J_{\mu\nu} = i \left(X_\mu \frac{\partial}{\partial X_\nu} - X_\nu \frac{\partial}{\partial X_\mu} \right)$ of AdS_{d+1} are subject to the following commutation relation

$$[J_{\mu\nu}, J_{\rho\sigma}] = -i(g_{\mu\sigma} J_{\nu\rho} + g_{\nu\sigma} J_{\mu\sigma} - g_{\mu\rho} J_{\nu\sigma} - g_{\nu\sigma} J_{\mu\rho}) \ . \tag{1.1}$$

The action of the isometry group on AdS_{d+1} is transitive i.e. action of the elements of $SO(d, 2)$ maps any two points of AdS_{d+1} to each other or in other words, the orbits are diffeomorphisms. Therefore AdS_{d+1} can be obtained as a coset space [11] by performing the following quotient by the isotropy group

$$AdS_{d+1} = \frac{SO(d, 2)}{SO(d, 1)} \ .$$

If a point p on a manifold is fixed under the action of a subgroup, then that subgroup constitutes the isotropy group (aka the stabilizer group) of that point. $SO(d, 1)$ constitutes the isotropy group for $SO(d, 2)$. In this way, AdS_{d+1} admits a differentiable structure and is called a *homogeneous spacetime*. The isometry group $SO(d, 2)$ admits $SO(2) \times SO(d)$ as the maximally compact subgroup where, $SO(2)$ part represents the time translation symmetry and $SO(d)$ the orthogonal transformation of $\mathbb{R}^d$ part.

To be more concrete, we state a metric that is of most interest to us and that we frequently encounter in this thesis *i.e.* of the Poincarè patch

$$ds^2 = \frac{L^2}{u^2} du^2 + \frac{u^2}{L^2}(-dt^2 + d\vec{x}^2) \ ,$$

this chart only covers half of the AdS_{d+1}. The transverse directions are noncompact thus, the coordinates cover the full range (i.e. $\{t, x^i\} \in \mathbb{R}^d$), whereas, the radial coordinate ranges over $0 \leq u \leq \infty$. The $\mathbb{R}^{d-1,1}$ plane where the metric blows up as $u \to \infty$, is referred to as the conformal boundary of the Poincarè patch. On the other hand, the timelike Killing vector ∂_t becomes null at $u = 0$ hypersurface and thus acts as a Killing horizon. It will be useful to mention that this Killing horizon is only an *apparent* horizon because the signals cannot propagate past it and is thus not a singularity because in the global choice of coordinates the metric can be extended beyond $u = 0$.

Another useful form of the parametrization of the Poincarè patch encountered regularly in the literature is obtained by making transformation $u \to L/z$, where $0 \leq z \leq \infty$ while the ranges of transverse directions remain the same

$$ds^2 = \frac{L^2}{z^2}(dz^2 - dt^2 + d\vec{x}^2) \ .$$

The maximal compact subgroup $SO(1, 1) \times SO(d, 1)$ of $SO(d, 2)$ is manifest in the Poincarè patch. Where $SO(d, 1)$ is the Poincarè transformation on $(t, \vec{x})$ and $SO(1, 1)$ is realized as the symmetry under dilatations $(u, t, \vec{x}) \to (\lambda^{-1} u, \lambda t, \lambda \vec{x})$. Geometrically in Poincarè patch, AdS_{d+1} can be

---

[1]this also happens to be the d-dimensional conformal group.
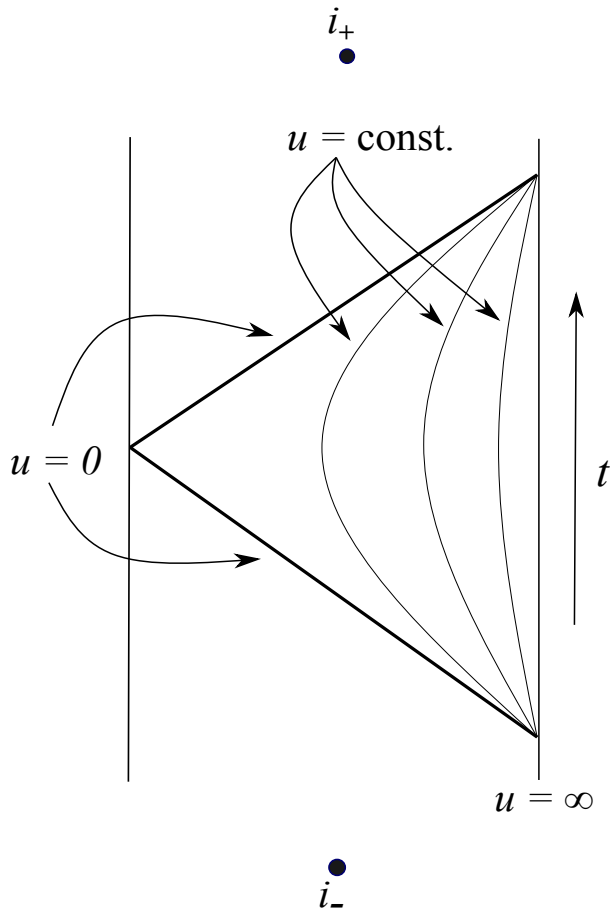
Figure 1.2: Poincarè patch of AdS$_{d+1}$

parametrized by the radial coordinate as a stack of copies of Minkowski spacetimes whose size dilates as the radial coordinate varies from horizon to the boundary. Each foliation is related to the Minkowski spacetime by a Weyl transformation this can be achieved by approaching different points at different rates.

In order to facilitate the study of geodetic motion we use a global chart in static coordinates. They can be obtained by the following parametrization

$$X_{d+1} = \sqrt{L^2 + r^2} \, \cos \frac{t}{L} \ ,$$
$$X_0 = \sqrt{L^2 + r^2} \, \sin \frac{t}{L} \ ,$$
$$X_i = r\omega_i, \quad (i = 1, ..., d) \ ,$$

where, ω_i such that $\sum_i^d \omega_i^2 = 1$ parametrizes S^{d-1}. The resulting pull-back metric on the AdS hyperboloid followed by unwrapping the time direction turns out to be

$$ds^2 = -\left(1 + \frac{r^2}{L^2}\right)dt^2 + \frac{dr^2}{\left(1 + \frac{r^2}{L^2}\right)} + r^2 d\Omega_{d-1} \ , \tag{1.2}$$

with the coordinate ranges $r \in (0, \infty)$ and $t \in (-\infty, \infty)$. AdS$_{d+1}$ is quite peculiar when one studies geodesic motion - being a negatively curved spacetime, massive particles are pushed periodically toward the origin and cannot reach the boundary. AdS$_{d+1}$ thus acts as a harmonic trap for massive particles.
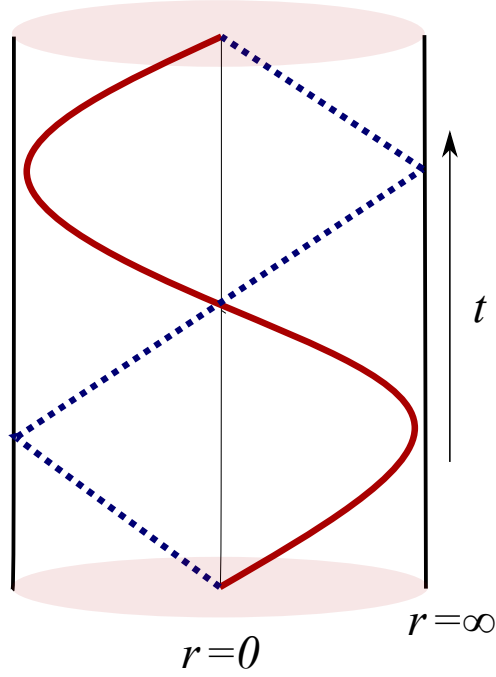
Figure 1.3: Geodesic motion in global AdS, red curves denotes the trajectory of the massive particle and the blue curve denotes that of the massless particle.

The trajectory for the massive particles is given by the following condition

$$-1 = g_{\mu\nu} \frac{d\dot{x}^{\mu}}{d\tau} \frac{d\dot{x}^{\nu}}{d\tau} \ ,$$

where affine parameter τ denotes the proper time. The above equation simplifies to the following form

$$\dot{r} = \pm \sqrt{E^2 - \left(1 + \frac{r^2}{L^2}\right)} \ ,$$

where E is given the interpretation of being energy per unit rest mass. Integration of the above equation yields the trajectory for the massive particle. With the boundary condition of $r(0) = 0$ we have the trajectory of the massive particle to be given by

$$r(\tau) = L\sqrt{E^2 - 1} \sin \frac{\tau}{L} \ .$$

It can be easily inferred from the above equation or alternatively by using the turning point condition $\dot{r} = 0$ that the particle does not go all the way up to the spatial boundary but instead turns back at $r_{max} = L\sqrt{E^2 - 1}$ towards the origin.

The null curves are obtained by integrating the following equation

$$\int_0^{\tilde{t}} dt = \int_0^{\infty} \frac{dr}{\left(1 + \frac{r^2}{L^2}\right)} \ ,$$

where we chose the positive sign for the outgoing null curve in the null condition obtained from the metric. This leaves us with the time taken to reach spatial infinity to be

$$\tilde{t} = \frac{L\pi}{2} \; .$$

Although being a hyperbolic spacetime, the boundary of AdS_{d+1} is an infinite proper distance away from any point in the bulk, but null geodesics escape to its conformal boundary in a finite amount of coordinate time t. This implies that in order to make particle dynamics well-defined, we also have to specify appropriate boundary conditions. With reflective boundary conditions in place, AdS_{d+1} effectively behaves like a box. This curious feature can be traced back to its spatial boundary being a timelike surface. As a consequence, AdS_{d+1} does not admit a (spacelike) Cauchy surface where one can specify initial data and hence make *Cauchy problem* well-posed. This can be summarized by saying that AdS_{d+1} is a *globally non-hyperbolic* spacetime. The fact that it takes the massless particles a finite time to reach spatial boundary is the artifact of the coordinate system. It is because coordinate time has no physical meaning as it cannot be registered by any observer. It instead takes an infinite amount of proper time to reach spatial infinity - the time which can be recorded by any physical clock in spacetime. To see this, note that

$$\frac{dt}{d\tau} = \frac{E}{\left(1 + \frac{r^2}{L^2}\right)} \; ,$$

and plug this back into the equation for the null curve to obtain the result that it indeed takes an infinite amount of proper time to reach the spatial boundary.

In asymptotic AdS spacetimes, the volume and area of the spatial sections scale in the same way. From the global metric (1.2) and working with a boundary cutoff Λ, the boundary area of the AdS is given by

$$A_\Lambda = \Lambda^{d-1} \int d\omega_{d-1} \; ,$$

where $\int d\omega_{d-1}$ is the volume of the spherical section of the AdS.

Similarly, the volume enclosed by the above boundary is

$$V_\Lambda = \int d\omega_{d-1} \int_0^\Lambda dr \frac{r^{d-1}}{\sqrt{1 + r^2/L^2}} \; ,$$

$$= \frac{L}{d-1} \Lambda^{d-1} \int d\omega_{d-1} \; .$$

We can safely remove the cutoff and realize that

$$\lim_{r \to \infty} \left(\frac{A_\Lambda}{V_\Lambda}\right) = \frac{d-1}{L} \; .$$

This makes holography easy to realize in asymptotic AdS spacetimes because there are enough degrees of freedom living on the boundary to capture the bulk physics and thereby adding leverage to t'Hooft and Susskind's anticipation of holography.

1.3.2 Conformal Field Theory

Conformal field theories (CFTs) occur as the fixed points of the Renormalization group (RG) flow. However the introduction of the renormalization scale in QFT breaks conformal invariance

- at the fixed points, the QFT description becomes scale invariant hence, the physical description remains the same under arbitrary rescaling of length scales. This scale invariance actually implies invariance under a larger group of symmetries called the *conformal group* [12, 13]. Conformal transformations rescale lengths but preserve angles between vectors. The causal structure (null-like, timelike and spacelike character) of the events in Minkowski spacetime is not altered under conformal transformations therefore, they preserve causality.

Under conformal transformations $x'^\mu = x^\mu + \epsilon^\mu(x)$, metric undergoes a position dependent overall rescaling

$$g_{\mu\nu}(x) \longrightarrow g'_{\mu\nu}(x') = \Omega^2(x')g_{\mu\nu}(x') .$$

Since our CFT_d lives in the boundary, the metric obeys what is called the conformal Killing equation which for the Minkowskian case boils down to

$$\partial_\mu \epsilon_\nu + \partial_\nu \epsilon_\mu = \frac{2}{d}\eta_{\mu\nu}\partial \cdot \epsilon .$$

For 2-dimensional CFT, the conformal group is infinitely large and has an infinite set of generators with each executing the transformations in the coordinate plane by analytic functions. The most general solution to the conformal killing equation for $d \neq 2$ is at the most quadratic in x

$$\epsilon_\mu(x) = a_\mu + \omega_{\mu\nu}x^\nu + \lambda x_\mu + b_\mu x^2 - 2(b \cdot x)x_\mu .$$

With a finite number of parameters, the conformal group is finite dimensional. The significance of the parameters as well as the associated generators are listed below

Parameters	Generators	Transformations
a_μ	P_μ	Translations
$\omega_{\mu\nu}x^\nu$	$J_{\mu\nu}$	Lorentz trans.
λx^μ	D	Dilatations
$b_\mu x^2 - 2(b \cdot x)x_\mu$	K_μ	SCT

The first two entries are easily discernible as they belong to the familiar Poincarè group and correspond to uniform translations and Lorentz transformations. The conformal group can be viewed as the extension of the Poincarè group with additional transformations like dilatations and Special Conformal Transformations (SCTs) respectively. The corresponding generators perform the local scalings and the translations of the point at infinity.

Altogether, we have $(d+2)(d+1)/2$ number of generators and each of which annihilates the vacuum of CFT. These generators obey the conformal commutation relations and their algebra isomorphic to standard form[2] of $SO(d,2)$ algebra (1.1) with generators of the following form

$$J_{\mu\nu} = M_{\mu\nu} , \qquad J_{\mu d} = \frac{K_\mu - P_\mu}{2} , \qquad J_{\mu,d+1} = \frac{K_\mu + P_\mu}{2} , \qquad J_{d,d+1} = D .$$

The Lorentz generators $M_{\mu\nu}$ forms $SO(d,2)$ subgroup and Dilatation operator D generates the $SO(1,1)$ subgroup of $SO(d,2)$. The action of a maximal compact subgroup $SO(d) \times SO(2)$ and its covering acts on $S^{d-1} \times \mathbb{R}$ after including the point at infinity. Since the conformal group is larger than the Poincarè group, it strictly constrains the mathematical structure of the correlation functions.

---

[2]with signature (-,+,....,+,-)

Representations of the conformal group are built by looking at the operators which are eigenfunctions of the dilatation operator. The eigenvalues of dilatation operator Δ, are called the *scaling dimensions* such that a spinless field under scaling $x \longrightarrow x' = \lambda x$ transforms as

$$\phi(x) \longrightarrow \phi'(x') = \lambda^\Delta \phi(x) \ .$$

The operator P_μ acts as a raising operator and K_μ acts as a lowering operator on the scaling dimension of the field. The scaling dimensions of the fields in a unitary theory are bounded below by the scaling dimension of the free scalar field. Hence, there exists *primary operators* in each representation of the conformal group having the lowest dimensions which are annihilated by K_μ. The representations of the conformal group are labeled by the scaling dimension together with the set of lorentz representation indices.

1.3.3   Putting it all together - matching symmetries

The matching of the global symmetries on both sides of the correspondence lends support for the holographic duality to be true. Conformal group $SO(d,2)$ acts on the boundary field theory which as alluded to earlier, contains Poincarè group $SO(d,1)$ as a subgroup. Moreover, the conformal group is a larger group having additional symmetry under rescalings and inversions. On the other hand, the diffeomorphism invariance of the gravitational theory is technically a gauge invariance of the theory under the choice of coordinates however, the true symmetries of the AdS are the invariance under the isometry group $SO(d,2)$. Isometries of AdS constitute the subgroup of diffeomorphisms which corresponds to the large gauge transformations that leave the asymptotic structure of the bulk invariant. The Poincarè subgroup of $SO(d,2)$ acts on the constant z foliation of the AdS which is Minkowskian spacetime, and $SO(1,1)$ is realized as the symmetry under dilatations. This matching of the symmetries of the bulk and boundary theories points to the intricate equivalence between the two descriptions and is successfully realized as the gauge-gravity duality.

1.4   Decoupling argument for AdS/CFT Duality

As stressed in the earlier sections, the holographic nature of the gravitational theory has been elevated to the status of the fundamental principle for any theory of quantum gravity. On the other hand, string theory already claims to be the leading candidate for the unified quantum theory of all the fundamental interactions including gravity. So, it is plausible that it must adhere to the holographic principle. Fortunately for the string theory, that turned out to be the case. String theory gives the concrete realization of the holographic principle in the form of Juan Maldacena's discovery of AdS/CFT duality in 1997 [5]. It is the conjectured non-perturbative description of the gravitational theory in asymptotically AdS spacetimes (also called the bulk) in terms of the gauge theory residing at its asymptotic boundary.

Central to the discovery of the AdS/CFT duality was the realization by Polchinski in 1995 that string theory is not only the theory of one-dimensional strings but also incorporates the higher-dimensional extended objects called D-branes. He was able to identify D-branes with the solitonic solutions found in supergravity known as extremal p-branes. D-branes naturally arise in string theory upon providing the Dirichlet boundary conditions to the endpoints of the open strings. Open string endpoints are constrained to not leave the D-branes and are free to move along the

directions parallel to D-branes. Upon quantization, the open string spectrum describes the dynamical fluctuations of the D-branes. Since the string endpoints are charged, consequently, the D-brane worldvolume carries a gauge field.

AdS/CFT duality can be arrived at by studying string theory from two different perspectives and identifying the two decoupled systems in the end. The first perspective is called the open string approach and it stems from studying the low energy excitations of the stack of D-branes described by open strings. The D-branes of interest to us are the extended objects in three spatial dimensions and are referred to as D3 branes. The world volume of D3 branes fills (3+1)-dimensional volume of (9+1)-dimensional ambient spacetime. Consider the following setup where we have a stack of N coincident D3-branes sitting in ten-dimensional Minkowski spacetime. In the low energy limit, only massless excitations are accessible, therefore this stack of D3-branes describes $U(N)$ gauge field in its world volume together with the D-brane excitations given by scalar modes. String theory in this kind of setup supports two kinds of perturbative excitations - open strings and closed strings. Open strings are the excitations of the D-brane and the closed strings are identified as empty spacetime excitations. In the low energy limit $E < \frac{1}{l_s}$, we only have massless string states excitations described by the effective action

$$S = S_{bulk} + S_{brane} + S_{int} \ . \tag{1.3}$$

Furthermore, in the low energy limit, $\alpha' \to 0$, S_{bulk} reduces to 10-dimensional SUGRA action, also brane action S_{brane} just reduces to the action of $\mathcal{N} = 4$ Super Yang-Mills theory living in (3+1) dimensional D3-brane worldvolume along with some higher derivative corrections. The interaction term in the action describes the coupling between the bulk and the brane modes of excitations. In the low energy limit, gravity becomes free as the 10-dimensional Newton's constant approaches zero. As a result, we are left with two decoupled systems: Free gravity in the bulk described by closed strings in 10-dimensional Minkowski spacetime and $\mathcal{N} = 4$ SYM in the worldvolume of D3-branes. To summarize, in the low energy limit $\alpha' \to 0$

$$S_{bulk} + S_{brane} + S_{int} \xrightarrow{(\alpha' \to 0)} S_{SUGRA} + S_{SYM} \ .$$

The second approach is called the closed string perspective and it stems from treating D-branes as the low energy supergravity solution. The D3-branes being a finitely extended object carrying finite tension gravitate and thus the stack of N coincident D-branes deforms the spacetime with the metric given by the exact SUGRA solution

$$ds^2 = \frac{1}{\sqrt{H(r)}} \left(-dt^2 + \sum_{i=1}^{3} d\vec{x}^2 \right) + \sqrt{H(r)}(dr^2 + r^2 d\Omega_5^2) \ ,$$

where $H(r) = 1 + \frac{R^4}{r^4}$ and the second term of the metric is the flat metric in transverse coordinates. The characteristic length is related to the parameters of string theory description through

$$R^4 = 4\pi g_s \alpha'^2 N \ ,$$

and describes the range of the gravitational effects. For the validity of the SUGRA solution, we require $R \gg \sqrt{\alpha'}$, in other words, the description is valid if $g_s \ll 1 \ll Ng_s$. The gravitational effects of the stack of D3-branes are weak for the length scales much larger than the characteristic length scale R therefore, the geometry of the far away region is governed by an asymptotically flat Minkowski background.

This stack of branes appears as a massive point object from the transverse directions of the brane, therefore the branes appear to be a point surrounded by five-sphere S^5. The geometry has an infinite throat region and the radius of S^5 approaches a constant value giving rise to the horizon. This near horizon geometry (region $r \ll R$) is described by the metric

$$ds^2 = \frac{r^2}{R^2} \left(-dt^2 + \sum_{i=1}^{3} d\vec{x}^2 \right) + \frac{R^2}{r^2} dr^2 + R^2 d\Omega_5^2 \, ,$$

which can be identified as the metric of $AdS_5 \times S^5$. In this perspective, the observer at infinity perceives two kinds of low energy physics: low energy excitations at a large distance from the branes and arbitrary energy excitations redshifted to low energy emanating from the horizon. The modes taking part in this low energy description decouple from each other in the asymptotic region because gravity becomes free at large distances. Thus physics governing the two types of excitations is again captured by the two decoupled systems- closed strings propagating in asymptotic flat region and Type-IIB string theory in the $AdS_5 \times S^5$ background respectively.

To conclude, in both cases one of the decoupled systems is always the same as described by the flat space supergravity which naturally leads us to identify the second system in both cases. Therefore we have a conjectured duality between the two systems in the alternate descriptions called the AdS/CFT correspondence. Which is stated in terms of *the duality between Type II-B superstring theory compactified on the 5-dimensional sphere, thereby, yielding (4+1) dimensional Anti-de Sitter (AdS_5 bulk) spacetime i.e. $AdS_5 \times S^5$, and maximally supersymmetric $\mathcal{N} = 4$ superconformal $U(N)$ Yang-Mills theory living on (3+1) dimensional boundary of that bulk.*

{Type II-B string theory in $AdS_5 \times S^5$} = {$\mathcal{N} = 4$, SU(N) gauge theory} .

For this isomorphism between the two theories to work, it is necessary for the dimensionless free parameters on both sides to match. For the Type II-B string theory, the dimensionless parameters are the AdS radius in units of string length $\frac{R}{l_s}$ and the string coupling constant. On the other hand for SU(N) SYM theory, the free parameters are coupling constant g_{YM} and the rank of the gauge group, N. They are related by

$$4\pi g_s = g_{YM} \, ,$$
$$\left(\frac{R}{l_s} \right)^4 = g_{YM}^2 N \, .$$

With string coupling g_s remaining fixed, string theory description dramatically simplifies to classical SUGRA approximation when the curvature scale is large in the units of string length

$$\frac{R}{l_s} \gg 1 \, .$$

This consequently implies that the rank of the gauge group is very large. The effective coupling in the large N limit is determined by the planar diagram theory to be the t'Hooft coupling

$$\lambda = g_{YM}^2 N \, .$$

We, therefore see that the perturbative weak coupling regime of gauge theory requires that one is dealing with the theory of quantum gravity. On the other hand, in the regime when classical gravity description is valid, one is essentially dealing with the strongly coupled gauge theory in the dual description.

Although in its original form, Maldacena arrived at it from a string theoretic setup using a top-down approach as discussed above, the later work by Gubser, Klebanov, and Polyakov[6] and

Witten[7] showed that AdS/CFT correspondence can be more conveniently engineered on certain holographic backgrounds using so-called *bottom up* construction without appealing to the full machinery of the superstring theory. We can also state the correspondence more generally in the following way: *to SUGRA living in $AdS_{d+1} \times \mathcal{M}$ we can find an isomorphism between a conformal field theory supported on the asymptotic conformal boundary of AdS spacetime.*

In order to formulate the mathematical statement of the equivalence between the two sides of the duality more concretely, we need to recall some valuable lessons drawn by the study of the scalar field dynamics in the AdS spacetime. For a scalar field $\phi(z,x)$ of mass m propagating in the bulk, there exists a dual primary operator labeled by its scaling dimension, $\mathcal{O}_\Delta(x)$ such that the mass of the scalar field and the scaling of the dual operator are related by

$$\Delta = \frac{d}{2} + \sqrt{\frac{d^2}{4} + m^2 L^2} \ .$$

With the appropriate choice of boundary conditions, the scalar field of mass m has the boundary asymptotic behavior

$$\phi(z,x) = z^{\Delta_-}\phi_0(x) + z^{\Delta_+}\phi_1(x) \ .$$

The solution with exponential behavior governed by Δ_+ is a normalizable solution and pertains to the quantum excitation in the bulk which decays at the boundary. This particular mode can be identified with the vacuum expectation value of the dual operator $\mathcal{O}_\Delta$. While the leading behavior with exponent Δ_- is a non-normalizable solution that does not decay at the boundary and defines a classical background field at the boundary with boundary value

$$\lim_{z \to \epsilon} \phi(z,x) = \phi_0(\epsilon,x) = \epsilon^{\Delta_-}\phi_0(x) \ ,$$

where $\phi_0(x)$ acts as a renormalized source of the dual operator $\mathcal{O}_\Delta$. The scalar fields with negative mass squared are dual to relevant operators in the boundary. Quite interestingly, Breitenlohner and Freedman found a window that allows for the $m^2 < 0$ tachyonic solutions to propagate in AdS and decay near the boundary without causing instabilities. The stability is relevant for the masses bounded from below[14] by

$$m^2 L^2 \geq -\frac{d^2}{2} \ .$$

The mathematical statement of the equivalence of both descriptions is captured by the equality of the generating functionals of the two theories constituting the two sides of the duality

$$\mathcal{Z}_{SUGRA}[\Phi_i] = \langle \mathcal{T} e^{i\int_{\partial\mathcal{M}} \Phi_{0i}\mathcal{O}_{\Delta_i}} \rangle_{CFT} \ ,$$

with the Dirichlet boundary condition that the bulk SUGRA field configurations Φ_i asymptotes to the boundary values Φ_{0i} each of which acts as the sources in the field theory for local CFT operators $\mathcal{O}_i$ dual to the bulk field. Also, $\mathcal{T}$ is the time ordering symbol for the boundary field theory. The correlation functions can be computed as

$$\langle \mathcal{O}_{\Delta_1}(x_1)....\mathcal{O}_{\Delta_n}(x_n) \rangle = \frac{\delta}{\delta\Phi_0(x_1)}....\frac{\delta}{\delta\Phi_0(x_n)} \log \mathcal{Z}_{SUGRA}[\{\Phi(x_i)\}]\Big|_{\{\Phi_0(x_i)\}=0} \ ,$$

where x_i's are also used to label the indices on the scalar fields.

For completeness sake, we must also mention other formulation due to Banks *et al.* of the dictionary [15] distinct from the above mentioned GPKW dictionary. In this version, the correlation functions of the appropriately weighted bulk fields are computed, and subsequently, their boundary limit is taken. The procedure comprises of extrapolating the bulk fields to the boundary in the following manner

$$\lim_{z \to 0} z^{-\Delta} = \mathcal{O}(x) \ ,$$

and treating them as boundary operators. The leading behavior of the bulk correlators gives the field theory correlation functions of the boundary operators dual to the bulk fields in the following way

$$\langle \mathcal{O}(x_1)....\mathcal{O}(x_n) \rangle_{CFT} = \lim_{z \to 0} z^{-n\Delta} \langle \phi(x_1,z)....\phi(x_n,z) \rangle_{bulk} \ .$$

This version is often mentioned as BDHM dictionary in the literature [16]. It can be shown that both versions of the dictionaries essentially compute the same correlators up to a numerical constant

$$\frac{\delta}{\beta(x_1)}....\frac{\delta}{\beta(x_n)} \mathcal{Z}_{bulk}[\beta] \bigg|_{\beta=0} \sim \lim_{z \to 0} \langle \phi(x_1,z)....\phi(x_n,z) \rangle_{bulk} \ ,$$

where β is the coefficient of the non-normalizable mode.

As of yet, this correspondence still has the status of the conjecture, but it has passed multiple robust tests making our belief in its consistency even stronger.

The duality between the quantities in the bulk and the boundary description is summarized in terms of the dictionary, which enables one to translate the quantities between the two duals. The basic entries in the dictionary are presented in the following table.

Basic entries in AdS/CFT duality dictionary	
Bulk quantities	Boundary quantities
Generating functional	Generating functional
Curvature radius in Planck units, $\left(\frac{R}{l_p}\right)^{D-2}$	dof per spacetime point, N^2
Curvature radius per unit string length, $\left(\frac{R}{l_s}\right)^{D-1}$	t'Hooft coupling λ
Scalar field, ϕ	Scalar primary operator, $\mathcal{O}$
Spin of field	Spin of operator
Charge of field	Charge of operator
Gauge field A_μ	Global conserved current, J^μ
Fierz-Pauli field, $h_{\mu\nu}$	Energy Momentum tensor, $T_{\mu\nu}$
Dirac spinor, ψ	Fermionic operator, $\mathcal{O}_\psi$
Evolution along bulk radial dimension	RG flow
Local isometries	Global spacetime symmetry
Blackhole temperature	Temperature of thermal state
Black hole charge	Chemical potential
On shell bulk action	Free energy
Area of horizon	Entropy
Instability of blackholes	Phase transitions
⋮	⋮

To summarize, the content of the AdS/CFT duality is that the quantum gravity state of the bulk is dual to the quantum state of the boundary CFT. The set of classical bulk geometries is dual to certain CFT states and the tools of quantum information theory enable us to recognize those states. We are typically interested in knowing which geometric regions of the bulk completely describe the given boundary regions and vice-versa, exploiting the information content enables us to gain mileage to map the corresponding regions under the duality. In the following chapters, we will summarize the achievements of this successful venture and will specifically focus on the utility of one very useful quantum information tool namely the complexity of the quantum state.

Chapter 2

Holographic Quantum Complexity

2.1 Quantum information tools are "not enough"

Our current understanding of holography is that the bulk spacetime represents an encoding of entanglement structure i.e. EPR type quantum mechanical correlations of the dual field theory degrees of freedom [17]. In order to exploit this relationship fully, recent years have seen an overlap between the quantum gravity and quantum information theory that goes under the banner name *it from qubit* program. This venture aims at unveiling the correct relationship between the bulk and the boundary degrees of freedom by leveraging quantum information theoretic tools. Entanglement entropy turned out to be an efficient tool enabling us to form such deep connections between both sides of the holographic duality. Entanglement entropy quantifies how the quantum information is encoded in a quantum state. If we have a subsystem of the quantum system described by a subregion $\mathcal{A}$ of the CFT and its complement is $\bar{\mathcal{A}}$, then for this two-partite system the full Hilbert space factorizes as

$$\mathcal{H} = \mathcal{H}_{\mathcal{A}} \otimes \mathcal{H}_{\bar{\mathcal{A}}} \ .$$

If the reduced state describing the subsystem $\mathcal{A}$ is a mixed state, then the pure state $|\Psi\rangle \in \mathcal{H}$ is said to be entangled. The reduced state of $\mathcal{A}$ is defined by

$$\rho_{\mathcal{A}} = \mathrm{Tr}_{\bar{\mathcal{A}}}(|\Psi\rangle \langle \Psi|) \ ,$$

and is obtained after tracing over the complement of the subregion and generally describes a mixed state. Entanglement entropy is a measure of the departure of the quantum state of the system from the pure state, and for a subregion $\mathcal{A}$ it is defined to be the von Neumann entropy of the reduced density matrix

$$S_{\mathcal{A}} = -\mathrm{Tr}_{\mathcal{A}}(\rho_{\mathcal{A}} \log \rho_{\mathcal{A}}) \ .$$

This formula simply quantifies the number of Bell pairs that are shared between $\mathcal{A}$ and the rest of the system, in other words, it measures the degree of entanglement between the subsystem and its complement.

In light of the striking connections uncovered between thermodynamics and the simplest of the gravitational systems like black holes in the 1970s, the question naturally arises whether the underlying boundary degrees of freedom contains sufficient information to exactly determine the bulk geometry, alternatively to the Einstein's field equations. The advent of AdS/CFT correspondence presents us with the right tools with which to directly tackle this question as was done subsequently in [18]. In this work, it has been shown that Einstein's equations satisfy what is called

the first law of thermodynamics

$$\delta S_A = \delta E_A^{hyp} \ ,$$

where the change in the entanglement entropy of the spherical region A of the CFT is δS_A and δE_A^{hyp} is the corresponding hyperbolic energy of the perturbed state about the vacuum state. The authors of [19] were precisely able to demonstrate that the holographic version of the relation analogous to the first law of thermodynamics applied to the boundary theory as expounded in [18] translates directly to Einstein's equation at least to linear order in perturbation about the pure AdS geometry. The "*first law of thermodynamics*" referred to above is universal as it applies to arbitrary perturbations around the vacuum state of the CFT and is true for an arbitrary number of dimensions. This significant development provides enough impetus for the anticipation that the thermodynamics of the boundary degrees of freedom encodes the knowledge about bulk geometry.

Generalizing the notion of Bekenstein-Hawking entropy in the light of the holographic principle, Ryu and Takayanagi [20, 21] discovered a holographic formula giving the geometrical dual of the entanglement entropy of a subregion of the boundary field theory. This Ryu-Takayanagi formula (RT-formula) as it came to be known, computes the field theory quantity called the holographic entanglement entropy which is von Neumann entropy by equating it to a geometrical quantity in the bulk. RT-formula equates the entanglement entropy of the boundary CFT states lying in some spatial sub-region $\mathcal{A}$, to the codimension-2 minimal area surface ($\gamma(\mathcal{A})$) in the bulk homologous to $\mathcal{A}$ up to a universal constant factor

$$S_\mathcal{A} = \mathcal{M}in. \left(\frac{Area(\gamma(\mathcal{A}))}{4G_N} \right) \ .$$

The covariant generalization to the RT formula valid for the nonstatic spacetimes was soon proposed in [21] and the general features like sub-additivity, positivity, etc. have been proven subsequently. The RT formula posits that spacetime emerges from the more fundamental degrees of freedom in such a manner that the bulk geometry is charted out by the EPR-like correlations of the CFT states. The entanglement entropy of the vacuum state of QFT is generally a UV divergent quantity because of the infinite number of dof contributing towards entanglement on either side of the entangling surface. One is therefore required to work with a UV cutoff together with the choice of the regularization scheme. The RT formula given above is the leading order result in the G_N expansion in the bulk (corresponding to the order N^2 in large- N gauge theory) had been verified by application of the replica trick in [22, 23, 24]. And more generally, the quantum corrections to it had been computed in [25, 24] the whole upshot of including the quantum corrections is to account for the von Newmann entropy of the bulk fields in the region called the entanglement wedge of $\mathcal{A}$ where entanglement wedge is simply the bulk domain of dependence of the partial Cauchy slice whose boundary is $\gamma(\mathcal{A}) \cup \mathcal{A}$. The corrected formula is able to account for the fine-grained entropy of the QFT coupled to gravity as is evident from the successful derivation of the Page curve from the gravitational path integral in the recent work [26, 27].

This program is very much in the spirit of Wheeler's plan of describing the fundamental physics in terms of the information-theoretic quantities but in the modern quantum mechanical sense christened as *It from Qubit.* The aim of the *it from qubit* program is to describe the emergence of the gravitation by analyzing the quantum information theoretic aspects of the dual QFT picture. The geometrization of the entanglement in the RT prescription has brought the significance of the entanglement to the forefront which is soon followed up by the very insightful work

of Mark Raamsdonk positing that entanglement acts as a glue responsible to stitch two disconnected spacetimes together.

Maldacena's identification of the thermofield double state with the dual description of the eternal black hole in AdS is the linchpin to this very insightful deduction. Maldacena in 2001 professed that the pure state prepared between two disjoint copies of CFTs residing on the left and the right asymptotic boundaries of the spacetime in the following way

$$|TFD\rangle = \frac{1}{\sqrt{Z(\beta)}} \sum_n e^{\frac{-\beta E_n}{2}} |E_n\rangle_L \otimes |E_n\rangle_R ~, \tag{2.1}$$

is dual to eternal AdS black hole in the bulk [28], whose two sides join the left and right exterior regions through a wormhole. The two copies which reside on the two boundaries are in the entangled state specified by $|TFD\rangle$. Here, β is the inverse temperature, E_i are the energy eigenvalues corresponding to the eigenkets $|E_i\rangle$ further labeled by the CFT to which they belong, and $Z(\beta)$ is the normalization constant which also happens to be the partition function i.e. $Z(\beta) = \mathrm{Tr}(e^{-\beta H})$. Notice that tracing out either of the Hilbert spaces produces a thermal state, therefore, this state can also be regarded as the purification of the thermal density matrix. The interpretation that one can ascribe to this state on the gravity side is that the quantum superposition of the disconnected asymptotically AdS geometries is dual to eternal AdS black hole with an Einstein-Rosen bridge connecting the two sides.

Drawing the lessons from Maldacena's work and the RT proposal, Raamsdonk has argued that for a non-entangled state corresponding to two non-interacting systems described by two disjoint CFTs, the product state is dual to the disconnected pair of spacetimes. He has further shown that the effect of gradually building up the entanglement between the two is just synonymous with the process of forming the quantum superposition of the disconnected spacetimes [29, 17]. The resulting state has features consistent with Maldacena's identification of the TFD state being dual to the eternal black hole in AdS. Hence, the entanglement between the dof in the two components is responsible for building up the classical connectivity between the initially disconnected spacetimes. Further down the line on the other hand, as per the RT argument, the effect of decreasing the entanglement between the quantum states is just the pinching off of the area of the RT surface consequently, bulk spacetime falls apart. Not only that, but increasing the entanglement also brings two distant regions closer and vice-versa.

Following this lead, Maldacena and Susskind have concluded that quantum entanglement between the microstates of two black holes is responsible to connect their interiors by ER bridges which they paraphrased by the slogan ER=EPR [30]. ER=EPR scenario leverages the fact that the length of the ER bridge grows extremely fast and also its throat pinches off with time in a manner as to not allow any signal propagation through itself is consistent with the knowledge that entanglement does not imply non-local signal propagation. They have used Raamsdonk's argument to ascribe the growing distance between the left and right portion of the ERB being the effect of the reduction of the entanglement. Putting these observations together, they have reached a conclusion that when EPR correlated quantum mechanical degrees of freedom collapse to form black holes, they are necessarily connected by the ER bridge. Quite interestingly this all leads to a speculative proposal that if two arbitrarily distant observers jump inside their neighboring black holes that happen to be maximally entangled with each other, the observers are bound to meet inside the horizon.

Another noteworthy offspring of the study of the RT proposal is the work of Brian Swingle who recognized the discrete representation of the time slice of AdS_{2+1} in terms of the hierarchical structure of tensor network called the MERA [31, 32]. Generally, a tensor network is an ansatz

for groundstate wavefunction of the discrete quantum system that also parametrizes the relevant subspace of the Hilbert space containing that wavefunction [33, 34]. The hierarchical structure emerges as the outcome of progressively removing local entanglement between the degrees of freedom at the short range followed by the coarse-graining procedure carried out iteratively in a manner that preserves long range entanglement. In the case of the critical gapless quantum systems, the same amount of entanglement is removed at every step followed by the coarse-graining procedure and the corresponding tensor network is called MERA. MERA can be manifested as a quantum circuit entangled at every scale that also includes information about the renormalization group. The coarse-graining or the renormalization direction in the MERA serves as the emergent radial direction of the holographic bulk with the circuit depth increasing logarithmically with the system size. More concretely, if the number of coarse-graining operations is given by w, then w also measures the layer depth of the MERA and for 1-dimensional critical quantum system, the metric of the entanglement geometry is given by

$$ds^2 = L^2_{AdS}(dw^2 + e^{-2w}dx^2) \ ,$$

where x is the horizontal distance in the MERA lattice. The logarithmic dependence upon the renormalization scale is given by $w = \log z$, then it is easy to see that this is simply the metric of the Poincarè chart of the AdS in disguise. Thus the discrete sites of the MERA where the quantum mechanical degrees of freedom lives forms the bulk AdS spacetime. After all the entanglement between the sites has been removed, the entanglement geometry terminates when the quantum state gets factorized into the product state. This analogy is pushed further when entanglement entropy is successfully reproduced by tracing over the bonds of the extremal surface of the MERA which is reminiscent of the RT surface in the discrete space and is called the causal cone. What has been said in the above paragraph applies to the discrete systems, but the extension to the continuum quantum mechanical systems has also been proposed. The analogy is strengthened further when including the finite temperature states in the MERA representation. In that case, thermal effects dominate the coarse-grained states as the energy scale of the lattice approaches the thermal energy and the state soon factorizes to a maximally mixed state. This behavior is given the interpretation of approaching the event horizon of the black hole because the local observer grazing close to the event horizon would observe the infinite blue shift in the black-hole temperature and the spacetime abruptly ends.

As alluded to in the last chapter one of the major aims of the AdS/CFT duality has been the question of bulk reconstruction wherein we are interested in knowing which bulk subregions could be described or reconstructed using the given boundary subregion or vice-versa, this modus operandi has been termed as subregion duality or entanglement wedge reconstruction in the literature. The primary geometrical construct in this paradigm is known as the entanglement wedge which is a subregion of the bulk encoding the same information about the CFT state as the subregion of the boundary over which that quantum state is defined. There have been several interesting developments on this front and we will give a brief summary of the current line of research. The first important development towards realizing this was the first order computation of quantum corrections to RT formula [25, **?**]. The authors (hereafter dubbed JLM) updated the notion of holographic entanglement entropy by defining the generalized entropy to be

$$S_{gen} = \frac{\mathcal{A}}{4G_N} + S_{bulk} + O(G_N) \ ,$$

by taking into account the von Neumann entropy computed over the reduced density matrix of the other matter fields present in the region of the bulk contained within the RT curve and the

boundary subregion of interest. It has been noted that the bulk entanglement entropy accounts for the first loop quantum corrections to the RT formula at order G_N^0 where the RT formula is already the leading order classical result at order $G_N^{0\ -1}$ (or $\mathcal{O}(1/N^{-2})$ in CFT). The omitted terms at order G_N constitute the various counterterms that cancel the UV divergences in order to render an overall finite quantity. Subsequently, it has been proved that generalized entropy obeys the generalized second law i.e. S_{gen} like the conventional notion of entropy, is a non-decreasing function of time. It is to be noted that JLM proved the result for the static spacetimes which was extended to include dynamic spacetimes in [35, 36]. These later developments maintain that the above result for the generalized entropy holds true for a broad class of surfaces homologous to the subregion of interest in the CFT. And thus pointed out the relevance of what is called the *Quantum Extremal Surface* (QES) that extremizes the generalized entropy i.e. the classical entropy including all its quantum corrections are exteremized. The FLM prescription extended the generalization by only including the first order corrections at the tree level result of entanglement entropy. Whereas, the QES proposal posits it to be true to all orders in the quantum corrections by deforming the FLM extremal surface to QES. In other words, the deformation of the extremal surface to QES is the nonperturbative result of including all the quantum corrections to the entanglement entropy

$$S_{gen} = \mathcal{M}in \left[\frac{\mathcal{A}(\gamma)}{4G_N} + S_{bulk}(\gamma) \right] \ .$$

The region over which the bulk entanglement entropy S_{bulk} is evaluated is the region of the bulk bounded by the minimal surface γ (homologous to the boundary interval) and the CFT interval and is called the entanglement wedge [37]. Thus the FLM and QES prescriptions only agree up to the first order i.e. $\mathcal{O}(G_N^0)$ but at $\mathcal{O}(G_N)$ and higher, the QES result departs from the extremal surface result and correctly accounts for the entanglement entropy. It has been shown in [38, 39] that the notion of QES correctly reproduces the information preserving unitary features of the Page curve for black hole evaporation. More precisely, it is shown that the information only escapes the blackhole after Page time when the bulk entanglement entropy of the escaping Hawking radiation equals the BH entropy and the early Hawking radiation carries the information about the black hole interior. Apart from accounting for the encoding of the blackhole information, the QES proposal has deep implications in general for the subject of the entanglement wedge reconstruction.

The program of entanglement wedge reconstruction has its roots in the works [40, 41, 42, 37, 43, 36]. The question of primary interest in this scheme is to fully understand the duality between the entanglement wedge and the subregions of the boundary where all the relevant degrees of freedom reside. The precursor to the entanglement reconstruction program was the HKLL prescription which is based upon extrapolate dictionary and tries to express local bulk operators in terms of boundary operators by using a construct called the *smearing function* having support on spacelike separated boundary subregion. But a perplexing feature of the procedure is that the choice of the smearing function is not unique and different choices of smearing functions reproducing the same bulk field may have support on the different boundary regions. The authors of [44] address this redundancy by proposing that the states of the bulk field are encoded in the boundary theory via the mechanism of quantum error correction. In this picture, the different boundary operators to which a given bulk operator is mapped are interpreted as the redundant encoding of the same bulk operator, which protects the bulk operator against the accidental erasure of certain boundary subregions. For the sake of completeness, we would like to mention the proposal by [**?**] of interpreting the redundancy of the reconstruction as the result of gauge free-

dom associated with the gauge symmetries of the boundary theory that changes the support without changing the action on the physical states.

In the previous paragraphs, we have seen that the requirement of having a geometrical dual heavily constrains the entanglement structure for the CFT state. Indeed, it supports the viewpoint that entanglement between various CFT degrees of freedom are crucial for the existence of the bulk spacetime geometry [17]. In other words, information theoretic properties of dual field theory are encoded in classical spacetime. There is an impressive list of quantum entanglement related CFT observables that have been related to classical geometric features of the bulk (see [45] for a review). Despite this, entanglement entropy or its close cousins like error correcting codes and tensor networks are *not enough* [46] in capturing the essential features of bulk geometry masked behind the black hole horizons. Take for example the growth of the Einstein-Rosen Bridge (ERB) behind the horizon. Entanglement entropy saturates in a short time upon reaching thermalization whereas, ER bridge continues to grow linearly with time long after the system hits thermalization [46]. This is also evident from the dual bulk description where the horizon totally obscures the region of spacetime from being explored by minimal surface. To explain the ERB growth, Susskind [47, 48, 49, 50] has recently borrowed another tool from quantum information theory and added to the holographic dictionary, namely the *computational complexity* as we will see in the following sections.

2.2   Role of Computational Complexity

In an attempt to understand the interplay between physics and quantum information, recently there has been quite an overlap between the physics literature and the literature on quantum information theory. All such attempts had been unanimously aimed at quantifying the information in a better way and in the process of doing that, physicists have borrowed quantities pertinent to the study of quantum information (QI) theory from the quantum information literature. Computational complexity being one such quantity of common interest to the members of both communities.

As expounded in the previous chapter, the need to adopt complexity as the quantity of interest in physics arose from trying to explain the curious feature of the growing interiors of black holes. Classically, black hole interiors seem to grow forever long after the scrambling time and quantum mechanically the growth is limited by Poincarè time. It is to be noted that the thermal entropy saturates after the thermalization time, therefore, it cannot be able to account for this late time growth. In the spirit of the holographic principle, specifically its realization in the form of AdS/CFT correspondence, where one seeks to find the dual description of the bulk phenomena in terms of the boundary gauge theory and vice-versa, Susskind was led to conjecture the association between the black hole interiors (Einstein Rosen bridges) with the computational complexity of the boundary state [47, 48]. The conjecture does not come as a surprise if one compares the late time evolution profile of the computational complexity of the quantum mechanical state with the ERB growth. However, we are still very far from formulating the precise workable microscopic characterization of quantum complexity in the context of Quantum Field Theory (QFT). Understanding complexity fully in the context of field theory to the present date remains a challenging problem, and its resolution is guaranteed to reward us with deep implications toward a more thorough understanding of holography. Several attempts have been made to define complexity in the continuum limit (see [51, 52, 53, 54, 55, 56, 57, 58, 59, 60, 61, 62, 63, 64, 65, 66, 67, 68] for an incomplete but representative list). However, it is fair to say that up to now there exists neither any universal and unanimous definition of complexity in the continuum limit nor an ex-

haustive study of its possible universality classes. In particular, in the continuum, complexity even in principle is a UV divergent quantity because it is defined to be within a tolerance (ϵ) with respect to the target state. Demanding more precision in replicating the target state requires the insertion of more number of gates which leads to a dependence on the inverse tolerance which is a divergent term. A similar trend emerges from the bulk perspective as we will see that both of the definitions involve the integrations over infinite regions of spacetime (bulk IR divergence). Usually, the divergent or explicitly cutoff dependent quantities in QFT are not considered physical as their value can be changed by changing the UV cutoff. But this characteristic UV dependence of complexity is a feature that seems to be relaxed while defining complexity in QFT.

Complexity and entropy for the classical systems although not the same but are very much similar - both scale classically linearly with the number of degrees of freedom. But in the quantum regime, since the states can be realized as lying in the Hilbert space, there is an exponential number of parameters and thus a huge difference emerges between the maxima of the entropy and that of maximum complexity. Complexity is the quantity associated with the states in the Hilbert space of the field theory living on the boundary which quantifies the difficulty of preparing a state (called the target state), starting from the given reference state. This is a well-defined quantity for discrete systems, like quantum circuits in information theory. Therefore we will first start by giving an exposition of the complexity of classical and quantum discrete systems and will subsequently bridge the gap leading us to the notion of holographic quantum complexity.

2.3 Computational Complexity in Classical Setting

Computational complexity is a quantity that quantifies the degree of difficulty in performing a computational task. In order to gain intuition, we first set out to discuss the simpler case of a classical system. A typical classical system well suited for our purpose consists of the chain of N classical spins, or it can equally well be the sequence of N coins as the degrees of freedom. The typical state of the system can be designated by the spin (coin) configuration and can be specified in bits, e.g. (10010111010001...), with 0 to denote spin down (tails) state and 1 to denote spin up (heads) state. First of all, we notice the inbuilt $\mathbb{Z}_2$ duality transformation that just amounts to saying that we could as well have started from the flipped configuration or by calling 0 the spin-up state and vice-versa. It is evident from the setup that the total number of spin configurations is 2^N. And maximal entropy attained after thermalization time is just the logarithm of the number of those configuration states i.e. $S_{max} = N \log 2$. Typically thermalization time for the classical systems is of the order of polynomial exponent in the number of bits. By the definition of complexity as the minimum number of simple spin flip operations and in the light of $\mathbb{Z}_2$ symmetry, it is easy to see that complexity of the classical spin system cannot exceed $N/2$. Moreover, the typical time scales to attain maximum complex configurations are also of the same order as the thermalization time. Elementary considerations of this sort demonstrate the indistinguishability of entropy and complexity for the classical systems. Even after the system thermalizes, subtle changes drive the complex states back to the simplest state all over again after what is called the Poincarè recurrence time which is typically of the order of the number of states i.e. 2^N.

2.4 Quantum Computational Complexity

However, for the quantum mechanical systems, we will argue that the situation will change drastically. Instead of the classical bits, we now have their quantum mechanical analogs called the qubits at our disposal as the degrees of freedom. For modeling a chain of N qubits, we now have to specify the quantum mechanical state of the system by expanding in terms of 2^N eigenstates[69]

$$|\psi\rangle = \sum_{i=1}^{2^N} a_i |i\rangle \ .$$

The availability of an exponential number of complex coefficients a_i's for tuning allows for quantum complexity to depart hugely from its classical counterpart. While maximum entropy and the thermalization times for the quantum mechanical systems remain the same, the quantum complexity is now exponential in the number of degrees of freedom. Also, the time to attain maximal complexity remains the same order as the maximal complexity, i.e. $t_{comp} \simeq e^N$. This implies that the late-time evolution of quantum complexity is able to account for the certain subtle changes that keep occurring in the quantum mechanical system long after it has thermalized. Any generic state of the quantum system is exponentially complex and it takes them an exponential amount of time in order to acquire exponential complexity as depicted in the figure
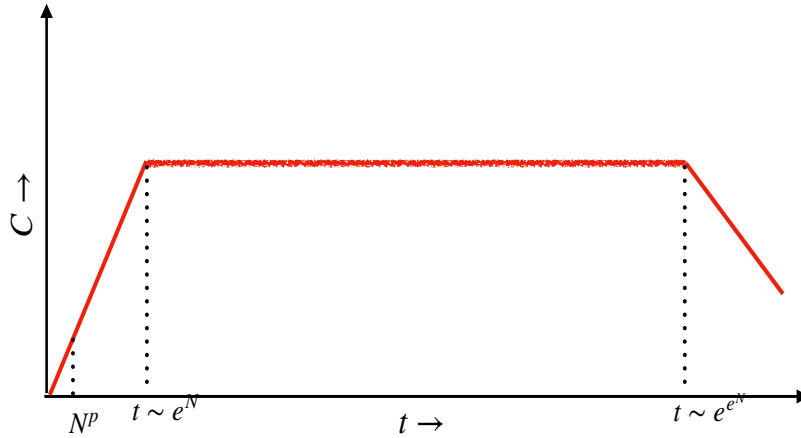
Figure 2.1: Time evolution of the complexity of a quantum state.

Initially, the complexity exhibits a linear growth in time after which the growth saturates to a mean equilibrium value exponential in N and fluctuates around it for a long time before a very rare large fluctuation kicks its back to the state of least complexity [70]. This happens once the whole unitary group has been explored after doubly exponential Poincarè recurrence time, $t_{recur} \simeq e^{e^N}$.

After the qualitative exposition of the nature of complexity, it is time to develop a quantitative framework. In order to be able to do that we need a set of ingredients that goes into defining the computational complexity as it arises in quantum mechanics. These ingredients are a quantum mechanical system, a space of states labeled the initial reference state $|R\rangle$, final target state $|T\rangle$ together with the set of gates $\{g_i\}$ to perform a task. Here, for example, the task constitutes of preparing the state $|T\rangle$ by the action of simple operations (packaged in as U) on $|R\rangle$ up to a tol-

erance of ϵ, such that according to some distance measure[1],

$$|| \, |T\rangle - U \, |R\rangle \, || \le \epsilon \, .$$

It is obvious that there are many different possible choices of U that one can make. But computational complexity tries to quantify the minimum number of simple operations one is required to do in order to execute a task. Now, the simple gates act upon the states lying in the Hilbert space, therefore they are represented as the unitary operators. Moreover, we cannot have one-qubit operators because we also want to allow for the entanglement between the states. It turns out for our purpose, that the two-qubit gates suffice, and this is the property we signify as being a simple operator.

Mathematically, the problem can be modeled in the following way. Starting from the reference state, we form what is called a quantum circuit by applying a unitary operator U

$$|T\rangle = U \, |R\rangle \, ,$$

which has the following decomposition in terms of the simple gates

$$U = g_n g_{n-1} .... g_1 \, .$$

The circuit complexity of U is then the minimum number of allowable gates it takes to constitute U in the above manner. We have also assumed that the allowable gates are k-local gates[2], but the dependence upon k is rather weak [70].

2.5 Nielsen's Geometrization of Circuit Complexity

This section is an exposition of Nielsen's geometrical approach to circuit complexity as the Hamiltonian control problem of finding the optimal circuit. To cope with the problem of giving a precise definition to complexity for continuous systems, Nielsen et. al. [71, 72] provide a definition of circuit complexity in field theory as the minimum number of unitary gates in the space of unitary operators which has a Finsler geometry. The complexity of a target state, given a reference state, is defined as the geodesic length in the Finsler manifold with suitable cost functions which acts like a Lagrangian in a typical variational problem.

We begin by synthesizing the n-qubit unitary operation U as

$$U = \overleftarrow{\mathcal{P}} \, exp \left[\int_0^1 d\tau \, H(\tau) \right] \, ,$$

in terms of time dependent control hamiltonian $H(t)$ expanded in a basis of generalized Pauli matrices M_I

$$H(\tau) = \sum_I Y^I(\tau) M_I \, ,$$

and the expansion coefficients Y^I are termed control functions. Path ordering operator $\overleftarrow{\mathcal{P}}$, indicates that the circuit is built starting from right to left. The operators M_I form the basis of the

---

[1] According to some appropriate operator norm.

[2] k-local gates constitutes the hamiltonian that is expressible as the sum of terms, each of which acts on the system of k-qubits.

tangent vector space in the group manifold and $H(\tau)$ is the velocity vector to the trajectory in the same space of unitaries. The optimal path in the space of unitaries obeys the boundary conditions $U(\tau = 0) = \mathbb{1}$ and $U(1) = U$. The complexity of this path is defined as the minimal value of the cost functional

$$\mathcal{C}[U] \equiv \mathcal{M}in. \int_0^1 d\tau \, F(U(\tau), \dot{U}(\tau)) \ .$$

Extremized cost functional acts as a geodesic length in the Finsler manifold with cost functions F acting as lagrangian in a typical variational problem. The cost functions are postulated to fulfill the following restrictions of

- **Smoothness:** $F(U, v) \in C^\infty$, in other words, F is a smooth function.

- **Positivity:** $F(U, v) \geq 0$, and $F = 0$ for all $v = 0$.

- **Positive homogeneity:** $F(U, \lambda) = \lambda F(U, v)$ for $\lambda \in \mathbb{R}$, the field of Reals.

- **Triangle inequality:** $F(U, v + v') \leq F(U, v) + F(U, v')$ for all tangent vectors v and v'.

Despite this attempt at achieving precision, there is still arbitrariness in the choice of cost functions that fixes the Finsler metric and complexity depends upon the choice of the metric. Nielsen was able to identify a multitude of choices for cost functions as

$$F_1(U, \dot{U}) = \sum_I |Y^I| \ , \qquad\qquad F_2(U, \dot{U}) = \sqrt{\sum_I (Y^I)^2} \ ,$$

$$F_p(U, \dot{U}) = \sum_I p_I |Y^I| \ , \qquad\qquad F_q(U, \dot{U}) = \sqrt{\sum_I q_I (Y^I)^2} \ ,$$

the role of penalty factors p_I and q_I is to penalize relatively difficult gates or directions on the relevant group manifold.

The beauty of this approach is to be able to translate the computational problem into the problem of minimizing the path length in differential geometry. As a consequence, the tools of geodesic analysis can be potentially applied to the problem of quantum circuit lower bounds. In this way of formulating things, the complexity of a target state, given a reference state, is modeled as the geodesic length in the Finsler manifold with suitable cost functions.

2.6 Quantum Field Theoretic Formulations

As we have mentioned in several places earlier, the quantum field theoretic formulation of circuit complexity is still lacking. An interesting stab at achieving this is the work of Jefferson and Meyers [51] who applied Nielsen's approach to the Gaussian states of free scalar field theory. They started off by placing the field theory on the discrete lattice thus achieving the family of N coupled harmonic oscillators. The reference state is chosen so that it has vanishing entanglement which is appropriately modeled by the Gaussian state of the following form

$$\psi_R(x) = \left(\frac{\omega_0}{\pi}\right)^{N/4} e^{-\frac{1}{2} x^T A_R x} \ ,$$

with $A_R = \omega_0 1$. The target state is chosen to be the ground state of the system of coupled harmonic oscillators

$$\psi_T = \prod_{i=0}^{N-1} \left(\frac{\omega_i}{\pi}\right)^{1/4} e^{-\frac{1}{2}x^T A_T x} ,$$

where, A_T is a matrix similar to the diagonal matrix with N distinct eigenvalues. The authors showed that the straight line geodesic in the normal mode subspace constitutes the optimal circuit.

After identifying the set of simple unitary gates that perform infinitesimal transformations on the states and appropriate cost functionals, the complexity is readily found to be given in terms of the normal mode frequency by

$$\mathcal{C} = \frac{1}{2}\sqrt{\sum_{k=0}^{N-1} \left(\log \frac{\omega_k}{\omega_0}\right)^2} ,$$

where, ω_k is is the normal mode frequency

$$\omega_k^2 + m^2 + \frac{4}{\delta^2}\sin^2\left(\frac{\pi k}{N}\right) ,$$

and δ is the lattice spacing. The agreement with the holographic CA answer is achieved when the cost functional $\mathcal{F}_1$ is chosen. The authors are aware of the fact that the holographic setup applies to the strongly coupled field theory, whereas the system under scrutiny is free field theory. But the aim is to draw insights into the nature of appropriate cost functionals and study the similarities with the holographic results. The universal features like the appearance of the logarithmic terms are emulated in the CA prescription where logarithmic divergences come from the joint terms, hence the free scalar field complexity reproduces CA complexity rather the CV complexity.

This setup has further been extended to study the complexity of the free fermionic system in [53, 56]. Furthermore, the authors of [59] studied the perturbative effect of turning on the ϕ^4 in the complexity functional with the conclusion that the effect of including interaction is to make the circuit depth the monotonic increasing function of the dimensionality of the space in which field theory is formulated. The states of interest are nearly Gaussian states and as a result, the gate set is also enlarged. Consequently, it is inferred that the complexity of the interacting field theoretic system has a slightly raised value at the Wilson-Fischer fixed point compared to the Gaussian fixed point.

2.7 Holographic Quantum Complexity

In AdS/CFT, the dual CFT picture of the eternal AdS black hole is an entangled state of the two copies of CFT living on the asymptotic regions called the thermofield double state[28]. Two such boundaries are joined by an Einstein-Rosen bridge (ERB) in the bulk spacetime. This ERB in the bulk continues to grow long after the boundary field theory attains thermal equilibrium. The spirit of AdS/CFT correspondence begs an answer to the natural question as to what dual quantity would suffice to capture this late-time growth.

Two geometrical duals with their own merits and motivations are conjectured to answer this question and are subsequently called the Complexity Volume [47, 48] and the Complexity Action

[49, 50] conjectures hereafter paraphrased by CV and CA conjecture respectively. CV conjecture tries to quantify the difficulty in sending a signal across ERB. It posits that the complexity of the field theory is given by the volume, $V_{max}(t)$ of the maximal spacial slice extending into the bulk and terminating on the boundary at the spacial slice on which the quantum state resides modulo some constants present for the dimensional reasons.
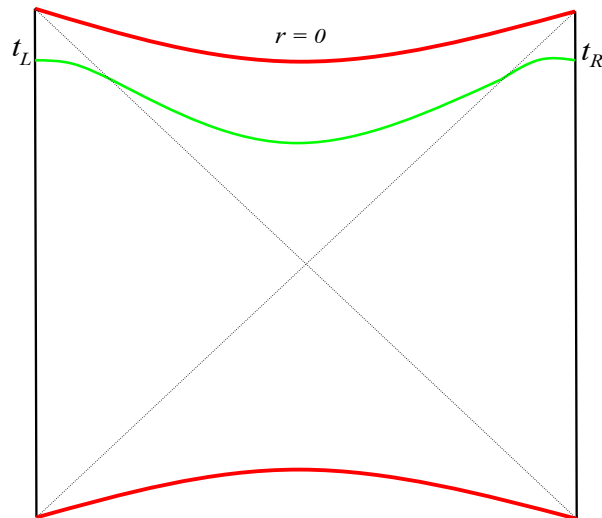
Figure 2.2: Maximal volume slice shown as green curve connecting points at the boundary, ERB is the region of the green curve lying behind the horizons.

In the adjoining figure, t_L and t_R denote respectively, the times on the left and the right boundary. This choice of picking two times in the dual CFT has the interpretation of choosing a quantum state

$$|\psi(t_L, t_R)\rangle = e^{-i(H_L t_l + H_R t_R)}|TFD\rangle \ ,$$

where H_L and H_R are the hamiltonians corresponding to the CFT living on the two boundaries and $|TFD\rangle$ is the thermofield double state (2.1). Recall that state $|TFD\rangle$ is close to being maximally entangled such that the reduced density matrix obtained by tracing over either side gives us a thermal state.

Quantitatively, the complexity volume duality is expressed as

$$\mathcal{C}_V(t) = \frac{V_{max}(t)}{G_N L} \ .$$

Where, $V(t)$ is the maximal volume of the spacelike slice anchored at the boundary time, t. And L is some characteristic length scale associated with the spacetime bulk like AdS radius or horizon radius. However, the choice of this background dependent quantity is ambiguous. For the purpose of illustrating the divergence structure of the CV complexity, we present the simplest

case [**?**, 73] of the Poincare patch of pure AdS_{d+1} background. The volume complexity evaluates to the following

$$\mathcal{C}_V = \frac{L_{AdS}^{d-1}V_x}{(d-1)\epsilon^{d-1}} \, ,$$

where, V_x is the boundary volume and plays the role of IR divergence, and ϵ is the UV cutoff. This is the result expected of any extensive quantity in a local field theory, it counts the total number of degrees of freedom on a lattice having a number of V_x/ϵ^{d-1} lattice sites. This all seems plausible because the preparation of some entangled state from the product state on the lattice would require a number of elementary operations proportional to the volume of the lattice. The CA conjecture [49, 50] posits that the complexity is proportional to the bulk on-shell action integral evaluated over the Wheeler-deWitt (WdW) patch of the boundary spatial slice on which the field theory state is specified. The WdW patch of a given spatial slice on the boundary is defined to be the bulk subregion covered by the union of all possible spacelike surfaces in the bulk which terminates on the same spatial slice at the boundary. Action complexity is defined as
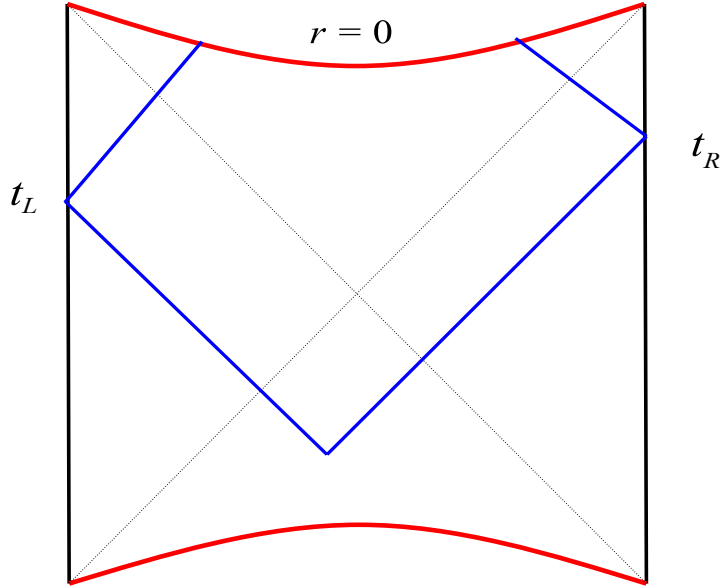
Figure 2.3: Wheeler-de Witt patch is the region enclosed by the lightlike curves, shown here in blue.

$$\mathcal{C}_A(t) = \frac{A_{WDW}(t)}{\pi\hbar}$$

Where, $A_{WDW}(t)$ is the classical bulk action including the boundary terms evaluated over the

WDW patch anchored at the boundary time, t. If there are no matter fields in the bulk, the action is given by [74, 73] the gravitational part

$$I_{WdW} = \frac{1}{16\pi G_N} \int_{WdW} d^{d+1}x \sqrt{g} \, (R - 2\lambda) + \frac{1}{8\pi G_N} \int_{\partial WdW} d^d x \sqrt{h} \, K - \frac{1}{8\pi G_N} \int_{\Sigma} d\lambda d^{d-1}\theta \sqrt{\gamma} \kappa$$
$$+ \frac{1}{8\pi G_N} \int_{\Sigma} d^{d-1}x \sqrt{\sigma} a \; .$$

The first term comprises the bulk Einstein-Hilbert action term with the cosmological constant, and for the rest of this work, the Gibbons Hawking boundary term will be evaluated at the timelike boundaries. The third term is the boundary term for the null boundaries of the WdW patch and the constant κ comes from writing out the null geodesic equation for the outward directed normal for the null surface, k

$$k^\mu \nabla_\mu k^\nu = \kappa k^\nu \; .$$

There are also joint contributions which are codimension-two surfaces formed by the intersection of the null-null or null-timelike surfaces. The null boundary contributions are in general complicated and we have just written them out for the sake of completeness. In the entirety of this thesis, we will use the alternative prescription proposed in [75] of simplifying the calculations by deforming the lightlike boundaries into timelike surfaces and then taking the null limit. This prescription is particularly advantageous for two reasons, first we don't have to deal with the null-null joint pieces which will get smoothed out into the timelike surface, and secondly, we will be able to use the GHY prescription to deal with the timelike boundaries instead of the different prescription by [76] to deal with the lightlike boundaries, thereby making our job a lot easier. We will still have to include the last term for the intersection of two timelike surfaces for which, $a = \log |n_1.n_2|$ where n_i's are the outward unit normals to the timelike surfaces.

Both these bulk measures of complexity are manifestly UV divergent, so regularization is necessary as remarked before. In the CV proposal there is an inherent ambiguity - to make the expression dimensionally consistent one must include a *characteristic length scale*, L, of the geometry for which there is no unique prescription. For the CA proposal, there are also a couple of issues *viz.* the ambiguities resulting from the null boundary terms. Some boundaries of the WdW patch are codimension one null/lightlike submanifolds *with* joints/edges. The presence of such null boundaries and their joints (edges) entails that the GHY boundary terms be properly defined as discussed in [76]. As we mentioned above, we take adopt a different approach to this problem [50, 77, 75]. Since we have to UV-regulate the WdW patch anyways, we use a particular regularization that deforms the WdW null boundary to timelike and in the process also smoothens out the joints. In this way, we can compute the GHY terms in one step without any issues. It is to be noted that instead of being an apparent shortcoming, the ambiguities arising in the holographic definition of complexity are a mere reflection of the inherent feature of the way the complexity is defined in field theory modulo the choice of the gate set. Here we quote a typical CA result to compare with the CV result obtained for the pure AdS$_{d+1}$ case.

$$\mathcal{C}_A = \frac{4l^{d-1}V_x}{\epsilon^{d-1}} \log(d-1) \; .$$

Note that $\mathcal{C}_A$ has the same divergence structure as $\mathcal{C}_V$ for the case of pure AdS i.e. it is an extensive quantity with the same IR dependence on the volume of lattice and the UV cutoff. However, as a dimensional accident in (1+1) dimensions, the action complexity vanishes. Moreover, the

rate of growth of complexity with respect to either of the boundary times gives in the limit of late time

$$\lim_{t \to \infty} \frac{d\mathcal{C}(t)}{dt} = \frac{2M}{\pi \hbar} \ .$$

A relation in agreement with Lloyd's conjectured bound of the rate of computation bounded above by the energy of the system

$$\frac{d\mathcal{C}(t)}{dt} \leq \frac{2E}{\pi \hbar} \ ,$$

making our belief in the validity of the CA conjecture stronger [78].

It would be a good place to ponder about having two different formulations of what appears to be the same field theory quantity. It has been noted that at the leading order CA and CV display the same divergence structure at the leading order (modulo an overall constant). However past studies reveal [74, 75] that the subleading coefficients might disagree across the two formulations. This hints at the fact that the two bulk/holographic prescriptions of complexity might correspond to different schemes of defining complexity in the boundary field theory. We will be in a relatively good position to remark on these matters once the field theoretic formulation of the complexity is available.

It is worthwhile at this point to mention that the two universal properties of complexity i.e. linear growth of complexity with time at late times and the universal time delay also called the *switchback effect* exhibited by complexity in response to the perturbations, inspired the authors in [79] to conjecture the existence of a more general class of codimension-one geometric observables as equally viable candidates encoding the complexity of the boundary theory as

$$\mathcal{C} = \frac{1}{G_N L} \int_{\Sigma_{F_2}} d^d \sigma \sqrt{h} \, F_1(g_{\mu\nu}, X^\mu) \ ,$$

where F_1 is a scalar functional of the background metric and the embedding coordinates $X^\mu(\sigma)$. The integration region is the codimension-one slice of the bulk region homologous to the boundary region where the CFT state is defined and is extremized with respect to the scalar functional F_2. These observables reduce after taking appropriate limits to the conventional CV proposal. Furthermore, the authors of this study went ahead and in [80] noticed that there is also no uniqueness in defining the holographic action complexity in terms of the codimension-zero observables in the bulk. They proposed the existence of yet another infinite class of codimension-zero gravitational observables exhibiting the same universal features as mentioned above that reduce to the CA duality under certain limits. These codimension-0 regions of integration $\mathcal{M}$ are bounded by the future and past codimension-1 hypersurfaces $\Sigma_\pm$ anchored on the boundary time slice where the CFT state is defined and is selected by extremizing the appropriate scalar functionals of the background metric and the embedding coordinates. Finally, the geometric codimension-0 candidate for holographic complexity takes the following form

$$\mathcal{C} = \frac{1}{G_N L^2} \int_{\mathcal{M}} d^{d+1} x \sqrt{g} \, G_1(g_{\mu\nu}) + \frac{1}{G_N L} \int_{\Sigma_+} d^d \sigma \sqrt{h} \, F_{1,+}(g_{\mu\nu}, X_+^\mu) + \frac{1}{G_N L} \int_{\Sigma_-} d^d \sigma \sqrt{h} \, F_{1,-}(g_{\mu\nu}, X_-^\mu) \ ,$$

where, $F_{1,\pm}(g_{\mu\nu}, X_\pm^\mu)$ and $G_1(g_{\mu\nu})$ are independent scalar functionals of their arguments shown in the parenthesis. This whole general scheme is appropriately dubbed *complexity equals anything* proposal for holography. The limit to the conventional CA duality is straightforward where G_1

functional is chosen to be the on-shell gravitational action in that case $\mathcal{M}$ becomes the WdW patch and the boundary integrals of $F_{1,\pm}$ assumes the form of GHY integrand evaluated over the boundaries $\Sigma_\pm$.

Another fruitful direction deserving mention is the one pursued in [81] where the authors pioneered the exploration of the circuits in the unitary representations of the Virasoro algebra

$$[L_m, L_n] = (m-n)L_{m+n} + \frac{c}{12}m(m^2-1)\delta_{m+n,0} ,$$

whose symmetry generators take the form

$$U(\sigma) = \overleftarrow{\mathcal{P}} \exp\left[\int_0^\sigma d\tau \, Q(\tau)\right] .$$

Where control functions are provided by the Fourier modes

$$\epsilon_n(\sigma) = \frac{1}{2\pi}\int_0^{2\pi} d\theta \, \epsilon(\sigma,\theta)e^{in\theta} ,$$

so that the unitary generators become

$$Q(\sigma) = \sum_{n \in \mathcal{Z}}\left(L_{-n} - \frac{c}{24}\delta_{n,0}\right) .$$

The reference state is chosen to be the eigenstate

$$L_0|h\rangle = h|h\rangle ,$$
$$L_n|h\rangle = 0 \quad \text{for} \quad n > 0 .$$

The cost functionals along the circuit are the usual F_1 and F_2 whose functional form is

$$F_1(\sigma) = |\langle\psi(\sigma)|\partial_\sigma\psi(\sigma)\rangle| ,$$
$$\text{and} \quad F_2(\sigma) = \sqrt{\langle\partial_\sigma\psi(\sigma)|\partial_\sigma\psi(\sigma)\rangle} .$$

These cost functionals are shown to be equivalent in the limit of large central charge $F_2 \simeq F_1\left(1 + \mathcal{O}\left(1/c\right)\right)$. Another slightly different version proposes [52] quantifying the contribution of the gates towards the complexity by minimizing the path length in the space of unitaries over the circuit using the Fubini-Study metric

$$ds_{FS}(\sigma) = \sqrt{\langle\partial_\sigma\psi(\sigma)|\partial_\sigma\psi(\sigma)\rangle - |\langle\psi(\sigma)|\partial_\sigma\psi(\sigma)\rangle|^2} \, d\sigma$$

One nice feature of the FS approach is that the directions modifying the state by an overall phase do not contribute toward circuit complexity. The complexity is then identified with the minimal length of the geodesic in the following manner

$$\mathcal{C}(\sigma) = \mathcal{M}in \int_0^\sigma ds_{FS}(\tau) .$$

In our study of Warped Conformal Field Theories, we will observe that the notion of complexity formulated in this manner is also related to the Polyakov action of 2D gravity. It is also worth mentioning that the Polyakov action has deep implications for the path integral formulation of circuit complexity through the Liouville action.

For the sake of completeness, we would like to mention other successful realizations of holographic quantum complexity. The first one of these is in terms of what is known as tensor networks, which as we already mentioned in section 1, are the representation of the wavefunction for discrete quantum systems. The evolution of quantum circuits also exhibits a growth pattern resembling tensor networks. It makes the identification of the growth of a number of nodes in a tensor network with complexity plausible. One convenient scheme of studying real space renormalization in terms of wavefunctions instead of that in momentum space (as in the Wilsonian approach) is called MERA [34, 82]. Motivated by the calculations of entanglement entropy by counting the number of entangling links, MERA is identified with the lattice realization of AdS spacetime[31, 83, 32, 84]. In this scheme, the tensors span the bulk and are thought of as discretized AdS geometry which provides the gravitational dual of the quantum theory living at the boundary. MERA so far captures only the discrete toy models of AdS/CFT therefore to overcome this discrepancy, the continuous analog of MERA called the cMERAS is introduced in[85, 86, 87, 88, 89, 90, 91], but which is restricted to the study of free field theories. Therefore to effectively study strongly coupled holographic CFTs, [92, 93]developed a scheme for optimizing the structure of lattice in Euclidean path integral setting by introducing a position dependent UV cutoff. Performing this minimization requires associating a metric functional recognized as Liouville action for each state which corresponds to the computational complexity in tensor network realization and varying the background metric for path integrals which is called the path integral complexity. [94] demonstrates that the complexity characteristics also have similarity with the quantum information metric under marginal deformations moreover, the metric is shown to be well approximated by the maximal volume of the time slice in the bulk [95, 96]. The consistency with AdS/CFT is established by reproducing the correct linear growth of the ERB with time.

Chapter 3

Holographic Complexity of LST and Single Trace $T\bar{T}$

3.1 Introduction

In this chapter, we focus our attention on the decoupled theory on a stack of $k \gg 1$ NS5 branes wrapping $T^4 \times S^1$, the so called Little String theory (LST) in $1 + 1$ dimensions. Unlike Dp branes, the worldvolume theory living on the NS5 branes decouples from the bulk at finite value of the string length $l_s = \sqrt{\alpha'}$. This is a signature that the decoupled theory namely LST living on the NS5 branes is not a local field theory. In fact the decoupled theory on the NS5 branes is somewhat intermediate between string theory (which is not a local theory and gives rise to massless gravitons upon quantization) and a local quantum field theory. The holographic background obtained by taking the near horizon geometry of the NS5 branes is flat spacetime with a linear dilaton $\mathbb{R}^{1,1} \times \mathbb{R}_\phi$. Such a holographic duality has been studied quite extensively in [97, 98].

Next, let us introduce $p \gg 1$ F1 strings wrapping the S^1. The near horizon geometry of the F1 strings is given by AdS_3. Thus the full geometry interpolates between AdS_3 in the IR (which corresponds to the near horizon geometry of the F1 strings) to flat spacetime with a linear dilaton in the UV (which corresponds to the near horizon geometry of just the NS5 branes). Correspondingly, the boundary field theory interpolates between a local CFT_2 dual to AdS_3 in the IR to LST in the UV. The interpolating geometry discussed above is often referred to in the literature as $\mathcal{M}_3$.

After the advent of $T\bar{T}$ deformation [99, 100], it was realized in [101] that there is a deformation of string theory in AdS_3 that shares many properties in common with the double trace $T\bar{T}$ deformation.[1] Such a deformation, often referred to in the literature as the single trace $T\bar{T}$ deformation, of string theory in AdS_3, changes the UV asymptotics of the bulk geometry from AdS_3 to flat spacetime with a linear dilaton keeping fix the IR regime of the geometry. Analysis in [101] shows that the dual background geometry interpolates between AdS_3 in the IR to flat spacetime with a linear dilaton in the UV. Holography in this background (often referred to as $\mathcal{M}_3$) can be realized as a concrete example of holography in non-AdS background that is smoothly connected to AdS_3.

This work is a part of a growing body of literature over the last few years to employ holography to investigate various aspects of nonlocal field theories such as LST which admit gravity duals [102, 103, 104, 105, 106, 107]. We are optimistic that holography will be as productive in demys-

---

[1]Details of the single trace $T\bar{T}$ deformation appear in section 4.2.

tifying properties of nonlocal quantum field theories such as the LST as it has been for enhancing our understanding of strongly coupled regimes of local field theories.

One shortcoming of holographic complexity volume and complexity action proposals for evaluating circuit complexity of the boundary theory is that there is no explicit reference to the boundary reference state as well the unitary gates which are involved in the circuit and these issue is still under investigation. In the AdS/CFT case the reference state is clearly *not* the CFT vacuum since the holographic (volume as well as action) for complexity is nonzero for pure AdS dual to the CFT vacuum state. We are unable to shed any further light on this issue here either and as a result our results suffer from the same reference state ambiguity. However since the LST_2 under consideration is obtained as a irrelevant deformation of a CFT_2 we can imagine using the *same exact* unitary gates and the *same exact* reference state as used for the initial CFT_2 which we UV-deformed. This is reasonable since the complexity expressions obtained here reduce to the familiar pure AdS expression once the UV deformation is removed. We *can* say something about the target state though. In the CFT_2 case the target state of the zero temperature geometry was the CFT vacuum, invariant under the $SL(2,\mathbb{R}) \times SL(2,\mathbb{R})$ symmetry. In the LST_2 case, the target state is the "no string" vacuum state which is the vacuum of the BRST cohomology of the coset $\frac{SL(2,\mathbb{R}) \times U(1)}{U(1)}$ at zero temperature [107]. For the finite temperature the target is the thermofield double state, both in case of the CFT and the LST, defined by $\left|\psi\right\rangle = \sum_n e^{-\beta \omega_n/2} \left|n\right\rangle_1 \otimes \left|n\right\rangle_2$ for energy eigenstates $\left|n\right\rangle$.

For interesting works on complexity in the context of double trace $T\bar{T}$ deformed CFT see [108, 109, 110].

3.2 Review of string theory in AdS_3, single trace $T\bar{T}$ and LST

Let us consider critical superstring background $AdS_3 \times \mathcal{M}$ that preserves $\mathcal{N} = 2$ or more supersymmetry where $\mathcal{M}$ is a compact spacelike manifold of dimension seven. A well studied example of this kind is type II strings on $AdS_3 \times S^3 \times T^4$ that preserves $(4,4)$ supersymmetry. The worldsheet theory describing strings propagating in AdS_3 with NS-NS fluxes turned on and R-R fluxes switched off is described by the WZW sigma model on the group manifold $SL(2,\mathbb{R})$. The worldsheet theory is invariant under the left and right moving component of $sl(2,\mathbb{R})$ current algebra at level k. The radius of AdS_3, R_{ads}, is related to the level of the current algebra as $R_{ads} = \sqrt{k}l_s$, where $l_s = \sqrt{\alpha'}$ is the string length.

Via the AdS/CFT correspondence, string theory on AdS_3 is dual to a two-dimensional CFT living on the boundary of AdS_3. For supergravity approximation to be reliable, we will consider $k \gg 1$. In the presence of the NS-NS three form H-flux, the spacetime theory has the following properties:

1. The spacetime theory has a normalizable $SL(2,\mathbb{C})$ invariant vacuum:

   - The NS vacuum, which corresponds to global AdS_3 in the bulk.
   - The R vacuum, that corresponds to massless $(M = J = 0)$ BTZ in the bulk.

2. The NS sector states contain a sequence of discrete states coming from the discrete series representation of $SL(2,\mathbb{R})$ followed by a continuum of long strings. The continuum starts above a gap of order $\frac{k}{2}$ [111].
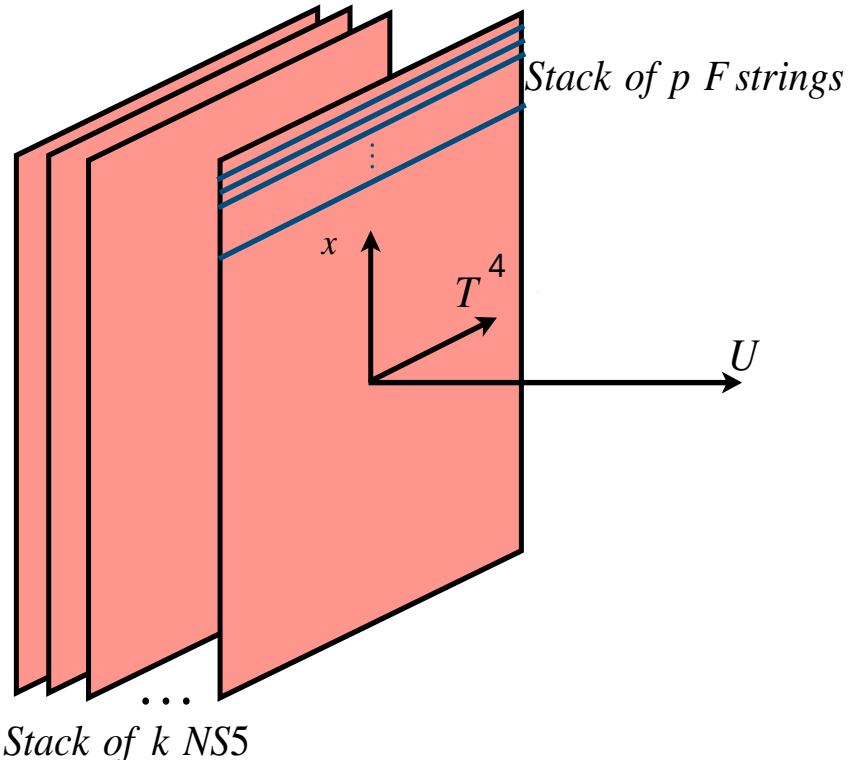
Figure 3.1: The configuration of k coincident NS5 branes with a number of p F_1 strings wrapping the S^1 direction.

3. The R-sector states contain a continuum above a gap of order $\frac{1}{k}$. Here the status of the discrete series states is not quite clear.

In the discussion that follows, we will focus only the long strings in the R-sector.
It was argued in [112] that, for string theory on $AdS_3 \times \mathcal{M}$, the theory living on a single long string is described by a sigma model on

$$\mathcal{M}_{6k}^{(L)} = \mathbb{R}_\phi \times \mathcal{M} \, , \tag{3.1}$$

with central charge $6k$. The theory on $\mathbb{R}_\phi$ has a dilaton that is linear in ϕ with a slope given by

$$Q^{(L)} = (k-1)\sqrt{\frac{2}{k}} \, . \tag{3.2}$$

The theory on the long strings has an effective coupling given by $\exp\big(Q^{(L)}\phi\big)$. Thus the dynamics of the long strings becomes strongly coupled as they move towards the boundary. But there is a wide range of positions on the radial direction where the long strings are weakly coupled. A natural question that one may ask at this point is: what is the full boundary theory dual to string theory in AdS_3. The answer to that question is, in general (for generic k), not known, but there are evidences to believe that the theory on the long strings are well described by the symmetric product CFT

$$(\mathcal{M}_{6k}^{(L)})^p / S_p \, , \tag{3.3}$$

where p can be thought of as the number of fundamental (F1) strings that form the background.

50

String theory in AdS_3 contains an operator $D(x,\bar{x})$ [113] (where x and $\bar{x}$ are coordinates of the two-dimensional spacetime theory), in the long string sector that has many properties in common with the $T\bar{T}$ operator. For example $D(x,\bar{x})$ is a $(2,2)$ quasi-primary operator of the spacetime Virasoro and has the same OPE with the stress tensor as the $T\bar{T}$ operator. However, there is an important difference between the $T\bar{T}$ operator and the operator $D(x,\bar{x})$: $T\bar{T}$ is a double trace operator whereas $D(x,\bar{x})$ is single trace.[2] In fact

$$D(x,\bar{x}) = \sum_{i=1}^{p} T_i \bar{T}_i \ , \tag{3.4}$$

where $T_i \bar{T}_i$ can be thought of as the $T\bar{T}$ operator of the ith block $\mathcal{M}_{6k}^{(L)}$ in the symmetric product CFT $(\mathcal{M}_{6k}^{(L)})^p/S_p$. For an elaborate discussion along this line see [114, 115]

Next, let us consider deformation of the long string symmetric product by the operator $D(x,\bar{x})$. This corresponds to deforming the ith block CFT $\mathcal{M}_{6k}^{(L)}$ by the operator $T_i\bar{T}_i$ and then symmetrized. Note that such a deformation is irrelevant and it involves flowing up the renormalization group (RG) trajectory. The deformation of the spacetime theory by $D(x,\bar{x})$ induces on the worldsheet a truly marginal deformation:

$$\int_{(\mathcal{M}_{6k}^{(L)})^p/S_p} d^2x D(x,\bar{x}) \sim \int_{\Sigma} d^2z J_{SL}^- \bar{J}_{SL}^- \ , \tag{3.5}$$

where $z,\bar{z}$ are the complex coordinates of the worldsheet Riemann surface Σ, J_{SL}^- and $\bar{J}_{SL}^-$ are respectively the left and right moving null $sl(2,\mathbb{R})$ currents of the worldsheet theory.

The above current-anti-current deformation of the worldsheet $\sigma-$model is exactly solvable, and standard worldsheet techniques yield the metric (in string frame), dilaton and the B-field as [116, 117]

$$ds^2 = f^{-1}(-dt^2 + dx^2) + kl_s^2 \frac{dU^2}{U^2} \ ,$$

$$e^{2\Phi} = \frac{g_s^2}{kU^2}f^{-1} \ , \tag{3.6}$$

$$dB = \frac{2i}{k^{3/2} l_s U^2}f^{-1}\epsilon_3 \ ,$$

where $f = \lambda + \frac{1}{kU^2}$, λ is the dimensionless coupling [3] of the marginal worldsheet deformation and g_s is the asymptotic string coupling in AdS_3 with $g_s^2 = e^{2\Phi(U\to 0)} \equiv e^{2\Phi_0}$. This background is popularly known as $\mathcal{M}_3$. The background $\mathcal{M}_3$ (4.6) interpolates between AdS_3 in the IR ($U \ll 1/\sqrt{k\lambda}$) to flat spacetime with a linear dilaton, $\mathbb{R}^{1,1} \times \mathbb{R}_\phi$ in the UV ($U \gg 1/\sqrt{k\lambda}$). The coupling λ sets the scale at which the transition happens.

The deformed sigma model background (4.6) can also be obtained as a solution to the equations of the motion of three dimensional supergravity action [118, 107]

$$S = \frac{1}{16\pi G_N} \int d^3X \sqrt{-g} e^{-2(\Phi - \Phi_0)} \left(R + 4g^{\mu\nu}\partial_\mu\Phi\partial_\nu\Phi - \frac{1}{12}H^2 - 4\Lambda \right) \ , \tag{3.7}$$

---

[2]Here single trace refers to the fact that $D(x,\bar{x})$ can be expressed as a single integral over the worldsheet of a certain worldsheet vertex operator. The operator $T\bar{T}$ on the other hand is double trace because it can be expressed as a product of two single trace operators in the sense just described.

[3]Note that without loss of generality, the value of λ can be set to an appropriate value as discussed in [101].

where G_N is the three-dimensional Newton's constant in AdS_3, $g_{\mu\nu}$ is the string frame metric, R is the Ricci scalar (in string frame), Φ is the dilaton, $H = dB$ is the 3-form flux and Λ is the cosmological constant.

As an example, the above construction can be realized as follows. Let us consider a stack of k NS5 branes in flat space wrapping a four dimensional compact manifold (T^4 or K_3). The near horizon geometry of the stack of k NS5 branes is given by $\mathbb{R}^{1,1} \times \mathbb{R}_\phi$ with a dilaton that is linear in the radial coordinate ϕ (where $\phi = \log(\sqrt{k}U)$). The string coupling goes to zero near the boundary ($U \to \infty$) whereas it grows unboundedly as one goes deep in the bulk ($U \to 0$). Next, let's add p (with $p \gg 1$) F1 strings stretched along $\mathbb{R}^{1,1}$. This stabilizes the dilaton and the string coupling saturates as $g_s \sim 1/\sqrt{p}$. Thus for large p the string coupling is weak and one can trust string perturbation theory. The F1 strings modifies the IR geometry ($U \ll 1/\sqrt{k\lambda}$) to AdS_3. The smooth interpolation between $\mathbb{R}^{1,1} \times \mathbb{R}_\phi$ in the UV to AdS_3 in the IR corresponds to interpolation between near horizon geometry of the NS5 brane system to that of the F1 strings [119, 107]. The spacetime theory interpolates between a CFT$_2$ with central charge $6kp$ in the IR to two-dimensional LST in the UV. The theory is nonlocal in the sense that the short distance physics is not governed by a fixed point.

LST can be realized as the decoupled theory on the NS5 branes. It has properties that are somewhat intermediate between a local quantum field theory and a full fledged critical string theory. Unlike a local field theory, at high energy E, LST has a Hagedorn density of states $\rho \sim e^{\beta_H E}$ where $\beta_H = 2\pi l_s \sqrt{k\lambda}$. On the other hand, LST has well defined off-shell amplitudes [120] and upon quantization it doesn't give rise to massless spin 2 excitation. Both these properties are very similar to local quantum field theories. For a detailed review of LST see [97, 98]

The above discussion has a simple generalization to backgrounds at finite temperature [101, 119, 121]:

$$ds^2 = -\frac{f_1}{f}dt^2 + \frac{1}{f}dx^2 + kl_s^2 f_1^{-1}\frac{dU^2}{U^2} \ ,$$

$$e^{2\Phi} = \frac{g_s^2}{kU^2}f^{-1} \ , \tag{3.8}$$

$$dB = \frac{2i}{k^{3/2}l_s U^2}f^{-1}\epsilon_3 \ ,$$

where as before $f = \lambda + \frac{1}{kU^2}$ and $f_1 = 1 - \frac{U_T^2}{U^2}$ where U_T is the radius of the outer horizon of the black hole. There is also an inner horizon at $U = 0$. For the Penrose diagram see figure 3.5. From the worldsheet sigma model point of view, the above background can be obtained from the coset description $\frac{SL(2,\mathbb{R}) \times U(1)}{U(1)}$ [118, 107, 121]. One can also check that solution (3.8) satisfies the equations of motion obtained from the supergravity action (4.7).

Going to the Euclidean continuation, and demanding the smoothness of the metric at the horizon, one can read off the temperature of the black hole (3.8) as

$$T_{bh} = \frac{1}{2\pi l_s}\frac{U_T}{\sqrt{1 + \lambda kU_T^2}} \ . \tag{3.9}$$

When $U_T \ll \frac{1}{\sqrt{k\lambda}}$, the horizon sits deep inside the bulk where the local geometry is well approximated by AdS_3. To good approximation such a black hole is described by BTZ. For $U_T \gg \frac{1}{\sqrt{k\lambda}}$ the horizon sits in the asymptotic linear dilaton regime of the geometry. The black hole here is well described by coset $\frac{SL(2,\mathbb{R})}{U(1)} \times U(1)$.

As U_T increases the black hole temperature (3.9) increases but saturates to an Hagedorn temperature

$$\beta_H = \frac{1}{T_H} = 2\pi l_s \sqrt{k\lambda} \; , \tag{3.10}$$

as $U_T \to \infty$. This is an indication of the Hagedorn nature of the spacetime theory (LST) in the UV.

Note that in the discussion that follows, we will consider only the positive sign of the coupling λ. In that case the spectrum of the deformed theory is real and the theory is unitary. Holography in the background (4.6) and (3.8) has been studied extensively in [101, 122, 102, 123, 103, 104, 107]. For the other sign of the coupling see [119, 124, 125].

3.3 Holographic Complexity in $\mathcal{M}_3$ at zero temperature

The aim of this section to compute the computational complexity of the LST dual to the background $\mathcal{M}_3$ (4.6) using holographic methods, namely the Complexity-Volume (CV) [48] and Complexity-Action (CA) [49, 50] prescriptions. We will perform these complexity computations for *both* zero temperature (in section 4.3) and finite temperature cases (in section 3.4). Computational complexity like entanglement entropy, is a manifestly UV-divergent quantity, and for local quantum field theories the UV divergence structure of computational complexity is rigidly constrained [73, 74]. In this section we reveal the UV-divergences which arise in a nonlocal field theory such as two-dimensional LST, and compare and contrast them with those arising in a local quantum field theory (a CFT$_2$).

3.3.1 Volume complexity at zero temperature

The volume complexity prescription computes the complexity of the dual boundary theory in terms of the volume of a maximal volume spacelike slice , Σ,

$$C_V = \frac{V_\Sigma}{G_N \, L} \; , \quad \text{with} \quad V_\Sigma = \int_\Sigma d^{D-1}x \, \sqrt{\gamma_\Sigma} \; , \tag{3.11}$$

where $\gamma_{\mu\nu}$ is the pullback metric on the maximal volume slice. As mentioned before, L represents a suitable characteristic scale of the geometry. However, we are working in the string frame with a non-trivial dilaton background and the volume complexity proposal needs to be generalized. This generalized prescription is guided by the requirement of furnishing the correct powers of the string coupling G_N in the complexity expression[4].The appropriate generalization is given by,

$$C_V = \frac{\tilde{V}_\Sigma}{\kappa_0^2 \, L} \; , \quad \text{with} \quad \tilde{V}_\Sigma = \int_\Sigma d^{D-1}x \, e^{-2(\Phi-\Phi_\infty)} \sqrt{\gamma_\Sigma} \; . \tag{3.12}$$

One can check that this generalization furnishes the correct powers of G_N [5] in the denominator using the string convention, $\kappa_0^2 e^{-2(\Phi_\infty-\Phi_0)} = 8\pi G_N$ where e^{Φ_∞} is the flat space string coupling and e^{Φ_0} is the string coupling of AdS_3.

---

[4]Similar considerations led the authors in [126] to a generalization of the Ryu-Takayanagi formula for holographic entanglement entropy for bulk backgrounds supporting a non-trivial dilation in the string frame.

[5]See [126] for a similar prescription for the Ryu-Takayanagi formula for the entanglement entropy

For the putative (string frame) maximal volume spacelike surface Σ given by $t = t(U)$, in the zero temperature $\mathcal{M}_3$ geometry (4.6), the induced metric is

$$ds_\Sigma^2 \equiv \gamma_{ab}dx^a dx^b = \left(\frac{k\,l_s^2}{U^2} - f^{-1}t'(U)^2\right)dU^2 + f^{-1}\,dx^2 , \quad \text{where} \quad t' \equiv \frac{dt}{dU} . \tag{3.13}$$

In the string frame, the volume of such a spacelike slice anchored at a time T [6] on the boundary is,

$$\tilde{V}(T) = e^{2(\Phi_\infty - \Phi_0)}\int dx\,dU\,e^{-2(\Phi-\Phi_0)}\sqrt{\gamma_\Sigma}$$

$$= \frac{k^{3/2}l_s L_x}{e^{-2(\Phi_\infty - \Phi_0)}}\int_0^\infty dU\,U\,f^{1/2}\sqrt{1 - \frac{U^2\,t'(U)^2}{k\,l_s^2\,f}} . \tag{3.14}$$

Here $L_x = \int dx$ is the spatial extent (IR cutoff) of the boundary theory target space. Extremizing this volume leads to the following Euler-Lagrange equation:

$$U\left(1 + \lambda\,k\,U^2\right)t'' + \left(4 + 3\lambda\,k\,U^2\right)t' - \frac{2U^4}{l_s^2}t'^3 = 0 . \tag{3.15}$$

The solution is found by employing series expansion method, lets assume the near boundary expansion of $t(U)$ of the form:

$$t(U) = T + \frac{a_1}{U} + \frac{a_2}{U^2} + \frac{a_3}{U^3} + \dots . \tag{3.16}$$

And plugging back in (4.35) and solving them order by order in $\frac{1}{U}$, we obtain the result that all the coefficients vanish. Thus the maximal volume slice is $t(U) = T$, a result that can be anticipated from the time reflection symmetry: $t \to -t$, of the background. Thus, the volume of the maximal volume slice is,

$$\tilde{V}_\Sigma(T) = \frac{k^{3/2}\,l_s\,L_x}{e^{-2(\Phi_\infty - \Phi_0)}}\int_0^\infty dU\,U\,f^{1/2} = \frac{k\,l_s\,L_x}{e^{-2(\Phi_\infty - \Phi_0)}}\int_0^\infty dU\sqrt{1 + k\lambda U^2} , \tag{3.17}$$

which diverges as $U \to \infty$. So we impose a UV cutoff at $U = l_s/\epsilon$ to regulate it. The regulated volume is then,

$$\tilde{V}_\Sigma(T) = \frac{k\,l_s\,L_x}{e^{-2(\Phi_\infty - \Phi_0)}}\left[\frac{l_s}{2\epsilon}\sqrt{1 + \frac{k\,\lambda\,l_s^2}{\epsilon^2}} + \frac{\sinh^{-1}\left(\frac{\sqrt{k\,\lambda}\,l_s}{\epsilon}\right)}{2\sqrt{k\,\lambda}}\right] . \tag{3.18}$$

As expected, due to time translation symmetry the expression is independent of T. Therefore from (4.20) volume complexity turns out to be:

$$C_V \equiv \frac{\tilde{V}_\Sigma}{\kappa_0^2\,L} = \frac{k\,l_s\,L_x}{G_N\,L}\left[\frac{l_s}{2\epsilon}\sqrt{1 + \frac{k\,\lambda\,l_s^2}{\epsilon^2}} + \frac{\sinh^{-1}\left(\frac{\sqrt{k\,\lambda}\,l_s}{\epsilon}\right)}{2\sqrt{k\,\lambda}}\right] . \tag{3.19}$$

Note that by convention the length scale L appearing here is the characteristic length scale associated with the geometry. Comparison with results from action complexity helps us resolve this ambiguity $L = \ell = \sqrt{k}\,l_s$, the AdS radius, and the volume complexity is thus,

$$C_V = \frac{cL_x}{3\beta_H}\left[\frac{\beta_H}{2\epsilon}\sqrt{4 + \frac{\beta_H^2}{\pi^2\epsilon^2}} + 2\pi\,\sinh^{-1}\left(\frac{\beta_H}{2\pi\epsilon}\right)\right] , \tag{3.20}$$

---

[6]The T here is not to be confused with the temperature T_{bh} (3.9) in section 3.4.

where c is the Brown-Henneaux central charge of the undeformed CFT_2 given by

$$c = \frac{3\sqrt{k}l_s}{2G_N} \ . \tag{3.21}$$

A comment on the non-locality: An *"effective central charge"* for LST

Let us recall that β_H can be thought of the length scale below which non-locality kicks in. Thus, an interesting limits to study would be $\epsilon/\beta_H \ll 1$ where the short distance physics is that of a non-local theory. In this limit the volume complexity takes the form

$$\lim_{\epsilon/\beta_H \to 0} C_V \ = \ \frac{cL_x}{3\beta_H} \left[\frac{\beta_H^2}{2\pi\epsilon^2} + 2\pi \log\left(\frac{\beta_H}{\pi\epsilon}\right) + \pi + O\left(\frac{\epsilon}{\beta_H}\right) \right] \ . \tag{3.22}$$

Evidently the divergence structure of the volume complexity (4.43) does not appear like that of a local quantum field theory.

For the case of a local quantum field theory, complexity being an extensive quantity should be proportional to the degrees of freedom given by the number of lattice sites $\propto \ L_x/\epsilon$ scales inversely with the cutoff ϵ (lattice spacing). The quadratic and logarithmic divergences in (4.43) are a reflection of the fact that the boundary theory, being a LST, is a non-local field theory and fittingly the non-locality parameter β_H features in the coefficient of this quadratic as well as the logarithmic divergences. One can check by making the non-locality vanish in the limit $\epsilon/\beta_H \gg 1$, the volume complexity expression (4.41) indeed reduces to that of a local field theory,

$$\lim_{\epsilon/\beta_H \gg 1} C_V = \frac{2c}{3\beta_H} \frac{L_x}{(\epsilon/\beta_H)} = \frac{2c}{3} \frac{L_x}{\epsilon} \ . \tag{3.23}$$

This expression of complexity (being proportional to the product of c, the central charge the number of degrees of freedom per lattice site, and L_x/ϵ, which gives the total number of lattice sites) counts the total number of degrees of freedom in a local field theory.

Now a remarkable physical fact emerges when one considers the coefficient of the log term (which is universal) in the expression of volume complexity (4.43) in the deep UV ($\epsilon \ll \beta_H$), which is

$$\tilde{N} = c\frac{L_x}{\beta_H} \ . \tag{3.24}$$

This coefficient counts the total number of "regularized/effective" degrees of freedom in the theory if we regard the lattice spacing of LST to be the Hagedorn scale, β_H instead of the UV cutoff ϵ of the original IR CFT, namely, $c\frac{L_x}{\epsilon}$[127, 103].

Another interesting fact emerges when we focus on the quadratic divergence in (4.43). One can rewrite this term in a manner which "looks" like a local field theory as follows,

$$C_V = \frac{cL_x\beta_H}{6\pi^2\epsilon^2} + \ldots = \frac{2\tilde{c}(\epsilon)}{3}\frac{L_x}{\epsilon} + \ldots, \quad \text{where} \quad \tilde{c}(\epsilon) = c\frac{\beta_H}{4\pi^2\epsilon} \ , \tag{3.25}$$

where $\tilde{c}(\epsilon)$ now has to be interpreted as an *"effective central charge"* for LST which is a monotonically increasing function of UV energy scale, $\frac{1}{\epsilon}$, and in particular this "effective central charge" diverges as the UV cutoff is removed.

The full volume complexity (4.41) as a function of ϵ/β_H has the following interesting properties:

1. C_V in (4.41) as a function of ϵ/β_H is always positive and monotonically decreases from UV to IR ($C_V'(\epsilon/\beta_H) \geq 0$).

2. In the deep UV (for $\epsilon/\beta_H \ll 1$), C_V diverges as (4.43).

3. In the deep IR (for $\epsilon/\beta_H \gg 1$), C_V decreases to 0 as (4.44).

The complete variation C_V as a function of ϵ/β_H is given in figure 4.1. Thus one can conclude that for length scales below β_H (the non-locality scale of LST), stringy physics takes over and the theory departs from behaving like a local field theory.

3.3.2 Action complexity at zero temperature

Now we compute the action complexity, $C_{\mathcal{A}}$, for the zero temperature $\mathcal{M}_3$ geometry. Action complexity has the dual advantage that (a) there are no arbitrary length scales appearing in its definition, and (b) neither does one need to solve a variational problem (maximal volume). Instead one just performs action integrals over the so called *WdW patch* which is defined to be the union of all spacelike curves in the bulk anchored at a fixed time slice on the boundary:

$$C_{\mathcal{A}} = \frac{S_{WdW}}{\pi\hbar} \ . \tag{3.26}$$

The Penrose diagram of the $\mathcal{M}_3$ spacetime with the WdW patch is displayed in figure 4.6.
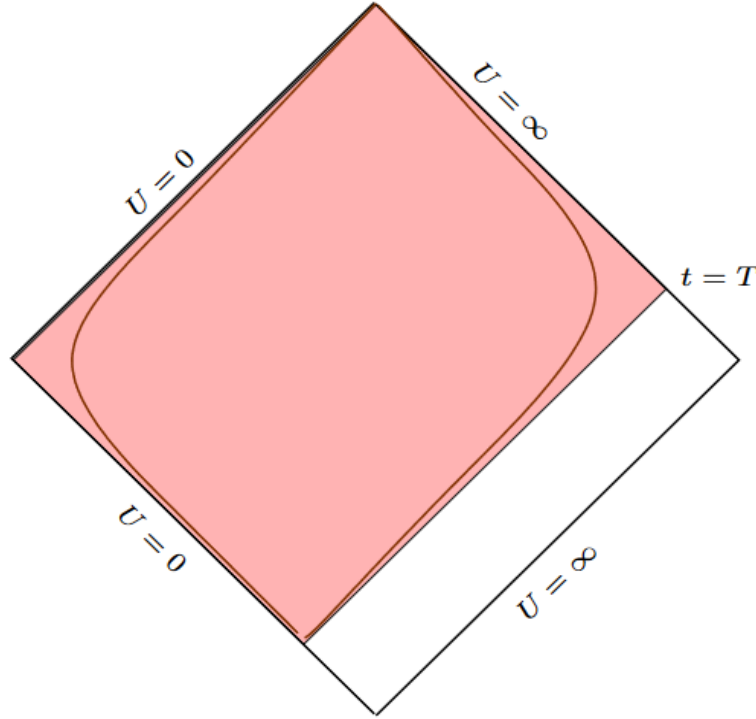
Figure 3.2: Penrose diagram of the $\mathcal{M}_3$ geometry with the Wheeler-deWitt (WdW) patch shaded in pink for the boundary time T. The brown curves are timelike surfaces which can be continuously deformed into the null boundaries of the WdW patch.

The gravity action in the string frame is:

$$S = \frac{1}{16\pi G_N} \int_M d^3X \sqrt{-g}\, e^{-2(\Phi-\Phi_0)} \left(R + 4g^{\mu\nu}\partial_\mu\Phi\partial_\nu\Phi - \frac{H^2}{12} - 4\Lambda \right)$$
$$+ \frac{1}{8\pi G_N} \int_{\sum \partial M} \sqrt{\gamma}\,(\cdots) + \frac{1}{8\pi G_N} \int_{\cap\partial M} \sqrt{h}\,(\cdots) \ . \tag{3.27}$$

56

The $(\cdots)$'s represent the appropriate surface/boundary $(\cup\partial M)$ terms and joint $(\cap\partial M)$ terms needed to make the variation of the action well defined as well as reparametrization invariant. Since (some) boundaries of the WdW patch are null, the usual GHY terms are not the suitable ones. This issue of determining the boundary terms for null boundaries was settled in [76]. However, we will take an alternative prescription spelled out in [75][7] where the null boundaries of the WdW patch are first deformed into a single smooth timelike surface using a deformation parameter (regulator), and then we are free to use the usual GHY term. After working out the GHY term we remove the regulator and obtain the result for the null WdW boundary. This affords an enormous simplification as it eliminates the necessity to compute the joint terms (terms in the action from joints or edges along which two null surfaces intersect) as well as preserving diffeomorphism and reparametrization invariance of the GHY contribution from beginning to end. Our regularization reproduces the same results as the prescription of [76] for the well known cases of pure AdS, AdS-Schwarzschild, AdS-RN etc. but the status of the equivalence of these two prescriptions for arbitrary generic geometries is yet unexplored. In general the issue of different regularization prescriptions is still being investigated e.g. for a comparison of the two regularizations introduced in [73], see [108, 109].

There is an additional issue regarding boundary terms here since we are working in the string frame while the usual GHY term applies for surface terms in the Einstein frame. In the string frame the GHY surface term has a contribution from the dilaton factor. This is determined by starting out with the usual GHY term in the Einstein frame and then Weyl transforming the expression to string frame. For $2 + 1$-dimensional bulk [8], the string frame GHY term is

$$S_{GHY} = \frac{1}{8\pi G_N} \int d^2x \sqrt{-\gamma}\, e^{-2(\Phi - \Phi_0)} \left(K - 4 n^M \partial_M \Phi \right) \; . \tag{3.28}$$

Volume (EH) pieces of the onshell action

The volume terms in the bulk action (4.87) are

$$S = \frac{1}{16\pi\, G_N} \int_{WdW} d^3X \sqrt{-g}\, e^{-2(\Phi - \Phi_0)} \left(R + 4 g^{\mu\nu} \partial_\mu \Phi \partial_\nu \Phi - \frac{1}{12} H^2 - 4\Lambda \right). \tag{3.29}$$

For the zero temperature $\mathcal{M}_3$ background, the Ricci scalar is,

$$R = \frac{-6 + 8\lambda\, k\, U^2}{k\, l_s^2\, \left(1 + \lambda\, k\, U^2\right)^2} \; , \tag{3.30}$$

and the dilaton is given by,

$$\Phi = \Phi_0 - \frac{1}{2} \ln\left(1 + \lambda\, k\, U^2\right) \; . \tag{3.31}$$

The Wheeler-deWitt patch (WdW) for the boundary time $t = T$ is bounded by the null rays

$$dt_\pm \;\; = \;\; \mp \sqrt{k}\, l_s\, \frac{\sqrt{f}}{U} dU \; , \tag{3.32}$$

---

[7] see also [77].

[8] For D-dimensions
$$S_{GHY} = 2 \int d^2x \sqrt{-h}\, e^{-2\Phi} \left(K - 2 \left(\frac{D-1}{D-2}\right) n^M \partial_M \Phi \right).$$

obeying boundary condition, $t(U \to \infty) = T$. The t-integrals in the volume terms (3.29) (Einstein-Hilbert terms) can be readily done:

$$t_+(U) - t_-(U) = 2\sqrt{k}\,l_s \int_U^\infty dU' \frac{\sqrt{f(U')}}{U'} \ . \tag{3.33}$$

This integral is divergent and hence we will modify our WdW patch to begin at a UV-cutoff surface $U = l_s/\epsilon$ instead of spatial infinity:

$$t_+(U) - t_-(U) = 2\sqrt{k}\,l_s \int_U^{l_s/\epsilon} dU' \frac{\sqrt{f(U')}}{U'} \ . \tag{3.34}$$

Various bulk contributions are listed as follows (in the intermediate steps one may consider the change of variables $U \to z = \frac{U}{l_s/\epsilon}$ and $U' \to z' = \frac{U'}{l_s/\epsilon}$ to perform the integrals exactly).

The Ricci scalar term in the action:

$$\begin{aligned}
S_R &\equiv \frac{1}{16\pi G_N} \int_{WdW} d^3X \sqrt{-g}\, e^{-2(\Phi-\Phi_0)}\, R \\
&= \frac{kL_x}{8\pi G_N} \int_0^{l_s/\epsilon} dU\, U \frac{-6 + 8\lambda k U^2}{(1+\lambda k U^2)^2} \int_U^{l_s/\epsilon} \frac{dU'}{U'} \sqrt{f(U')} \ .
\end{aligned} \tag{3.35}$$

The above integral can be performed analytically but the full expression is a bit cumbersome. In the deep UV (when $\epsilon/\beta_H \ll 1$), S_R takes the following form

$$\begin{aligned}
\lim_{\epsilon/\beta_H \ll 1} S_R &= -\frac{cL_x}{6\beta_H}(7 + 8\log 2)\log\left(\frac{\beta_H}{\pi\epsilon}\right) + \frac{2cL_x}{3\beta_H}\log^2\left(\frac{\beta_H}{\pi\epsilon}\right) \\
&\quad + \frac{cL_x}{18\beta_H}(\pi^2 + 24\log 2) + O\left(\epsilon^2/\beta_H^2\right) \ .
\end{aligned} \tag{3.36}$$

In the IR (when $\epsilon/\beta_H \gg 1$), S_R takes the form

$$\lim_{\epsilon/\beta_H \gg 1} S_R = -\frac{cL_x}{4\pi\beta_H}\frac{\beta_H}{\epsilon} + \frac{7cL_x}{288\pi^3\beta_H}\left(\frac{\beta_H}{\epsilon}\right)^3 + O\left(\beta_H^4/\epsilon^4\right) \ . \tag{3.37}$$

The dilaton kinetic term in the action:

$$\begin{aligned}
S_\Phi &\equiv \frac{1}{16\pi G_N} \int_{WdW} d^3X \sqrt{-g}\, e^{-2(\Phi-\Phi_0)}\, (4g^{\mu\nu}\partial_\mu\Phi\partial_\nu\Phi) \\
&= \frac{L_x k^3 \lambda^2}{2\pi G_N} \int_0^{l_s/\epsilon} dU \frac{U^5}{(1+\lambda k U^2)^2} \int_U^{l_s/\epsilon} \frac{dU'}{U'} \sqrt{f(U')} \ .
\end{aligned} \tag{3.38}$$

In the UV S_Φ takes the following form:

$$\begin{aligned}
\lim_{\epsilon/\beta_H \ll 1} S_\Phi &= \frac{cL_x}{24\pi^2\beta_H}\left(\frac{\beta_H}{\epsilon}\right)^2 + \frac{cL_x}{6\beta_H}(3 + 8\log 2)\log\left(\frac{\beta_H}{\pi\epsilon}\right) - \frac{2cL_x}{3\beta_H}\log^2\left(\frac{\beta_H}{\pi\epsilon}\right) \\
&\quad - \frac{cL_x}{36\beta_H}(-3 + 2\pi^2 + 48\log 2) + O\left(\epsilon^2/\beta_H^2\right) \ .
\end{aligned} \tag{3.39}$$

One might be a bit alarmed at the appearance of the "log squared" divergences in the expressions (4.94) and (4.96), which did not arise in the volume complexity cases but as it will turns out, such log squared divergent contributions will cancel out among each other.

58

In the IR, S_Φ takes the form

$$\lim_{\epsilon/\beta_H \gg 1} S_\Phi = 0 + O\left(\beta_H^5/\epsilon^5\right) \,. \tag{3.40}$$

The cosmological constant term in the action:

$$
\begin{aligned}
S_\Lambda &\equiv \frac{1}{16\pi G_N} \int_{W\,dW} d^3X \sqrt{-g}\, e^{-2(\Phi-\Phi_0)} \left(-4\,\Lambda\right) \\
&= \frac{L_x k}{2\pi G_N} \int_0^{l_s/\epsilon} dU\, U \int_u^{l_s/\epsilon} \frac{dU'}{U'} \sqrt{f(U')} \,.
\end{aligned} \tag{3.41}
$$

In the UV S_Λ takes the following form

$$\lim_{\epsilon/\beta_H \ll 1} S_\Lambda = \frac{cL_x}{24\pi^2\beta_H}\left(\frac{\beta_H}{\epsilon}\right)^2 + \frac{cL_x}{6\beta_H}\log\left(\frac{\beta_H}{\pi\epsilon}\right) + \frac{cL_x}{12\beta_H} + O\left(\epsilon^2/\beta_H^2\right) \,. \tag{3.42}$$

In the IR, S_Φ takes the form

$$\lim_{\epsilon/\beta_H \gg 1} S_\Lambda = \frac{cL_x}{6\pi\beta_H}\frac{\beta_H}{\epsilon} + \frac{cL_x}{144\pi^3\beta_H}\left(\frac{\beta_H}{\epsilon}\right)^3 + O\left(\beta_H^4/\epsilon^4\right) \,. \tag{3.43}$$

The Kalb-Ramond term in the action:

$$
\begin{aligned}
S_H &\equiv \frac{1}{16\pi G_N} \int_{W\,dW} d^3X \sqrt{-g}\, e^{-2(\Phi-\Phi_0)} \left(-\frac{H^2}{12}\right) \\
&= -\frac{L_x}{4\pi G_N\, k} \int_0^{l_s/\epsilon} \frac{dU}{U^3 f^2} \int_U^{l_s/\epsilon} \frac{dU'}{U'} \sqrt{f(U')} \,.
\end{aligned} \tag{3.44}
$$

In the UV S_H takes the following form

$$\lim_{\epsilon/\beta_H \ll 1} S_H = -\frac{cL_x}{6\beta_H}\log\left(\frac{\beta_H}{\pi\epsilon}\right) + O\left(\epsilon^2/\beta_H^2\right) \,. \tag{3.45}$$

In the IR, S_Φ takes the form

$$\lim_{\epsilon/\beta_H \gg 1} S_H = -\frac{cL_x}{12\pi\beta_H}\frac{\beta_H}{\epsilon} + \frac{cL_x}{288\pi^3\beta_H}\left(\frac{\beta_H}{\epsilon}\right)^3 + O\left(\beta_H^4/\epsilon^4\right) \,. \tag{3.46}$$

Surface term at $U = 0$

This is the AdS Poincaré horizon which is a null surface on which the induced metric h degenerates. Instead we will work with the timelike surface, $U = \delta$, evaluate the GHY term and take the limit, $\delta \to 0$ of the final expression. The metric on this timelike surface, $U = \delta$, is,

$$ds^2 = \frac{1}{f}\left(-dt^2 + dx^2\right) \,. \tag{3.47}$$

The components of the unit outward normal vector for such a constant U surface are:

$$n^U = -\frac{U}{\sqrt{k l_s}} \,, \qquad n^t = n^x = 0 \,. \tag{3.48}$$

Using the Christoffel Symbols:

$$\Gamma^U_{UU} = -\frac{1}{U} \ , \qquad \Gamma^t_{t\rho} = \Gamma^x_{x\,\rho} = -\frac{1}{f}\frac{df}{dU} \ , \tag{3.49}$$

and the unit norma vector (3.48), we get the extrinsic curvature of $U = \delta$ surface,

$$K = -\frac{2}{\sqrt{k}\,l_s\,(1 + \lambda k\delta^2)} \ . \tag{3.50}$$

The GHY surface term at the Poincaré horizon

$$\begin{aligned}
S^0_{GHY} &= \lim_{\delta \to 0} \frac{1}{8\pi G_N} \int dx \int_{t_-(\delta)}^{t_+(\delta)} dt \, \sqrt{-\gamma(\delta)}\, e^{-2(\Phi - \Phi_0)}\, (K - 4n^\rho \partial_\rho \Phi) \\
&= \lim_{\delta \to 0} \frac{2\,L_x}{8\pi G_N}\, k\delta^2 \left(\frac{-2 - 4\lambda k\delta^2}{1 + \lambda k\delta^2}\right) \int_\delta^{l_s/\epsilon} \frac{dU'}{U}\sqrt{f(U)} = 0 \ .
\end{aligned} \tag{3.51}$$

Action Contributions from the null boundaries of the WdW patch

The null boundaries of the WdW patch are defined by

$$(t - T) = \mp\sqrt{k}\,l_s A(U) \ ; \quad \text{where} \quad A(U) \equiv \int_{l_s/\epsilon}^U dU'\frac{dU'\sqrt{f(U')}}{U'} \ ; \tag{3.52}$$

where T is defined in (4.36). However, we will deform the pair of null surfaces to a single smooth timelike surface by introducing a dimensionless parameter, ε,[9]

$$\frac{(t - T)^2}{k\,l_s^2} - (1 + \varepsilon)A^2(U) = 0 \ . \tag{3.53}$$

Taking differentials of both sides leads to,

$$\frac{dt^2}{f} = (1 + \varepsilon)\frac{k\,l_s^2 dU^2}{U^2} \ . \tag{3.54}$$

Using (4.106), the induced metric on this timelike surface can be written as

$$ds^2 = \frac{1}{f^2}(-dt^2 + dx^2) + \frac{k\,l_s^2}{U^2}dU^2 = -\frac{\varepsilon\,k\,l_s^2}{U^2}dU^2 + \frac{1}{f^2}dx^2 \ . \tag{3.55}$$

The negative sign in the first term clearly indicates that this is a timelike surface. The unit outward normals to the surface (4.105) are,

$$n^t = -\frac{t - T}{\sqrt{(1 + \varepsilon)^2 A^2(U) - \frac{(t-T)^2}{k\,l_s^2}}}\frac{\sqrt{f(U)}}{\sqrt{k}l_s}, \quad n^U = -\frac{(1 + \varepsilon)A(U)}{\sqrt{(1 + \varepsilon)^2 A^2(U) - \frac{(t-T)^2}{k\,l_s^2}}}\frac{U}{\sqrt{k}l_s} \ , \quad n^x = 0 \ . \tag{3.56}$$

The trace of the extrinsic curvature

$$K \equiv \nabla_L n^L = \partial_L n^L + \Gamma^L_{LM} n^M = \partial_t n^t + \partial_U n^U + \Gamma^L_{LU} n^U \ . \tag{3.57}$$

---

[9]This is distinct from the UV regulator, ϵ.

takes the form

$$K = \frac{2}{\sqrt{\varepsilon}\sqrt{k}l_s(1 + \lambda k U^2)} . \tag{3.58}$$

Thus the GHY term for this surface in the null limit ($\varepsilon \to 0$) is

$$
\begin{aligned}
S_{GHY}^{\partial W dW} &= \lim_{\varepsilon \to 0} \frac{1}{8\pi G_N} \int d^2 X e^{-2(\Phi - \Phi_0)} \sqrt{-\gamma} \left[K - 4n^M \partial_M \Phi \right] \\
&= \frac{L_x k}{4\pi G_N} \int_0^{l_s/\epsilon} dU\, U\, \frac{2\lambda + \frac{1}{kU^2}}{\sqrt{f}} = \frac{cL_x}{12\pi^2 \beta_h} \frac{\beta_H^2}{\epsilon^2} \sqrt{1 + 4\pi^2 \frac{\epsilon^2}{\beta_H^2}} .
\end{aligned}
\tag{3.59}
$$

In the UV, $S_{GHY}^{\partial W dW}$ diverges as

$$\lim_{\epsilon/\beta_H \ll 1} S_{GHY}^{\partial W dW} = \frac{cL_x}{12\pi^2 \beta_h} \frac{\beta_H^2}{\epsilon^2} + \frac{cL_x}{6\beta_H} + O\left(\epsilon^2/\beta_H^2\right) . \tag{3.60}$$

In the IR one can write

$$\lim_{\epsilon/\beta_H \gg 1} S_{GHY}^{\partial W dW} = \frac{cL_x}{6\pi \beta_H} \frac{\beta_H}{\epsilon} + \frac{cL_x}{48\pi^3 \beta_H} \left(\frac{\beta_H}{\epsilon}\right)^3 + O\left(\beta_H^4/\epsilon^4\right) . \tag{3.61}$$

Full Action complexity at zero temperature

Putting together all the pieces, the full on-shell action over the WdW patch is obtained by summing over the contributions (4.93),(4.95),(4.98),(4.101),(3.51) and (4.111). The full action complexity (4.86) thus obtained is presented in figure 3.3. In the UV linear dilaton regime (i.e. when
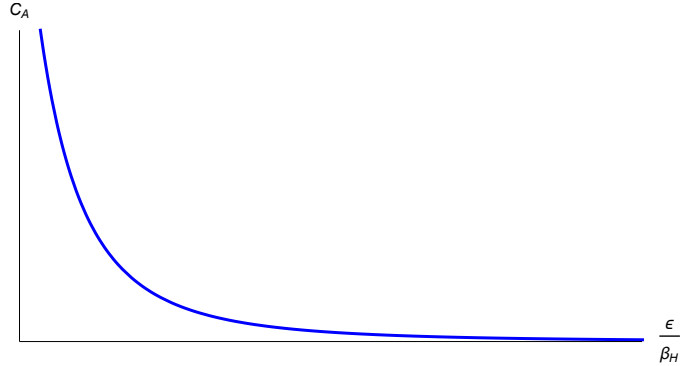
Figure 3.3: $C_{\mathcal{A}}(\epsilon/\beta_H)$ vs ϵ/β_H at $T = 0$.

$\epsilon/\beta_H \ll 1$), the action complexity (obtained by summing over the contributions (4.94),(4.96), (4.99),(3.51),(4.102), and (4.112),) diverges as

$$C_{\mathcal{A}} = \frac{L_x c}{3\pi^2 \beta_H} \left[\frac{\beta_H^2}{2\pi \epsilon^2} - 2\pi \log\left(\frac{\beta_H}{\pi \epsilon}\right) + \pi + O\left(\frac{\epsilon}{\beta_H}\right) \right] . \tag{3.62}$$

Comparison of (6.2) with the volume complexity expression (4.43) reveals that the leading divergence structure (i.e. the quadratic divergent term) and the constant term in both cases are identical. The subleading logarithmic divergences differ by a negative sign. This is not a novel observation. Past studies have revealed that the coefficients of the subleading divergent pieces might be

different [75] hinting to the fact that the two bulk/holographic prescriptions of complexity might actually correspond to different schemes of defining complexity in the boundary field theory. In the IR (i.e. when $\epsilon/\beta_H \gg 1$) the action complexity takes the form

$$\lim_{\epsilon/\beta_H \gg 1} C_{\mathcal{A}} = \frac{cL_x}{18\pi^3\beta_H}\left(\frac{\beta_H}{\epsilon}\right)^2 + O\left(\beta_H^5/\epsilon^5\right) \; . \tag{3.63}$$

Thus in pure AdS_3 the action complexity goes to zero. This is in precise agreement with the analysis performed in [74]. Unlike the volume complexity, the action complexity in $\mathcal{M}_3$ decreases much faster. A comparison between volume complexity and action complexity in $\mathcal{M}_3$ is given in figure 4.7. Similar to the volume complexity, the action complexity diverges in the UV (when
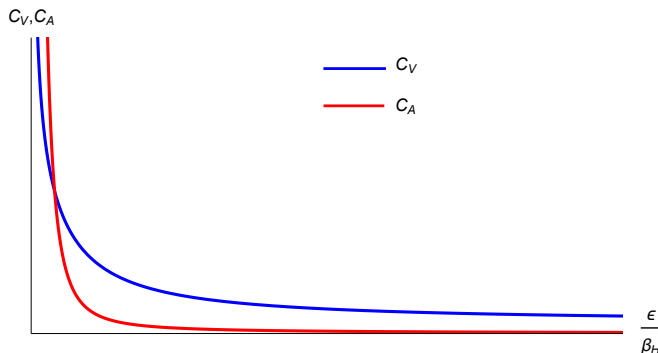
Figure 3.4: Comparison between C_V and $C_{\mathcal{A}}$ at zero temperature. For large ϵ/β_H, the action complexity decays much faster than volume complexity.

$\epsilon/\beta_H \to 0$). Then as ϵ/β_H increases, the action complexity decreases (much faster than volume complexity) monotonically eventually going to 0 in the deep IR.

3.4 Holographic Complexity in $\mathcal{M}_3$ at finite temperature

In this section, we compute the holographic complexity for LST at finite temperature. Our main aim is to look for new exotic divergence structures which do not arise in the zero temperature case and are endemic to finite temperatures exclusively. Although we have a good idea of what kind of finite temperature corrections one generates for complexity of *local* quantum field theories and there we can rule out appearance of such exotic new divergences for finite temperatures, there is hardly such intuition for the case of nonlocal quantum field theories such as LST. In particular, we will be content by computing the action complexity as the integrals that can be performed numerically very easily without any approximations. Volume complexity on the other hand is a different story, the equations for the maximal volume slice are nonlinear and we could hope to solve (even numerically) perturbatively only in simple limits such as high temperatures or low temperatures. Instead of making such simplifying assumptions, we have decided to compute the action complexity exactly and evaluate the integrals numerically. For this finite temperature case one has to use the finite temperature $\mathcal{M}_3$ background (3.8). In particular, we consider the thermofield double state of two LST's for which the dual bulk geometry is an eternal $\mathcal{M}_3$ black hole. An important thing to note is the geometry here is that of the two-sided eternal hole with four quadrants - right (I), future (II), left (III) and past (IV) wedges. The future wedge (II) is the region between the inner and the outer horizons. The Penrose diagram of the finite temperature $\mathcal{M}_3$ spacetime with the WdW patch is displayed in figure 3.5. Although we denote the four
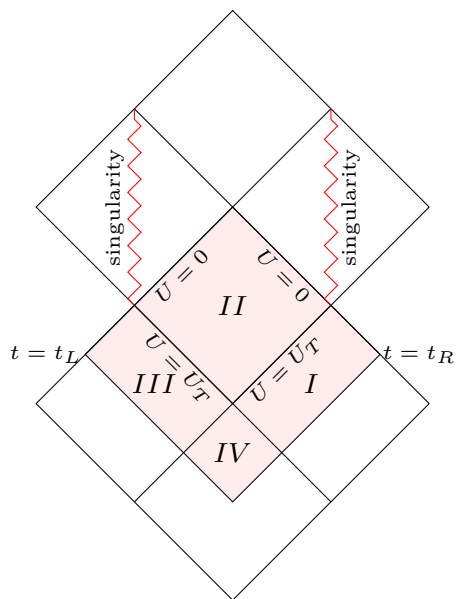
Figure 3.5: Penrose diagram of the eternal $\mathcal{M}_3$ black hole geometry with the Wheeler-deWitt (WdW) patch shaded in pink for the boundary time t_L and t_R.

wedges of the eternal black hole by I, II, III, IV precisely in the sense discussed above, in the discussion that follows, we will refer to the four section obtained by taking an intersection of the WdW patch with the full two-sided eternal hole as regions I, II, III, IV.

So in the zero temperature limit of this two-sided geometry, one will get *twice* the action complexity value for that of the single sided zero temperature geometry. The Wheeler-deWitt patch for the eternal geometry is anchored at the Schwarzschild times, t_R in the right quadrant and t_L in the left quadrant. Of course in terms of boundary time coordinate, the left quadrant time is then, $-t_L$. We also consider the case when $t_L = -t_R = t$ is very large, since in this case the past wedge, quadrant IV pinches off and its contribution to the complexity the vanishes. Also it is worth mentioning that since the metric in left and right wedges I and III are time-independent and has reflection symmetry around $t = 0$, the complexity contributions from the left and right are identical and independent of t_R or t_L. The action complexity contributions at finite temperature (two sided $\mathcal{M}_3$ black hole) are worked out in the following subsections, first the contributions from the bulk (volume) of the WdW patch followed by contributions from the surface/edges of the WdW patch. The results are then plotted in the figure 3.6. We find the finite temperature complexity qualitatively displays similar monotonic behavior as a function of ϵ/β_H and that there are no new exotic divergence structures appearing up to second order in finite temperature corrections ($O\left(U_T^2\right)$) in action complexity (see Appendix A).

3.4.1 Action complexity at finite temperature

Bulk terms for finite temperature action complexity

The bulk action (3.29) consists of four types of contributions, namely from the Ricci scalar term, from the cosmological constant term, the dilaton kinetic term and the NS-NS H-field strength term. We will write the metric in infalling null coordinate v and radial coordinate r which are well defined in the quadrants I and II (see figure 3.5). In terms of these the (string frame) metric

in quadrants I and II looks like

$$ds^2 = -\frac{f_1}{f} dv^2 + \frac{2\sqrt{k}\, l_s}{\sqrt{f}\, U} dv\, dU + \frac{dx^2}{f} \ . \tag{3.64}$$

The v coordinate is related to the Schwarzschild coordinates, t, U by the relation:

$$v = t + U_* \ , \tag{3.65}$$

where the (UV regularized) tortoise coordinate, $U_*(U)$ is defined by

$$U_* = \begin{cases} \int_{\frac{l_s}{\epsilon}}^{U} dU' \frac{\sqrt{k}l_s}{f_1(U')} \frac{\sqrt{f(U')}}{U'}, & \text{region } I \ , \\ \int_0^U dU' \frac{\sqrt{k}l_s}{-f_1(U')} \frac{\sqrt{f(U')}}{U'}, & \text{region } II. \end{cases} \tag{3.66}$$

Of course these coordinates do not cover the left wedge III or the past region IV. However, since the metric in region III is time-independent (and time-reflection symmetric), it turns out that the contribution from III is exactly equal to that of region I. As mentioned before we are looking at large / late times, $t_R = -t_L = t \to \infty$, in this limit the wedge IV pinches off and there is no contribution from it. Here are the list of the bulk term contributions to the action complexity.

The Ricci scalar term:
The Ricci scalar term in the supergravity action in region I contributes

$$\begin{aligned} S_R^I &= \frac{L_x}{16\pi\, G_N} \int_{U_T}^{\frac{l_s}{\epsilon}} dU \int_{t_R+2U_*(U)}^{t_R} dv \sqrt{-g}\, e^{-2(\Phi-\Phi_0)} R \\ &= \frac{L_x k^{\frac{1}{2}}}{8\pi\, G_N} \int_{U_T}^{\frac{l_s}{\epsilon}} dU U \left(\frac{2U_T^2 k\lambda\,(2k\lambda U^2 - 5) + 8k\lambda U^2 - 6}{(k\lambda U^2 + 1)^2} \right) \left(\int_U^{\frac{l_s}{\epsilon}} dU' \frac{\sqrt{\lambda k U'^2 + 1}}{(U'^2 - U_T^2)} \right) \ . \end{aligned} \tag{3.67}$$

Owing to the symmetry between region I and III in the Penrose diagram, the region III integrals give same contribution as region I with just the change $t_R \Longleftrightarrow t_L$ interchange. Since, anchorage time does not feature in the integrals involving regions outside the outer horizon, we simply the exact same contribution from the region III. Therefore,

$$S_R^{III} = S_R^I \ . \tag{3.68}$$

Next, the contribution coming from region II is given by

$$\begin{aligned} S_R^{II} &= \frac{L_x}{16\pi\, G_N} \int_0^{U_T} dU \int_{t_L+2U_*(U)}^{t_R} dv \sqrt{-g}\, e^{-2(\Phi-\Phi_0)} R \\ &= \frac{L_x k^{\frac{3}{2}} l_s}{16\pi\, G_N} \int_0^{U_T} dU U \left(\frac{2U_T^2 k\lambda\,(2k\lambda U^2 - 5) + 8k\lambda U^2 - 6}{kl_s^2\,(k\lambda U^2 + 1)^2} \right) \left(t_R - t_L - 2l_s \int_0^U dU' \frac{\sqrt{\lambda k U'^2 + 1}}{(U'^2 - U_T^2)} \right). \end{aligned} \tag{3.69}$$

The contribution from S_R^{II} trivially goes to zero in the limit $U_T \to 0$. In the late times limit, there is no contribution from region IV since it gets pinched off.

The cosmological constant term:
This term is particularly simple since it is proportional to the volume of the WdW patch. The contribution to the onshell action from regions outside the horizons (region I, III) is

$$\begin{aligned} S_\Lambda^I &= \frac{4L_x}{16\pi k l_s^2\, G_N} \int_{U_T}^{\frac{l_s}{\epsilon}} dU \int_{t_R+2U_*(U)}^{t_R} dv \sqrt{-g}\, e^{-2(\Phi-\Phi_0)} \\ &= \frac{4L_x k^{\frac{1}{2}}}{16\pi l_s\, G_N} \int_{U_T}^{\frac{l_s}{\epsilon}} dU U \left(-2l_s \int_{\frac{l_s}{\epsilon}}^{U} dU' \frac{\sqrt{\lambda k U'^2 + 1}}{(U'^2 - U_T^2)} \right) \ . \end{aligned} \tag{3.70}$$

As argued before $S_\Lambda^{III} = S_\Lambda^I$. The contribution to the volume of the WdW patch from inside the horizon region namely region II is given by

$$S_\Lambda^{II} = \frac{4L_x k^{\frac{1}{2}}}{16\pi l_s G_N} \int_0^{U_T} dU U \left(t_R - t_L - 2l_s \int_0^U dU' \frac{\sqrt{\lambda k U'^2 + 1}}{(U'^2 - U_T^2)} \right) . \tag{3.71}$$

As expected the S_Λ^{II} vanishes in the limit $U_T \to 0$ and for large t_R, $S_\Lambda^{IV} \to 0$.

The Dilaton kinetic term:

The dilaton kinetic term in the supergravity action coming from region I is given by:

$$\begin{aligned}
S_\Phi^I &= \frac{4L_x}{16\pi G_N} \int_{U_T}^{\frac{l_s}{\epsilon}} dU \int_{t_R + 2U_*(U)}^{t_R} dv \sqrt{-g} e^{-2(\Phi - \Phi_0)} g^{\mu\nu} \partial_\mu \Phi \partial_\nu \Phi \\
&= \frac{L_x k^{\frac{5}{2}} \lambda^2}{2\pi G_N} \int_{U_T}^{\frac{l_s}{\epsilon}} dU \left(\frac{U^5}{(k\lambda U^2 + 1)^2} - \frac{U^3 U_T^2}{(k\lambda U^2 + 1)^2} \right) \left(\int_U^{\frac{l_s}{\epsilon}} dU' \frac{\sqrt{\lambda k U'^2 + 1}}{(U'^2 - U_T^2)} \right) .
\end{aligned} \tag{3.72}$$

The contribution from the region III is same is that of region I namely $S_\Phi^{III} = S_\Phi^I$. The contributions from the region II inside the horizon in this case is

$$S_\Phi^{II} = \frac{4L_x k^{\frac{3}{2}} l_s}{16\pi G_N} \int_0^{U_T} dU U \left(\frac{k^2 \lambda^2 U^2 (U^2 - U_T^2)}{l_s^2 (k\lambda U^2 + 1)^2} \right) \left(t_R - t_L - 2l_s \int_0^U dU' \frac{\sqrt{\lambda k U'^2 + 1}}{(U'^2 - U_T^2)} \right) . \tag{3.73}$$

As a check one can see that $S_\Phi^{II} \to 0$ as $U_T \to 0$ and for late time t_R, $S_\Phi^{IV} \to 0$.

The Kalb-Ramond term:

The contribution to action complexity from the Kalb-Ramond term in region I is given by:

$$\begin{aligned}
S_H^I &= -\frac{L_x}{12 \times 16\pi G_N} \int_{U_T}^{\frac{l_s}{\epsilon}} dU \int_{t_R + 2U_*(U)}^{t_R} dv \sqrt{-g} e^{-2(\Phi - \Phi_0)} H^2 \\
&= -\frac{L_x}{4\pi G_N k^{\frac{3}{2}}} \int_{U_T}^{l_s/\epsilon} \frac{dU}{U^3 f^2} \left(\int_{\frac{l_s}{\epsilon}}^U dU' \frac{\sqrt{\lambda k U'^2 + 1}}{(U'^2 - U_T^2)} \right) .
\end{aligned} \tag{3.74}$$

The contribution from the region II interior to the future horizon is,

$$S_H^{II} = \frac{L_x}{8\pi G_N k^{\frac{3}{2}} l_s} \int_0^{U_T} \frac{dU}{U^3 f^2} \left(t_R - t_L - 2l_s \int_0^U dU' \frac{\sqrt{\lambda k U'^2 + 1}}{(U'^2 - U_T^2)} \right) . \tag{3.75}$$

Again, predictably this inside horizon contribution vanishes in the zero temperature limit. Finally, the contribution from region III is identical to that of region I $S_H^{III} = S_H^I$. For large t_R, $S_H^{IV} \to 0$.

GHY term for the null boundaries of the WdW patch

Let's first consider the right boundaries of the null WdW patch defined by the equations

$$v = t_R \qquad \text{(future)} \quad \& \quad v - 2U_* = t_R \qquad \text{(past)} , \tag{3.76}$$

where U_* is the tortoise coordinate for the outside horizon region (region I) (3.66). In region I, these two null boundaries can be combined and deformed into a continuous timelike surface defined by equation

$$\frac{(t - t_R)^2}{k l_s^2} - (1 + \varepsilon) A^2(U) = 0 , \quad \text{where} \quad A(U) = \int_{l_s/\epsilon}^U dU' \frac{\sqrt{f(U')}}{U' f_1(U')} . \tag{3.77}$$

where ε is the deformation parameter which when sent to zero, takes the above timelike surface into a pair of null surfaces.[10] Note that by definition, $A(U) < 0$. Let us denote this surface by Γ. The induced metric on the deformation surface Γ is given by

$$ds^2 = -\varepsilon \frac{kl_s^2}{f_1 U^2} dU^2 + \frac{dx^2}{f} \ . \tag{3.78}$$

Hence,

$$dx \, dU \, \sqrt{-\gamma} \, e^{-2(\Phi - \Phi_0)} = \sqrt{\varepsilon} k^{3/2} l_s dx \, dU \, U \sqrt{\frac{f}{f_1}} \tag{3.79}$$

where γ denotes the determinant of the induced metric on the surface Γ. Next, we compute the trace of the extrinsic curvature of the surface (3.77). The components of the unit outward normal are

$$n^t = -\frac{t - t_R}{\sqrt{k} \, l_s \sqrt{(1 + \varepsilon)^2 \, A^2 - \frac{(t - t_R)^2}{kl_s^2}}} \sqrt{\frac{f}{f_1}} \ ,$$

$$n^U = -\frac{(1 + \varepsilon) \, U \, A}{\sqrt{k} \, l_s \sqrt{(1 + \varepsilon)^2 \, A^2 - \frac{(t - t_R)^2}{kl_s^2}}} \sqrt{f_1} \ , \tag{3.80}$$

$$n^x = 0 \ .$$

Using the above information one can write

$$\left(K - 4n^U \partial_U \Phi \right)\Big|_\Gamma = 2 \frac{1 + 2\lambda k U^2}{1 + \lambda k U^2} \frac{\sqrt{f_1}}{\sqrt{k} \, l_s \sqrt{\varepsilon}} + \frac{1}{\sqrt{k} \, l_s \sqrt{\varepsilon}} \frac{1}{\sqrt{f_1}} \frac{U_T^2}{U^2} \ . \tag{3.81}$$

Thus the GHY term contribution from the right null boundary in region I is given by

$$\begin{aligned} S_{GHY}^{\partial W dW I} &= \frac{1}{8\pi G_N} \int d^2X \, \sqrt{-\gamma} \, e^{-2(\Phi - \Phi_0)} \left(K - 4n^U \partial_U \Phi \right)\Big|_\Gamma \\ &= \frac{L_x \, k}{4\pi G_N} \int_{U_T}^{ls/\epsilon} dU \, U \frac{2\lambda + \frac{1}{kU^2}}{\sqrt{f}} + \frac{L_x \, k}{8\pi G_N} U_T^2 \int_{U_T}^{ls/\epsilon} dU \frac{\sqrt{f}}{U f_1} \ . \end{aligned} \tag{3.82}$$

Evidently, when one sets $U_T = 0$, this reduces precisely to the GHY contribution for the zero temperature case for the right null boundary of WdW patch (4.111), One can exactly evaluate the integral (3.82) to obtain

$$\begin{aligned} S_{GHY}^{\partial W dW I} &= \frac{L_x \, k}{4\pi G_N} \left(\sqrt{\lambda} \frac{l_s^2}{\epsilon^2} + \frac{1}{2k\sqrt{\lambda}} - U_T^2 \sqrt{f \, (U_T)} \right) \\ &+ \frac{L_x \, k}{8\pi G_N} U_T^2 \left(\sqrt{\lambda} \ln \left(\frac{2\sqrt{\lambda k} l_s}{\epsilon} \right) + \sqrt{f \, (U_T)} \ln \left(\sqrt{1 + \lambda k U_T^2} - \sqrt{\lambda k} U_T \right) \right) \\ &- \frac{L_x \, k}{8\pi G_N} U_T^2 \left(\sqrt{\lambda} \sinh^{-1} \left(\sqrt{\lambda k} U_T \right) - \frac{\sqrt{f \, (U_T)}}{2} \lim_{U \to U_T^+} \ln \left(\frac{2U_T \, (1 + \lambda k U_T^2)}{U - U_T} \right) \right) \ . \end{aligned} \tag{3.83}$$

---

[10]This "null-to-timelike" deformation parameter ε is in principle independent of the UV regulator ϵ, but can be chosen, without inconsistency to be equal to ϵ (see [75]).

Next, we evaluate the GHY contribution from the part of the right null boundary of the WdW patch from within the horizon in region II. In this case it is simpler to work with the deformed timelike surface

$$t_R - t = (1 - \delta) \sqrt{k} \, l_s \, B(u) \, , \qquad \text{where} \qquad B(u) \equiv \int_0^U \frac{dU' \sqrt{f(U')}}{U' (-f_1(U'))} \, . \qquad (3.84)$$

The induced metric on the right null boundary of the WdW patch is

$$ds^2 = -2\delta \frac{kl_s^2}{U^2 (-f_1)} dU^2 + \frac{dx^2}{f} \, . \qquad (3.85)$$

The unit outward normal is given by

$$n^t = \frac{1}{\sqrt{2\delta}} \sqrt{\frac{f}{-f_1}}, \qquad n^U = \frac{(1 - \delta) \, U \sqrt{-f_1}}{\sqrt{2\delta} \, \sqrt{k} \, l_s}, \qquad n^x = 0 \, . \qquad (3.86)$$

The full integrand of the GHY term is

$$K - 4n^L \partial_L \Phi = \frac{1}{\sqrt{2\delta}\sqrt{k} \, l_s} \left(-\frac{1}{\sqrt{-f_1}} \frac{U_T^2}{U^2} + 2 \left(\frac{1 + 2\lambda kU^2}{1 + \lambda kU^2} \right) \sqrt{-f_1} \right) . \qquad (3.87)$$

Thus, the GHY term contribution from the right null boundary of the WdW patch in region II is

$$
\begin{aligned}
S_{GHY}^{\partial WdW_R II} &= \frac{1}{8\pi G_N} \int d^2X \, \sqrt{-\gamma} \left(K - 4n^L \partial_L \Phi \right) \\
&= -\frac{L_x k}{8\pi G_N} U_T^2 \left(\frac{\sqrt{f(U_T)}}{2} \lim_{U \to U_T^-} \ln \left(\frac{U_T (1 + \lambda kU_T^2)}{U_T - U} \right) - \sqrt{\lambda} \sinh^{-1} \left(\sqrt{\lambda k} U_T \right) \right) \\
&\quad + \frac{L_x k}{4\pi G_N} U_T^2 \sqrt{f(U_T)} \, .
\end{aligned} \qquad (3.88)
$$

Thus summing the contributions from both outside and inside the horizon, (3.83) and (3.88) we obtain the GHY type contributions to action from the right null boundary of the WdW patch as

$$
\begin{aligned}
S_{GHY}^{\partial WdW_R} &= \frac{L_x \, k}{8\pi G_N} U_T^2 \left(\sqrt{\lambda} \ln \left(\frac{2\sqrt{\lambda k} l_s}{\epsilon} \right) + \sqrt{f(U_T)} \ln \left(\sqrt{1 + \lambda kU_T^2} - \sqrt{\lambda k} U_T \right) \right) \\
&\qquad\qquad + \frac{L_x \, k}{4\pi G_N} \left(\sqrt{\lambda} \frac{l_s^2}{\epsilon^2} + \frac{1}{2k\sqrt{\lambda}} \right) \, .
\end{aligned} \qquad (3.89)
$$

Joint contributions for the intersection of null boundaries of WdW patch

Here we compute the contribution to the action (complexity) supported on the joint or edge along which the null boundaries of the WdW patch intersects. The future boundaries of the WdW patch are along the inner horizon, $U = 0$ (refer to figure 3.5). Since we have deformed the null boundaries of the WdW to timelike and we take the null limit only at the very end, we are considering a joint of two timelike surfaces along $U = 0$. The right future null boundary has been deformed to a timelike surface (3.87) with the unit outward normal given in (3.86). Analogously the left future null boundary of the WdW patch, namely, $t - t_L = U_*$ can be deformed to timelike,

$$t - t_L = (1 - \delta)\sqrt{k} l_s B(U) \qquad (3.90)$$

67

where $B(U)$ has already been defined in eq. (3.87). The unit outward normal for this timelike deformed boundary is,

$$\bar{n}_t = \frac{1}{\sqrt{2\delta}}\sqrt{\frac{-f_1}{f}}, \quad \bar{n}_U = -\frac{1-\delta}{\sqrt{2\delta}}\frac{\sqrt{k}l_s}{U\sqrt{-f_1}}, \quad \bar{n}_x = 0. \tag{3.91}$$

From the expression of the unit outward normals (3.86) and (3.91), it is evident that, $n.\bar{n} = 1$ and hence

$$\ln|n.\bar{n}| = 0. \tag{3.92}$$

Thus the joint contribution (evaluated in the Einstein frame) vanishes,

$$S^{U=0}_{\cap \partial W\, dW} = \frac{1}{8\pi G_N}\int dx \lim_{U\to 0}\left(\sqrt{\tilde{g}_{xx}}\ln|n.\bar{n}|\right) = 0. \tag{3.93}$$

because $\lim_{U\to 0}\sqrt{\tilde{g}_{xx}} \to \frac{\sqrt{k}U}{g_s^2}$. Here $\tilde{g}$ denotes the Einstein frame metric, $\tilde{g} = e^{-4(\Phi-\Phi_0)}g$.

Full Action complexity at finite temperature

Thus the full action complexity for the finite temperature case in the late time limit, is given by gathering together contributions from regions $I, II, \& III$ (with the contributions from region III being identical to those from region I),

$$C_{\mathcal{A}} = \frac{1}{\pi\hbar}\left(2S^I_R + S^{II}_R + 2S^I_\Lambda + S^{II}_\Lambda + 2S^I_\Phi + S^{II}_\Phi + 2S^I_H + S^{II}_H + S^{\partial W\, dW_R}_{GHY} + S^{\partial W\, dW_L}_{GHY} + S^{U=0}_{\cap\partial W\, dW}\right). \tag{3.94}$$
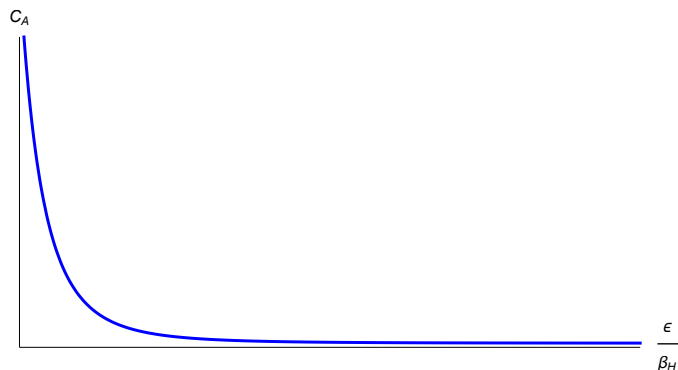
Figure 3.6: $C_{\mathcal{A}}(\epsilon/\beta_H)$ vs ϵ/β_H at finite temperature $(T_{bh}/T_H = 0.1)$.

Figure 3.6 shows the plot of action complexity at finite temperature as a function of ϵ/β_H. As in the case of zero temperature, the action complexity monotonically decreases from the UV to the IR. In Appendix A we have performed the asymptotic analysis of the action complexity term by term perturbatively in finite temperature up to second order $O(U_T^2)$ to extract the UV divergence structure. Turning on a finite temperature doesn't give rise to new exotic temperature dependent divergences (at least up to second order in U_T^2) that go away in the zero temperature limit at least up to second order in U_T. This is perhaps expected from the physical insight that the finite temperature introduces a horizon deep inside but does not change the asymptotic structure of the geometry and hence no new UV divergences are not expected to appear at finite temperature.

3.5 Discussion & Outlook

In this chapter, we studied string theory in the background that interpolates between AdS_3 in the IR to flat spacetime with a linear dilaton in the UV both at zero (4.6) and at finite temperature (3.8). We studied holographic complexity using the CV and CA conjecture in this background and investigated the effects of non-locality of LST through the lenses of holographic complexity. Here is a summary of our findings:

- At zero temperature, both the volume and action complexities are UV divergent and hence manifestly regulator dependent. In the regime where the UV cutoff (lattice spacing) is shorter than the Hagedorn scale of the LST, the leading piece diverges *quadratically* with the UV cutoff (4.43). We identify this quadratic divergence as the characteristic signature of non-local nature of the LST. Modulo an overall factor ambiguity (which is well known in the literature) the leading divergences for both complexities (volume and action) agree and have the same sign.

- There are subleading logarithmic divergences in both volume complexity (4.43) and action complexity expressions (6.2) which have the same magnitude but differ in sign. The universal coefficient (4.45) of this log divergent term can be interpreted as the total number of degrees of freedom in the LST with the Hagedorn scale, β_H treated as the lattice spacing.

- In the opposite regime, when the UV cutoff is much larger than the Hagedorn scale, the volume complexity expression expectedly reduces to that of a local field theory having linear divergence (corresponding to a single spatial dimension) (4.44). In fact this expression matches that of a CFT with the central charge equal to the Brown-Henneaux expression derived from a pure AdS_3 calculation. Similarly, in this limit the action complexity too reproduces the expected pure AdS_3 answer (4.114) [74, 73].

- At finite temperature we computed the action complexity since it can be computed exactly (numerically) without any approximations. The finite temperature complexity displays the same qualitative features as that of the zero temperature case, in particular it monotonically decrease with ϵ/β_H. We do not find any new exotic divergences at finite temperature compared to the zero temperature case, at least perturbatively up to second order in finite temperature corrections.

The leading divergence of both the volume and the action complexity, at short distances, goes as inverse of the square of the short distance cutoff scale ($C_{V,\mathcal{A}} \sim 1/\epsilon^2$). A striking feature of the above fact is that LST visualized as a six-dimensional theory on NS5/M5 in type IIA/M-theory, will also exhibit the same quadratic (leading) and logarithmic (subleading) divergences. This is due to the fact that the two-dimensional LST we are interested in can be thought of as a T^4 compactification of the six-dimensional LST. Such a six dimensional LST (in type IIA theory) flows to a fixed point in the IR, the so called six-dimensional $(2, 0)$ SCFT. The complexity of this SCFT$_6$ (unlike CFT$_2$/SCFT$_2$) has a leading divergence that goes like V_5/ϵ^5 [73, 74] (as opposed to $1/\epsilon$ in the case of CFT$_2$), where V_5 is the five dimensional spacial volume of the manifold on which the CFT$_6$ lives . For $\epsilon/\beta_H \ll 1$, the sub-leading divergence in both complexities (volume and action) turn out to be a log term. Once again, the presence of the log term is another signature of non-locality. In fact the absolute value of the log term can be considered as an effective number of degrees of freedom, cL_x/β_H of the system provided we treat β_H as the lattice spacing of the theory. It would be interesting to understand a precise relationship between the coefficient

of the log term and the regularized[11] degrees of freedom of LST. The coefficient of the log term comes with opposite signs in the volume and action complexity. It would also be nice to have a more physical understanding of this discrepancy.

The analysis of holographic Wilson loop [104], holographic entanglement entropy [103, 128, 129, 106] and thermodynamics [105, 119] in $\mathcal{M}_3$ naturally reveals the non-locality scale through some pathologies in the physical observables. For example, the free energy and the entropic c-function diverges as the RG scale approaches the non-locality scale of LST. The partition function in the thermodynamic limit develops a branch cut singularity as the temperature approaches the Hagedorn temperature of LST. In our analysis of holographic complexity, we didn't come across such pathologies. We believe that such a pathology will be encountered in the analysis of subregion complexity. It would be interesting to do the exercise of subregion complexity to verify this fact. Recently, some progress has been made in understanding a solvable irrelevant deformation of a CFT$_2$ by a Lorentz symmetry breaking operator that goes in the name of $J\bar{T}$ deformation [130, 115]. Single trace $J\bar{T}$ deformation has been studied in [115, 131] with further generalizations studied in [114, 124]. It would be interesting to understand the holographic complexity in these more general setups. Since the presence of $J\bar{T}$ deformation breaks Lorentz invariance, it would be interesting to understand its effect on volume and action complexity. This comprises of our aim in the next chapter, where we try to quantify the additional effects of lorentz violation in the divergence structure of the complexity.

---

[11]We call it "regularized" degrees of freedom because the actual number of degrees of freedom of LST is infinite [127, 103].

Chapter 4

Holographic Complexity of LST and Single Trace $T\bar{T}$, $J\bar{T}$ and $T\bar{J}$ Deformations

4.1 Introduction

In a previous chapter constituting the content of [132] we focused our attention on the decoupled regime of the theory of a stack of large number ($k \gg 1$) of NS5 branes wrapping $T^4 \times S^1$, the so called Little String theory (LST) in $1+1$ dimensions. This system is unlike the theory of a stack of Dp branes, since the worldvolume theory living on the NS5 branes decouples from the bulk at *finite* value of the string length $l_s = \sqrt{\alpha'}$. This implies that this decoupled theory, namely LST living on the NS5 branes, still retains stringy nonlocality and is *not* a local quantum field theory. In fact this decoupled theory living on the NS5 branes is to some extent intermediate between string theory (which is nonlocal theory containing massless gravitons) and a local QFT. The dual holographic background is then obtained by taking the near horizon geometry of the NS5 branes - it is a metrically flat spacetime with a linear dilaton $\mathbb{R}^{1,1} \times \mathbb{R}_\phi$ turned on all the way to spatial infinity. Such a holographic duality has been studied quite extensively in the past [97, 98]. Now if one introduces $p \gg 1$ F1 strings wrapping a S^1 along the NS5 directions, the near horizon geometry of the F1 strings is given by AdS$_3$. Thus the full geometry interpolates between AdS$_3$ in the IR (which corresponds to the near horizon geometry of the F1 strings) to flat spacetime with a linear dilaton in the UV (which corresponds to the near horizon geometry of just the NS5 branes). Correspondingly, the boundary field theory interpolates between a local CFT$_2$ dual to AdS$_3$ in the IR to LST in the UV. The interpolating geometry discussed above is often referred to in the literature as $\mathcal{M}_3$. In the wake of the recent developments in the subject of $T\bar{T}$ deformation [99, 100], it was proposed in [101] that there exists an analogous deformation of string theory in AdS_3 that shares many properties in common with the double trace $T\bar{T}$ deformation. This is often referred to as the single trace $T\bar{T}$ deformation in the literature which changes the UV asymptotics of the bulk geometry from AdS_3 to flat spacetime with a linear dilaton keeping fix the IR regime of the geometry. Analysis in [101] shows that the dual background geometry interpolates between AdS_3 in the IR to flat spacetime with a linear dilaton in the UV. Holography in this background (often referred to as $\mathcal{M}_3$) can be realized as a concrete example of holography in non-AdS background that is smoothly connected to AdS_3. Naturally this non-AdS holography set up has attracted a lot of attention and there has been a lot of studies where holography has been exploited to investigate various aspects of nonlocal field theories such as LST which admit gravity

71

duals, e.g. [102, 103, 104, 105, 106, 107]. In the previous chapter reporting our recent work [132] we probed this theory using holographic complexity as a probe. There we computed the volume and action complexity, both at zero and finite temperature. The complexity expressions contained imprints of the stringy nonlocality on the UV divergence structure. To be specific, we encountered quadratic and logarithmic divergences, evidently not to be associated with local field theory in 1 space dimension (where we expect a linear divergence) when the UV cutoff is smaller than the (Hagedorn) length scale, $\beta_H = 2\pi l_s \sqrt{k\,\lambda}$, set by the $T\overline{T}$ coupling λ). When the UV cutoff is held larger than the Hagedorn scale, complexity displays a linear UV divergence, much akin to a local field theory in 1 space dimension. For completeness we computed the holographic complexity at finite temperature as well, however no unanticipated newer type of UV divergences were encountered in perturbation theory around zero temperature.

The purpose of this chapter is to extend the our work in [132] constituting the content of the last chapter to a more general linear combination of irrelevant single trace deformations, namely the single trace $T\overline{T}, J\overline{T}$ and $T\overline{J}$ of a CFT$_2$ which contains/involves conserved left (right)-moving current $J(\overline{J})$. These irrelevant deformations drive the UV theory to nonlocality, in the sense that the UV is not a local fixed point as the high energy density of states exhibits a exponential Hagedorn growth [105]. Moreover, the effect of turning on the irrelevant current $J(\overline{J})$ couplings is to explicitly break Lorentz boost symmetry in the UV. The dual gravity (string) background was introduced in [114, 124] which interpolates between AdS$_3$ in the IR to a linear dilaton background in the UV. From the string viewpoint, the UV is the near horizon limit of the stack of k NS5 branes with p F1 strings propagating in the world volume while incorporating NS-NS H-flux along the world volume directions violating Lorentz boost invariance [114, 115, 131]. Our main motivation to investigate this set up is to capture the imprint of Lorentz boost symmetry violation in the holographic complexity, to be specific in the UV divergence structure of holographic complexity. In particular, we are interested in finding out whether the imprints of Lorentz symmetry violation and nonlocality on the UV divergence are separate or different kind. Also since the theory does not respect boost symmetry, we would like to know how the UV divergences in complexity change as we move from one Lorentz frame to another. Another motivation of the present work is to study subsystem holographic complexity [133, 134, 73] which we had omitted in our previous work [132]. Subsystem complexity, just like entanglement entropy of a subsystem's reduced density matrix is expected to display phase transitions as the subsystem size is tuned. In particular, in the work [106], which looked at entanglement entropy of this system, namely the $T\overline{T}, J\overline{T}$ and $T\overline{J}$ deformed CFT$_2$, entanglement entropy undergoes a (Hagedorn) phase transition when the subsystem size is tuned to a critical spatial size determined by the strength of the irrelevant couplings.

The plan of the chapter is as follows. In section 4.2, we give a briefly recap aspects of string theory in AdS_3, its single trace $T\overline{T}, J\overline{T}, T\overline{J}$ deformations and highlight interesting features of LST for the sake of completeness. We also review some features of the dual holographic background (bulk). In this regard we would like to point out that one may work with either a 3+1-dimensional bulk as was done in the works on entanglement entropy [106], or equivalently one can perform a KK reduction on the y circle fiber and work with an effective bulk background in 2+1 dimensions [114]. Here we take the second approach because it affords us performing immediate comparison or checks with our previous work [132] at every step. In section 4.3, we set out to compute the holographic complexity of the $T\overline{T}, J\overline{T}, T\overline{J}$ deformed CFT$_2$ by implementing the CV prescription[1] in two distinct (boundary) Lorentz frames, which we dub as the *stationary frame* and *static*

---

[1]Actually we used a generalized prescription of the volume complexity put forth in our previous work [132] in the string frame since a non-trivial dilaton field turned on in the bulk, and this modification is necessary to get the

frame (for reasons which will become obvious), related to each other by a Lorentz boost. In either frame, the volume complexity diverges quadratically with a subleading logarithmic divergence. However, anticipated, due to lack of boost symmetry, the coefficients of the quadratic and logarithmic divergence differ in the two frames (and even the finite piece differs). We find that the Lorentz violation effects (governed by the parameter $\epsilon_\pm$) and nonlocality effects (governed by the parameter λ) are inextricably linked - the UV divergence structure depends on a *single* parameter, namely $\mu = \lambda - (\epsilon_+ + \epsilon_-)^2$ in the stationary frame, and the parameter $\lambda' \equiv \lambda - 4\epsilon_+\epsilon_-$ in the static frame. There is no way to cleanly separate the effects of nonlocality and Lorentz boost asymmetry. This is perhaps mildly disappointing since our hope was to be able to see the effects of nonlocality and Lorentz violation in separate or independent UV divergence structures. These results are consistent with the results obtained in the previous chapter [132] - setting $\epsilon_\pm = 0$ reproduces the volume complexity of the LST dual to the $\mathcal{M}_3$ geometry. The quadratic and logarithmic divergences of the volume complexity immediately reveals the nonlocal nature of the dual field theory (LST) as for a local theory the complexity is expected to scale with volume $\mathcal{V}$ (here length) and hence should diverge as lattice cell volume inverse $\mathcal{V}/\epsilon^d$. In either frames, the non-locality scale is set by the respective Hagedorn length $\rho_H \propto \sqrt{k\mu}\, l_s$ in the stationary frame and $\beta'_H \propto \sqrt{k\lambda'}\, l_s$ in the static frame. When the lattice spacing is larger than the Hagedorn length scales in the respective frame ($\epsilon \gg \rho_H$ or $\epsilon \gg \beta'_H$), the complexity expression reduces to that of a local field theory with a linear divergence (volume scaling). However if the lattice spacing is shorter than the Hagedorn length scale $\epsilon \ll \rho_H$, or $\epsilon \ll \lambda'_H$, stringy physics takes over and the theory departs from behaving like a local field theory. Finally we note that the logarithmic divergent pieces (subleading divergence) in the complexity expressions in either frame which are accompanied by a dimensionless universal constant coefficient. This coefficient can be given the interpretation of the total number of "regularized/effective" degrees of freedom in the spacetime theory in the nonlocal stringy regime as opposed to the true degrees of freedom of LST which naively diverges [127, 103]. Next in Sec. 4.4, we proceed to evaluate the subregion complexity, in both the stationary and static frames. The exact results for subregion complexity are obtained numerically, and the results are displayed graphically, subregion complexity plotted as function of the subregion size, $\mathcal{C}_V$ vs L for several different choices of the set of parameters $\lambda, \epsilon_\pm$. In either frame, the plots clearly show the Hagedorn phase transition - at a critical subregion size, $L_c = \frac{\pi\sqrt{k\lambda\lambda'}l_s}{2\sqrt{\mu}}$ in the stationary frame and $L'_c = \frac{1}{2}\pi\sqrt{k\lambda}l_s$ in the static frame. For subregion sizes larger than the critical size, the subregion complexity grows linearly with subregion size (length), characteristic of a CFT$_2$ while for subregion sizes lower than the critical subregion length, subregion complexity grows quadratically with subsystem size (length), which is more like a nonlocal LST. The reason we identify this transition as the Hagedorn transition because the critical length, read off from the numerics (plot), is identical to the phase transition point of entanglement entropy [106]! The fact that the critical length is different in the two frames related by a Lorentz boost simply reflects the boost asymmetry of the LST. In Sec. 4.7 we explore a very interesting special point in the parameter space of the couplings, namely when $\lambda = \epsilon_+ = 0$ (or $\lambda = \epsilon_- = 0$) which is dual to the null warped AdS$_3$ geometry (with nonvanishing dilaton and NS-NS B field). Although this might appear to be a slight digression, we explore this case since this falls under the same broader umbrella of sting theory in AdS$_3$. Since this limit is singular, instead of naively taking this limit in the final complexity expression of the general case, and redo some of the intermediate steps. The complexity is only well defined (real) when the UV cut

---

correct powers of G_N. Similar considerations led the authors in [126] to a generalization of the Ryu-Takayanagi formula for holographic entanglement entropy for bulk backgrounds supporting a non-trivial dilation in the string frame.

off is restricted $\epsilon \leq \sqrt{k}\epsilon_- l_s$, a trait which lends support to the claims in the literature that the null warped AdS$_3$ spacetime is the holographic dual to field theory which *does not* possess a UV completion. For the null WAdS$_3$, the UV divergence structure is also special, one obtains UV divergences to all orders! In other words the complexity is not an analytic function of the UV cut off. This alludes to the fact that the boundary theory is highly nonlocal (and does not possess boost symmetry either). We also compute the subregion complexity numerically for a boundary interval of length, L and present our results graphically via subregion C_V vs L plot in Fig. 4.5 for a (allowable) range of the warping parameter ϵ_-. The subregion complexity monotonically increases with the subregion size and approaches the subregion complexity of a CFT$_2$ (i.e. pure AdS$_3$ linear regime) as L is progressively increased. However, unlike what we found for the case of general values of the couplings $\lambda, \epsilon_\pm$, there is no Hagedorn like phase transition. These results were obtained in the stationary frame, and there is no static frame for this case since the associated boost transformation which takes one from the stationary to static frame, becomes singular. Next, in Sec. 4.6 we set out to compute the action complexity for the LST (i.e. the $T\overline{T}, J\overline{T}, T\overline{J}$ deformed CFT$_2$). Here we realize that the construction of null surfaces bounding the so called Wheeler-de Witt (WdW) patch is simplest in the boosted frame in the boundary since it leads to a static metric in the bulk. So we exclusively stick to this coordinate system for the entire section/calculation. We leave the construction of lightsheets as sociated with the WdW patch and the subsequent evaluation of the action-complexity for the stationary frame for future work. While computing the WdW we are confronted with a choice, either to the use the $3 + 1$-d bulk geometry or to work with the $2 + 1$-d bulk geometry by dimensionally reducing over the y-fiber. Although we present the calculation performed in the dimensionally reduced $2 + 1$-d set up, pleasantly the action complexities obtained using the $3 + 1$-d and $2 + 1$-d bulk actions agree *provided we retain the total derivative terms in the lower dimensional action one gets while performing a dimensional reduction.* Usually such total derivative terms are omitted from the dimensionally reduced action as they do not contribute to the equations of motion, but they do contribute to (action) complexity. The action complexity results display the exact same divergence structures, quadratic and logarithm when $\epsilon \ll \beta'_H$. Modulo an overall constant (courtesy the ambiguity in the choice of the "characteristic length-scale of the geometry" in the definition of the volume complexity), the leading quadratic divergence piece matches for both the volume and action complexities. However we find that the subleading logarithmic divergence, while having the same magnitude in both prescriptions, *differs by a sign* in the volume and action complexity expressions. This is not a total surprise. Past studies have revealed that the coefficients of the subleading divergent pieces might be different [75] hinting to the fact that the two bulk/holographic prescriptions of complexity might actually correspond to different schemes of defining complexity in the boundary field theory. These are also consistent with the results of our previous paper [132] constituting the content of the previous chapter. As a final check, we extract the behavior of the action complexity in the deep IR limit (i.e. $\epsilon \gg \beta'_H$) where it indeed reproduces the pure AdS$_3$ or CFT$_2$ vacuum state complexity [74, 73] (for both prescriptions). In Sec. 4.7, we revisit the null Warped AdS$_3$ background (with dilaton and B-field) located at point in the coupling space, $\lambda = \epsilon_+ = 0$ and compute the action complexity of dual WCFT$_2$ using this bulk background. As remarked before, the static frame does not exist for this case, on cannot obtain the results by simply plugging $\lambda = \epsilon_+ = 0$ in the results of Sec. 4.6. We to tackle the calculation in the stationary frame itself where the construction of the WdW patch boundaries is more complicated than for a static geometry (but far simpler than that for the more general $\lambda, \epsilon_+ \neq 0$ case). We find that the action complexity null warped AdS$_3$ vanishes! We believe this is purely a dimensional accident, the action complexity for pure AdS$_{d+1}$ analogously vanishes [74, 132] due to an

overall factor of $(d - 2)$. Finally, in section 4.8 we conclude by discussing our results and provide an outlook for future work. In the appendices, we gather some results for ready references in the main sections. In Appendix B we recap the sigma model with the $T\bar{T}, J\bar{T}, T\bar{J}$ deformations and the 4d target spacetime which follows and work out the action complexity terms for the 4d geometry. Next in Appendix B.1 we recap the KK reduction over the y circle fiber following the conventions of [114], and obtain the dimensionally reduced 3d metric, Dilaton, B-field and KK scalar and KK gauge fields (the KK gauge fields obtained after reducing the 4d NS-NS B-field were missing in [114]. Subsequently we demonstrate the action complexity integrals for the 3d background work out to be the same as those from the 4d background worked out in the previous section provided we *retain the total derivative terms in the 3d action*. In Appendix B.2 we compute the new GHY term contribution as a result of keeping the total derivative term in the 3d lagrangian (action) and the net GHY contribution. In Appendix B.3 we compute the holographic entanglement entropy for the WCFT dual to null warped AdS$_3$, for a boundary interval of size L, thereby closing a gap in the literature. For null WCFT we find that the entanglement entropy is log divergent, just like that of an local CFT$_2$, but the coefficient of the log divergence (central charge) now depends on the warping parameter.

For other interesting works on complexity in the context of double trace $T\bar{T}$ deformed CFT see [108, 109, 110].

4.2   Review of string theory in AdS$_3$, single trace $T\bar{T}$ and LST

We first consider critical superstring background AdS$_3 \times \mathcal{M}$, with $\mathcal{M}$ being a compact seven dimensional spacelike manifold, which preserves $\mathcal{N} \geq 2$ supersymmetry. A classic example of this kind of a set up consists of type II strings on AdS$_3 \times S^3 \times T^4$ preserving $(4, 4)$ supersymmetry. The worldsheet theory of strings propagating in AdS$_3$ with NS-NS fluxes switched on but R-R fluxes turned off is a WZW nonlinear sigma model of the noncompact group manifold $SL(2, \mathbb{R})$. The worldsheet theory is symmetric under the holomorphic (left moving) and antiholomorphic (right moving) components of $sl(2, \mathbb{R})$ current algebra with level k. The AdS radius , R_{AdS}, is related to the level of the current algebra by the relation $R_{AdS} = \sqrt{k}l_s$, $l_s = \sqrt{\alpha'}$ being the string length.

According to the AdS/CFT correspondence, string theory on (asymptotically) AdS$_3$ is dual to a two-dimensional CFT living on the conformal boundary of AdS$_3$. For supergravity approximation to be valid, we will have to work in the parameter regime $k \gg 1$. In the presence of the NS-NS three form H-flux, the spacetime theory has the following properties:

1. The spacetime theory has a normalizable $SL(2, \mathbb{C})$ invariant vacuum state:

   - The NS vacuum, which corresponds to global AdS$_3$ as the bulk.
   - The R vacuum, that corresponds to massless spinless $(M = J = 0)$ BTZ as the bulk.

2. The NS sector consists of a sequence of discrete states coming from the discrete series representation of $SL(2, \mathbb{R})$ followed by a continuum of long strings. The continuum starts above a gap of order $\frac{k}{2}$ [111].

3. The R-sector states contain a continuum above a gap of order $\frac{1}{k}$. Here the fate of the discrete series states is unclear.

In the discussion that follows, we focus exclusively on the long strings of the R-sector.
In [112], it was argued, that for string theory on $AdS_3 \times \mathcal{M}$, the theory supported on a single long string is described by a sigma model on

$$\mathcal{M}_{6k}^{(L)} = \mathbb{R}_\phi \times \mathcal{M} , \qquad (4.1)$$

with central charge $6k$. The theory on $\mathbb{R}_\phi$ has a dilaton field Φ that is linear in the coordinate ϕ with a slope given by

$$Q^{(L)} = (k-1)\sqrt{\frac{2}{k}} . \qquad (4.2)$$

Thus the theory on the long string worldsheet has an effective interaction strength given by $\exp\left(Q^{(L)}\phi\right)$ and as a result the dynamics of the long strings becomes strongly coupled as they approach spatial infinity (boundary). But there is a wide range of positions on the radial direction where the long strings are weakly coupled. A natural question that one may ask at this point is: what is the full boundary theory dual to string theory in AdS_3. The answer to that question, for generic k, is unknown, but there are strong evidences to convince that the theory on the long strings is described by the symmetric product CFT

$$(\mathcal{M}_{6k}^{(L)})^p/S_p , \qquad (4.3)$$

where p represents the number of fundamental (F1) strings that form the background.
String theory in AdS_3 admits an operator $D(x, \bar{x})$ [113] (where x and $\bar{x}$ are coordinates of the two-dimensional spacetime theory), in the long string sector that has many properties in common with the $T\bar{T}$ operator. For example $D(x, \bar{x})$ is a $(2,2)$ quasi-primary operator of the spacetime Virasoro and has the same OPE with the stress tensor as the $T\bar{T}$ operator. However, there is an important difference between the $T\bar{T}$ operator and the operator $D(x, \bar{x})$: $T\bar{T}$ is a double trace whereas $D(x, \bar{x})$ is single trace.[2] In fact

$$D(x, \bar{x}) = \sum_{i=1}^{p} T_i \bar{T}_i , \qquad (4.4)$$

where $T_i \bar{T}_i$ can be thought of as the $T\bar{T}$ operator of the ith block $\mathcal{M}_{6k}^{(L)}$ in the symmetric product CFT $(\mathcal{M}_{6k}^{(L)})^p/S_p$. For an elaborate discussion along this line see [114, 115]
Next, consider the deformation of the long string symmetric product by the operator $D(x, \bar{x})$. This deforms the ith block CFT $\mathcal{M}_{6k}^{(L)}$ by the operator $T_i \bar{T}_i$ and is subsequently symmetrized. Such a deformation is evidently irrelevant and it involves *flowing up* the renormalization group (RG) trajectory. This $D(x, \bar{x})$ deformation of the spacetime theory translates to turning on the worldsheet a truly marginal deformation:

$$\int_{(\mathcal{M}_{6k}^{(L)})^p/S_p} d^2x D(x, \bar{x}) \sim \int_\Sigma d^2z J_{SL}^- \bar{J}_{SL}^- , \qquad (4.5)$$

where $z, \bar{z}$ are the complex coordinates of the worldsheet Riemann surface Σ, J_{SL}^- and $\bar{J}_{SL}^-$ are respectively the left and right moving null $sl(2, \mathbb{R})$ currents of the worldsheet theory.

---

[2]Here single trace refers to the fact that $D(x, \bar{x})$ can be expressed as a single integral over the worldsheet of a certain worldsheet vertex operator. The operator $T\bar{T}$ on the other hand is double trace because it can be expressed as a product of two single trace operators in the sense just described.

The above current-anti-current deformation of the worldsheet $\sigma-$model is exactly solvable, and standard worldsheet techniques yield the metric (in string frame), dilaton and the B-field as [116, 117]

$$ds^2 = f^{-1}(-dt^2 + dx^2) + kl_s^2 \frac{dU^2}{U^2} \ ,$$

$$e^{2\Phi} = \frac{g_s^2}{kU^2}f^{-1} \ , \qquad\qquad (4.6)$$

$$dB = \frac{2i}{k^{3/2} l_s U^2}f^{-1}\epsilon_3 \ ,$$

where $f = \lambda + \frac{1}{kU^2}$, λ is the dimensionless coupling [3] of the marginal worldsheet deformation and g_s is the asymptotic string coupling in AdS_3 with $g_s^2 = e^{2\Phi(U\to 0)} \equiv e^{2\Phi_0}$. This background is popularly known as $\mathcal{M}_3$. The background $\mathcal{M}_3$ (4.6) interpolates between AdS_3 in the IR ($U \ll 1/\sqrt{k\lambda}$) to flat spacetime with a linear dilaton, $\mathbb{R}^{1,1} \times \mathbb{R}_\phi$ in the UV ($U \gg 1/\sqrt{k\lambda}$). The coupling λ sets the scale at which the transition happens.

The deformed sigma model background (4.6) can also be obtained as a solution to the equations of the motion of three dimensional supergravity action [118, 107]

$$S = \frac{1}{16\pi G_N} \int d^3X \sqrt{-g}e^{-2(\Phi-\Phi_0)} \left(R + 4g^{\mu\nu}\partial_\mu\Phi\partial_\nu\Phi - \frac{1}{12}H^2 - 4\Lambda \right) \ , \qquad\qquad (4.7)$$

where G_N is the three-dimensional Newton's constant in AdS_3, $g_{\mu\nu}$ is the string frame metric, R is the Ricci scalar (in string frame), Φ is the dilaton, $H = dB$ is the 3-form flux and Λ is the cosmological constant.

As an example, the above construction can be realized as follows. Let us consider a stack of k NS5 branes in flat space wrapping a four dimensional compact manifold (T^4 or K_3). The near horizon geometry of the stack of k NS5 branes is given by $\mathbb{R}^{1,1} \times \mathbb{R}_\phi$ with a dilaton that is linear in the radial coordinate ϕ (where $\phi = \log(\sqrt{k}U)$). The string coupling goes to zero near the boundary ($U \to \infty$) whereas it grows unboundedly as one goes deep in the bulk ($U \to 0$). Next, let's add p (with $p \gg 1$) F1 strings stretched along $\mathbb{R}^{1,1}$. This stabilizes the dilaton and the string coupling saturates as $g_s \sim 1/\sqrt{p}$. Thus for large p the string coupling is weak and one can trust string perturbation theory. The F1 strings modifies the IR geometry ($U \ll 1/\sqrt{k\lambda}$) to AdS_3. The smooth interpolation between $\mathbb{R}^{1,1} \times \mathbb{R}_\phi$ in the UV to AdS_3 in the IR corresponds to interpolation between near horizon geometry of the NS5 brane system to that of the F1 strings [119, 107]. The spacetime theory interpolates between a CFT_2 with central charge $6kp$ in the IR to two-dimensional LST in the UV. The theory is nonlocal in the sense that the short distance physics is not governed by a fixed point.

LST can be realized as the decoupled theory on the NS5 branes. It has properties that are somewhat intermediate between a local quantum field theory and a full fledged critical string theory. Unlike a local field theory, at high energy E, LST has a Hagedorn density of states $\rho \sim e^{\beta_H E}$ where $\beta_H = 2\pi l_s \sqrt{k\lambda}$. On the other hand, LST has well defined off-shell amplitudes [120] and upon quantization it doesn't give rise to massless spin 2 excitation. Both these properties are very similar to local quantum field theories. For a detailed review of LST see [97, 98].

One can generalize this scenario further by turning on holomorphic and antiholomorphic currents in the spacetime theory $J(x), \overline{J}(\overline{x})$ [114, 113]. In that case, parallel to the construction of $D(x,\overline{x})$, one can also construct *single trace* operators, namely, $A(x,\overline{x})$ and $\overline{A}(x,\overline{x})$ of dimension

---

[3]Note that without loss of generality, the value of λ can be set to an appropriate value as discussed in [101].

$(1, 2)$ and $(2, 1)$ respectively [113]. $A(x, \overline{x})$ has the same conformal dimension and OPE's with the currents as the irrelevant double trace $J(x)\overline{T}(\overline{x})$ operator. Analogously, the single trace marginal $\overline{A}(x, \overline{x})$ is related to the irrelevant double trace $T(x)\overline{J}(\overline{x})$ operator in the spacetime CFT. In the symmetric product CFT, one can think of the operator of $A, \overline{A}$ as

$$A(x, \overline{x}) = \sum_{j=1}^{p} J_j(x) \, \overline{T}_j(\overline{x}); \; \overline{A}(x, \overline{x}) = \sum_{j=1}^{p} T_j(x) \, \overline{J}_j(\overline{x}). \tag{4.8}$$

Turning on $A, \overline{A}(x, \overline{x})$, in addition to the $D(x, \overline{x})$ operators, in the spacetime corresponds to the perturbing the worldsheet lagrangian by the following marginal operators,

$$\delta \mathcal{L}_{WS} = \lambda \, J_{SL}^-(z)\overline{J}_{SL}^-(\overline{z}) + \epsilon_+ \, K(z)\overline{J}_{SL}^-(\overline{z}) + \epsilon_- \, J_{SL}^-(z)\overline{K}(\overline{z}). \tag{4.9}$$

One has to strictly consider the positive sign of the coupling λ because only for that sign of the coupling the spectrum of the deformed theory is real and the theory is unitary.
The worldsheet $U(1)$ currents $K(z)$ and $\overline{K}(\overline{z})$ are associated with left and right-moving momenta on a S^1 in the bulk spacetime labelled by the coordinate y. Such a deformation will lead to the sigma model action [114],

$$S(\lambda, \epsilon_+, \epsilon_-) = \frac{k}{2\pi} \int d^2z \left(\partial\phi\overline{\partial}\phi + h\partial\overline{\gamma}\overline{\partial}\gamma + \frac{2\epsilon_+ h}{\sqrt{k}}\partial y\overline{\partial}\gamma + \frac{2\epsilon_- h}{\sqrt{k}}\overline{\partial}y\partial\overline{\gamma} + \frac{f^{-1}h}{k}\partial y\overline{\partial}y \right) \tag{4.10}$$

where $f^{-1} = \lambda + e^{-2\phi}$, $h^{-1} = \lambda - 4\epsilon_+\epsilon_- + e^{-2\phi}$. This corresponds to the $4d$ background [114],

$$\frac{ds^2}{l_s^2} = kh \left(d\gamma + \frac{2\epsilon_-}{\sqrt{k}}dy \right) \left(d\overline{\gamma} + \frac{2\epsilon_+}{\sqrt{k}}dy \right) + kd\phi^2 + dy^2 \tag{4.11}$$

with a dilaton

$$e^{2\Phi} = g_s^2 e^{-2\phi} h, \tag{4.12}$$

and a NS-NS B-field,

$$B_{\gamma\overline{\gamma}} = -\frac{hk}{2}, \qquad B_{y\gamma} = -B_{\gamma y} = \epsilon_+ h\sqrt{k}, \qquad B_{y\overline{\gamma}} = -B_{\overline{\gamma}y} = -\epsilon_- h\sqrt{k} \tag{4.13}$$

See Appendix **??** for some of the details omitted here.

4.2.1 The Holographic $2 + 1$-d background

Upon performing a KK reduction along the y-circle [114], target space NS-NS sector background described by the 3d metric

$$ds^2 = kl_s^2 \frac{h(\phi)}{f(\phi)}\mathrm{d}\phi^2 + kl_s^2 \frac{h(\phi)^2}{f(\phi)}d\gamma d\overline{\gamma} - kl_s^2 h(\phi)^2(\epsilon_+\mathrm{d}\gamma + \epsilon_-\mathrm{d}\overline{\gamma})^2, \tag{4.14}$$

and the dilaton, Φ and a 2-form gauge field H background[4],

$$e^{2\Phi} = g_s^2 e^{-2\phi}\sqrt{f(\phi)h(\phi)}, \qquad\qquad B_{\gamma\overline{\gamma}} = \frac{kh(U)l_s^2}{2}. \tag{4.15}$$

---

[4]In addition there are $U(1)$ gauge fields originating from the KK reduction of the 4d metric and 4d B-field, refer to Appendix B.1 for the full list.

The functions h, f are defined by

$$h(\phi) = \frac{1}{\lambda - 4\epsilon_+\epsilon_- + e^{-2\phi}}, \qquad\qquad f(\phi) = \frac{1}{\lambda + e^{-2\phi}}, \qquad (4.16)$$

where $\lambda, \epsilon_\pm$ are the irrelevant dimensionless couplings for $T\bar{T}, J\bar{T}$, & $\bar{J}T$ deformations respectively. Here ϕ is the radial coordinate while the $\gamma, \bar{\gamma}$ are lightlike coordinates parallel to the boundary. In this work we will work instead with the following coordinates,

$$e^\phi = \sqrt{k}U, \qquad\qquad x = \frac{\sqrt{k}l_s}{2}(\gamma + \bar{\gamma}), \qquad\qquad t = \frac{\sqrt{k}l_s}{2}(\gamma - \bar{\gamma})$$

Thus, U is the radial coordinate (RG scale) while t, x are boundary time and space coordinate. In terms of these new coordinates metric reads,

$$ds^2 = \frac{h(U)}{f(U)}\left[kl_s^2\frac{dU^2}{U^2} - h(U)\left(1 + f(U)(\epsilon_+ - \epsilon_-)^2\right)dt^2\right.$$

$$\left. - 2h(U)f(U)(\epsilon_+^2 - \epsilon_-^2))\,dtdx + h(U)\left(1 - f(U)(\epsilon_+ + \epsilon_-)^2\right)dx^2\right]. \quad (4.17)$$

while the dilaton and the Kalb-Ramond field are given by,

$$e^{2\Phi} = \frac{g_s^2}{\sqrt{(k\lambda U^2 + 1)(kU^2(\lambda - 4\epsilon_-\epsilon_+) + 1)}}, \qquad dB = \frac{2h(U)}{k^{3/2}l_s U^2\sqrt{1 - 4\epsilon_+\epsilon_-f(U)}}\epsilon_3. \qquad (4.18)$$

Here we have,

$$h(U) = \frac{kU^2}{1 + (\lambda - 4\epsilon_+\epsilon_-)kU^2}, \qquad\qquad f(U) = \frac{kU^2}{1 + \lambda kU^2},$$

(We notice that if we replace $\lambda \to \lambda' = \lambda - 4\epsilon_+\epsilon_-$, then $f(U) \to h(U)$. This fact will be put to use in the calculations to follow in the coming sections). This background interpolates between AdS_3 in the IR to linear dilaton flat spacetime in the UV. In the dual sense this geometry represents an integrable RG flow connecting a Lorentz invariant local CFT (fixed point) in the IR to a Lorentz violating nonlocal theory in the UV, namely a deformed little string theory (LST).

4.3 Holographic Volume Complexity

In this section we compute the computational complexity of the LST deformed by irrelevant single trace $J\bar{T}$ and $T\bar{J}$ deformation using holography, in particular, the Complexity-Volume (CV) [48] prescription. Computational complexity like entanglement entropy, is a manifestly UV-divergent quantity, and for ordinary quantum field theories the UV divergence structure of computational complexity is rigidly constrained [73, 74]. In this section we reveal the UV-divergences which might arise in a nonlocal and lorentz violating field theory, such as two-dimensional CFT deformed by single trace $J\bar{T}$ and $T\bar{J}$ and compare and contrast them with those arising in a lorentz invariant local quantum field theory (a CFT$_2$). The volume complexity prescription computes the complexity of the dual boundary theory in terms of the volume of a maximal volume space-like slice, Σ,

$$C_V = \frac{V_\Sigma}{G_N L}, \quad \text{with} \quad V_\Sigma = \int_\Sigma d^{D-1}x\,\sqrt{\gamma_\Sigma}, \qquad (4.19)$$

where $\gamma_{\mu\nu}$ is the pullback metric on the maximal volume slice. As mentioned before, L represents a suitable characteristic scale of the geometry. Here, we are working in the string frame with a non-trivial dilaton background and the volume complexity proposal needs to be generalized. The appropriate generalization is given by [126],

$$C_V = \frac{\tilde{V}_\Sigma}{\kappa_0^2 L} , \quad \text{with} \quad \tilde{V}_\Sigma = \int_\Sigma d^{D-1}x \, e^{-2(\Phi-\Phi_\infty)}\sqrt{\gamma_\Sigma} . \tag{4.20}$$

One can check that this generalization furnishes the correct powers of G_N [5] in the denominator using the string convention, $\kappa_0^2 e^{-2(\Phi_\infty-\Phi_0)} = 8\pi G_N$ where e^{Φ_∞} is the flat space string coupling and e^{Φ_0} is the string coupling of AdS_3. In anticipation of the fact that the dual boundary field theory is Lorentz violating, we compute the volume complexity in two different Lorentz frames and the comparison is drawn between the results.

4.3.1 Volume Complexity in stationary coordinates (x, t)

We specify the a spacelike hypersurface by the condition, $t = t(U)$, $\forall x$. The pullback of the ambient metric in the so called stationary coordinates (4.17) on the hypersurface becomes:

$$ds_\Sigma^2 = \left(\frac{kl_s^2}{U^2} - h(U)(1 + f(U)(\epsilon_+ - \epsilon_-)^2)t'(U)^2\right) dU^2 - 2h(U)f(U)(\epsilon_+^2 - \epsilon_-^2))t'(U)dUdx$$
$$+ h(U)(1 - f(U)(\epsilon_+ + \epsilon_-)^2)dx^2. \tag{4.21}$$

The general form of the volume of any hypersurface in string frame with appropriate inclusion of the dilaton factors in the integral measure is,

$$V_\Sigma(t_*) = e^{2(\Phi_\infty-\Phi_0)} \int dx\, dU \, e^{-2(\Phi-\Phi_0)}\sqrt{\gamma_\Sigma},$$
$$= \frac{kl_s L_x}{e^{-2(\Phi_\infty-\Phi_0)}} \int_0^\infty dU \sqrt{1 + k\mu\, U^2}\sqrt{1 - \frac{t'(U)^2 U^4}{l_s^2\,(1 + k\mu\, U^2)}}.$$

where, L_x is the IR cutoff of the boundary LST and we have defined

$$\mu := \lambda - (\epsilon_- + \epsilon_+)^2 \tag{4.22}$$

for later convenience. To find the maximal volume one needs to extremize this volume functional. The corresponding Euler-Lagrange equation is,

$$-Ul_s^2 t''(U)\left(1 + k\mu U^2\right) + l_s^2 t'(U)\left(3k\mu U^2 + 4\right) - 2U^4 t'(U)^3 = 0. \tag{4.23}$$

To solve this nonlinear differential equation perturbatively, we employ the near boundary power series expansion of the form

$$t(U) = T + \frac{a}{U} + \frac{b}{U^2} + \frac{c}{U^3} + \frac{d}{U^4} + ... \tag{4.24}$$

Plugging this "large U" expansion in the Euler Lagrange equation and solving iteratively in powers of U^{-1} we get all coefficients to vanish, $a = b = c = d = \ldots = 0$. With this knowledge, the volume V_Σ of the maximal slice turns out to be:

$$V_\Sigma(t_*) = \frac{kl_s L_x}{e^{-2(\Phi_\infty-\Phi_0)}} \int dU \sqrt{1 + kU^2\mu}. \tag{4.25}$$

---

[5]See [126] for a similar prescription for the Ryu-Takayanagi formula for the entanglement entropy

Therefore by (4.19), the volume complexity turns out to be

$$C_V \equiv \frac{V_\Sigma(t_*)}{\kappa_0^2 L} \; = \; \frac{k\, l_s\, L_x}{G_N\, L} \left[\frac{l_s}{2\epsilon} \sqrt{1 + \frac{k\, \mu\, l_s^2}{\epsilon^2}} + \frac{\sinh^{-1}\left(\frac{\sqrt{k\mu}\, l_s}{\epsilon} \right)}{2\sqrt{k\, \mu}} \right]. \tag{4.26}$$

Note that by convention the length scale L appearing here is the characteristic length scale associated with the geometry. Comparison with results from action complexity helps us resolve this ambiguity $L = \ell = \sqrt{k}\, l_s$, the AdS radius, and the volume complexity is after evaluating the integral is

$$\begin{aligned} C_V(T) &= \frac{cL_x}{3\epsilon} \sqrt{\frac{3\rho_H^2}{4\pi^2\epsilon^2} + 1} + \frac{2\pi c L_x}{3\sqrt{3}\gamma_H} \sinh^{-1}\left(\frac{\sqrt{3}\rho_H}{2\pi\epsilon} \right), \\ &= \frac{cL_x}{3\rho_H} \left(\frac{\rho_H}{\epsilon} \sqrt{1 + \frac{3\rho_H^2}{4\pi^2\epsilon^2}} + \frac{2\pi}{\sqrt{3}} \sinh^{-1}\left(\frac{\sqrt{3}\rho_H}{2\pi\epsilon} \right) \right). \end{aligned} \tag{4.27}$$

Here as before, ϵ is the UV cutoff required to regularize the divergent integral by placing the boundary at $U = \frac{l_s}{\epsilon}$ and $c = \frac{3\sqrt{k}l_s}{2G_N}$ is the Brown-Hanneaux central charge of the IR CFT_2. The expression in the first line is rewritten in terms of the Hagedorn density of states, ρ_H [105] in the second line:

$$\rho_H = \frac{2\pi}{\sqrt{3}} \sqrt{k\mu}l_s. \tag{4.28}$$

We immediately notice that the leading divergence is quadratic followed by a logarithmic divergence. The unexpected quadratic (and logarithmic) divergence is taken to be as the sign of nonlocality and lorentz violation. However it appears that the Lorentz violation effects and nonlocality effects are combined into a single parameter, namely $\mu = \lambda - (\epsilon_+ + \epsilon_-)^2$ and there is no way to cleanly separate the effects of one from the other. This is perhaps mildly disappointing since our expectation was to be able to see the effects of nonlocality and Lorentz violation in separate divergence structures. Also, we see that in order for the notion of complexity to make sense, we have to restrict $\mu \geq 0$. This condition is important in ensuring the existence of a smooth dual gravity background geometry as mentioned in earlier works [106, 124]. As a consistency check we note that the complexity expression (4.27) smoothly reduces to the previously known $\mathcal{M}_3$ expression as the lorentz violating couplings $\epsilon_\pm$ [132] are turned off.

Let's now examine the behavior of the theory in the two opposite extreme limits. Thinking of ρ_H as the distance scale below which non-local and lorentz violating effects kicks in, one of the interesting limit to study would be the UV limit $\epsilon/\rho_H \ll 1$ where the short distance physics is that of the non-local lorentz violating field theory:

$$\lim_{\epsilon/\rho_H \to 0} C_V = \frac{cL_x}{\sqrt{3}\rho_H} \left(\frac{\rho_H^2}{2\pi\epsilon^2} + \frac{\pi}{3} \ln\left(\frac{3\rho_H^2}{\pi^2\epsilon^2} \right) + O\left(\epsilon/\rho_H \right) \right). \tag{4.29}$$

The divergence structure as is evident from this expression, does not match with that of the lorentz covariant local field theory. For the latter case, the complexity being an extensive quantity counting the degrees of freedom in the field theory is expected to diverge linearly i.e. L_x/ϵ.

Another interesting regime to study is the IR behavior where, $\rho_H/\epsilon \ll 1$.

$$\lim_{\rho_H/\epsilon \to 0} C_V = \frac{2cL_x}{3\,\epsilon}. \tag{4.30}$$

This expression reproduces the expected result for a local field theory [74] by correctly counting the total number of degrees of freedom.

In conclusion, we notice that the volume complexity for the LST deformed with Lorentz violating and nonlocal couplings leads to the exact same divergences which nonlocality by itself would have produced and we see no distinctive signature of Lorentz violation.

4.3.2   Volume complexity in static (X, T) coordinates

As alluded to in the introduction, due to the presence of additional irrelevant $\{\epsilon_{\pm}\}$ couplings, the field theory is lorentz violating. As a result, the bulk geometry also inherits this character. Therefore we feel it is instructive to repeat the CV calculation in a different Lorentz frame, namely the "static coordinate system" obtained after performing the following lorentz boosts on the stationary coordinate system of the previous section,

$$
X = \frac{1}{2\sqrt{\epsilon_+\epsilon_-}}((\epsilon_+ + \epsilon_-)x + (\epsilon_+ - \epsilon_-)t),
$$

$$
T = \frac{1}{2\sqrt{\epsilon_+\epsilon_-}}((\epsilon_+ - \epsilon_-)x + (\epsilon_+ + \epsilon_-)t), \tag{4.31}
$$

the resulting metric is:

$$
ds^2 = kl_s^2 \frac{dU^2}{U^2} - h(U)\, dT^2 + f(U)\, dX^2. \tag{4.32}
$$

Using CV prescription, the maximal codim-1 surface Σ is required to be given by the equation $T = T(U)$ with appropriate functional form which extremizes the volume element. Since there are no crossterms of form $dtdX$, it is appropriate to refer this as a static coordinate system.

The induced metric is

$$
ds_\Sigma^2 \equiv \gamma_{ab}dx^a dx^b,
$$

$$
= \left(\frac{kl_s^2}{U^2} - h(U)T'(U)^2\right) dU^2 + f(U)\, dX^2. \tag{4.33}
$$

In the string frame, the volume of such a spacelike slice anchored at a time T_* on the boundary is,

$$
\tilde{V}(T) = e^{2(\Phi_\infty - \Phi_0)} \int dx\, dU\, e^{-2(\Phi - \Phi_0)}\sqrt{\gamma_\Sigma},
$$

$$
= \frac{k^{3/2}l_s L_x}{e^{-2(\Phi_\infty - \Phi_0)}} \int_0^\infty dU\, \frac{kU^2}{\sqrt{f(U)h(U)}} \sqrt{f(U)\left(\frac{kl_s^2}{U^2} - h(U)T'(U)^2\right)}. \tag{4.34}
$$

Here $L_x = \int dx$ is the spatial extent (IR cutoff) of the boundary theory target space and λ' is defined to be $\lambda - 4\epsilon_+\epsilon_-$. Extremizing this volume leads to the following Euler-Lagrange equation:

$$
l_s^2 \left(UT''(U)\left(1 + k\lambda'U^2\right) + T'(U)\left(3k\lambda'U^2 + 4\right)\right) - 2U^4 T'(U)^3 = 0. \tag{4.35}
$$

The solution is found by employing series expansion method, lets assume the near boundary expansion of $T(U)$ of the form:

$$
T(U) = T_* + \frac{a_1}{U} + \frac{a_2}{U^2} + \frac{a_3}{U^3} + \dots. \tag{4.36}
$$

And plugging back in (4.35) and solving them order by order in $\frac{1}{U}$, we obtain the result that all the coefficients vanish. Thus the maximal volume slice is $T(U) = T_*$, a result that can be anticipated from the time reflection symmetry: $T \to -T$, of the background. Thus, the volume of the maximal volume slice is,

$$\tilde{V}_\Sigma(T) = \frac{k^{3/2} l_s L_x}{e^{-2(\Phi_\infty - \Phi_0)}} \int_0^\infty dU \frac{U}{\sqrt{h(U)}}, \tag{4.37}$$

$$= \frac{k l_s L_x}{e^{-2(\Phi_\infty - \Phi_0)}} \int_0^\infty dU \sqrt{1 + kU^2 \lambda'}, \tag{4.38}$$

which diverges as $U \to \infty$. So we impose a UV cutoff at $U = l_s/\epsilon$ to regulate it. Also, we have defined λ' to be $\lambda - 4\epsilon_- \epsilon_+$. The regulated volume is then,

$$\tilde{V}_\Sigma(T) = \frac{k l_s L_x}{e^{-2(\Phi_\infty - \Phi_0)}} \left[\frac{l_s}{2\epsilon} \sqrt{1 + \frac{k \lambda' l_s^2}{\epsilon^2}} + \frac{\sinh^{-1}\left(\frac{\sqrt{k \lambda'} l_s}{\epsilon}\right)}{2\sqrt{k \lambda'}} \right]. \tag{4.39}$$

As expected, due to time translation symmetry the expression is independent of T_*. Therefore from (4.20) volume complexity turns out to be

$$\mathcal{C}_V \equiv \frac{\tilde{V}_\Sigma}{\kappa_0^2 L} = \frac{k l_s L_x}{G_N L} \left[\frac{l_s}{2\epsilon} \sqrt{1 + \frac{k \lambda' l_s^2}{\epsilon^2}} + \frac{\sinh^{-1}\left(\frac{\sqrt{k \lambda'} l_s}{\epsilon}\right)}{2\sqrt{k \lambda'}} \right]. \tag{4.40}$$

Again following the remarks of the preceding section, $L = \ell = \sqrt{k} l_s$, the AdS radius and the volume complexity is thus,

$$\mathcal{C}_V = \frac{cL_x}{3\beta_H'} \left[\frac{\beta_H'}{2\epsilon} \sqrt{4 + \frac{\beta_H'^2}{\pi^2 \epsilon^2}} + 2\pi \, \sinh^{-1}\left(\frac{\beta_H'}{2\pi\epsilon}\right) \right], \tag{4.41}$$

where, β_H' is the inverse Hagedorn temperature

$$\beta_H' = 2\pi l_s \sqrt{k \lambda'}. \tag{4.42}$$

We would like to draw the reader's attention to the important fact that the holographic volume complexity expression in the static frame (4.41) does not match with that in the stationary frame (4.27). This is the artifact of the dual field theory being Lorentz violating in nature i.e. the complexity measured in different frames related by a Lorentz boost transformation do not agree. Similar observation had also been made in regard to entanglement entropy in [106]. This is indeed gratifying to note. A comment on the nonlocality and Lorentz violation
Let us recall that β_H' can be thought of the length scale below which nonlocality and Lorentz violation effects kicks in. Thus, an interesting limits to study would be $\epsilon/\beta_H' \ll 1$ where the short distance physics is that of a nonlocal and Lorentz violating theory. In this limit the volume complexity takes the form

$$\lim_{\epsilon/\beta_H' \to 0} \mathcal{C}_V = \frac{cL_x}{3\beta_H'} \left[\frac{\beta_H'^2}{2\pi\epsilon^2} + 2\pi \log\left(\frac{\beta_H'}{\pi\epsilon}\right) + \pi + O\left(\frac{\epsilon}{\beta_H'}\right) \right]. \tag{4.43}$$

Evidently the divergence structure of the volume complexity (4.43) does not appear like that of a local quantum field theory.
For the case of a local quantum field theory, complexity being an extensive quantity should be proportional to the degrees of freedom given by the number of lattice sites $\propto L_x/\epsilon$ scales inversely with the cutoff ϵ (lattice spacing). The quadratic and logarithmic divergences in (4.43) are a reflection of the fact that the boundary theory, being a LST, is a nonlocal, Lorentz violating field theory and fittingly a special combination of nonlocality and Lorentz violation parameters, namely β_H', features in the coefficient

of this quadratic as well as the logarithmic divergences. One can check, that by making the nonlocality and Lorentz violation vanish in the limit $\epsilon/\beta'_H \gg 1$, the volume complexity expression (4.41) indeed reduces to that of a local field theory,

$$\lim_{\epsilon/\beta'_H \gg 1} \mathcal{C}_V = \frac{2c}{3\beta'_H} \frac{L_x}{(\epsilon/\beta'_H)} = \frac{2c}{3} \frac{L_x}{\epsilon} \ . \tag{4.44}$$

This expression of complexity (being proportional to the product of c, the central charge the number of degrees of freedom per lattice site, and L_x/ϵ, which gives the total number of lattice sites) counts the total number of degrees of freedom in a local field theory.

This quadratic UV divergence of the LST in 1-space dimensions, i.e. a "hypervolume" divergence is a fascinating observation. Let compare and contrast it with the divergence structure arising in (holographic) entanglement entropy (EE). The EE for nonlocal field theories one encounters a similar phenomenon, the RT prescription yields a volume law instead of a perimeter (area) law for a subregion EE, e.g. see [127, 135, **?**, **?**] in addition to the LST EE [103]. However, physical understanding of the volume dependence (divergence) of EE for nonlocal field theories is perhaps intuitively obvious. Given a subregion, for a local field theory the entangling degrees of freedom are localized on the boundary. Once the theory becomes nonlocal, the entangling degrees of freedom are not only localized on the boundary of the subregion but also along direction orthogonal to the boundary, i.e. throughout the volume of the subregion. Hence the appearance of the volume divergence for EE. However, for the case of complexity is qualitatively different, it is *already* a volume law for local field theories, so it is not obvious intuitively why the "hypervolume" law and in particular why the power of divergence is "volume + 1" instead of "volume + n" for arbitrary positive integral n. At this point we can only speculate which specific aspect of nonlocality of LST is captured by the hypervolume divergence: in the strong dilaton region (UV), the LST effectively behaves like it has grown an extra spatial dimension, much alike IIA string theory which grows an extra dimension when the dilaton turns strong (strong coupling). This appearance of an effective extra (noncompact) spatial dimension could potentially explain the "**volume** + 1" divergence structure. Although this analogy is not exact or direct since the LST studied in our work is obtained from NS5 branes in IIB frame/theory, while the 10 dimensional string to 11 dimensional M-theory is realized in the IIA frame, and the emergent dimension is a compact (circle). Similar observations/ suggestions i.e. LST behaving like it develops an extra spatial dimension at strong coupling, have been made in early works in LST in IIA frame, e.g. in [136]. Perhaps a more definitive statement can only be made when the holographic complexity of nonlocal field theories which are not necessarily LST (or derived from string theory) are computed. These theories will not share the stringy property of developing extra spatial dimensions at strong coupling and might have a different kind of divergence structure.

Next consider the coefficient of the log term (which is universal) in the expression of volume complexity (4.43) in the deep UV ($\epsilon \ll \beta'_H$), which is

$$\tilde{N} = c\frac{L_x}{\beta'_H} \ . \tag{4.45}$$

Evidently, this coefficient counts the total number of "regularized/effective" degrees of freedom in the theory if we regard the lattice spacing of LST to be the Hagedorn scale, β'_H instead of the UV cutoff ϵ of the original IR CFT, namely, $N \sim c\frac{L_x}{\epsilon}$. Regarding the universality of the log divergence piece in volume complexity and action complexity: We regret that the language in the draft led the referee to infer that we are claiming that the log divergence is universal across different holographic proposals of complexity (e.g. volume and action). There are now numerous proposals of holographic complexity (complexity=volume, complexity=action, complexity=spacetime volume 2.0, etc., finally culminating in the claim by Belin et. al. [79] that there might be infinite number of such spatial codimension-one bulk geometric prescriptions of holographic complexity which are as good candidates as the ones suggested originally. It has been generally observed that although the leading divergence pieces across different prescriptions match, the coefficients of the subleading divergences do not match, either in sign or in magnitude. It could be that various prescriptions of holographic complexity correspond to field theory duals

which are distinct but are in the same universality class in the sense of RG (although the study of field theory complexity is at a very premature stage to make such classifications of universality classes under RG). However, *once we pick a proposal*, the coefficient of the log divergence is universal in the usual sense - if we rescale the UV energy scale, the coefficient of the log divergence does not get rescaled. Such coefficients which do not get rescaled usually capture some universal physics e.g. in the RT proposal it gives the c-function.

Another interesting fact emerges if we rewrite the quadratic UV divergence term (4.43), in a manner which mimics a local field theory:

$$\mathcal{C}_V = \frac{cL_x\beta_H'}{6\pi^2\epsilon^2} + \ldots = \frac{2\tilde{c}(\epsilon)}{3}\frac{L_x}{\epsilon} + \ldots, \quad \text{where} \quad \tilde{c}(\epsilon) = c\frac{\beta_H'}{4\pi^2\epsilon} \ , \tag{4.46}$$

If we pretend this is a local theory with a linear divergence structure, then the coefficient of the linear divergence if identified as an "effective central charge" is now a UV scale dependent parameter $\tilde{c}(\epsilon)$, in fact it is a monotonically increasing function of UV scale (energy), $\frac{1}{\epsilon}$. So this "effective central charge" diverges as the UV cutoff is withdrawn. Similar observations have been made about LST, namely a divergent central charge, elsewhere in the literature.

Now we compare the complexity results for the static frame and the stationary frame. They share several common features:

1. The static frame volume complexity, $\mathcal{C}_V$ (4.41) as a function of ϵ/β_H' and the stationary frame complexity, $\mathcal{C}_V'$ (4.27) as function of ϵ/ρ_H are always positive and monotonically decreases from UV to IR.

2. In the extreme UV regime (when $\epsilon \ll \beta_H', \rho_H$), $\mathcal{C}_V$ diverges as (4.43), and $\mathcal{C}_V'$ too diverges as (4.29).

3. In the extreme IR regime, (when $\epsilon \gg \beta_H', \rho_H$), $\mathcal{C}_V$ decreases to 0 as (4.44) and so does $\mathcal{C}_V'$ according to (4.30).

Finally we plot the static frame complexity, $\mathcal{C}_V$ and the stationary frame complexity, $\mathcal{C}_V'$ as a function of the cutoff, ϵ in figure 4.1.
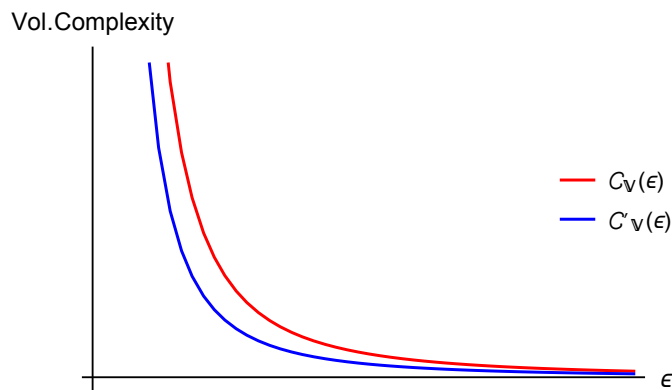
Figure 4.1: Static frame complexity, $\mathcal{C}_V$ and stationary frame complexity, $\mathcal{C}_V'$ as a function the UV cutoff scale ϵ.

In conclusion, we notice that the volume complexity for the LST deformed with Lorentz violating and nonlocal couplings leads to the exact same kind of divergences which nonlocality by itself would have produced (quadratic and logarithmic divergences). The distinctive signature of Lorentz boost violation is that the coefficients of the quadratic and logarithmic divergences as well as the finite piece in complexity differ in the two frames related by a Lorentz boost.

4.4 Subregion volume complexity

The volume complexity computed in the last section was unable to capture the distinguishing signatures of lorentz violation form nonlocality. In the hope that the subregion complexity might have something more to tell us about the differences between signatures of nonlocality and Lorentz violation, in this section we explore the features of subregion volume complexity for a boundary subregion of size L. To this end we need to focus our attention to the portion of the maximal volume slice which is contained within the Ryu-Takayanagi (RT) surface (curve) homologous to the aforementioned boundary spacelike interval (of size L).

First we have to determine the RT surface, which is a codimension 2 surface in the bulk, homologous to the boundary subregion. The volume functional on a codimension-2 slice (in this case a curve) is obtained by looking at the constant time section of the $U = U(x)$ surface.

$$ds^2 = \left(kl_s^2 \frac{U'^2}{U^2} + h(U)(1 - f(U)(\epsilon_+ + \epsilon_-)^2)\right) dx^2, \tag{4.47}$$

where, the prime denotes the derivative with respect to the parameter x parameterizing the RT curve. Now in the string frame, this co-dimension-2 surface has the following volume functional, which in the present case turns out to be the length of the curve

$$\int dx \, \mathcal{L}(U(x), U'(x), x) = \frac{1}{U} \sqrt{kU'^2 l_s^2 \left(k\lambda U^2 + 1\right)\left(kU^2\lambda' + 1\right) + kU^4 \left(kU^2\mu + 1\right)}. \tag{4.48}$$

where, the primes over the quantities denotes their derivative with respect to x.

Now one has to minimize this string frame length functional to obtain the RT curve. However, instead of minimizing the action functional following the variational method (Euler-Lagrange equations), we instead follow the procedure of [106] and start by analyzing the integrals of motion. The condition that lagrangian is independent of time, gives us the first integral of motion

$$c_1 = \frac{\partial \mathcal{L}}{\partial t'} \quad (= 0), \tag{4.49}$$

Since the lagrangian is cyclic in parameter x, the corresponding "hamiltonian" should be conserved:

$$
\begin{aligned}
c_2 &= U' \frac{\partial \mathcal{L}}{\partial U'} - \mathcal{L}, \\
&= \frac{-kU^3 \left(kU^2\mu + 1\right)}{\sqrt{kU'^2 l_s^2 \left(k\lambda U^2 + 1\right)\left(kU^2\lambda' + 1\right) + kU^4 \left(kU^2\mu + 1\right)}}, \\
&= -\sqrt{k} U_0 \sqrt{kU_0^2\mu + 1},
\end{aligned}
\tag{4.50}
$$

c_2 being a constant, we have used the boundary conditions at $x = 0$ to evaluate c_2, i.e. $U(0) = U_0$ and $U'(0) = 0$ to evaluate it.

Solving for $U'(x)$ and choosing the positive root,

$$U'(x) = \frac{U^2 \sqrt{k\mu U^2 + 1}\sqrt{k\mu \left(U^4 - U_0^4\right) + U^2 - U_0^2}}{U_0 l_s \sqrt{\left(k\lambda U^2 + 1\right)\left(k\lambda' U^2 + 1\right)}\sqrt{k\mu U_0^2 + 1}}. \tag{4.51}$$

To obtain the subregion size we integrate the above equation by specifying the appropriate limits of integration.

$$\int_0^x dx' = \int_{U_0}^U \frac{d\tilde{U}}{\tilde{U}'(x)}. \tag{4.52}$$

After the integration limits had been specified, the subregion size is given as the function of the turning point U_0 by:

$$L = \int_{U_0}^{\infty} dU \, \frac{dU}{U'(x)} \tag{4.53}$$

If we choose to look at deep linear dilatonic region, $(k\lambda U^2 >> 1)$ we obtain a simplification:

$$L = \frac{\pi\sqrt{k\lambda\lambda'}l_s}{2\sqrt{\mu}} + O\left(\frac{1}{U_0^2}\right). \tag{4.54}$$

However, we can only analytically solve for L perturbatively, but the characteristic features of subregion length in the linear dilaton region are immediately obvious. As we move U_0 closer to the boundary, L asymptotes to a constant value:

$$L_c = \frac{\pi\sqrt{k\lambda\lambda'}l_s}{2\sqrt{\mu}}. \tag{4.55}$$

This behaviour is typical of the theory having a Hagedorn phase transition as had already been alluded to before in the literature [106] in the context of the study of entanglement entropy.

For the sake of comparison and building intuition, we check that different special cases can indeed be reproduced from the general case equation (4.53) :

- **AdS (Case $\lambda = \epsilon_\pm = 0$):** The simplest of the all is the pure AdS geometry which has been the subject of an extensive study for which, the relation between the subregion length and the turning point is well known:

$$L = \frac{2l_s}{U_0}. \tag{4.56}$$

- **WAdS (Case $\lambda = \epsilon_+ = 0$):** The next case is when only the $J\overline{T}$ coupling is turned on. This case had also been thoroughly investigated and the gravity dual is warped AdS (WAdS) spacetime [**?**].

$$\int_0^{L/2} dx' = \int_{U_0}^{\frac{l_s}{\epsilon}} dU \, \frac{U_0 l_s \sqrt{1 - kU_0^2\epsilon_-^2}}{U^2\sqrt{1 - kU^2\epsilon_-^2}\sqrt{U^2 - U_0^2 + k\epsilon_-^2(-U^4 + U_0^4)}} \tag{4.57}$$

$$\Rightarrow L = \frac{2l_s}{U_0} + 2kU_0 l_s \epsilon_-^2 \ln\left(\frac{2l_s}{U_0\epsilon}\right) + O(\epsilon_-^4). \tag{4.58}$$

Upon turning off the coupling $(\epsilon_- \to 0)$, one simply recovers the pure AdS result.

- $\mathcal{M}_3$ **(Case $\epsilon_+ = \epsilon_- = 0$):** When only $T\overline{T}$ coupling is turned on,

$$\int_0^{L/2} dx' = \int_{U_0}^{l_s/\epsilon} dU \, \frac{U_0 l_s \sqrt{k\lambda U^2 + 1}\sqrt{k\lambda U_0^2 + 1}}{U^2\sqrt{(U^2 - U_0^2)(k\lambda(U^2 + U_0^2) + 1)}},$$

$$L = \frac{1}{2}\pi\sqrt{k\lambda}l_s + O\left(\frac{1}{U_0^2}\right), \tag{4.59}$$

we recover the result already encountered earlier in [103].

Alternatively, treating coupling as the perturbation parameter,

$$L = \frac{2l_s}{U_0} + k^2\lambda^2 U_0^3 l_s \ln\left(\frac{2l_s}{U_0\epsilon}\right) + O(\lambda^3). \tag{4.60}$$

With $\lambda \to 0$, we again recover the AdS result.

Thus we have successfully reproduced the features of the RT curves for the special cases of the pure AdS, warped AdS and the $\mathcal{M}_3$ from our general formula relating the RT curve turning point and the subregion length (4.53). We will use this relation to obtain the expression for the subregion volume complexity next. Now this will be done numerically since the analytic answer can only be obtained perturbatively. However we are not interested in perturbative answers, so will do this exactly but numerically. But just as we have done for the RT curve, before presenting the final results for the general case, we first perform sanity checks by studying various special cases where the effects of locality and Lorentz violation are removed and comparing those expressions to existing results in the literature obtained in the contexts where the boundary dual is a local CFT_2, instead of an LST_2.

4.4.1 Subregion volume (complexity) for $\lambda = \epsilon_\pm = 0$: Poincare patch of AdS$_3$

The first check is the maximal volume corresponding to the subregion size ($\mathcal{V}(L)$) for the simplest of the cases - pure AdS_{2+1}. This can be evaluated analytically exactly. The induced metric on a codimension-1 submanifold of a constant time slice is

$$ds^2 = \frac{kl_s^2}{z^2}(dz^2 + dx^2). \tag{4.61}$$

Then subregion volume is,

$$
\begin{aligned}
\mathcal{V}(L) &= \int_0^{l_s/\epsilon} dz \int_0^{x(z)} dx' e^{-2(\Phi(z) - \Phi_\infty)} \sqrt{\gamma}, \\
&= kl_s^2 \left(\frac{L}{2\epsilon} - \frac{\pi}{2} \right).
\end{aligned}
\tag{4.62}
$$

The linear UV divergence is expected of any lorentz covariant local CFT in one spatial dimension. This is a well known result [133].

4.4.2 Subregion volume complexity $\epsilon_\pm = 0$ ($T\overline{T}$ deformation or $\mathcal{M}_3$)

The next case that we are going to treat appropriately belongs to the subject matter of the preceding work [132] on pure $\mathcal{M}_3$ complexity. However the subregion complexity calculation did not appear there, therefore for the sake of completeness, we reproduce here the corresponding result for subregion complexity.

The pullback of the ambient metric on co-dim-1 surface bounded by the RT surface for the pure $\mathcal{M}_3$ case is:

$$ds^2 = kl_s^2 \frac{dU^2}{U^2} + h(U)dx^2. \tag{4.63}$$

The (maximal) volume corresponding to this subregion as the function of the turning point U_0 is given by:

$$
\begin{aligned}
\mathcal{V} &= \int_{U_0}^{l_s/\epsilon} dU \int_0^{x(U)} dx\, e^{-2(\Phi(U) - \Phi_0)} \sqrt{\gamma}, \\
&= kl_s \int_{U_0}^{l_s/\epsilon} dU \sqrt{1 + k\lambda U^2} \int_{U_0}^{U} \frac{d\tilde{U}}{\tilde{U}'(x)}.
\end{aligned}
\tag{4.64}
$$

We have to eliminate U_0 in favor of L to express the maximal volume in terms of subregion length. However if we insist on analytical expression, then the inversion can only be achieved iteratively. In order to not compromise on precision, we instead perform the calculations numerically to exhibit the quantitative features of the subregion complexity.

(a) $\mathcal{C}_V$ vs L for $\lambda = 1$ (b) $\mathcal{C}_V$ vs L for $\lambda = 10$ (c) $\mathcal{C}_V$ vs L for $\lambda = 100$
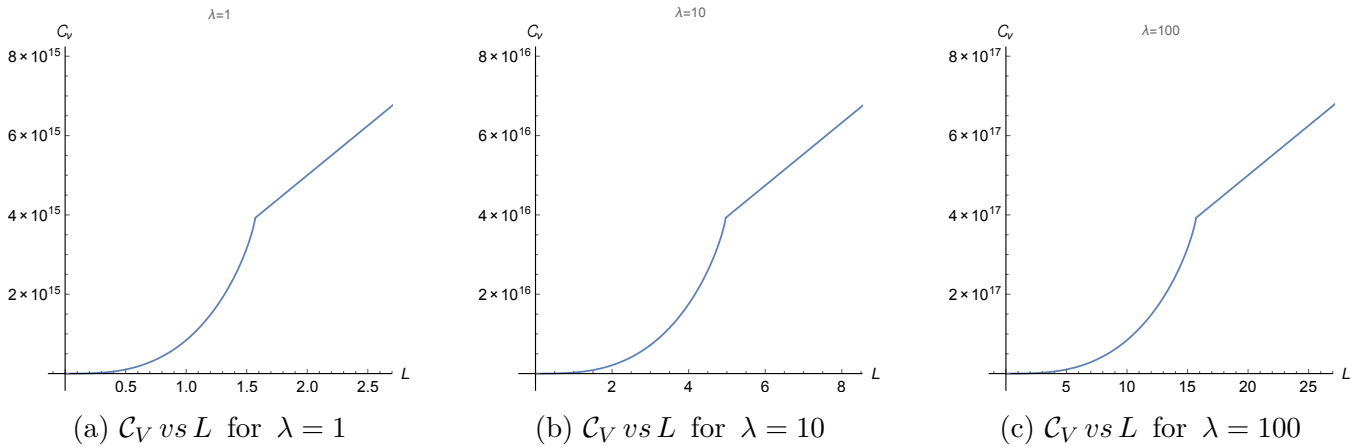
Figure 4.2: Subregion volume complexity ($\mathcal{C}_V$) vs. subregion size (L) graphs for $T\overline{T}$ deformed CFT$_2$ (LST) for different values of the deformation parameter ($T\overline{T}$ coupling) λ exhibiting Hagedorn phase transition. The critical suregion size at the transition point increases monotonically with λ.

We present the numerical plots demonstrating the dependence of complexity (modulo the factor of $8\pi G_N \sqrt{k}l_s$) on the subregion length L in Fig. 4.2 for three different values (differing order os magnitude) of λ, the $T\overline{T}$ deformation coupling parameter (differing orders of magnitude). In all the plots we observe the following universal traits

- The subregion volume complexity is a monotonically increasing function of the subregion size.

- The subregion volume complexity undergoes a sharp phase transition as the subregion size is increased beyond a certain critical size as depicted by the presence of a kink in each of the plots.

- Once the subregion size is larger than the critical subregion (kink), the subregion volume complexity grows linearly with subregion size. This is characteristic of the AdS geometry as pointed out in the previous subsection 4.4.1. The RT curve extends deep into bulk where the geometry is close to AdS$_3$.

- The parabolic portion of the curve, for subregion size (length) is less than the critical length, pertains to the linear dilaton region because that is where the subregion size slowly approaches to a constant value L_c regardless of the position of the turning point U_0 of the RT curve. The RT curve here remains stuck mostly in the deep UV region i.e. near the boundary.

The linear growth of the complexity with the subregion size when the subregion size is larger then the Hagedorn scale (see next section for more details) is plausible because in this situation the LST behaves more like a local CFT and the number of degrees of freedom in the Lorentz covariant local theory can be thought of as uniformly distributed along the boundary subregion. The kink signifies the termination of the linear dilaton geometry and bulk being subsequently taken over by the AdS geometry. It will turn out that same universal features will emerge when we introduce Lorentz violating effects in the system i.e. when the couplings $\epsilon_\pm$ are nonzero. In order to avoid repetition, we will leave further quantitative discussion to the next section where we tackle the case when Lorentz violating effects are turned on.

4.4.3 Subregion volume complexity for $T\overline{T}$, $J\overline{T}$ and $\overline{J}T$

Armed with the hints and insights from the previous sections for the various subcases (i.e. pure AdS and $\mathcal{M}_3$), we are now ready to tackle the most general case with both the locality violating, and Lorentz violating couplings turned on and obtain the general characteristics for the subregion volume complexity.

89

As was done in the previous section, we first record the pullback of the ambient metric on codimension two surface constant t surface bounded by RT curve for the general case of the non local as well as both of the lorentz violating couplings turned on is:

$$ds^2 = kl_s^2 \frac{dU^2}{U^2} + h(U)(1 - f(U)(\epsilon_+ + \epsilon_-)^2)dx^2. \tag{4.65}$$

The maximal volume arising from the above geometry is given by:

$$\begin{aligned}
\mathcal{V} &= \int_{U_0}^{l_s/\epsilon} dU \int_0^{x(U)} dx\, e^{-2(\Phi(U)-\Phi_0)}\sqrt{\gamma}, \\
&= kl_s \int_{U_0}^{l_s/\epsilon} dU \sqrt{1 + k\mu U^2} \int_{U_0}^U \frac{d\tilde{U}}{\tilde{U}'(x)}.
\end{aligned} \tag{4.66}$$

For the reasons alluded to earlier in the previous subsection, we again opt for a numerical approach to uncover the features of subregion complexity. The corresponding plots for $\mathcal{V}$ *vs* L (note that modulo the factor of $8\pi G_N \sqrt{k}l_s$, the complexity $\mathcal{C}_V$ and maximal slice volume $\mathcal{V}$ are the same) for various values of the Lorentz violating couplings against the fixed value of $\lambda = 170$, are appended below in Fig. 4.3. In all the plots we notice some features which are in common with the $\mathcal{M}_3$ ($T\overline{T}$ deformation) set up, namely

- The subregion volume complexity is a monotonically increasing function of the subregion size

- The subregion complexity undergoes a phase transition as the subregion size is varied. For small subregions, we encounter a parabolic growth up to a kink at some critical subregion length, followed by the linear growth which is characteristic of dual AdS geometry in the deep IR. The parabolic region of the curve corresponds to the UV region i.e. linear dilaton geometry because that is where, the subregion length slowly approaches zero.

- For fixed λ (i.e. nonlocality scale held fixed), the critical subregion size at the phase transition point in the plots increases (shifts rightwards) as the Lorentz-violating coupling ϵ_+ (ϵ_-) is increased. Interestingly the critical subregion size changes (increases) even if *just one* of the couplings ϵ_+ is made nonzero. We will keep this in mind when we are looking at the static frame complexity where it will turn out that the critical subregion size is a function of the product $\epsilon_+\epsilon_-$.

In order to facilitate comparisons, its convenient to scale all the diagrams in a single plot by plotting the logarithms of complexity (modulo the factor of $8\pi G_N \sqrt{k}l_s$) and the subregion size L. From the graphs, one can directly appreciate the appearance of the transition point L_c where the complexity characteristics transitions sharply from parabolic to the AdS like linear dependence. A phase transition in the holographic entanglement entropy as a function of subregion size for this same system has been shown in [106]. However, what is interesting is that, complexity not only undergoes an analogous phase transition, but that the subregion complexity phase transition **occurs at the exact same critical subregion length as that of the entanglement entropy phase transition**, as evident from table 4.1 displaying the numerical value of the critical length extracted from the plots and the theoretical expression for the critical subregion length for entanglement entropy (refer to Eq. (4.55)).
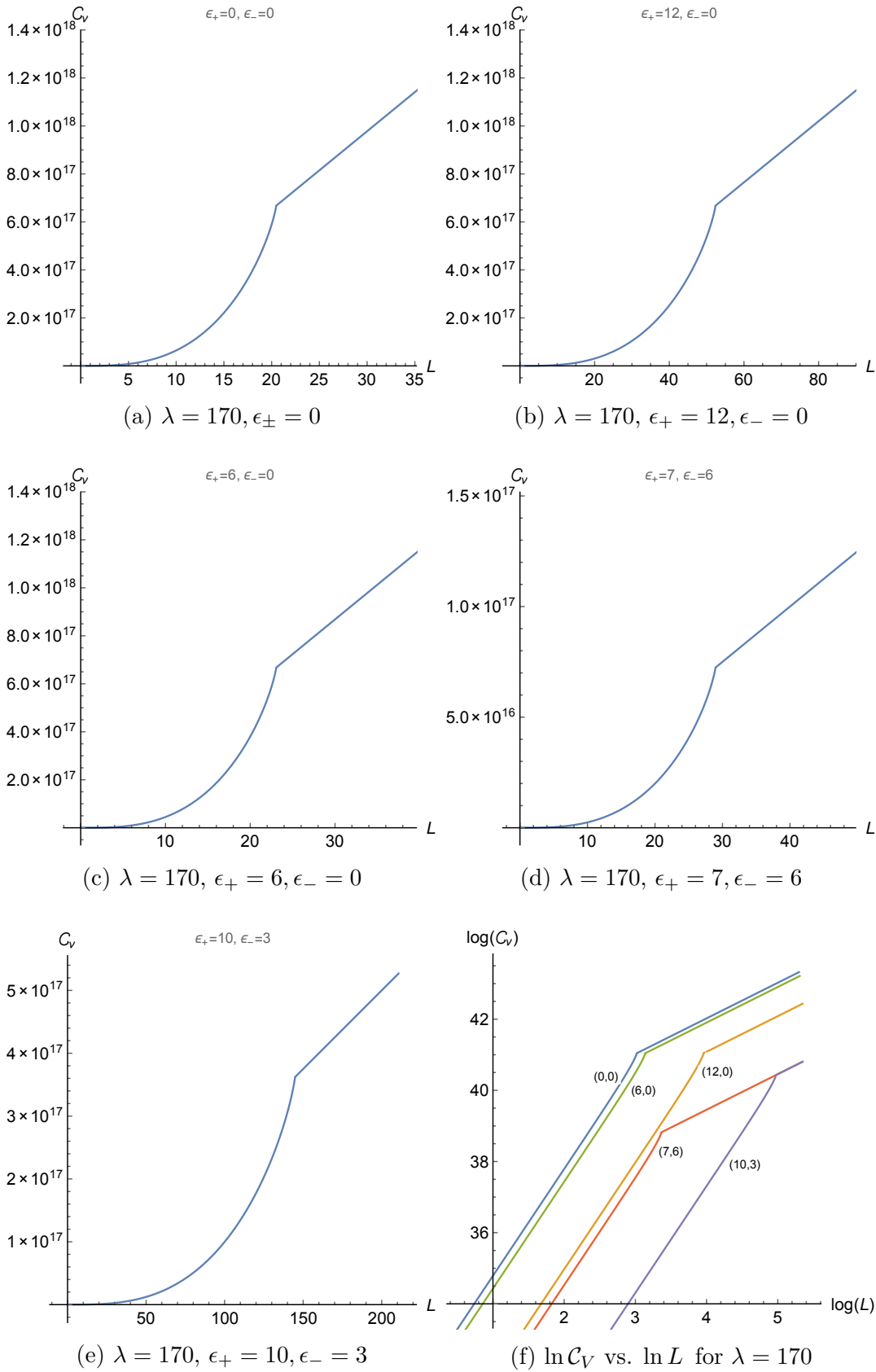
Figure 4.3: Subregion volume complexity ($\mathcal{C}_V$) vs. subregion size (L) graphs for $T\overline{T}$, $J\overline{T}$ & $\overline{J}T$ deformed CFT$_2$ (LST) for fixed values of the deformation parameter ($T\overline{T}$ coupling) $\lambda = 170$ exhibiting Hagedorn phase transition. The last plot is a log-log graph clearly displaying the scaling exponents (slopes).

Critical subregion size for complexity for $\lambda = 170$		
Lorentz violating couplings (ϵ_+, ϵ_-)	Entanglement entropy transition point length L_c (in units of AdS radius)	Subregion complexity transition point from graphs (in units of AdS radius)
(0,0)	20.48	20.47
(6,0)	23.06	23.05
(12,0)	52.37	52.33
(7,6)	28.96	28.94
(10,3)	144.82	144.9
(13,0)	267.03	266.84

Table 4.1: Table comparing the critical subregion size for phase transition in Entanglement entropy from theory and the critical subregion size for subregion volume complexity extracted from the plots

This fact that the subregion complexity undergoes a phase transition for the exact same the transition point (critical region size) as entanglement entropy, lends credence to the claim that complexity is a very effective physical observable (perhaps more useful that entanglement entropy) capable of detecting phase transitions (in the present case the Hagedorn phase transition) which perhaps cannot always be captured by usual field theory probes such as correlation functions of local operators.

4.4.4 Subregion volume complexity in static frame

Lorentz violating effects are our principal object of interest in this chapter and in particular for the system under study i.e. LST our aim is to disentangle the effects of Lorentz violating from nonlocality. One way to perhaps isolate the characteristics of complexity corresponding to Lorentz violating effects in field theories is to examine complexity in different inequivalent Lorentz (boosted) frames. With such hope in this section we compute subregion complexity in a boosted frame (static frame) Eq. (4.32). To determine the RT curve we will first need the pullback (γ_{ab}) of the static metric on the one dimensional prospective RT curve is

$$ds_\gamma^2 = \left(kl_s^2 \frac{U'^2}{U^2} + f(U) \right) dX^2. \tag{4.67}$$

The length functional for this curve, parameterized as $U = U(X)$, in the string frame is given by

$$\int dX \, \mathcal{L}\left(U(X), U'(X), X\right) = \int dX e^{-2(\Phi - \Phi_0)} \sqrt{\gamma} = \int dX \frac{kU^2}{\sqrt{f(U)h(U)}} \sqrt{kl_s^2 \frac{U'^2}{U^2} + f(U)}. \tag{4.68}$$

Employing the same set of steps employed in the previous section we first compute the integrals of motion.

$$C_2 = U' \frac{\partial \mathcal{L}}{\partial U'} - \mathcal{L} = -\frac{kU^3\sqrt{f(U)}}{\sqrt{h(U)}\sqrt{U^2 f(U) + kU'^2 l_s^2}} = -\frac{kU^3\sqrt{kU^2\lambda' + 1}}{\sqrt{kU'^2 l_s^2 \left(k\lambda U^2 + 1\right) + kU^4}} \tag{4.69}$$

Integrals of motion after applying boundary conditions $U(0)) = U_0$ and $U'(0) = 0$ at the turning point to the above equation is

$$C_2 = -\sqrt{k}U_0\sqrt{kU_0^2\lambda' + 1}. \tag{4.70}$$

Equating and solving for $U'(X)$ gives

$$U' = \frac{U\sqrt{f(U)}\sqrt{U^4 h(U_0) - U_0^4 h(U)}}{\sqrt{k}U_0^2\sqrt{h(U)}l_s} \tag{4.71}$$

Inverting this, the subregion size can be expressed in terms of the turning point U_0 as

$$L = 2\int_0^{L/2} dX = 2\int_{U_0}^{\infty} \frac{dU}{U'} = 2\sqrt{k}U_0^2 l_s \int_{U_0}^{\infty} \frac{\sqrt{h(U)}}{U\sqrt{f(U)}\sqrt{U^4 h(U_0) - U_0^4 h(U)}} \tag{4.72}$$

In the linear dilaton region, $(kU^2 >> 1)$, one can perturbatively solve the above equation to obtain

$$L = \frac{1}{2}\pi\sqrt{k\lambda}l_s + O\left(1/U_0^2\right) \tag{4.73}$$

This limiting value of L in the static frame, named L_c' gives critical length of the subregion at the point of Hagedorn phase transition

$$L_c' = \frac{1}{2}\pi\sqrt{k\lambda}l_s \tag{4.74}$$

This is the critical subregion size where entanglement entropy (RT curve) undergoes the Hagedorn phase transition in the static frame. An important thing to note here that despite the Lorentz violating couplings, $\epsilon_\pm$, being turned on this leading order expression is independent of $\epsilon_\pm$, and instead depends just on the nonlocality parameter λ. The issue of whether this is true to all orders will be settled After determining the RT curve, now we determine the subregion complexity as the string frame area of the co-dimension one maximal area spacelike surface bound from the inside by the RT curve. The (pullback) metric on the maximal area (spacelike) hypersurface is:

$$ds^2 = kl_s^2\frac{dU^2}{U^2} + f(U)dX^2. \tag{4.75}$$

Thus the maximal volume arising from the above hypersurface bounded between the RT curve and the boundary is:

$$\mathcal{V} = \int_{U_0}^{l_s/\epsilon} dU \int_0^{X(U)} d\tilde{X} e^{-2(\Phi(U)-\Phi_\infty)}\sqrt{\gamma} = kl_s \int_{U_0}^{l_s/\epsilon} dU\sqrt{1 + kU^2\lambda'}\int_{U_0}^{U} \frac{d\tilde{U}}{\tilde{U}'} \tag{4.76}$$

We again opt for exact but numerical means in computing the subregion volume (complexity) instead of an analytic but perturbative (approximate) approach. The plots for subregion complexity vs. subregion size for various representative values of the Lorentz violating couplings $\epsilon_\pm$ and a fixed value the $T\bar{T}$ coupling $\lambda = 170$ are displayed in figure (4.4).

(a) $\lambda = 170, \epsilon_\pm = 0$

(b) $\lambda = 170, \epsilon_+ = 6, \epsilon_- = 0$

(c) $\lambda = 170, \epsilon_+ = 12, \epsilon_- = 0$

(d) $\lambda = 170, \epsilon_+ = 7, \epsilon_- = 6$

(e) $\lambda = 170, \epsilon_+ = 10, \epsilon_- = 3$

(f) $\ln \mathcal{C}_V$ vs. $\ln L$ for $\lambda = 170$
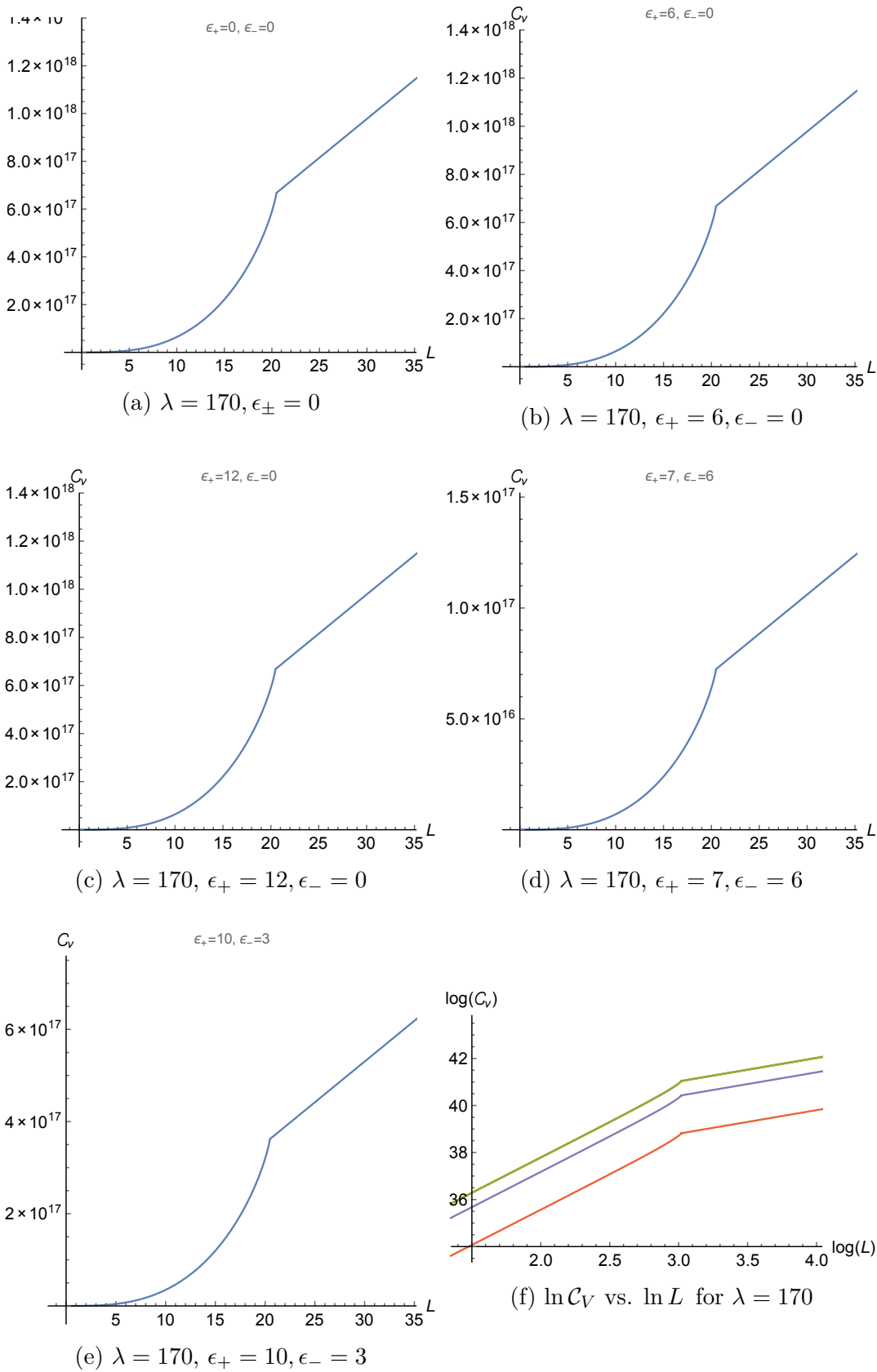
Figure 4.4: Static frame subregion volume complexity ($\mathcal{C}_V$) vs. subregion size (L) graphs for $T\overline{T}$, $J\overline{T}$ & $\overline{J}T$ deformed CFT$_2$ (LST) for fixed $\lambda = 170$ exhibiting Hagedorn phase transition. The last plot is a log-log graph clearly displaying the scaling exponents (slopes).

94

Here we list the salient features of these plots:

- Subregion volume complexity is a monotonically increasing function of the subregion size and it undergoes a phase transition as the subregion size is varied (just like subregion complexity in the stationary frame) beyond a certain critical length, which turns out to be L'_c of Eq. (4.74), i.e. the same critical subregion size at which entanglement entropy undergoes a phase transition (refer to table 4.2).

- For subregion size less than the critical size, L'_c, complexity grows quadratically with subregion size while for subregion sizes greater than L'_c, complexity grows linearly as evident from the log-log plot. The physics of this is the same as in that of the stationary frame - for small subregion sizes the RT curve is confined to the near boundary linear dilaton region, i.e. the deep UV regime of the boundary theor which is a nonlocal theory (LST on scales comparable to the string length scale), while for large subregion sizes the RT curve is well inside the bulk where the geometry is AdS, i.e. the deep IR regime of the boundary theory - LST on length scales far larger than the string scale and hence can be regarded as local CFT.

- Unlike in the stationary frame, in the static the critical subregion size at the transition point, extracted from the location of the kinks in the plots, does not change as the Lorentz violating couplings $\epsilon_\pm$ are varied while keeping the nonlocality scale λ fixed. Refer to the table This strongly hints that perhaps the static frame complexity is a probe which is better suited to isolate or extract the effects of nonlocality while the complexity in the stationary frame manifests a mixed characteristic of both nonlocality and Lorentz violation.

- When either one or both of Lorentz violating couplings $\epsilon_\pm$ vanish, their graphs overlap to overlap. This is potentially due to the fact that the static frame subregion complexity becomes effectively the function of $\lambda' = \lambda - 4\epsilon_+\epsilon_-$, so that it is insensitive to distinguish between the various values of λ' for vanishing value of the product $\epsilon_+\epsilon_-$. So the characteristic signatures of Lorentz violation in the divergence structure is the one which is accompanied by the coefficient $\epsilon_+\epsilon_-$.

Location of the critical length L_c for $\lambda = 170$		
Lorentz violating couplings (ϵ_+,ϵ_-)	Critical suregion size for entanglement entropy (EE) L'_c computed from Eq. (4.74)	Critical subregion size for subregion complexity in static frame extracted from $\mathcal{C}_V$-L graphs Fig. 4.4
(0,0)	20.48	20.47
(6,0)	20.48	20.48
(12,0)	20.48	20.49
(7,6)	20.48	20.48
(10,3)	20.48	20.48
(13,0)	20.48	20.48

Table 4.2: Table comparing the critical subregion size for phase transition in Entanglement entropy from theory and the critical subregion size for subregion volume complexity extracted from the plots in the static Lorentz frame

As before, in the case of stationary frame subregion complexity, here we find it instructive to supply the table listing the critical subregion size from the plots for various cases of Loerntz violating couplings at a fixed λ and compare it with the perturbatively calculated analytical estimate Eq. (4.74). It is evident

form table [4.2](#) subregion volume complexity displays a phase transition *at the exact same critical sub-region size* as that of entanglement entropy in the static frame. Thus, we can echo the same message from the end of the previous section regarding the utility of complexity as a physical probe for detecting phase transitions (perhaps even in those circumstances where other probes such as correlators of local operators might fail). However, unfortunately as long as λ remains nonzero it appears one cannot isolate the effects of Lorentz violation from nonlocality in this system (LST) in this static frame. In fact, to the contrary, what we have seen in this exercise is that even if $\epsilon_\pm$ are not both zero, but if the product $\epsilon_+\epsilon_-$ vanishes, then the subregion complexity phase transition point is a pure function of the the nonlocality scale λ i.e. in this boosted frame, the phase transition is independent of the Lorentz violating effects.

4.5 Holographic volume complexity of null WAdS$_3$

In this section we consider a special limit in the parameter space of the irrelevant couplings of the LST, for which the bulk dual is the null Warped AdS geometry, which is smoothly realised by sending $\lambda \to 0$ and one of the Lorentz violating coupling (say ϵ_-) to zero. In this limit, the (stationary frame) bulk metric Eq. [(4.17)](#) becomes,

$$ds^2 = kl_s^2 \frac{dU^2}{U^2} - h(U)\left(1 + f(U)\epsilon_-^2\right)dt^2 + 2h(U)f(U)\epsilon_-^2\,dt\,dx + h(U)\left(1 - f(U)\epsilon_-^2\right)dx^2 \qquad (4.77)$$

The Lorentz parameter ϵ_- can be identified with the warping parameter ϵ_-. The boundary theory in this case is a *warped* CFT [137, 138], a highly nonlocal Lorentz violating field theory with the CFT symmetry algebra now reduced to a product of Virasoro (left) and a $U(1)$ Kac-Moody algebra (right). In particular, for the null warped WAdS$_3$, the dual warped CFT is not UV complete, beyond a certain critical energy (deep UV) the theory is nonunitary since the energy spectrum is complex [105]. Although correlation functions are hard compute in this warped CFT, we demonstrate that this feature (UV incompleteness) easily captured by complexity.

4.5.1 Volume Complexity

The maximal volume spacelike slice does not need to be worked out afresh as it can treated as a special case of the stationary frame metric of the generic $T\overline{T}$, $J\overline{T}$-$\overline{J}T$ deformed bulk geometry. However this limit could be singular so instead of indirectly evaluating the volume (complexity) by taking the naive $\lambda, \epsilon_+ \to 0$ limit of the maximal volume expression of the string frame [(4.39)](#) (or complexity [(4.40)](#)) we compute the integral directly,

$$V_\Sigma(T) = L_x k l_s \int dU \sqrt{1 - \epsilon_-^2 kU^2} = \frac{L_x k l_s^2}{2\epsilon}\sqrt{1 - \frac{k\epsilon_-^2 l_s^2}{\epsilon^2}} + \frac{\sqrt{k}l_s L_x}{2\epsilon_-}\sin^{-1}\left(\frac{\sqrt{k}\epsilon_+ l_s}{\epsilon}\right)$$

$$\Rightarrow \mathcal{C}_V = \frac{L_x \sqrt{k} l_s}{2 G_N \epsilon}\sqrt{1 - \frac{k\epsilon_-^2 l_s^2}{\epsilon^2}} + \frac{L_x}{2\epsilon_- G_N}\sin^{-1}\left(\frac{\sqrt{k}\epsilon_- l_s}{\epsilon}\right) \qquad (4.78)$$

Here, we see that the resultant complexity, unlike for the generic case, [(4.27)](#), fails to remain real unless $\epsilon > \sqrt{k}l_s\,\epsilon_-$. Thus the UV cut off cannot be made arbitrarily small. This validates our faith that complexity successfully captures the UV incompleteness of the warped CFT dual to null warped AdS$_3$. In the limit of a small warping parameter ϵ_- (to be precise expanding in $\epsilon_-\sqrt{k}l_s/\epsilon$), the leading term is linearly divergent,

$$\mathcal{C}_V \sim \frac{L_x \sqrt{k} \, l_s}{G_N \, \epsilon} - \frac{L_x \left(\sqrt{k}l_s\right)^3 \epsilon_-^2}{6 G_N \, \epsilon^3} \qquad (4.79)$$

i.e. like a local field theory in one space dimensions (or pure AdS bulk)! Again this is a reflection that the UV regime (near boundary region) where the nonlocality effects kicks in is excluded from consideration. The complexity characteristics of Warped CFT in general from both the holographic and field theory methods has been taken up in greater detail in the next chapter.

4.5.2 Subregion volume complexity for null WAdS$_3$

Finally we work out the subregion volume complexity for the interesting special case of null warped AdS$_3$. In this case first the result will be obtained analytically in the approximation of small warping ϵ_- to underscore the fact that subregion complexity is a better probe of nonlocality in this example compared to other probes such as subregion entanglement entropy. Then the exact result will be presented by evaluating the subregion complexity integral numerically without any approximations. First, recall that In this case, the turning point of the RT surface (curve) in terms of the subregion size is already worked out by inverting (4.57),

$$U_0 = \frac{2l_s}{L} + \frac{8kl_s^3\epsilon_-^2}{L^3}\ln\left(\frac{L}{\epsilon}\right) + O(\epsilon_-^4) \tag{4.80}$$

In terms of the turning point, the subregion volume complexity calculation of null WAdS$_3$ is given by the nested integral,

$$C_V = \frac{\sqrt{k}l_s}{8\pi G}\int_{U_0}^{\frac{l_s}{\epsilon}} dU\sqrt{1-kU^2\epsilon_-^2}\int_{U_0}^{U} d\tilde{U}\frac{U_0\sqrt{1-kU_0^2\epsilon_-^2}}{\tilde{U}^2\sqrt{1-k\tilde{U}^2\epsilon_-^2}\sqrt{\tilde{U}^2-U_0^2+k\epsilon_-^2(-\tilde{U}^4+U_0^4)}} \tag{4.81}$$

$$= \frac{\sqrt{k}l_s}{8\pi G}\int_{U_0}^{\frac{l_s}{\epsilon}}\left[\frac{\sqrt{U^2-V^2}}{UV}-\left(\frac{kU\sqrt{U^2-U_0^2}}{2U_0}-kU_0\ln\left(\frac{U+\sqrt{U^2-U_0^2}}{U_0}\right)\right)\epsilon_-^2+O\left(\epsilon_-^4\right)\right]dU \tag{4.82}$$

$$= \frac{\sqrt{k}l_s}{8\pi G}\left[\left(1+\frac{4kl_s^2}{L^2}\epsilon_-^2\right)\frac{L}{2\epsilon}-\frac{kl_s^2L}{12\epsilon^3}\epsilon_-^2-\frac{\pi}{2}O\left(\epsilon_-^4\right)\right] \tag{4.83}$$

In order to get eqn (4.83), we have expanded the integrands in equation (4.81) in a Taylor series with respect to ϵ_-. In the above expression of C_V, we can clearly see that if we take the warping factor to be zero, equation (4.83) reproduces the subregion complexity for the pure AdS_3. For, pure AdS_3, we recover the expression for subregion volume complexity [133],

$$C_V = \frac{\sqrt{k}l_s}{8\pi G}\left[\frac{L}{2\epsilon}-\frac{\pi}{2}\right] \tag{4.84}$$

Another very important feature of this result (4.83) is that the subregion C_V (the divergence structure) reflects the nonlocal nature of the dual warped conformal field theory unlike the holographic entanglement entropy in the appendix B.3. While we are using a string background with all NS-NS sector fields turned on in the bulk, this local theory like divergence structure (linear divergence) of EE for Warped AdS$_3$ has been reported using other holographic backgrounds where the bulk theory is either topologically massive gravity (TMG) [139, 140] or new massive gravity (NMG) [141]. Thus in this example, we see that subregion complexity is a more sensitive or refined probe of nonlocality and Lorentz violation compared to entanglement entropy.

Next we present the plot[6] of Subregion C_V as a function of L in the figure below obtained by direct numerical evaluation of (4.81).

---

[6]We have used parametric plot function in mathematica here and used Eq. (4.57) for the expression of L as,

$$L = \int_{U_0}^{\frac{l_s}{\epsilon}} dU\frac{2U_0l_s\sqrt{1-kU_0^2\epsilon_-^2}}{U^2\sqrt{1-kU^2\epsilon_-^2}\sqrt{U^2-U_0^2+k\epsilon_-^2(-U^4+U_0^4)}} \tag{4.85}$$
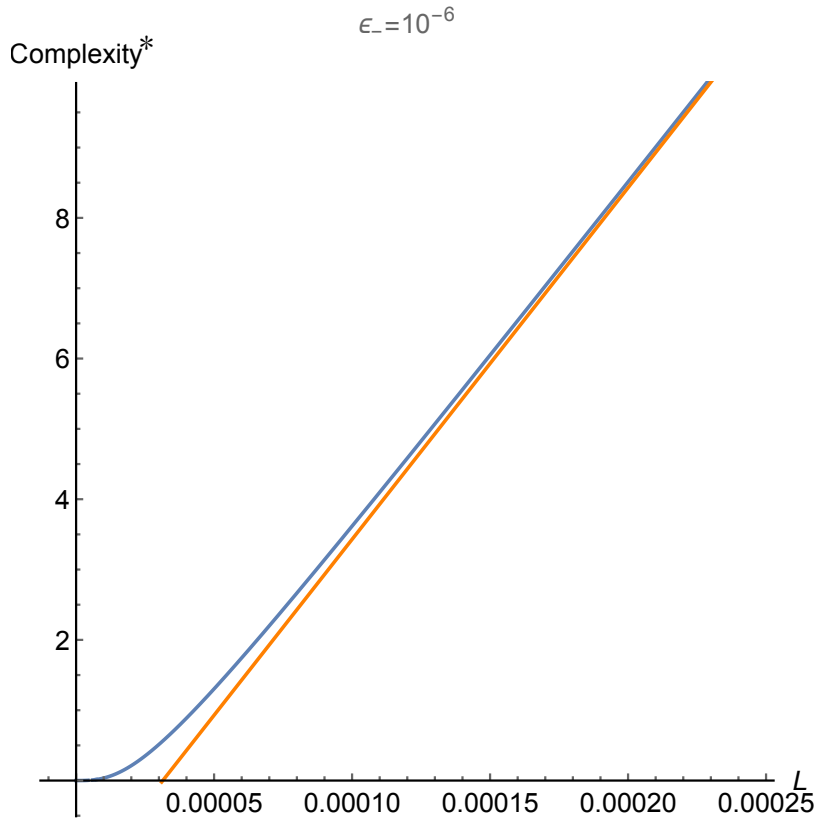
Figure 4.5: Subregion Volume Complexity vs L plot for null warped AdS$_3$. For this plot we have set $k = 10^4$, $l_s = 10^{-2}$ and $\epsilon = 10^{-5}$. Here, the y-axis represents $Complexity^* = Complexity \times 8\pi G_N$ while the x-axis is the subregion size L in units of the AdS radius ($\sqrt{k}l_s = 1.0$). The orange curve is the plot for pure AdS$_3$ while the blue curve is the plot for null WAdS$_3$.

The value of $\epsilon_- = 10^{-6}$ is used for this plot because from Eq. (4.78), it is clear that the value of ϵ_- has to be smaller than the value of ϵ. Also note that here, the y-axis is actually complexity scaled by the universal constant $8\pi G_N$. We summarize the salient features of this plot

- Subregion complexity monotonically increases as a function of the subregion size.

- Unlike in the case of generic nonvanishing λ, ϵ_+ the subregion complexity does not undergo any phase transition.

- The effect of nonlocality or Lorentz violation is very small in general and only prominent when the subregion is orders of magnitude smaller than the AdS radius. For larger generic subregion sizes the WAdS subregion $\mathcal{C}_V$ coincides with that for pure AdS$_3$ (this part needs to be discussed later.)

- Sensible plots are only obtained when the cut off $\epsilon > \epsilon_-$[7]. This is again a reflection of the fact that the dual boundary theory is not a UV complete theory, it is best thought of as an effective theory with the spectrum truncated at high energies.

One might ask whether one can switch to the static frame and evaluate the complexity of LST dual to null warped AdS$_3$ in the that frame just like it was done in the case of generic $J\overline{T}, \overline{J}T$ couplings to demonstrate/check for boost symmetry violation. However in this regard we would like to point out that boost transformation ((4.31)) is singular in the null warped AdS$_3$ limit, i.e. when $\epsilon_+ \to 0$. Thus neither

---

[7]To be precise one must keep $\epsilon > \epsilon_- \sqrt{k}l_s$ but here we have set $\sqrt{k}l_s = 1$ so effectively we must keep $\epsilon_- < \epsilon$

such a boost transformation and by extension, nor does a static frame exist for null warped AdS$_3$. In this special point of the parameter space, we will have to be content with the volume complexity, subregion volume complexity and action complexity in the stationary coordinate system exclusively.

4.6 Action complexity

In this section we compute the action complexity, $C_{\mathcal{A}}$, for the LST obtained by $T\overline{T}, J\overline{T}, \overline{J}T$ deformation of a CFT$_2$ using the holographic dual metric, dilaton and Kalb-Ramond background. Action complexity is an alternative prescription of holographically evaluating the dual boundary theory complexity which offers distinct advantages over volume complexity in that (A) no arbitrary length scales appearing in its definition, just the fundamental constants $\hbar$ and G_N, and (B) one does need to solve a variational problem which can be challenging exercise in general for Lorentzian signature spacetimes. Instead one just performs (action) integrals over the *WdW patch*. The WdW patch is defined as the union of all spacelike hypersurfaces in the bulk anchored at a fixed time slice on the boundary:

$$C_{\mathcal{A}} = \frac{S_{WdW}}{\pi\hbar} \ . \tag{4.86}$$

The Penrose diagram of the dual bulk geometry (upon suppressing the transverse boundary direction) is identical to that of the $\mathcal{M}_3$ spacetime, which was presented in our previous work [132]. For completeness, we reproduce the Penrose diagram here with the WdW patch displayed in pink
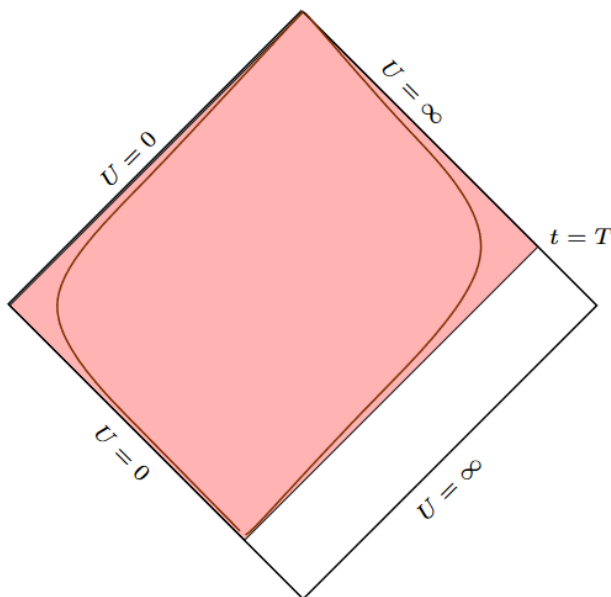
Figure 4.6: Penrose diagram of the dual bulk geometry with the Wheeler-deWitt (WdW) patch shaded in pink for the boundary time T. The brown curves are timelike surfaces which can be continuously deformed into the null boundaries of the WdW patch by means of a regulator parameter.

The bulk action in the string frame is:

$$S = \frac{1}{16\pi G_N} \int_M d^{d+1} X \sqrt{-g} e^{-2(\Phi-\Phi_0)} \left(R + 4g^{\mu\nu}\partial_\mu\Phi\partial_\nu\Phi - \frac{H^2}{12} - 4\Lambda \right)$$
$$+ \frac{1}{8\pi G_N} \int_{\sum \partial M} \sqrt{\gamma} \left(\cdots \right) + \frac{1}{8\pi G_N} \int_{\cap \partial M} \sqrt{h} \left(\cdots \right) . \tag{4.87}$$

The $(\cdots)$'s represent the supplementary surface/boundary $(\cup\partial M)$ terms and joint $(\cap\partial M)$ terms necessary for the variation of the action to be well defined, as well as reparametrization invariant. Since (some) boundaries of the WdW patch are null, the usual GHY terms are not the suitable ones. The issue of determining the boundary terms for null boundaries was settled in [76]. However, we will take an alternative prescription spelled out in [75][8] where the null boundaries of the WdW patch are first deformed into a single smooth timelike surface using a deformation parameter (regulator), and then we are free to use the usual GHY term. After working out the GHY term we remove the regulator and obtain the result for the null WdW boundary. This affords an enormous simplification as it eliminates the necessity to compute the joint terms (terms in the action from joints or edges along which two null surfaces intersect) as well as preserving diffeomorphism and reparametrization invariance of the GHY contribution from beginning to end. Our regularization reproduces the same results as the prescription of [76] for the well known cases of pure AdS, AdS-Schwarzschild, AdS-RN etc. but the status of the equivalence of these two prescriptions for arbitrary generic geometries is yet unexplored. In general the issue of different regularization prescriptions is still being investigated e.g. for a comparison of the two regularizations introduced in [73], see [108, 109].

Unlike for the $\mathcal{M}_3$ case, here one has to make a choice here: one can either work with the full 4 dimensional bulk action, or one might dimensionally reduce (over the y-direction fiber) and work with an effective 3 dimensional bulk action. While computing the entanglement entropy for this system, the authors of [106] found that the 4d and 3d results disagree and they opted to work with the full 4d bulk. Happily for us, it turns out that both 4d and 3d actions deliver identical results for complexity, *provided one does not drop the total derivative terms in the dimensionally reduced action.* Conventionally in the literature these total derivative terms are dropped since they do not contribute to the classical equations of motion. However while computing complexity these terms do contribute and one cannot discard them if the complexity before and after dimensional reduction has to match. In appendix Sec. **??**, the KK reduction is reviewed and the exact match between the 4D and 3D actions is carried out after retaining all total derivative terms in the dimensionally reduced (3D) action.

$$
\begin{aligned}
S_{(3D)} = \frac{1}{16\pi G_N} \int d^3x \sqrt{-g}\, e^{-2(\Phi-\Phi_0)} \Big(& R - (\partial\sigma)^2 - 2\,\Box\sigma - \frac{1}{4}e^{2\sigma}\mathcal{F}^2 - 4\Lambda \\
& + 4g^{\mu\nu}\partial_\mu\Phi\partial_\nu\Phi + 4g^{\mu\nu}\partial_\mu\Phi\partial_\nu\sigma \\
& - \frac{1}{12}\widetilde{H}^2 - \frac{1}{4}e^{-2\sigma}\widetilde{F}^2 \Big).
\end{aligned}
\tag{4.88}
$$

It is evident that after dimensionally reducing to 3 dimensions the KK scalar, σ contributes to the action a term which has a second order derivative, namely $\Box\sigma$ (This is a total derivative term which is usually dropped). This will also to lead an extra contribution to the surface terms (GHY terms) in the string frame, apart from the usual GHY surface term arising from the metric. The full surface term contribution for the $2+1$-dimensional bulk in string frame is

$$
S_{GHY} = \frac{1}{8\pi G_N} \int d^2x \sqrt{-\gamma}\, e^{-2(\Phi-\Phi_0)} \left(K + n^\mu\partial_\mu\sigma \right)
\tag{4.89}
$$

For the derivation, the reader may refer to Sec. B.2. For the action complexity calculation, in the first order of business is to determine the WdW patch, i.e. the light cones emanating from the boundary timeslice. However, solving the WdW patch is very complicated in the stationary frame coordinates (4.17) where constant t surfaces are not orthogonal to the vector $\partial/\partial t$. Life is much simpler in the static frame coordinates (4.32) as the constant T surfaces are orthogonal to the time direction vector $\partial/\partial T$. So we perform the action complexity calculation exclusively in the static frame (4.32).

---

[8]see also [77].

Volume (EH) pieces of the onshell action

In this section we present the volume piece contributions ("EH terms") to the action complexity using the dimensionally reduced $2 + 1$-dimensional background. As mentioned previously, the evaluation of the gravitational action ("EH terms") in the string frame in 4 dimensional and the dimensionally reduced 3 dimensional backgrounds give identical results, for this equivalence, the reader is referred to the Sec. B.1.2.

First we have to determine the WdW patch. The calculation is most straightforward in the static coordinates (T, X, U) because the lightcones are easy to determine. The Wheeler-deWitt patch (WdW) for the boundary time $T = T_*$ is bounded by the null rays

$$dt_{\pm} = \mp \sqrt{k}\, l_s \frac{1}{U\sqrt{h(U)}} dU, \tag{4.90}$$

obeying boundary condition, $T(U \to \infty) = T_*$. The T-integrals in the volume terms (4.88) (Einstein-Hilbert plus matter type terms) can be readily done:

$$T_+(U) - T_-(U) = 2\sqrt{k}\, l_s \int_U^{\infty} d\tilde{U} \frac{1}{\tilde{U}\sqrt{h(\tilde{U})}} \ . \tag{4.91}$$

This integral is divergent and hence we will modify our WdW patch to begin at a UV-cutoff surface $U = l_s/\epsilon$ instead of spatial infinity:

$$T_+(U) - T_-(U) = 2\sqrt{k}\, l_s \int_U^{l_s/\epsilon} d\tilde{U} \frac{1}{\tilde{U}\sqrt{h(\tilde{U})}} \ . \tag{4.92}$$

Having determined the WdW patch, we list the various bulk action term contributions (4.88) along with their UV and IR limits are listed as follows.

The Ricci scalar sector term: These terms are from the 4 dimensional Ricci scalar or equivalently in 3 dimensions from the full KK reduced sector derived from the 4 dimensional metric. For details the reader is referred to Sec. B.1.2.

$$\begin{aligned} S_R &\equiv \frac{1}{16\pi G_N} \int_{WdW} d^3x \sqrt{-g}\, e^{-2(\Phi - \Phi_0)} \left(R^{(3)} - 2\left(\partial\sigma\right)^2 - 2\Box\sigma - \frac{1}{4}e^{2\sigma}\mathcal{F}^2 \right), \\ &= \frac{L_x k}{8\pi G_N} \int_0^{l_s/\epsilon} dU\, U \frac{(8\lambda'kU^2 - 6)}{(\lambda'kU^2 + 1)^2} \int_U^{l_s/\epsilon} dU' \frac{1}{U'\sqrt{h(U')}} \ . \end{aligned} \tag{4.93}$$

The above integral can be performed analytically but the full expression is a bit cumbersome. In the deep UV (when $\epsilon/\beta_H \ll 1$), S_R takes the following form

$$\begin{aligned} \lim_{\epsilon/\beta_H \ll 1} S_R = &-\frac{cL_x}{6\beta_H'}(7 + 8\log 2)\log\left(\frac{\beta_H'}{\pi\epsilon}\right) + \frac{2cL_x}{3\beta_H'}\log^2\left(\frac{\beta_H'}{\pi\epsilon}\right) \\ &+ \frac{L_x c}{18\beta_H'}(\pi^2 + 24\log 2) + O\left(\left(\frac{\epsilon}{\beta_H'}\right)^2\right) \ . \end{aligned}$$

In the IR (when $\epsilon/\beta_H \gg 1$), S_R takes the form

$$\lim_{\epsilon/\beta_H \gg 1} S_R = -\frac{cL_x}{4\pi\beta_H'}\frac{\beta_H'}{\epsilon} + \frac{7cL_x}{288\pi^3\beta_H'}\left(\frac{\beta_H'}{\epsilon}\right)^3 + O\left(\left(\frac{\beta_H'}{\epsilon}\right)^4\right) \ . \tag{4.94}$$

The dilaton kinetic term in the action: We refer the reader to Sec. B.1.2 for the details.

$$\begin{aligned} S_\Phi &\equiv \frac{1}{16\pi G_N} \int_{WdW} d^3x \sqrt{-g}\, e^{-2(\Phi - \Phi_0)} 4g^{\mu\nu}\partial_\mu\Phi\partial_\nu\Phi, \\ &= \frac{\lambda'^2 k^3 L_X}{2\pi G_N} \int_0^{\frac{l_s}{\epsilon}} dU \frac{U^5}{(1 + \lambda'\, kU^2)^2} \int_U^{\frac{l_s}{\epsilon}} \frac{dU'}{U'\sqrt{h(U')}}. \end{aligned} \tag{4.95}$$

In the UV regime, S_Φ takes the following form:

$$\lim_{\epsilon \ll \beta'_H} S_\Phi = \frac{cL_x}{24\pi^2\beta'_H}\left(\frac{\beta'_H}{\epsilon}\right)^2 + (3 + 8\ln 2)\frac{cL_x}{6\beta'_H}\ln\left(\frac{\beta'_H}{\pi\epsilon}\right) - \frac{2cL_x}{3\beta'_H}\ln^2\left(\frac{\beta'_H}{\pi\epsilon}\right)$$
$$+ \left(3 - 2\pi^2 - 48\ln 2\right)\frac{cL_x}{36\beta'_H} + O\left(\frac{\epsilon}{\beta'_H}\right)..$$

(4.96)

One might be a bit alarmed at the appearance of the "log squared" divergences in the expressions (4.94) and (4.96), which did not arise in the volume complexity cases but as it will turns out, such log squared divergent contributions will cancel out among each other.

In the IR, S_Φ takes the form

$$\lim_{\epsilon/\beta_H \gg 1} S_\Phi = 0 + O\left(\beta_H^5/\epsilon^5\right) .$$

(4.97)

The cosmological constant term in the action: The details are worked out in Sec. B.1.2. Here we present the main results starting from the 3 dimensional action,

$$S_\Lambda \equiv \frac{1}{16\pi G_N}\int d^3x\sqrt{-g}e^{-2(\Phi-\Phi_0)}\left(-4\Lambda\right),$$
$$= \frac{L_x k}{2\pi G_N}\int_0^{l_s/\epsilon} dU\, U\int_U^{l_s/\epsilon} dU'\frac{1}{U'\sqrt{h(U')}} .$$

(4.98)

In the UV, S_Λ takes the following form

$$\lim_{\epsilon/\beta'_H \ll 1} S_\Lambda = \frac{c}{24\pi^2}\frac{L_x}{\beta'_H}\left(\frac{\beta'_H}{\epsilon}\right)^2 + \frac{c}{6}\frac{L_X}{\beta'_H}\ln\left(\frac{\beta'_H}{\pi\epsilon}\right) + \frac{c}{12}\frac{L_x}{\beta'_H} + O\left(\frac{\epsilon}{\beta'_H}\right) .$$

(4.99)

In the IR, S_Φ takes the form

$$\lim_{\epsilon \gg \beta_H} I_\Lambda = \frac{cL_x}{6\pi\epsilon} + \frac{cL_x}{144\pi^3\beta'_H}\left(\frac{\beta'_H}{\epsilon}\right)^3 + O\left(\left(\frac{\beta'_H}{\epsilon}\right)^5\right).$$

(4.100)

The Kalb-Ramond term in the action: Finally the spacetime volume type contribution from the Kalb-Ramond field in 4 dimensions or the full Kalb-Ramond derived fields in 3 dimensions after dimensional reduction (a Kalb-Ramond two-form field and a Kalb-Ramond one-form gauge field). The details including the matching before and after dimensional reduction are worked out in the appendix Sec. B.1.2. The main results starting with the action piece are presented here,

$$S_H \equiv \frac{1}{16\pi G_N}\int d^3x\,\sqrt{-g}e^{-2(\Phi-\Phi_0)}\left(-\frac{1}{12}\widetilde{H}^2 - \frac{1}{4}e^{-2\sigma}\widetilde{F}^2\right),$$
$$= \frac{L_x}{4\pi G_N k}\int dU\frac{h^2(U)}{U^3}\int_U^{\frac{l_s}{\epsilon}} dU'\frac{1}{U'\sqrt{h(U')}} .$$

(4.101)

In the UV, S_H takes the following form

$$\lim_{\epsilon/\beta_H \ll 1} S_H = \frac{cL_x}{6\beta'_H}\ln\left(\frac{\beta'_H}{\pi\epsilon}\right) + O\left(\frac{\epsilon}{\beta'_H}\right).$$

(4.102)

In the IR, S_H takes the form

$$\lim_{\epsilon/\beta_H \gg 1} S_H = \frac{cL_x}{12\pi\beta'_H}\left(\frac{\beta'_H}{\epsilon}\right) - \frac{cL_x}{288\pi^3\beta'_H}\left(\frac{\beta'_H}{\epsilon}\right)^3 + O\left(\left(\frac{\beta'_H}{\epsilon}\right)^5\right).$$

(4.103)

Action Contributions from the null boundaries of the WdW patch.

The WdW patch action receives surface contributions (GHY terms) from the boundaries of the WdW patch. The Poincaré horizon and the two joint terms (intersection of the null boundaries of the WdW patch with the Poincaré horizon) make vanishing contributions. The only non trivial contribution comes from the two null boundaries of the WdW patch.

The null boundaries of the WdW patch are defined by

$$(T - T_*) = \mp \sqrt{k} l_s A(U) ; \quad \text{where} \quad A(U) = \int_{l_s/\epsilon}^{U} \frac{d\tilde{U}}{\tilde{U}\sqrt{h(\tilde{U})}} . \tag{4.104}$$

However, we will deform the pair of null surfaces to a single smooth timelike surface by introducing a dimensionless parameter, ε,[9]

$$\frac{(T - T_*)^2}{kl_s^2} - (1 + \varepsilon)A^2(U) = 0 . \tag{4.105}$$

Taking differentials of both sides leads to,

$$h(U)dT^2 = (1 + \varepsilon)kl_s^2 \frac{dU^2}{U^2} . \tag{4.106}$$

Using (4.106), the induced metric on this timelike surface can be written as

$$ds^2 = -\varepsilon kl_s^2 \frac{dU^2}{U^2} + h(U)(1 - 4\epsilon_+\epsilon_-f(U))dX^2 . \tag{4.107}$$

The negative sign in the first term clearly indicates that this is a timelike surface. The unit outward normals to the surface (4.105) are,

$$n^T = \frac{-(T - T_*)}{\sqrt{(1 + \varepsilon)^2 A^2(U) - \frac{(T-T_*)^2}{kl_s^2}}} \frac{1}{\sqrt{k}l_s\sqrt{h(U)}}, \quad n^U = \frac{-(1 + \varepsilon)A(U)}{\sqrt{(1 + \varepsilon)^2 A^2(U) - \frac{(T-T_*)^2}{kl_s^2}}} \frac{U}{\sqrt{k}l_s}, \quad n^X = 0. \tag{4.108}$$

The trace of the extrinsic curvature,

$$K \equiv \nabla_L n^L = \partial_L n^L + \Gamma_{LM}^L n^M = \partial_T n^T + \partial_U n^U + \Gamma_{LU}^L n^U , \tag{4.109}$$

takes the form

$$K = \frac{1}{\sqrt{\varepsilon}\sqrt{k}l_s(1 + kU^2\lambda)} + \frac{1}{\sqrt{\varepsilon}\sqrt{k}l_s(1 + kU^2\lambda')} . \tag{4.110}$$

Thus the GHY term for this surface in the null limit ($\varepsilon \to 0$) is

$$S_{GHY}^{\partial WdW} = \frac{1}{8\pi G_N} \int_{\partial WdW} d^2x \sqrt{-\gamma}e^{-2(\Phi-\Phi_0)} (K + n^\mu \partial_\mu \sigma),$$

$$= \lim_{\varepsilon \to 0} \frac{L_x\sqrt{k}}{4\pi G_N} \int_0^{l_s/\epsilon} \frac{dU}{\sqrt{1 + kU^2\lambda'}} ,$$

$$= \frac{cL_x}{3\beta_H'} \ln \left(\sqrt{1 + \frac{\beta_H'^2}{4\pi^2\epsilon^2}} + \frac{\beta_H'}{2\pi\epsilon} \right) .$$

In the UV, $S_{GHY}^{\partial WdW}$ diverges as

$$\lim_{\epsilon/\beta_H \ll 1} S_{GHY}^{\partial WdW} = \frac{L_xc}{3\beta_H'} \ln \left(\frac{\beta_H'}{\pi\epsilon} \right) + O\left(\epsilon/\beta_H' \right) . \tag{4.111}$$

In the IR one can write

$$\lim_{\epsilon/\beta_H \gg 1} S_{GHY}^{\partial WdW} = \frac{L_xc}{6\pi\beta_H'} \left(\frac{\beta_H'}{\epsilon} \right) - \frac{L_xc}{144\pi^3\beta_H'} \left(\frac{\beta_H'}{\epsilon} \right)^3 + O\left(\beta_H'^4/\epsilon^4 \right) . \tag{4.112}$$

---

[9]This is distinct from the UV regulator, ϵ.

4.6.1 Action Complexity

Putting together all the pieces, the full on-shell action over the WdW patch is obtained by summing over the contributions (4.93),(4.95),(4.98),(4.101), and (4.111). In the UV regime or the linear dilaton region (when $\epsilon/\beta_H \ll 1$), the action complexity (obtained by summing over the contributions (4.94),(4.96), (4.99),(4.102),and (4.111)) diverges as

$$C_{\mathcal{A}} = \frac{L_x c}{3\pi^2 \beta_H} \left[\frac{\beta_H^2}{2\pi\epsilon^2} - 2\pi \log\left(\frac{\beta_H}{\pi\epsilon}\right) + \pi + O\left(\frac{\epsilon}{\beta_H}\right) \right]. \tag{4.113}$$

Comparison this action complexity result with the (static frame) volume complexity expression (4.43) reveals that the leading divergence structure (the quadratic divergent term) and the constant term in both cases are identical. The subleading logarithmic divergences differ by a negative sign. In the IR (when $\epsilon/\beta_H \gg 1$) the action complexity takes the form

$$\lim_{\epsilon/\beta_H \gg 1} C_{\mathcal{A}} = \frac{cL_x}{18\pi^3 \beta_H} \left(\frac{\beta_H}{\epsilon}\right)^2 + O\left(\beta_H^5/\epsilon^5\right) . \tag{4.114}$$

Thus in pure AdS_3 the action complexity goes to zero. This is in precise agreement with the analysis performed in [74], a dimensional accident (there is a coefficient $C_d = d - 2$ in the pure AdS_{d+1} complexity). Unlike the volume complexity, the action complexity decreases faster. A comparison between volume complexity and action complexity is presented in figure 4.7.
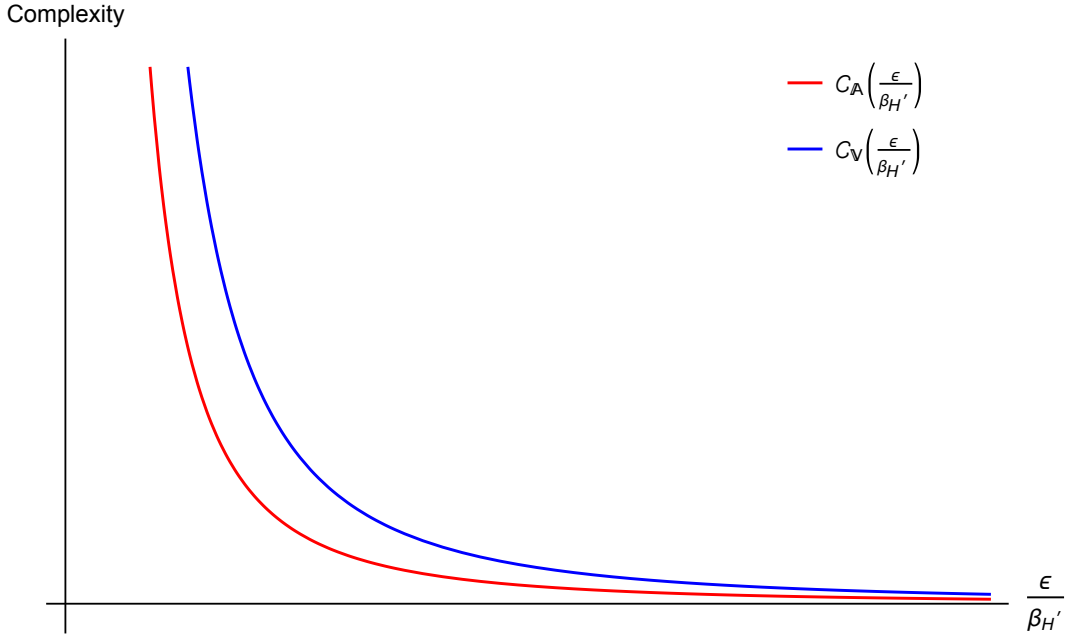
Figure 4.7: Comparison between C_V and $C_{\mathcal{A}}$ at zero temperature. For large ϵ/β_H, the action complexity decays much faster than volume complexity.

Thus overall, both the volume complexity and the action complexity diverges quadratically in the UV (when $\epsilon/\beta_H \to 0$). However, as ϵ/β_H increases, the action complexity decreases (much faster than volume complexity) monotonically eventually going to 0 in the deep IR. This discrepancy can be traced back to the boundary being $1 + 1$ dimensional, the action complexity has a coefficient $C_d = d - 2$. But in general it is understood that complexity is arbitrary or ambiguous up to such numerical factors and in general dimensions the volume and action complexity divergences will match both in the UV and IR.

4.7 Action Complexity for null WAdS$_3$

We conclude this work by presenting the results for the action complexity of the null warped AdS$_3$ defined by the limit $\lambda = \epsilon_+ = 0$. We refrain from taking this (singular) limit directly in the action complexity expressions e.g. in (6.2), and instead work it out from scratch to be rigorous. This time dilaton field is simply a constant $e^{2\Phi} = g_s^2$, which points out to the fact the dual boundary theory, a WCFT has a scale (Weyl) symmetry.

The null WAdS$_3$ metric in stationary coordinates is

$$ds^2 = k\, l_s^2 \frac{dU^2}{U^2} - kU^2 \left(1 + kU^2\epsilon_-^2\right) dt^2 + 2\left(kU^2\right)^2 \epsilon_-^2\, dt\, dx + kU^2 \left(1 - kU^2\epsilon_-^2\right) dx^2.$$

First we reorganize the null WAdS$_3$ metric in the form

$$ds^2 = \frac{kU^2}{1 - kU^2\epsilon_-^2} \left[\frac{l_s^2 \left(1 - kU^2\epsilon_-^2\right)}{(U^2)^2} dU^2 - dt^2 \right] + kU^2 \left(1 - kU^2\epsilon_-^2\right) \left[dx + \frac{kU^2\epsilon_-^2}{1 - kU^2\epsilon_-^2} dt \right]^2. \tag{4.115}$$

So the light rays ($ds^2 = 0$) are then given by the equations/conditions,

$$dt^2 = \frac{l_s^2 \left(1 - kU^2\epsilon_-^2\right)}{(U^2)^2} dU^2,$$

$$dx = -\frac{kU^2\epsilon_-^2}{1 - kU^2\epsilon_-^2} dt.$$

These equations can be simultaneously solved by

$$t_\pm(U) = T_0 \pm l_s \int_U^{l_s/\epsilon} dU \, \frac{\sqrt{1 - kU^2\epsilon_-^2}}{U^2}, \tag{4.116}$$

$$x_\pm(U) = x_0 \mp k\, l_s\epsilon_-^2 \int_U^{l_s/\epsilon} \frac{dU}{\sqrt{1 - kU^2\epsilon_-^2}}. \tag{4.117}$$

Here the $\pm$ refer to the future and past directed light rays starting from the cutoff surface at $x = x_0, t = T_0$. The WdW patch boundary at time T_0 is then described by the null surface obtained by the collection of null rays obtained by varying U and x_0. Assuming the range of x is from $[-L_x/2, +L_x/2]$, one sees that for a fixed U,

$$dx = dx_0.$$

As a result for the spacetime volume terms in the action (Ricci, cc, Kalb-Ramond piece etc.) the ranges of integration are

$$\int dx = \int dx_0 = L_x \ ,$$

and

$$\int_{t_-(U)}^{t_+(U)} dt = 2l_s \int_U^{l_s/\epsilon} dU \, \frac{\sqrt{1 - kU^2\epsilon_-^2}}{U^2}. \tag{4.118}$$

4.7.1 Bulk Action terms

The supergravity action we are going to evaluate in the volume is

$$S = \frac{1}{16\pi G_N} \int dU dt dx \sqrt{-g}\, e^{-2(\Phi(U)-\Phi(0))} \left(R - 4\Lambda - \frac{1}{12}\tilde{H}^2 + 4g^{\mu\nu}\partial_\mu\Phi\partial_\nu\Phi \right) \ .$$

Integral measure appearing in the string frame metric turns out to be

$$e^{-2(\Phi(U)-\Phi_0)}\sqrt{-g} = k^{3/2} l_s U \ .$$

- **Einstein Hilbert term in the action**

$$S_{EH} = \frac{1}{16\pi G_N} \int dU \, dt \, dx \sqrt{-g} \, e^{-2(\Phi(U)-\Phi(0))} \left(R - 4\Lambda \right) \ ,$$

$$= \frac{-\sqrt{k} L_x}{4\pi G_N} \int dU \, U \int_U^{l/\epsilon} dU' \frac{\sqrt{1 - \epsilon_-^2 \, k U'^2}}{U'^2} \ ,$$

$$= -\frac{c L_x}{24\pi \sqrt{k} \epsilon_- l_s} \left(\frac{\sqrt{k} \epsilon_- l_s}{\epsilon} \sqrt{1 - \frac{k \epsilon_-^2 l_s^2}{\epsilon^2}} + \sin^{-1}\left(\frac{\sqrt{k} \epsilon_- l_s}{\epsilon} \right) \right) \ . \tag{4.119}$$

- **Kalb Ramond term in the action**

$$S_{KR} = \frac{1}{16\pi G_N} \int dU \, dt \, dx \sqrt{-g} \, e^{-2(\Phi(U)-\Phi(0))} \left(-\frac{1}{12} \tilde{H}^2 \right) \ ,$$

$$= \frac{-L_x \sqrt{k}}{4\pi G_N} \int dU \, U \int_U^{l_s/\epsilon} dU' \frac{\sqrt{1 - \epsilon_-^2 \, k U'^2}}{U'^2} \ ,$$

$$= -\frac{c L_x}{24\pi \sqrt{k} \epsilon_- l_s} \left(\frac{\sqrt{k} \epsilon_- l_s}{\epsilon} \sqrt{1 - \frac{k \epsilon_-^2 l_s^2}{\epsilon^2}} + \sin^{-1}\left(\frac{\sqrt{k} \epsilon_- l_s}{\epsilon} \right) \right) \tag{4.120}$$

- **Dilaton term in the action**

$$S_{KR} = \frac{1}{16\pi G_N} \int dU \, dt \, dx \sqrt{-g} \, e^{-2(\Phi(U)-\Phi(0))} \left(4 g^{\mu\nu} \partial_\mu \Phi \partial_\nu \Phi \right) \ . \tag{4.121}$$

On account of dilaton being trivially a constant, the dilaton has vanishing contribution towards the gravitational action.

- **Gravitational action volume contribution**

$$S = \frac{1}{16\pi G_N} \int dU \, dt \, dx \sqrt{-g} \, e^{-2(\Phi(U)-\Phi(0))} \left(R - 4\Lambda - \frac{1}{12} \tilde{H}^2 + 4 g^{\mu\nu} \partial_\mu \Phi \partial_\nu \Phi \right) \ ,$$

$$= -\frac{c L_x}{12\pi \sqrt{k} \epsilon_- l_s} \left(\frac{\sqrt{k} \epsilon_- l_s}{\epsilon} \sqrt{1 - \frac{k \epsilon_-^2 l_s^2}{\epsilon^2}} + \sin^{-1}\left(\frac{\sqrt{k} \epsilon_- l_s}{\epsilon} \right) \right) \ , \tag{4.122}$$

$$= -\frac{c L_x}{6\pi \epsilon} + \frac{c k \epsilon_-^2 l_s^2 L_x}{36\pi \epsilon^3} + O(\epsilon_-^4) \ .$$

The choice of the coupling is bounded from above by the UV cutoff via $\epsilon > \epsilon_- \sqrt{k} l_s$.

4.7.2 GHY surface terms from null boundaries

Now for the GHY calculation let's first check that there is no mixed/cross term in the induced metric from the t, x part of the metric (4.115) by plugging in (4.116,4.117). For the future boundary of the WdW patch, keeping in mind that $dU < 0$,

$$dt_+ = -\frac{\sqrt{1 - kU^2 \epsilon_-^2}}{U^2} dU,$$

and,

$$dx_+ = dx_0 + l_s \frac{k \epsilon_-^2 \, dU}{\sqrt{1 - kU^2 \epsilon_-^2}}.$$

Then, the t, x part of the metric simplifies to

$$kU^2 \left(1 - kU^2 \epsilon_-^2\right) \left[dx_+ + \frac{kU^2 \epsilon_-^2}{1 - kU^2 \epsilon_-^2} dt_+\right]^2 = kU^2 \left(1 - kU^2 \epsilon_-^2\right) dx_0^2.$$

Similarly, one can also show that for the past boundary of the WdW patch, the t, x part of the metric (4.115) becomes,

$$kU^2 \left(1 - kU^2 \epsilon_-^2\right) \left[dx_- + \frac{kU^2 \epsilon_-^2}{1 - kU^2 \epsilon_-^2} dt_-\right]^2 = kU^2 \left(1 - kU^2 \epsilon_-^2\right) dx_0^2.$$

Now we can turn on the timelike deformation (note that this timelike deformation is a separate/disjoint deformation of the future and past null surfaces),

$$(t - T_0)^2 = (1 + \delta) l_s^2 A^2(U), \qquad \text{where,} \quad A(U) \equiv \int_U^{l_s/\epsilon} dU \frac{\sqrt{1 - kU^2 \epsilon_-^2}}{U^2} .$$

Plugging this in the t, U part of the metric (4.115), the timelike (near null) part of the induced metric on the deformed surface is

$$\frac{kU^2}{1 - kU^2 \epsilon_-^2} \left[\frac{l_s^2 \left(1 - kU^2 \epsilon_-^2\right)}{(U^2)^2} dU^2 - dt^2\right] = -\delta \frac{k \, l_s^2}{U^2} dU^2.$$

Thus the induced metric on the timelike deformed surfaces is,

$$ds_\gamma^2 = -\delta \frac{k \, l_s^2}{U^2} dU^2 + kU^2 \left(1 - kU^2 \epsilon_-^2\right) dx_0^2, \tag{4.123}$$

and so

$$\sqrt{-\gamma} = \sqrt{\delta} k \, l_s \sqrt{\left(1 - kU^2 \epsilon_-^2\right)}.$$

(The range of x-integration for this GHY term is $\int dx = \int dx_0 = L_x$.)

Now to figure out the normal to the surface we first recall that on the timelike deformed surfaces the changes in dt, dx, dU are constrained by the equations

$$dt = \mp\sqrt{(1 + \delta)} l_s \frac{\sqrt{1 - kU^2 \epsilon_-^2}}{U^2} dU, \quad dx_+ = dx_0 \pm l_s \frac{k \epsilon_-^2 \, dU}{\sqrt{1 - kU^2 \epsilon_-^2}}.$$

So on the deformed surface the (near null) timelike tangent vector can be taken to be,

$$T_1^\mu \propto \left(1, \mp\sqrt{(1 + \delta)} l_s \frac{\sqrt{1 - kU^2 \epsilon_-^2}}{U^2}, \pm l_s \frac{k \epsilon_-^2}{\sqrt{1 - kU^2 \epsilon_-^2}}\right)$$

while the spacelike tangent vector can be taken to be,

$$T_2^\mu \propto (0, 0, dx_0) = (0, 0, 1).$$

Let the components of the normal vector be,

$$N_\mu = (n_U, n_t, n_x)$$

So the normal vector components satisfy the equation $N_\mu T_1^\mu = N_\mu T_2^\mu = 0$ or,

$$n_U \mp \sqrt{(1 + \delta)} l_s \frac{\sqrt{1 - kU^2 \epsilon_-^2}}{U^2} n_t \pm l_s \frac{k \epsilon_-^2}{\sqrt{1 - kU^2 \epsilon_-^2}} n_x = 0.$$

and
$$n_x = 0.$$

Thus only n_U and n_t are non-zero. Thus the unnormalized normals can be taken to be,

$$n_U = 1 \qquad\qquad n_t = \pm\frac{U^2}{\sqrt{\delta+1}l_s\sqrt{1-kU^2\epsilon_+^2}} \qquad\qquad n_x = 0.$$

Let's first start working with the upper portion of the timelike (near null) surface (regulating surface). The normalised outward normal to the upper portion of the regulating timelike surface is

$$n^U = \frac{\sqrt{\delta+1}U}{\sqrt{\delta}\sqrt{k}l_s} \;, \qquad\qquad n^t = -\frac{\sqrt{1-kU^2\epsilon_-^2}}{\sqrt{\delta}\sqrt{k}U} \;, \qquad\qquad n^x = \frac{\sqrt{k}U\epsilon_-^2}{\sqrt{\delta}\sqrt{1-kU^2\epsilon_-^2}} \;.$$

The trace of the extrinsic curvature is

$$K = \nabla_\mu n^\mu = \partial_U n^U + \partial_t n^t + \partial_x n^x + \underbrace{(\Gamma_{UU}^U + \Gamma_{tU}^t + \Gamma_{Ux}^x)}_{\frac{1}{U}} n^U \;,$$

$$= \frac{2\sqrt{\delta+1}}{\sqrt{\delta}\sqrt{k}l_s} \;,$$

$$= \frac{2}{\sqrt{\delta}\sqrt{k}l_s} + O(\delta^{1/2}) \;. \tag{4.124}$$

Now for the lower portion of the deformed timelike surface, the outward unit normal is

$$n^U = \frac{\sqrt{\delta+1}U}{\sqrt{\delta}\sqrt{k}l_s} \;, \qquad\qquad n^t = \frac{\sqrt{1-kU^2\epsilon_-^2}}{\sqrt{\delta}\sqrt{k}U} \;, \qquad\qquad n^x = -\frac{\sqrt{k}U\epsilon_-^2}{\sqrt{\delta}\sqrt{1-kU^2\epsilon_-^2}} \;.$$

The normalization constant and the extrinsic curvature are same as that for the upper portion of the regulating surface.
The GHY integral evaluates to be

$$S_{GHY}^\delta = \frac{1}{8\pi G_N} \int_{L/2}^{-L/2} dx_0 \int_0^{l_s/\epsilon} dU\, e^{-2(\Phi-\Phi_0)}\sqrt{-\gamma}(K + n^\mu\partial_\mu\sigma) \;,$$

$$= \frac{\sqrt{k}L_x}{4\pi G_N} \int_0^{l_s/\epsilon} dU\, \sqrt{1-kU^2\epsilon_-^2} \;,$$

$$= \frac{c}{12\pi\sqrt{k}\epsilon_- l_s} \left(\frac{\sqrt{k}\epsilon_- l_s}{\epsilon}\sqrt{1 - \frac{k\epsilon_-^2 l_s^2}{\epsilon^2}} + \sin^{-1}\left(\frac{\sqrt{k}\epsilon_- l_s}{\epsilon} \right) \right) \;. \tag{4.125}$$

Full action complexity obtained by summing (4.122) and (4.125) evaluates to be zero. This, turns out to a dimensional accident as has been noted earlier in [74], it is artifact of the fact that in dimension $d = 2$ the action complexity being proportional to $\ln(d-1)$, vanishes. As has been pointed earlier, CA and CV might actually correspond to be two different schemes [75] of defining complexity in the boundary field theory. Since, we still do not yet have the field theoretic formulation of complexity at our disposal, it would be a bit too early at this stage of development to try to relate it to the boundary behaviour of complexity. However, we believe that once we have the complete field theoretic formulation, it will shed light into this bizarre behaviour of vanishing complexity.

4.8   Discussion & Outlook

In this work, we investigated aspects of the little string theory (LST), which is the holographic (boundary) dual of a string theory in a target space that interpolates between AdS_3 in the IR to an anisotropic spacetime with a linear dilaton and NS-NS B-field that violates Lorentz isometry in the UV. This LST can be regarded as a nonlocal Lornetz (boost) noninvariant UV deformation of a local CFT$_2$ by "single trace" analogue of the usual irrelevant $T\overline{T}, J\overline{T}, T\overline{J}$ operators. Our tool of investigation was holographic complexity, specifically the holographic volume complexity (CV) and holographic action complexity (CA) prescriptions. Our aim was to identify and, if possible, isolate the signatures of the Lorentz-violation in holographic complexity. This work extends our previous work [132] in two respects. In our previous work we looked at LST with just nonlocality ($T\overline{T}$ deformation) without turning on Lorentz-violating couplings ($J\overline{T}, \overline{J}T$ deformations), and we omitted the interesting or informative case of subregion complexity. Here we summarize of our findings:

- Volume complexity was evaluated for two different frames related by a boost - namely the stationary and static frame, while the action complexity was evaluated only in the static frame. Both the volume complexity and action complexity are UV divergent and hence manifestly regulator dependent. In the regime where the UV cutoff (lattice spacing) is shorter than the Hagedorn scale of the LST, the leading piece diverges *quadratically* with the UV cutoff (cf Eq. (4.29), (4.43), and Eq. (6.2)). We identify this leading quadratic divergence as the characteristic signature of nonlocal nature of the LST. Modulo an overall factor ambiguity (which is well known in the literature) the leading divergences for both complexities (volume and action) in the static frame agree and have the same sign.

- There are subleading logarithmic divergences in both volume complexity (4.43) and action complexity expressions (6.2) which have the same magnitude but differ in sign. The universal coefficient (4.45) of this log divergent term can be interpreted as the total number of degrees of freedom in the LST with the Hagedorn scale, β_H treated as the lattice spacing.

- The characteristic length scale of nonlocality is different in the stationary and static frames. For the stationary frame, this nonlocality scale is given by $\rho_H = \frac{2\pi}{\sqrt{3}} l_s \sqrt{k\left(\lambda - (\epsilon_+ + \epsilon_-)^2\right)}$ while in the static frame it is given by $\beta'_H = 2\pi l_s \sqrt{k\left(\lambda - 4\epsilon_+\epsilon_-\right)}$. This effect of changing the nonlocality scale upon boosting to a different Lorentz frame is the characteristic signature of the fact that the theory is not boost invariant.

- In the opposite regime, when the UV cutoff is much larger than the nonlocality scale, the volume complexity expectedly reduces to that of a local field theory having linear divergence (corresponding to a single spatial dimension) (4.44) matching that of a CFT with the central charge equal to the Brown-Henneaux expression derived from a pure AdS_3 calculation. Similarly, in this limit the action complexity too reproduces the expected pure AdS_3 answer (4.114) [74, 73].

- The subregion volume complexity as a function of the subregion size (length), in both the stationary and static frames, displays a sharp transition as the subregion size is varied across a critical subregion size in both frames. In the stationary frame this critical length is $L_c = \frac{\pi\sqrt{k\lambda\lambda'}}{2\sqrt{\mu}} l_s$) while in the static frame this critical scale is $L'_c = \frac{\pi\sqrt{k\lambda}}{2} l_s$ where $\lambda' \equiv \lambda - 4\epsilon_+\epsilon_-$ and $\mu \equiv \lambda - (\epsilon_+ + \epsilon_-)^2$. We identify this phase transition of subregion volume complexity with the Hagedorn phase transition which have been previously observed in entanglement entropy as well as the thermodynamics [105, 106].

- Upon setting $\lambda = \epsilon_+ = 0$, one obtains null warped AdS$_3$ metric in the bulk (with nonzero dilaton and B-field turned on). This point in the parameter space is out of the unitarity regime and hence

corresponds to a boundary dual WCFT which does not admit a UV completion. Nevertheless, one can still study it as an effective theory, which violates locality and Lorentz boost symmetry. The volume complexity expression confirms that the UV cutoff (lattice spacing) cannot be made arbitrarily small and is bounded by the warping parameter ϵ_-, namely $\epsilon > \sqrt{k} l_s \epsilon_-$. Below this the volume complexity does not make sense (turns imaginary). The action complexity on the other hand vanishes, perhaps due to a dimensional accident akin to the unwarped AdS$_3$ case. The subregion volume complexity is a monotonically increasing function of the subregion size L, but there is no Hagedorn like phase transition. Surprisingly, the holographic entanglement entropy of this null warped AdS$_3$ solution dual to the highly nonlocal, Lorentz violating WCFT has a logarithmic divergence, same as that of pure AdS$_3$ dual to local CFT$_2$. The universal coefficient of the log divergence however receives a contribution from the warping parameter.

The analysis of holographic Wilson loop [104], holographic entanglement entropy [103, 128, 129, 106] and thermodynamics [105, 119] for the LST naturally reveals the nonlocality scale through some pathologies in the physical observables. For example, the free energy and the entropic c-function diverges as the RG scale approaches the nonlocality scale of LST. The partition function in the thermodynamic limit develops a branch cut singularity as the temperature approaches the Hagedorn temperature of LST. So it is perhaps natural to expect that the subregion complexity would also show such singular/pathological traits when the subregion size approaches the nonlocality scale. This was one of the main reasons to include the subregion complexity in this work. But to the contrary, In our analysis of holographic complexity, we didn't come across such pathologies.

It would be interesting to work out the action complexity in the stationary frame. This will entail solving a more involved technical problem of constructing WdW patches for stationary metrics [142, 143]. Although we don't expect any radically different answers for the action complexity in the stationary frame compared to volume complexity (as evidenced by the strong similarities in static frame counterparts), it will still be nice to close this gap. We leave this exercise for a future work as well.

So far everything we have done here corresponds to the zero temperature case. Since the LST is a nonlocal theory for which we do not have much intuition, there might appear novel exotic divergences compared to the zero temperature case - so perhaps it is important that one studies the finite temperature case. In fact such a computation was performed in our previous paper [132] for the LST dual to $\mathcal{M}_3$. There we computed the finite temperature the action complexity using the bulk dual black hole geometry. In particular, we consider the thermofield double state of two LST's for which the dual bulk geometry is an eternal $\mathcal{M}_3$ black hole. Qualitatively, the action complexity[10] at finite temperature showed the same behavior as that of the zero temperature case. More importantly, *no newer divergences* compared to the zero temperature case was found (perturbatively up to second order in finite temperature corrections). For the $J\overline{T}, T\overline{J}$ deformed theory, such a black brane background dual to finite temperature LST with $J\overline{T}, T\overline{J}$ deformations (thermofield double) was recently worked out [144]. It would be interesting to carry out the computation of action complexity for this eternal black blane geometry - although from the insights gathered from our past paper and the patterns established in the current work, we do not expect to see novel UV divergence structures because for this LST Lorentz violating effects seem to be mixed with nonlocality effects and they come in a single joint package. We leave this exercise for future work.

Finally, one needs to study the characteristics of holographic complexity for a larger class of nonlocal theories, not necessarily LST as was done for the case of entanglement entropy [127, 135]. This will help us settle the issue of the hypervolume UV divergence structure i.e., whether one should always expect a general "volume + 1" scaling for the leading term or something more complicated related to the cause or origin of the nonlocality.

A well known issue in the holographic proposals for evaluating circuit complexity of the boundary theory

---

[10]For such a black brane bulk background analytic calculations of the maximal volume slice without any approximations are not possible, and so we abandoned the volume complexity scheme. Instead we numerically computed the action complexity exactly.

is that there is neither any direct specification of the reference state nor the unitary gates (operators) which constitute the circuits. These issues are still not settled in the holography literature. The only thing one can definitively state is that In the AdS/CFT case the reference state is clearly *not* the CFT vacuum, since the holographic complexity is nonzero for pure AdS geometry (equivalently the CFT vacuum state). We are unable to shed any further light on these issues in our current work. However, at the end of the day, the LST_2 we study is obtained by deforming a CFT_2 by a set of irrelevant deformations. Hence, we might as well use the *exact same* set of unitary gates and the *exact same* reference state as used for the initial CFT_2 which we UV-deformed. This is sensible since the LST complexity obtained here smoothly go over to the CFT (pure AdS) complexity once the UV deformation parameters are set to zero. We *can* comment on the target state though. In the CFT_2 case the target state was the CFT vacuum, invariant under the $SL(2, \mathbb{R}) \times SL(2, \mathbb{R})$ symmetry. For the LST_2 case obtained by a single trace $T\overline{T}$ deformation of the CFT_2 which was the subject of our last paper [132], the target state was the "no string" vacuum state, the vacuum of the BRST cohomology of the coset $\frac{SL(2,\mathbb{R}) \times U(1)}{U(1)}$ at zero temperature [107]. For the LST in this paper, obtained after further breaking the Lorentz boost symmetry, it is not yet clear that a coset description can be provided. The states can be labeled by the left over symmetry generators corresponding to time translations, translation in the x-direction and the $U(1)$ left and right moving sector charges $J, \overline{J}$. In fact the vacuum here has nontrivial quantum numbers, $U(1)$ charge(s) since after dimensional reduction of the y-circle the 3d bulk has nontrivial KK $U(1)$ gauge fields turned on.

Since this correspondence between LST and String backgrounds with asymptotically linear dilaton backgrounds is a non-AdS/non-CFT case of holography, perhaps a more direct exercise would be to work out the holographic dictionary in the vein of GKPW and/or as HKLL [145, 146, 147]. As we have already remarked in our previous work [132], one anticipates some surprising twists in the bulk-boundary map/dictionary in this case because such maps will reconstruct *local* supergravity excitations in the bulk, from *nonlocal* excitations of the LST in the boundary. In the traditional AdS/CFT setting such local bulk reconstruction maps are to a great extent determined by the (conformal) symmetry preserved by the boundary state, as well as *locality/microcausality* properties of the boundary CFT correlators, in the HKLL recipe locality in the bulk directions parallel to the boundary is a simple and direct consequence of boundary (CFT) locality, and the nontrivial challenge was to understand bulk locality in the emergent radial (holographic) direction from the locality in the boundary (transverse) directions. However in the case of LST, the field theory is *nonlocal* and Lorentz symmetry is broken. It will be interesting to identify which alternative properties of a nonlocal theory such as the LST plays the crucial role in emergence of the quasilocal semiclassical bulk space in both radial as well transverse directions.

In our study of the null $WAdS_3$ case, we observed a complicated dependence upon the UV cutoff as the function of the lorentz violating coupling, this is also true for the timelike warping of the bulk. This is consequence of the fact that dual field theory does not have a unitary UV completion. However, the spacelike $WAdS_3$ does have a well behaved UV complete dual field theory description in terms of what is called the $WCFT_2$ [148, 137] which is a highly nonlocal theory. It will be interesting to investigate the features of this theory using the tool of computational complexity, where we expect the proper scaling with system in the units of UV cutoff. This leads us to the subject of the next chapter where we try to address exactly that.

Chapter 5

Holographic Complexity of Warped Conformal Field Theories

Holography [5, 6, 7, 97] has not only provided us with tools which have revolutionized our understanding of phenomena in strongly coupled field theories, it has even led to the discovery of novel exotic phases of strongly coupled field theories and led to the identification of new conformal field theories. One such example are the Warped conformal field theories (WCFT) [148, 137], which are the proposed holographic duals of warped AdS$_3$ spacetimes [149]. WCFTs can be defined as the two dimensional field theories with $SL(2, \mathbb{R})_R \times U(1)_L$ Kac-Moody symmetry, which is the local extension of the algebra of two global translation and one global chiral scale symmetries. This is in contrast to the much older result [12] where an unitary two dimensional QFT with global Poincaré and scale invariance,

$$x^- \to x^- + a, \qquad x^+ \to x^+ + b,$$
$$x^- \to \lambda_- x^-, \qquad x^+ \to \lambda_+ x^+.$$

ends up having an enhanced to a direct product of two copies of the Virasoro algebra, corresponding to two dimensional conformal symmetry,

$$x^- \to f(x^-), \qquad x^+ \to g(x^+).$$

if the dilatation operator has discrete non-negative spectrum. Here $x^\pm$ are the two dimensional light-cone coordinates. In [148], however the field theory was assumed to possess only one-sided (chiral) global scale invariance

$$x^- \to x^- + a, \qquad x^+ \to x^+ + b,$$
$$x^- \to \lambda_- x^-.$$

There is a novel symmetry enhancement when one adds to the mix a chiral boost symmetry $x^+ \to x^+ + \omega\, x^-$. In such a case the symmetry algebra gets enhanced to an infinite dimensional symmetry algebra, namely that of a semidirect product of a Virasoro algebra and a $U(1)$ current algebra (Virasoro-Kac-Moody algebra), corresponding to the so called *warped conformal symmetry*,

$$x^- \to f(x^-), \qquad x^+ \to x^+ + g(x^-). \tag{5.1}$$

Field theories possessing such a warped conformal symmetry are the WCFTs. Since then warped conformal symmetry and WCFTs have been explored intensely using various field theory and holographic tools - it is worth nothing a few prominent works here. See [137], for a discussion about representations of the warped conformal symmetry and an analogue of the Cardy formula. Correlation functions have been

worked out [150]- two and three point functions get completely determined by the global warped conformal symmetry, while the four-point functions are determined up to an arbitrary function of the cross ratio. Several concrete examples of WCFTs have now been worked out, see [151, 152] for bosonic WCFTs, and [138, 153, 154, 155] for fermionic WCFT models and [156] for supersymmetric WCFTs. For other interesting works in WCFTs refer to [152, 131, 157, 158]. In this work we are particularly interested in holographic WCFTs, which are dual field theory candidates to gravitational theories on warped AdS_3 ($WAdS_3$) spacetimes. $WAdS_3$ are non-Einstein spacetimes which can be realized in topologically massive gravity [159, 160, 161, 162, 163] or in string theory [164, 165, 166, 167, 117]. The asymptotic symmetry group of these spacetimes is the semidirect product of a Virasoro algebra and a $U(1)$ affine Kac-Moody algebra [168, 169, 170, 171, 172]. These spacetimes are not asymptotically locally AdS, and hence they expand the scope of holography beyond asymptotically AdS. In particular we are interested in spacelike warped AdS_3 spacetimes, which are obtained when a spatial line or circle is fibered over AdS_2. Timelike and null warped AdS_3, where the $U(1)$ fiber is timelike and null respectively, are known to contain closed timelike curves (CTC) and hence are not expected to have sensible, well-behaved boundary duals. Spacelike warped AdS_3 spacetimes also admit black hole solutions [149].

Ideas from quantum information have brought new insights into various physics branches and had far-reaching consequences. It has given a new perspective in interpreting several geometric objects in the context of holography. A most studied information-theoretic tool is entanglement entropy. Typically, the entanglement entropy is computed using the von-Neumann entropy after partitioning the systems into two subsystems and tracing them out. This has been extensively explored in the context of AdS/CFT [173] and the Warped holography [140, 174, 175, 139, 176, 177]. Another information-theoretic quantity, primarily motivated by recent developments in black hole physics [46, 48], has come into the limelight is *circuit complexity*[72, 71]. In the context of holography, certain geometrical objects, e.g. maximal volume of a particular codimension-one bulk slice (complexity = volume) [47], gravitational action defined on Wheeler-DeWitt patch of a bulk Cauchy surface anchored at a specific time (complexity = action) [49], are conjectured to be the gravity dual to the circuit complexity of the dual field theory state. Circuit Complexity, an idea from the theory of quantum computation, basically quantifies the minimal number of operations or gates required to build a circuit that will take one from a given reference state($|\psi_R\rangle$) to the desired target state ($|\psi_T\rangle$). In recent times, circuit complexity has been explored in the context of quantum field theory [178, 52, 56, 53, 59, 63, 179, 180, 81, 64, 67, 68, 181, 182, 183] [1].

In this chapter, we will explore complexity both from the field theory and gravity side in the context of warped holography, complementing the studies of entanglement entropy in this context.

The constitution of the chapter is as follows. In section 5.1 we resort to holographic methods, in particular the complexity-volume (CV) prescription to compute the complexity of the warped conformal field theories dual to timelike and spacelike warped AdS_3 spacetimes realized in topologically massive gravity theory. We find that for the timelike case, the dependence on the UV cutoff is rather complicated - an indication of the fact the warped CFT is a nonlocal theory, but the holographic complexity is not defined for a arbitrary values of the UV cutoff. The complexity is only well defined when the cutoff is kept under a critical value determined by the warping parameter. Such a phenomenon has already been observed in the case of complexity of field theories dual to null warped AdS_3 spacetimes realized in the context of $T\overline{T}, J\overline{T}, \overline{J}T$ deformed CFT_2's in previous chapter that appeared in [186]. Such computations lend credence to the claim that the warped CFT_2's which are dual to null and timelike warped AdS_3 spacetimes do not have an unitary UV completion.Then we work out the holographic complexity of WCFTs dual to spacelike $WAdS_3$ spacetimes. These are free from pathologies (i.e. are unitary and UV complete) and the underlying symmetry structure is that of a semidirect product of a Virasoro and a $U(1)$ Kac-Moody algebra. The holographic complexity in this case scales extensively with system in units of the UV cutoff, a trait which is perhaps more expected from a local CFT_2, despite the fact that warped CFTs are highly nonlocal theories. There is a nontrivial dependence on the symmetry parame-

---

[1]This list is by no means exhaustive. Interested readers are referred to these reviews [184, 185], and citations are therein for more details.

ters c, k. In particular the complexity *does not* scale linearly with the Virasoro central charge c as it did in the case of local CFT$_2$, but instead with the $U(1)$ Kac-Moody level number, k. Although there is no restriction on the cutoff in terms of the warping parameter, it can be arbitrary, the complexity is still defined in a restricted domain of the parameter space of the symmetry algebra, namely $c/k \leq 25/8$. Next in section 3, we adopt the method of [81, 67, 64] to directly evaluate the circuit complexity of WCFT employing the Kac-Moody symmetry gates by evaluating the complexity functional. We find that for small c/k ratio but large k the answer is again proportional to k as what we obtain from the gravity side. We conclude the section after an elaborate comparison with the results coming from holography. Finally in Section 4, we discuss our results and provide an outlook for further future investigations. We note that there have been other, complementary studies of complexity of warped conformal field theories [187] as well holographic complexity of warped AdS$_3$ black holes [188, 189, 190].

5.1 Holographic Complexity of warped CFTs

In this section our goal is to study the complexity of two dimensional WCFTs using holography i.e. using the dual warped-AdS_3 solutions [References for WAdS/WCFT correspondence]. To be precise we use the holographic volume complexity prescription [48, 46, 47]. Although timelike and null warped AdS$_3$ spacetimes are not supposed to be dual to any UV complete boundary field theory we work out the holographic complexity of timelike WAdS$_3$ for the sake of completeness. The holographic volume complexity expression must exhibit a characteristic signature for the sickness of the boundary dual field theory. The holographic of null warped AdS$_3$ has already been considered in previous chapter [186] where it is obtained as the holographic dual to a little string theory (LST) obtained as a single trace $T\bar{T}, J\bar{T}, \bar{J}T$ deformation of a CFT$_2$, for a very special case of the deformation parameters ($\lambda = \epsilon_+ = 0$). There it has been observed that both the holographic volume and action complexity expressions become either complex or ill-defined if the UV cut off is arbitrarily large. Sensible (real positive) complexity expressions are only obtained when the UV cutoff is restricted by the warping parameter. Such a behavior of the complexity clearly signals the UV incompleteness of the putative WCFT (in this case an LST) dual to the null Warped AdS$_3$. To avoid redundancy, we skip the null warped case as it was already revisited in the previous chapter and in [186] and instead we begin our holographic computations with the case of the timelike warped AdS_3. We work specifically with the metric in a Poincaré patch of the timelike warped AdS$_3$, which can be obtained by taking the zero temperature limit of the warped black string metric equation (4.10) of [174] as reviewed in the appendix D.
The metric in Poincarè patch is (C) in appendix D and reads

$$ds^2 = \frac{-dt^2 + dx^2 + dz^2}{z^2} - \lambda^2 \frac{(dt + dx)^2}{4z^4} \ .$$

As usual $z = 0$ is the (conformal) boundary, and the (warped) AdS radius is set to unity. Here λ is a dimensionless parameter representing (timelike) warping.
In order to compute the volume complexity, we need to first work out the maximal volume spatial slice Σ - a spacelike hypersurface anchored at a specific time (say T_0) at the boundary which has the maximum volume among all spacelike hypersurfaces anchored at the same time, T_0. The volume complexity of the dual boundary theory at the time T_0 is then proportional to the volume $\mathcal{V}_\Sigma$ of the maximal volume slice Σ,

$$\mathcal{C}(T_0) = \frac{\mathcal{V}_\Sigma(T_0)}{G_N \, l} \tag{5.2}$$

Here l is a characteristic length scale of the geometry (which is a bit arbitrary to some extent). In the present case we will take it to be the (W)AdS$_3$ radius (which we have set to unity $l = 1$).
Let us parameterize a generic spatial surface (say γ) by $t = t(z), \forall x$. Then the induced metric on this

spacelike hypersurface is

$$ds_\gamma^2 = \left(\frac{1}{z^2} - \frac{\lambda^2 t'(z)^2}{4z^4} - \frac{t'(z)^2}{z^2} \right) dz^2 - \frac{\lambda^2 t'(z)}{2z^4} dxdz + dx^2 \left(\frac{1}{z^2} - \frac{\lambda^2}{4z^4} \right) .$$

The volume of the spacelike hypersurface γ is then,

$$\mathcal{V}_\gamma = \int dx \int_0^\infty dz \, \frac{1}{z^2} \sqrt{1 - t'(z)^2 - \frac{\lambda^2}{4z^2}}, \tag{5.3}$$

Extremizing this volume functional leads us to the following Euler-Lagrange equation

$$z \left(4z^2 - \lambda^2 \right) t''(z) + \left(\lambda^2 - 8z^2 \right) t'(z) + 8z^2 \, t'(z)^3 = 0 .$$

To solve this differential equation we assume the following ansatz for the spacelike slice anchored at the boundary as

$$t(z) := T_0 + T_1 z + T_2 z^2 + T_3 z^3 + T_4 z^4 + T_5 z^5 + T_6 z^6 + ... ,$$

when solved order by order in z. Since this is a second order equation, we need a second boundary condition, which is the constraint that asymptotically this is a spacelike surface ($\frac{dt}{dz}|_{z=0} = 0$). The solution to the Euler Lagrange equation is remarkably simple, it is the constant time slice $t(z) = T_0$. However plugging in the maximal volume slice $t = T_0$, in the expression for the volume naively gives divergent result since the space is noncompact. So we need to introduce a volume regulator in the form of a radial cutoff, $z = \epsilon$ instead of integrating all the way to the boundary $z = 0$. After regulating the volume, one obtains a finite (regulator dependent)[2] expression for the volume complexity of warped CFT dual to a timelike warped AdS$_3$ spacetime to be

$$\mathcal{C} = \frac{1}{G_N} \int dx \int_\epsilon^\infty dz \, \frac{1}{z^2} \sqrt{1 - \frac{\lambda^2}{4z^2}}$$

$$= \frac{L_x}{G_N} \left(\frac{1}{\lambda} \sin^{-1} \left(\frac{\lambda}{2\epsilon} \right) + \frac{1}{2\epsilon} \sqrt{1 - \frac{\lambda^2}{4\epsilon^2}} \right) \tag{5.4}$$

There are several features to note in this expression for complexity. First and foremost is that unlike that of a local CFT$_2$, the complexity of a warped CFT does not diverge linearly with the cutoff ϵ. This is consistent with the fact the warped CFTs are highly nonlocal, boost non-invariant field theories. The second key feature is that for a fixed cutoff, the complexity is a nonanalytic function of the warping parameter λ - the complexity does not make sense for all real values of the warping parameter λ. Alternately, for a fixed value of the warping parameter λ, complexity is a nonanalytic function of the cutoff ϵ. In fact the cutoff cannot be made arbitrarily small, there is a restriction imposed on it by the warping parameter λ. In order for the above complexity expression to make sense, we must always restrict the cutoff to $2\epsilon \geq \lambda$. This pathology is similar in nature to as we encountered in the previous chapter during our study of null WAdS [186]. This phenonmenon points out to the UV incompleteness of the warped CFTs dual to timelike and null warped AdS$_3$. (In case of null warped AdS$_3$ it can be shown that the dual LST has complex energy eigenvalues for energy scales large ϵ, thereby rendering the dual

---

[2]Note that just like entanglement entropy, complexity is also expected to be a manifestly (UV) cutoff dependent quantity for a continuum quantum field theory. In addition, generically for a quantum theory where states are described by a continuum of state vectors, the so called *circuit complexity* is intrinsically unbounded and can only be defined provided one introduces a tolerance parameter which is a sort of minimal volume cell in the Hilbert space of states. There have been attempts to define quantum complexity which is finite as well as tolerance free but there is no unanimity in such approaches.

theory nonunitary [105]. Also from the bulk sting background perspective, the transverse direction x is a compact (closed), and there appears closed timlike curves once one crosses into the deep UV (near boundary) region $2\epsilon < \lambda$. Then to obtain a causal macrosopic semiclassical bulk one is forced to truncate the spacetime time region $2\epsilon < \lambda$, just as in the dual LST one is forced to truncate the theory beyond a certain cutoff UV energy scales (Hagedorn) such that the spectrum of the truncated theory is real. Such pathological features render the warped CFTs dual to timelike or null warped AdS$_3$ spacetimes unsuitable for further investigations and in the remainder on will concern ourselves with the warped CFTs which are dual to exclusively spacelike warped AdS$_3$

5.1.1 Holographic volume complexity of spacelike WAdS$_3$

Here we consider the physically interesting case of warped CFTs dual to *spacelike* warped AdS$_3$ spacetime. Spacelike warped AdS has isometry group $SL(2, \mathbb{R}) \times U(1)$. The metric of spacelike WAdS$_3$ solution is given by [149]

$$ds^2 = \frac{l^2}{\nu^2 + 3} \left[-\cosh^2 \rho \, dt^2 + d\rho^2 + \frac{4\nu^2}{\nu^2 + 3} (dt \, \sinh \rho + du)^2 \right] . \tag{5.5}$$

When $\nu^2 > 1$ one obtains a spacelike stretched AdS$_3$, while a spacelike squashed AdS$_3$ is obtained when $\nu^2 < 1$. Evidently $\nu^2 = 1$ case represents undeformed pure AdS$_3$ spacetime. For computational convenience, we make the diffeomorphism $\tan \theta = \sinh \rho$, with $0 \leq \theta \leq \pi/2$ to bring the spacelike warped AdS$_3$ metric to the following form

$$ds^2 = \frac{l^2}{(\nu^2 + 3) \cos^2 \theta} \left(d\theta^2 - dt^2 + \frac{4\nu^2}{\nu^2 + 3} (dt \, \sin \theta + du \, \cos \theta)^2 \right) . \tag{5.6}$$

As was done previously, the next step towards computing the holographic volume complexity is to locate the maximal volume slice. To this end, let us parameterize a generic spacelike hypersurface by the condition $t = t(\theta) \, \forall u$. Then the pullback metric on this spacelike hypersurface $t = t(\theta)$ is given by

$$ds^2 = \frac{l^2}{(\nu^2 + 3) \cos^2 \theta} \left[-t'(\theta)^2 \, d\theta^2 + d\theta^2 + \frac{4\nu^2}{\nu^2 + 3} (\sin \theta \, t'(\theta) \, d\theta + du \, \cos \theta)^2 \right] , \tag{5.7}$$

with the volume

$$\mathcal{V} = \frac{2 \, l^2 \, \nu}{(\nu^2 + 3)^{3/2}} \int du \int d\theta \, \frac{1}{\cos \theta} \sqrt{1 - t'^2(\theta)} .$$

Extremizing the volume functional leads to the following Euler-Lagrange equation

$$-t''(\theta) + \tan \theta \, t'(\theta)^3 - \tan \theta \, t'(\theta) = 0 . \tag{5.8}$$

This second order nonlinear differential equation has following two nontrivial roots

$$t(\theta) = c_2 \pm \tan^{-1} \left(\frac{\sqrt{2} \sin \theta}{\sqrt{2c_1 + \cos 2\theta + 1}} \right) , \tag{5.9}$$

where $c_2 = T_0 - \tan^{-1} \left(\frac{1}{\sqrt{c_1}} \right)$. If one works out the normals to the above hypersurface(s), one finds

$$n_\tau = 1 \qquad\qquad n_\theta = -\frac{\cos(\theta)}{\sqrt{c_1 + \cos^2(\theta)}} \qquad\qquad n_u = 0 , \tag{5.10}$$

with norm

$$n^2 = -\frac{c_1 \left(\nu^2 + 3\right) \cos^2(\theta)}{l^2 \left(c_1 + \cos^2(\theta)\right)} .$$

Therefore, the hypersurface(s) represented by Eq.(5.9) is null at the boundary, $\theta = \pi/2$ and we will discard them as they do not represent maximal volume slices. However, a simple inspection of the Euler-Lagrange equation (5.8) reveals that $t'(\theta) = 0$ is also a solution to the Euler-Lagrange equation which is manifestly spacelike all the way (its normal being timelike at the boundary). Selecting this constant t spatial slice and evaluating the volume functional, we obtain the holographic complexity of spacelike warped AdS$_3$ is,

$$\begin{aligned}
\mathcal{C} &= \frac{2L_x l}{G_N} \frac{\nu}{(\nu^2 + 3)^{3/2}} \int d\theta \sec\theta , \\
&= \frac{2L_x l}{G_N} \frac{\nu}{(\nu^2 + 3)^{3/2}} \int_0^{1/\epsilon} d\rho , \\
&= \frac{2l}{G_N} \frac{\nu}{(\nu^2 + 3)^{3/2}} \frac{L_x}{\epsilon} .
\end{aligned} \tag{5.11}$$

Here we have introduced a radial cutoff ϵ (boundary UV cutoff) and an IR cutoff, L_x, in the transverse boundary direction, $\int du = L_x$ to regulate the complexity expression.

To translate this result in the language of field theory we use the WAdS$_3$/WCFT$_2$ holographic dictionary [149, 171, 172, 191]. WAdS$_3$ is realized in topologically massive gravity (TMG) as a classical solution which is asymptotically AdS$_3$ with radius l for every value of the gravitational Chern-Simons (CS) coupling $\mu(>0)$. The CS coupling, μ is related to the parameter ν appearing in the gravity solution, $\nu = \frac{\mu l}{3}$. The phase space corresponding to the metric has asymptotic symmetry algebra is a semidirect product of the Virasoro and Kac-Moody algebra with central charge c and the Kac-Moody level number k respectively:

$$\begin{aligned}
[L_n, L_m] &= (n - m)L_{n+m} + \frac{c}{12}(n^3 - n)\delta_{n+m} , \\
[L_n, P_m] &= -mP_{n+m} , \\
[P_n, P_m] &= -\frac{k}{2}n\delta_{n+m} ,
\end{aligned} \tag{5.12}$$

This asymptotic symmetry algebra is identified with the symmetry algebra of the holographic dual warped CFT$_2$. The holographic map between the boundary field theory parameters (c, k) and bulk gravity action parameters (G_N, l, ν) is [172],

$$c = \frac{5\nu^2 + 3}{\nu \left(\nu^2 + 3\right)} \frac{l}{G}, \quad k = \frac{\nu^2 + 3}{6\nu} \frac{l}{G}. \tag{5.13}$$

Thus the final expression for complexity of warped CFT dual to spacelike warped AdS$_3$ is

$$\mathcal{C} = \tilde{c} \frac{L_x}{\epsilon}, \tag{5.14}$$

where the parameter $\tilde{c}$ is a rather elaborate function of the symmetry algebra parameters c, k,

$$\tilde{c} = \frac{5^{\frac{5}{2}}}{2^{\frac{11}{2}} 3^{\frac{1}{2}}} k \left(\frac{3}{5} - \sqrt{1 - \frac{8c}{25k}}\right) \left(1 + \sqrt{1 - \frac{8c}{25k}}\right)^{\frac{3}{2}}. \tag{5.15}$$

for $\nu < 1.3416$ while for $\nu > 1.3416$,

$$\tilde{c} = \frac{5^{\frac{5}{2}}}{2^{\frac{11}{2}} 3^{\frac{1}{2}}} k \left(\frac{3}{5} + \sqrt{1 - \frac{8c}{25k}}\right) \left(1 - \sqrt{1 - \frac{8c}{25k}}\right)^{\frac{3}{2}}. \tag{5.16}$$

The holographic complexity expression of the WCFT dual to spacelike WAdS$_3$ ((5.14), (5.15) (5.16)) has the following features of note,

- Complexity scales extensively with the number of lattice sites, i.e. system size in units of the UV cutoff, $\mathcal{C} \propto L_x/\epsilon$ (here since the WCFT/system is spatially extended in one dimensions), much like that of a local field theory CFT$_2$. This is a bit counterintuitive since the WCFT is understood to be a nonlocal theory.

- Unlike in the case of the WCFTs dual to timelike or null WAdS$_3$ case, there is no restriction of the UV cutoff ϵ on the warping parameter k/c. This affirms the fact that the dual WCFT to spacelike WAdS is a unitary UV complete theory.

- In contrast to local CFT$_2$, for which the holographic complexity is proportional to the Virasoro central charge c, in the case of the WCFT$_2$ it is proportional to $\tilde{c}$, which is a complicated function of the Virasoro central charge and the $U(1)$ Kac-Moody level. We note that the complexity only makes sense for the range of parameters

$$\frac{c}{k} \leq \frac{25}{8}. \tag{5.17}$$

  So there is no way to set $k \to 0$ while keeping c finite.

- Finally we note that at $\nu = 3/\sqrt{5} \approx 1.3416$ or equivalently $c/k = 25/8$, there is a phase transition in complexity corresponding to switching of the branches of the solution (5.15) to (5.16). The branch which is connected to the unwarped pure AdS$_3$ solution is represented by (5.15). One can check that setting $\nu^2 = 1$ in (6.1) or equivalently by setting $c = \frac{2l}{G}$, $k = \frac{2l}{3G}$ in (5.15) one gets the pure AdS complexity[3].

5.2   Circuit complexity for warped CFTs

To provide impetus to the holographic result, in this section we compute the circuit complexity for dual warped conformal field theory using the approach as outlined in [81, 187].
Symmetry generators and their transformations:
As discussed in [148, 137], the Lorentzian theory has a global $SL(2,R)_R \times U(1)_L$ invariance. Furthermore, on the plane the algebra is defined by the commutators of the following operators [148, 137],

$$T_\zeta = -\frac{1}{2\pi} \int dx^- \, \zeta(x^-) T(x^-), \qquad\qquad P_\chi = -\frac{1}{2\pi} \int dx^- \, \chi(x^-) P(x^-). \tag{5.18}$$

The right moving and left moving modes are associated with x^- and x^+ respectively and $T(x^-)$, $P(x^-)$ are the local operators (the stress-tensor and momentum operator) on the plane. The ground state of the theory is invariant under the action of these symmetry generators.
To get an insight about the algebra, let us take an concrete example. If we go from a Lorentzian plane (x^+, x^-) to a Lorentzian cylinder using the coordinate transformations $x^- = e^{i\phi}$ and choose the test functions

$$\begin{aligned}
\zeta(x^-) &= \zeta_n = (x^-)^n = e^{i\,n\,\phi}, \\
\chi(x^-) &= \chi_n = (x^-)^n = e^{i\,n\,\phi},
\end{aligned} \tag{5.19}$$

---

[3]Incidentally, one could perhaps attempt to extract the volume complexity of spacelike WAdS$_3$ by taking the zero temperature (and zero angular velocity) limit of the holographic volume complexity expression for WAdS$_3$ black holes obtained in [190]. However that volume complexity expression does not reduce to the pure AdS volume complexity when one sets $\nu^2 = 1$, in fact the divergences in volume complexity *vanish entirely* in the unwarped pure AdS limit by setting $\nu^2 = 1$ and $M = 0$ in Eq. 4.6 of (5.15).

then following [148, 137] one can show that that Fourier modes satisfy Virasoro-Kac-Moody algebra mentioned in (5.12) with central charge c and the Kac-Moody level k after the following identification,

$$L_n = i\,T_{\zeta_{2n+1}}, \quad P_n = P_{\chi_n}. \tag{5.20}$$

Note that, the $T(x^-)$ generates infinitesimal coordinate transformation for the coordinate x^-. On the other hand $P(x^-)$ generates the infinitesimal gauge transformations in the gauge bundle parametrized by x^+. Following [148, 137] we can write down the following transformation rules for $T(x^-)$ and $P(x^-)$

$$T'(w^-) = f'^2\,T(x^-) + \frac{c}{12}\{f, w^-\} + f'g'P(x^-) - \frac{k}{4}g'^2,$$
$$P'(w^-) = f'P(x^-) - \frac{k}{2}g', \tag{5.21}$$

where, f, g are two arbitrary functions and $f' = \frac{\partial f(w^-)}{\partial w^-}, g' = \frac{\partial g(w^-)}{\partial w^-}$. Also we have used the fact that the finite transformations for the coordinates going from (x^-, x^+) to (w^-, w^+) is of the form mentioned in (5.1). Also, we can identify the Schwarzian term as,

$$\{f, w^-\} = \frac{f'''}{f'} - \frac{3}{2}\left(\frac{f''}{f'}\right)^2.$$

Now again going back to the case of mapping the theory defined on a plane to a cylinder, using the (5.21) we get,

$$T^\alpha(\phi) = -(x^-)^2\,T(x^-) + \frac{c}{24} + i\,2\,\alpha\,x^-P(x^-) + k\,\alpha^2,$$
$$P^\alpha(\phi) = i\,x^-P(x^-) + k\,\alpha \tag{5.22}$$

where we have used the following coordinate transformations,

$$x^- = e^{i\phi}, \quad x^+ = t + 2\,\alpha\,\phi. \tag{5.23}$$

α is an arbitrary tilt [148, 137]. The Fourier modes for $T^\alpha(\phi)$ and $P^\alpha(\phi)$ on the cylinder is defined as,

$$P_n^\alpha = -\frac{1}{2\pi}\int d\phi\, P^\alpha(\phi)e^{in\phi}, \qquad\qquad L_n^\alpha = -\frac{1}{2\pi}\int d\phi\, T^\alpha(\phi)e^{in\phi}. \tag{5.24}$$

Then using the (5.22) we can relate the Fourier modes on the cylinder with those on the planes in the following way,

$$L_n^\alpha = L_n + 2\,\alpha\,P_n - \left(k\,\alpha^2 + \frac{c}{24}\right)\delta_n,$$
$$P_n^\alpha = P_n - k\,\alpha\,\delta_n, \tag{5.25}$$

where L_n and P_n are the Fourier modes defined on the plane.

We need to know one more thing before we proceed further. We will be requiring to know the expectation values of $T^\alpha(\phi)$ and $P^\alpha(\phi)$ with respect some primary states. From [148, 137] we know that they are,

$$T^\alpha(\phi) = k\alpha^2 + \frac{c}{24}, \quad P^\alpha(\phi) = k\alpha. \tag{5.26}$$

Complexity measure for symmetry groups:
Now we use the method of [81] to compute the circuit complexity. In [81] authors have adapted the methods for computing circuit complexity [72] for conformal field theory. We primarily follow their approach. Starting from a suitable reference state $|\psi_R\rangle$ we can go a target state $|\psi_T\rangle$ by acting the reference state by a unitary operator

$$U(\tau) = \overleftarrow{\mathcal{P}}\exp\left(-i\int_0^\tau H(\tau')d\tau'\right).$$

At $\tau = 0$ this $U(\tau)$ becomes identity operator so that we get the reference matrix. Then,

$$|\psi_T\rangle = U(\tau = T)|\psi_R\rangle. \tag{5.27}$$

Here we have assumed that we will reach the target state after $\tau = T$ time. The Hermitian operator $H(\tau)$ is composed of a set of gates that satisfy a closed algebra and form a group. $\overleftarrow{\mathcal{P}}$ represents the path ordering as these gates do not commute in general. In [81], the authors following the arguments of [180] focuses on the symmetry group. Hence the gates are generated by the symmetry generators. This method has been used to compute circuit complexity for Virasoro and Kac-Moody groups [64, 67]. Using appropriate representation we can identify the instantaneous gates $Q(\tau') = -i\,H(\tau')$ as,

$$Q(\tau') = \frac{1}{2\pi} \int dx\, \epsilon(\tau', x) J(x), \tag{5.28}$$

where $J(x)$ is the conserved current and $\epsilon(\tau', x)$ is the control functions which counts how many times the particular generators have been acted at a given time τ'. One can view the circuit as a path on the underlying group manifold connecting two given points. For infinitesimally close points along the path we can write down the following,

$$U(\tau + d\tau) = e^{-Q(\tau)d\tau} U(\tau). \tag{5.29}$$

We also we need to relate this control function with the group elements to compute the circuit complexity. This can be done by noting the fact that under the symmetry transformations we can write the following for the group element $g(\tau, x)$,

$$g(\tau + d\tau, x) = e^{\epsilon(\tau, x)d\tau} g(\tau, x), \tag{5.30}$$

Then we can expand this to the first order we can relate the control function with the derivative of the group element [81, 64]. It can be easily seen that, $\epsilon(\tau, x)$ is nothing but the instantaneous velocity in the group space.

Finally we need to specify a suitable functional assigning computational cost to all of these symmetry transformations. In the original formulation by the Nielsen [72], typically one assign higher penalties for those gates which are 'difficult' to construct. Here we will follow the approach of [81, 64] to assign same cost all kind of symmetry transformations. Furthermore, following [81] we will define the cost functional by evaluating the gates $Q(\tau)$ in the instantaneous state at time τ. This is different from the Nielsen's original formulation. For more details we discussions on this interested readers are referred to [81, 64]. We mainly use the following cost-functional,

$$\mathcal{F} = |\mathrm{Tr}[\rho(\tau)Q(\tau)]|. \tag{5.31}$$

This is also known as "one-norm" cost-functional. There are plethora of choices for cost-functional. For more details of possible choices for cost-functional interested readers are referred to [71, 58]. The density matrix for the instantaneous state $\rho(\tau)$ in this can be generated from the initial density matrix ρ_0 by evolving with the unitary operator, $\rho(\tau) = U(\tau)\rho_0 U^\dagger(\tau)$. Then (5.31) can be re-written as,

$$\mathcal{F} = |\mathrm{Tr}[\rho_0 \tilde{Q}(\tau)]|, \tag{5.32}$$

where, $\tilde{Q}(\tau) = U^\dagger(\tau)Q(\tau)U(\tau)$. Furthermore the total cost can be found by integrating over this cost-functional over the entire path connecting reference and target states.

$$\mathcal{C} = \int d\tau \mathcal{F} = \frac{1}{2\pi} \int d\tau \left| \int dx\, \epsilon(\tau, x) \langle \psi_R | U^\dagger(\tau) J(x) U(\tau) | \psi_R \rangle \right|, \tag{5.33}$$

where we have used (5.28) and (5.32). Then we have to choose a suitable reference state and minimize (5.33). Note that, (5.33) is a functional of the group path $g(\tau)$. By minimizing it we are finding the

shortest path. Also as each path corresponds a circuit, shortest path corresponds to the optimal circuit. Finally, evaluating (5.33) on this path will give us the complexity associated with the optimal circuit which will take us from a given reference state to a desired target state.

Virasoro-Kac-Moody Circuit:

Armed with this discussion, now we turn our attention to the Virasoro-Kac-Moody symmetry group and compute the circuit complexity using the methods discussed above. In [187], the author has initiated a study regarding the circuit complexity for the Virasoro-Kac-Moody symmetry group. However, in [187], only the complexity functional has been written. In this chapter, we have taken a concrete step to write down the complexity functional and extremize it. This enables us to make a concrete comparison with the results coming from holography. This is the first time such concrete comparisons are being made for the complexity of warped holography to the best of our knowledge.

We now build the unitary circuit using the gates generating Virasoro-Kac-Moody symmetry [187]. The instantaneous gates are defined as,

$$
\begin{aligned}
Q_T(t) &= \int_0^{2\pi} \frac{d\phi}{2\pi} \, \epsilon(t,\phi) T^\alpha(\phi), \\
Q_P(t) &= \int_0^{2\pi} \frac{d\phi}{2\pi} \, \epsilon(t,\phi) P^\alpha(\phi)
\end{aligned}
\tag{5.34}
$$

where, $T^\alpha(\phi)$ and $P^\alpha(\phi)$ are the stress-tensor and momentum operator defined on the cylinder (5.22). The quantum circuit is then take the following form,

$$
U(\tau) = \overleftarrow{\mathcal{P}} \exp\left[\int_0^\tau \left(Q_T(\tau') + Q_P(\tau')\right) d\tau'\right].
\tag{5.35}
$$

Next to compute the complexity functional (5.33) we have to do the following:

- We choose the reference state $|\psi_R\rangle$ as the primary state $|p, h\rangle$ of the underlying warped CFT [148, 137].

- To compute the following,

$$
\tilde{Q}(\tau) = U^\dagger(\tau)\left(Q_T(\tau) + Q_P(\tau)\right)U(\tau).
\tag{5.36}
$$

we first note that, $U(\tau)$ is basically unitary representation of the symmetry group elements. Hence acting $U(\tau)$ on $Q_T(\tau)$ and $Q_P(\tau)$, amounts to transform $T^\alpha(\phi)$ and $P^\alpha(\phi)$ using the transformation rules mentioned in (5.21). We then get the following,

$$
\begin{aligned}
U^\dagger(\tau)T^\alpha U(\tau) &= f'(\tau,\phi)^2 \, T^\alpha(\phi) + \frac{c}{12}\{f(\tau,\phi),\phi\} + f'(\tau,\phi)g'(\tau,\phi)P^\alpha(\phi) - \frac{k}{4}g'(\tau,\phi)^2, \\
U^\dagger(\tau)P^\alpha U(\tau) &= f'(\tau,\phi)P^\alpha(\phi) - \frac{k}{2}g'(\tau,\phi).
\end{aligned}
\tag{5.37}
$$

Here, for a given path τ in the group manifold, f is the diffeomorphism on the circle just like the Virasoro case [81, 64] and g provides a translation along τ for given ϕ. Note that in contrast to [81, 64] we are using the notation f, g instead of F, G and to represent the inverse diffeomorphism and vice versa. Our notation is more in line with the original literature in the context of coadjoint orbit action in 2D gravity [?].

- Also we relate the velocity (the control functions) $\epsilon(\tau,\phi)$ with the group parameters. Note that, we can identify it as the instantaneous velocity in the group space from (5.30) just like the case of Virasoro [81, 64]. Hence following, the similar computation done in [81, 64], it can be related

to the derivatives of diffeomorphism on the circle, i.e for an infinitesimal change in τ, the how the diffeomorphism over the circle changes. So we get the following [81, 64],

$$\epsilon(\tau,\phi) = -\frac{\dot{f}(\tau,\phi)}{f'(\tau,\phi)} \tag{5.38}$$

Also, henceforth we will omit the arguments of the functions f, g and denote the τ and ϕ derivative as by "($\cdot$)" and ($'$) and respectively.

- Finally we replace the expectation values of $T^\alpha(\phi)$ and $P^\alpha(\phi)$ with respect to the primary states in the complexity functional (5.33) by the relations mentioned in (5.26).

Then putting all this together from (5.33) we get,

$$\mathcal{C} = \frac{1}{2\pi} \int_0^T d\tau \int_0^{2\pi} d\phi \left| -\dot{f}f'T_0 - \frac{c}{12}\frac{\dot{f}}{f'}\{f,\phi\} - \dot{f}\,g'\,P_0 + \frac{k}{4}\frac{\dot{f}}{f'}g'^2 - \dot{f}\,P_0 + \frac{k}{2}\frac{\dot{f}}{f'}g' \right| \tag{5.39}$$

where, $T_0 = \langle h|T^\alpha(f,g)|h\rangle$ and $P_0 = \langle h|P^\alpha(f,g)|h\rangle$. We have chosen the reference state $|\psi_R\rangle$ as the primary state $|h\rangle$. Next we minimize (5.39) with respect to f and g. Note that, there is no $\dot{g}$. So we obtain the following constraint condition for g',

$$g' = \frac{\beta(\tau) + \dot{f}\,P_0}{(k/2)(\dot{f}/f')} - 1. \tag{5.40}$$

Here $\beta(\tau)$ is an integration constant which will be determined from the initial conditions. Next using (5.40) we can eliminate g' from (5.39). We get,

$$
\begin{aligned}
\mathcal{C} =& \frac{1}{2\pi} \int_0^T d\tau \int_0^{2\pi} d\phi \left| \dot{f}f'\left(T_0(f) + \frac{P_0(f)^2}{k}\right) + \frac{\dot{f}}{f'}\left(\frac{c}{12}\{f,\phi\} + \frac{k}{4}\right) - \frac{\beta^2 f'}{k\dot{f}} \right| \\
=& \frac{1}{2\pi} \int_0^T d\tau \int_0^{2\pi} d\phi \left| \frac{\dot{F}}{F'}\left(T_0(\phi) + \frac{P_0(\phi)^2}{k}\right) - \frac{\dot{F}}{F'}\frac{c}{12}\{F,\phi\} + \dot{F}F'\frac{k}{4} - \frac{\beta^2\,F'}{k\dot{F}} \right|
\end{aligned}
\tag{5.41}
$$

Here in the second line we have expressed the action in terms of the inverse diffeomorphism, F, defined by $F\left(\tau, f(\tau,\phi)\right) = \phi$). Now using (5.26) we finally we get,

$$\mathcal{C} = \frac{1}{2\pi} \int_0^T d\tau \int_0^{2\pi} d\phi \left| \frac{\dot{F}}{F'}\left(2k\,\alpha^2 + \frac{c}{24} - \frac{c}{12}\{F,\phi\} + F'^2\frac{k}{4} - \left(\frac{F'}{\dot{F}}\right)^2\frac{\beta^2}{k}\right) \right| \tag{5.42}$$

Next we minimize (5.42). Then the Euler Lagrange equation is,

$$
\begin{aligned}
&\frac{c}{12}\frac{\dot{F}}{F'}\left(-\frac{F''}{F'^2} - \frac{6F''^3}{F'^4} + \frac{6F''F'''}{F'^3} - \frac{F''''}{F'^2} + \frac{\dot{F}'}{\dot{F}F'} + \frac{9F''^2\dot{F}'}{\dot{F}F'^3} - \frac{4F'''\dot{F}'}{\dot{F}F'^2} - \frac{6F''\dot{F}''}{\dot{F}F'^2} + \frac{2\dot{F}'''}{\dot{F}F'}\right) \\
&+ k\frac{\dot{F}}{F'}\left(\frac{4\alpha^2\dot{F}'}{\dot{F}F'} - \frac{\dot{F}'F'}{2\dot{F}} - \frac{4\alpha^2F''}{F'^2}\right) + \frac{1}{k}\frac{F'}{\dot{F}}\left(-\frac{2\beta\dot{\beta}}{\dot{F}} + \frac{2\beta^2\ddot{F}}{\dot{F}^2} - \frac{2\beta^2\dot{F}'}{F'\dot{F}}\right) = 0.
\end{aligned}
\tag{5.43}
$$

This is a nonlinear partial differential equation of very cubic order and it is not a priori obvious what are the consistent boundary and initial data on $F, \dot{F}, F', F''$ which will lead to the existence of an unique solution. The questions of consistent initial and boundary data, existence, uniqueness, boundedness of the solution etc. of this equation can perhaps be taken up in a future investigations. For now we content ourselves by arriving at a solution by plain guessing since for the purpose of this paper, *any* solution will allow us to make an estimate of the circuit complexity and afford a comparison with the holographic complexity computed in Sec. 2. By simple inspection, the most obvious solution of (5.43) is $\dot{F} = F' = 0$ when $\dot{\beta} = 0$, which yields

$$F(\tau,\phi) = c_1\,\tau + c_2\,\phi + c_3 \quad \& \quad \beta = \text{constant} \tag{5.44}$$

where, c_1, c_2, c_3 are constants. One can try to look for more general solutions which To be a diffeomorphism, $F(\tau, \phi)$ must have the same period as ϕ (for fixed τ) i.e [81],

$$F(\tau, \phi + 2\pi) = F(\tau, \phi) + 2\pi. \tag{5.45}$$

So from (5.44) we get,

$$c_2 = 1. \tag{5.46}$$

Also, $F(0, \phi) = \phi$ is the initial condition [81]. This implies, $c_3 = 0$. Finally we are left with the following,

$$F(\tau, \phi) = c_1 \tau + \phi. \tag{5.47}$$

Putting (5.47) in (5.42) we get,

$$\mathcal{C} = \frac{1}{2\pi} \int_0^T d\tau \int_0^{2\pi} d\phi \left[c_1 \left(2k\,\alpha^2 + \frac{c}{24} + \frac{k}{4} \right) - \frac{\beta^2}{k\,c_1} \right] = c_1\,T \left(2k\,\alpha^2 + \frac{c}{24} \right) + c_1\,T \left(\frac{k}{4} - \frac{\beta^2}{k\,c_1^2} \right). \tag{5.48}$$

The undermined coefficient c_1 is determined from the choice of the target state. The expression for complexity contains a dependence on the tilt parameter α and "time", T which labels the final (target) state in the trajectory (orbit) of the Kac-Moody symmetry gates. As remarked before the tilt parameter α is arbitrary for simplicity we can even set it to unity. In this formulation of complexity, there is no scope of any dependence of complexity with system size. Before we end this section, there are a few comments in order.

- Among various other choices for complexity functional, there is one other commonly use functional which can be defined as, $\mathcal{F} = \sqrt{-\text{Tr}[\rho_0\,\tilde{Q}^2(\tau)]}$. For our case then the complexity will take the following form,

$$\mathcal{C} = \int_0^T d\tau \sqrt{-\text{Tr}\left[\rho_0 \left(\tilde{Q}_T^2(\tau) + \tilde{Q}_P^2(\tau) \right) \right]}. \tag{5.49}$$

  It has been argued in [81] this will give the same complexity as before in large c limit. This is indeed the case for Virasoro symmetry group. Unless we take large c limit we can not expect that this complexity functional will give the same value as what we have quoted in (5.41).

- For our case it is natural that we have to take a large k limit as well since the leading semiclassical limit is defined by $l/G_N \gg 1$ which mandates large c, *as well as* large k since ν is order one). If we take $\frac{c}{k}$ small but finite while taking k large then, from (5.48) we can easily see the complexity becomes proportional to k:

$$\mathcal{C} \sim k\,c_1 \left(2\,\alpha^2 + \frac{1}{4} + \frac{c}{24k} \right) T \tag{5.50}$$

  This is similar to the result obtained from the holography which is also proportional to the k in this limit as evident from (5.14), (5.15) and (5.16).

- Last but the not the least, unlike the gravity result, we do not get any UV cut-off dependence (short distance singularities) in the complexity! In fact this supposed to be case, for Virasoro group also as mentioned in [64, 67]. So it will be tempting to use the other methods e.g. Fubini-Study approach [68, 67, 181] and try to get a more precise match.

5.3 Discussions

WAdS$_3$/WCFT$_2$ duality allows us to explore holography beyond asymptotically AdS spacetimes. WCFTs are nonlocal quantum field theories characterized by the infinite dimensional symmetry algebra, namely the Virasoro-Kac-Moody current algebra. In this work we have probed WCFTs by means of circuit complexity, a novel tool which has traditionally been used in quantum information and computation theory, but has gained importance in black hole physics and holography of late. In particular we studied the WCFT complexity in two independent schemes. First is the holographic volume complexity scheme and the other is the recently proposed circuit complexity based on circuits constructed purely by means of unitary gates which are the Kac-Moody symmetry transformations. We mainly focused on WCFTs which are putative duals of spacelike warped AdS$_3$ since the WCFTs dual to timelike or null warped AdS$_3$ are not expected to have unitary UV completion. (While discussing holographic complexity, we did discuss the timelike warped AdS$_3$ case just to illustrate the point that the complexity expression becomes nonanalytic and develops cuts when the UV cutoff is made arbitrarily small signaling UV incompleteness of the dual WCFT). For spacelike warped AdS$_3$ case, the dual WCFT$_2$ holographic complexity turns out to be linearly divergent. This is rather counterintuitive because such linear divergences are expected for *local* CFT$_2$ while WCFTs are nonlocal field theories. However, such a trend has been true for other observables like WCFT entanglement entropy [140, 139] which does display logarithmic divergence characteristic of local CFT$_2$s. The coefficient of the complexity linear divergence for CFT$_2$ is the central charge (up to a numerical factor), while for the case of WCFT$_2$ we see that this coefficient is a rather elaborate function of the Virasoro central charge, c as well as the $U(1)$ Kac-Moody level number, k and the complexity only makes sense for the range of parameters in the domain $c/k \leq 25/8$. So there is no simple way to take a large c limit while keeping k fixed, in fact one has take both c, k large while maintaining $c/k \leq 25/8$. However, one can take k large while keeping the ration c/k fixed, and in this limit, the holographic complexity has a leading behavior proportional to k. From the holographic standpoint, one might think of employing other schemes such as the action complexity. However we recall that for the case of CFT$_2$ dual to pure AdS$_3$, the action complexity vanishes due to dimensional accident (in arbitrary boundary spacetime dimensions, say d, the action complexity is proportional to a factor $\ln(d-1)$) [74]. Analogous vanishing of the action complexity has also been observed in the null warped AdS$_3$ [186] so we do not pursue this direction here in this work. See [188] for a calculation of the divergence-free time-rate of action-complexity growth in warped AdS black hole geometries.

Next we looked at the circuit complexity of WCFT based on a proposal [64] which advocates the use of the unitary gates corresponding to (exponentiating) Kac-Moody symmetry generators. Note that, the complexity functional mentioned in (5.39) is not actually geometric action functional supported on the coadjoint orbits of the Virasoro-Kac-Moody symmetry group [4]. In [64], a modification of the proposal advocated in [81] has been given. It will be interesting to use that modification to obtain a complexity functional for our case which will be same as warped coadjoint orbit action. Furthermore, extremizing the complexity functional(5.39) leads to a highly nonlinear PDE which seems intractable. But by simple investigation, we find can a special solution where the derivatives $f', \dot{f}$ are constants. This choice yields a very simple looking expression for the circuit complexity, one which depends on the symmetry parameters c and k, and the path length T between the reference and the target state. Of course it would be ideal if one could somehow arrive at a more general solution of the complexity functional extremization conditions, and figure out the most generic dependence on the parameters c, k. We leave that general analysis for future work. Since the complexity functional is proportional to the action on the coadjoint orbit and not physical space, there is no dependence on the system size. Also, by construction, this complexity functional is tolerance free and free from UV divergences. Thus perhaps one cannot perform a direct comparison of the resulting expressions of the two schemes of holographic complexity and circuit complexity employed here, apart from the fact that both are proportional to k in the leading order.

In Nielsen's original formalism [72, 71, 63], this $\mathcal{C}$ in (5.33), can furthermore be related to the number

---

[4]This is also true for the Virasoro case if we simply follow the approach of [81].

of gates, which in turn then make the complexity dependent on the system size. One first needs to perform that analysis for this case in order to relate the $\mathcal{C}$ that we have computed in (**??**) with the number of gates constituting the circuit. Also, one important thing that we have to keep in mind is that the penalty factor played an important role in such analysis. In our case, we have not penalized any gates. We leave these important issues for future investigations. Apart from this, it will be also interesting to investigate circuit complexity using other methods eg Fubini-Study, path integral approach along the lines of [181, 67, 92, 57, 61]. Last but the not the least, it will be worthwhile to investigate operator complexity related with the Hamiltonian evolution. In that context an useful approach might be to consider recently proposed 'Krylov complexity' [192] for our case. Again we hope to report on this issue in near future.

Chapter 6

Quantum complexity and bulk timelike singularities

The issue of the resolution of spacetime singularities in general relativity is one of the biggest unsolved questions in quantum gravity. Spacetime singularities are inevitable end-points in gravitational collapse matter [193, 194]. In such situations, general relativity breaks down and new UV physics is believed to take over. It is a general consensus that this new physics will resolve the singularities by smoothing them out, e.g. in string theory, the physics of new degrees of freedom such as strings and branes might remove or resolve the singularities arising in semiclassical gravity [195]. Various isolated examples of singularity resolution are known in string theory, eg. [196, 197] (see [198] for an overview). However, it is fair to say that so far in string theory (or for that matter in any UV-complete theory of quantum gravity), there is no universal or systematic mechanism for resolving generic spacetime singularities. Spacetime singularities come in three varieties, namely spacelike, timelike and null. Spacelike singularities those where entire space essentially ends or collapses at some given moment of time, e.g. the big bang (crunch) cosmological singularity or at the heart of neutral black holes. Since all of space collapses, there is no way to evade or avoid this crunch. Timelike singularities, on the other hand, are localized in some compact spatial region and one can in principle stay away from it at all times. Being timelike, some timelike singularities extend all the way up to past timelike infinity and thus constitute a singularity in the initial (metric) data itself! No wonder many researchers perhaps regard timelike singularities as representing unphysical or pathological configurations which should not be part of any UV complete theory of gravity. However, there are no rigorous results regarding the necessary and/or sufficient conditions in string theory which govern the resolution of generic timelike singularities. Part of the reason why generic spacelike singularities, especially cosmological singularities have been intractable in traditional worldsheet sigma model based string theory approaches is due to the fact that these backgrounds are time-dependent and they explicitly break supersymmetry thereby lacking analytical control. See [199, 200, 201, 202, 203] for some attempts towards this direction. Some have argued in favour of replacing the cosmological singularity by a closed string tachyon condensate [195, 204] building on Sen's idea [205] of the rolling open string tachyon on an unstable brane. Finally nonperturbative setups such as Matrix Models [206] and the AdS/CFT correspondence has been applied to treat cosmological singularities [207, 208, 209] with modest success. There has been some efforts in dealing with the resolution cosmological singularities in the higher spin gravity set up in as well, see e.g. [210, 211] in the context of $2 + 1$-dimensions where the singularity turns out to be a gauge artifact - by performing a higher spin (spin 3) gauge transformation the metric becomes regular! However, in some respects this is unsatisfactory as turning on higher spin gauge fields can perhaps have more dramatic consequences for observers. The present work has origins in some previous work [212, 75] where it was shown that the notion of complexity adds new ways aiding in the investigation/ interpretation or resolution of a class of cosmological singularities like AdS-Kasner singularity, topological crunch singularity and de Sitter crunch singular-

ity. Holographic complexity is a promising candidate towards providing essential insight in capturing the physics of the singularities. Most transparently, in the action complexity formulation, where the WDW patch receives a direct contribution from the singularity, seems to be an appropriate tool to probe the singularity. In fact, despite appearances, the action and volume complexity seem to agree, this renders complexity in general a viable tool in the investigation of bulk containing the singularities. Those studies clearly suggested that the complexity exhibits a monotonic decrease as one approaches the singularity. This monotonic decrease points to the fact that CFT quantum states have low quantum entanglement at the singularity. This phenomenon is reminiscent of the firewall phenomenon, where the disentangling of gravity degrees of freedom across a black hole horizon leads to the appearance of a naked singularity dubbed as the *firewall* [213]. Motivated by the success of this previous work [212, 75], in this work we turn our attention towards the study of naked *timelike* singularities. Naked timelike singularities are rife in bottom-up holography, in particular in metrics obtained as solutions to the effective holographic theories at zero temperature. Such singularities can be expected, at times, to be resolved by lifting them to full ten-dimensional SUGRA or by the inclusion of string/D-brane states[1]. The important question that concerns us is whether a given naked timelike singularity in semiclassical gravity is resolvable in a UV-complete quantum gravity theory e.g. string theory. The chief criterion to answer that issue in the literature is called Gubser criterion[216, 217]. Gubser criterion implies that

Naked singularities arising in bottom-up holography (effective holographic setups) that can be obtained as the extremal deformations of regular blackholes are resolvable in full ten-dimensional (UV complete) string theory.

In the following sections, we intend to explore the complexity of the class of spacetimes which comprises of naked timelike singularities. We will first study the simplest negative mass Schwarzschild-AdS spacetime and draw important conclusions regarding the behavior of the complexity. Later we will go ahead and study more complicated examples comprising of the timelike singularities in Kasner and Einstein-Dilaton system.

In AdS/CFT, the dual CFT picture that emerges of the eternal AdS black hole is that of a entangled state of the two copies of CFT living on the asymptotic regions called the thermofield double state [28]. Two such boundaries are joined by an Einstein-Rosen bridge in the bulk spacetime. This ER bridge in the bulk continues to grow long after the boundary field theory attains thermal equilibrium. The spirit of AdS/CFT correspondence begs an answer to the natural question of what dual quantity would suffice to capture this late-time growth.

Susskind conjectured two geometrical duals to address this question and are subsequently called the Complexity Volume [48] and the Complexity Action [49][50] conjectures hereafter paraphrased by CV and CA conjecture respectively.

CV conjecture tries to quantify the difficulty in sending a signal across ERB. It proposes that the complexity of the field theory is given by the volume, V of the maximal spacial slice extending into the bulk and terminating on the boundary at the spacial slice on which the quantum state resides. Quantitatively,

$$C_V(T) = \frac{V_{max}(T)}{G_N L} \, , \tag{6.1}$$

where $V(t)$ is the maximal volume of the spacelike slice anchored at the boundary time, T. And L is some characteristic length scale associated with the spacetime bulk like AdS radius or horizon radius. However, the choice of this background dependent quantity is ambiguous.

The CA conjecture [49][50] quantifies the holographic dual to the quantum complexity by evaluating the classical bulk action on the Wheeler-DeWitt patch (Wheeler-deWitt patch is the union of all the spacelike slices which extend into the bulk and terminate on the same given spacial slice on the boundary).

---

[1]There are some isolated examples of the resolution of some innocuous timelike singularities in string theory e.g. the *enhancon* [214] where a singular D-brane geometry is resolved when on zooms in close to the singularity and one finds that the D-branes form a shell with flat metric in the interior [215].

Action complexity conjecture posits that, the complexity of the boundary state at time, T is given by

$$C(T) = \frac{I_{WdW}(T)}{\pi\hbar} \ , \tag{6.2}$$

where I_{WdW} is the bulk action evaluated on the Wheeler de Witt patch (domain of dependence) for a timelike slice at a time, t. Since there is no matter in the bulk, the action is given by [74, 73] the gravitational part

$$I_{WdW} = \frac{1}{16\pi G_N} \int_{WdW} d^{d+1}x \sqrt{g} \ (R - 2\lambda) + \frac{1}{8\pi G_N} \int_{\partial WdW} d^d x \sqrt{h} \ K$$
$$- \frac{1}{8\pi G_N} \int_{\Sigma} d\lambda d^{d-1}\theta \sqrt{\gamma} \kappa + \frac{1}{8\pi G_N} \int_{\Sigma} d^{d-1}x \sqrt{\sigma} a \ .$$

The first term comprise of the bulk Einstein-Hilbert action term with the cosmological constant, and for the rest of this work, the Gibbons Hawking boundary term will be evaluated at the timelike boundaries. The third term is the boundary term for the null boundaries of the WdW patch and the constant κ comes from writing out the null geodesic equation for the outward directed normal for the null surface, k

$$k^\mu \nabla_\mu k^\nu = \kappa k^\nu \ .$$

There are also the joint contributions which are codimension-two surfaces formed by the intersection of the null-null or null-timelike surfaces. The null boundary contributions are in general complicated and we have just written them out for the sake of completeness. In the entirety of this chapter, we will use the alternative prescription proposed in [75] of simplifying the calculations by deforming the lightlike boundaries into timelike surfaces and then taking the null limit. This prescription is particularly advantageous for two reasons, first we don't have to deal with the null-null joint pieces which will get smoothed out into the timelike surface, and secondly, we will be able to use the GHY prescription to deal with the timelike boundaries instead of the different prescription by [76] to deal with the lightlike boundaries, thereby making our job a lot easier. We will still have to include the last term for the intersection of two timelike surfaces for which, $a = \log |n_1.n_2|$ where n_i's are the outward unit normals to the timelike surfaces.

There some operational advantages in choosing action complexity over volume complexity, the foremost is that, unlike volume complexity, action complexity does not depend upon quantities like arbitrary length scales. The second advantage of action complexity of is that solving for volume complexity is generally a hard variational problem which requires maximization unlike the action complexity wherein one is only required to evaluate the integrals. On the other hand, in geometries which have lesser symmetry, constructing the WdW patch is in itself a nontrivial exercise but the maximal volume slices are relatively easier to construct [186, 218].

The plan of the chapter is as follows. In Sec. 6.1 we study the negative mass Schwarzschild AdS geometry. This is known to have a pathological boundary dual, namely a CFT with no stable ground state. This geometry evidently violates the Gubser criterion since it cannot be realized as the extremal (zero temperature) limit of the positive mass Schwarzschild-AdS (SAdS) black hole or for that matter any asymptotically AdS geometry with a cloaked singularity. We first compute the action complexity numerical for a range of the parameters namely the mass parameter, the bulk IR cut off. The action and volume complexity are found to be positive in all cases and display the UV divergences characteristic of a local dual field theory. However both the action and volume complexity are found to lower than that of empty (global) AdS! We take this observation to be a clear sign of pathology - anything having a holographic complexity lower than empty AdS must imply instability of the dual CFT/ quantum gravity theory. Next, in Sec. 6.2, we look at an anisotropic asymptotically AdS geometry which is the timelike counterpart of AdS-Kanser spacetime. This contains a naked timelike singularity which too is not allowed according to the Gubser criterion - it cannot be obtained as the extermal limit of a cloaked

singularity and instead is obtained via a *Wick rotation* of the more familiar spacelike Kasner-AdS space-time. We compute the action complexity analytically for this case, and just like in the negative mass Schwarzschild AdS case, we find that it has a lower action complexity than empty (Poincaré) AdS space-time. Thus according to formulated complexity criterion, this solution should not be admissible or realizable as semiclassical geometry in any UV complete theory of quantum gravity. Next we work out the volume complexity of this timelike Kasner-AdS geometry and we find that for the range of Kasner exponent, $\alpha < 2/3$, the volume complexity is lower than that of empty AdS and thus must be ruled out. However for the complimentary range of values of the Kasner exponent, $2/3 < \alpha < 1$, the volume complexity is larger than empty Poincaré AdS, and thus appears to be an allowable singularity! We conclude that action complexity is as good a tool to diagnose admissible naked timelike singularities as Gubser criterion, but volume complexity is not a reliable probe. Encouraged by the results of these two types of timelike singularities, we move on to naked singularities arising in the (asymptotically AdS) Einstein-Scalar system in Sec. 6.3. These solutions are characterized by two parameters, Q, α. While Q can be any positive number, α lies in the restricted range $(0, 1)$. We show that according to the Gubser criterion when $\alpha \geq \frac{1}{\sqrt{3}}$, the geometry contains an admissible naked singularity while for the complimentary range $\alpha < \frac{1}{\sqrt{3}}$ the singularity is not admissible anymore. Following this we compute the action complexity (both analytically and numerically), and find that for $\alpha < \frac{1}{\sqrt{3}}$ the action contains a negative divergent contribution arising from the singularity, while for $\alpha \geq \frac{1}{\sqrt{3}}$, the complexity is positive and larger than that of empty (global) AdS$_4$. Thus action complexity criterion is in perfect agreement with the Gubser criterion on the appearance of naked timelike singularities in a UV complete quantum gravity theory. We compute the volume complexity next and find that, unlike action complexity, it does not show a sudden jump from negative to positive as the parameter α is dialed from 0 to 1. Thus, once again volume complexity fails to discriminate between forbidden and admissible naked timelike singularities. We conclude our work in Sec. 6.5 by discussing our results and provide an outlook for the future investigations to further test our complexity criterion.

6.1   Negative mass Schwarzschild-AdS singularity

Before delving into a case study of the timelike singularities appearing in the effective holographic theories, we would first like to try out a warm-up example of a timelike singularity, the field theory dual to which is known to be pathological. The boundary theory is pathological in the sense that it does not admit any ground state and the corresponding bulk dual is the negative mass Schwarzschild in AdS spacetime. The negative mass Schwarzschild-AdS geometry is a vacuum solution to the Einstein field equations with a negative cosmological constant, $\lambda = -\frac{(D-1)(D-2)}{2\,l^2}$. It is described by the metric (in Schwarzschild coordinates)

$$ds^2 = -f(r)dt^2 + \frac{dr^2}{f(r)} + r^2 d\Omega^2_{D-2} \ , \tag{6.3}$$

where the redshift factor,

$$f(r) = 1 + \frac{r^2}{l^2} + \frac{\mu}{r^{D-3}}$$

has an opposite sign mass term compared to the usual Schwarzschild geometry. Consequently, there is no coordinate singularity at hypersurface $r = 2M$, and nor is the boundary of a trapped surface horizon, i.e. an event horizon. However, the hypersurface $r = 0$, which is a *timelike* hypersurface, is still a curvature singularity, and is not hidden behind an event horizon. In other words, the bulk geometry constitutes of a naked timelike singularity. The chain of arguments provided in [219] necessitates the theory of Quantum Gravity (QG) to admit certain kinds of unresolvable timelike gravitational singularities. Instead, the lack of such singularities would often result in a badly behaved theory e.g. the instability of the groundstate. As alluded to earlier, the negative mass Schwarzschild-AdS bulk geometry supplies such
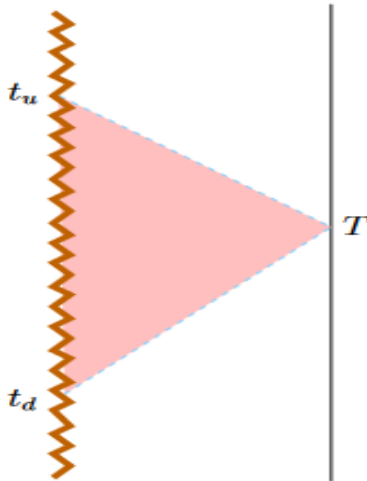
Figure 6.1: Penrose diagram for negative mass timelike Schwarzschild AdS geometry. The region shaded in pink is the WdW patch corresponding to boundary time T.

an example geometry which is known to have a sick (unphysical) holographic dual, namely a field theory with a ground state whose energy is unbounded from below [219], this background clearly violates the Gubser criterion.

We expect the complexity to reflect some pathological behavior that signifies the sickness of the boundary field theory. In the following sections, we work out the complexity using the action complexity conjecture first and later test our claims with the aid of the volume complexity conjecture in the subsequent section.

6.1.1 Action complexity for negative mass Schwarzschild AdS

In this section, we compute action complexity corresponding to the CFT state dual to the negative-mass Schwarzschild AdS black hole. The complexity thus computed is expected to reveal to us the universal divergent pieces. However, on the accounts of the dual CFT lacking any ground state [219], we expect to register some unphysical characteristics.

Consider a boundary state given at time $t = T$ for which we wish to compute the complexity as depicted in First of all, we need to determine the WdW patch. For this purpose, we follow past and future null rays originating at the boundary point T. The resulting WdW patch is bounded by the null rays

$$dt_{u/d} = \mp \frac{dr}{f(r)} \ ,$$

that can readily be written in the integrated form

$$t_{u/d}(r) = T \pm \int_r^\infty \frac{dr}{f(x)} \ .$$

The subscript u (d) corresponds to the future (past) boundary of the WdW patch. Having determined the boundaries for the WdW patch, we now compute the contributions to the action complexity.

- **Einstein-Hilbert term bulk contribution**

$$
\begin{aligned}
I_{EH} &= \tfrac{1}{16\pi G_N} \int_{WdW} d^D x \ \sqrt{-g} \ (R - 2\lambda) \ , \\
&= -\tfrac{(D-1)\,\Omega_{D-2}}{4\pi G_N l^2} \int_0^\Lambda dr \ r^{D-2} \int_r^\Lambda \tfrac{dx}{f(x)}.
\end{aligned}
\tag{6.4}
$$

The radial integral is IR divergent. So we regulate this contribution by means of the IR regulator, $r \leq \Lambda$. This contribution is manifestly negative because the integral is positive definite (integrand is positive and the limits of integration are in ascending order).

- **The GHY contribution from the timelike singularity** On one side, the WdW patch is bounded by the timelike singularity within the range of time coordinates lying between t_d and t_u. We will consider a fixed r surface with nonzero r and then set $r \to 0$ at the end. The induced metric on a constant r hypersurface is

$$ds^2 = -f(r)dt^2 + r^2 d\Omega_{D-2}^2.$$

For which the integral measure can easily be seen to be

$$d^{D-1}\sqrt{h} = f^{1/2}(r)\, r^{D-2} dt\, d\Omega_{D-2}.$$

The outward normal to this hypersurface turns out to be

$$n^r = -f^{1/2}(r),\; n^t = n^\Omega = 0.$$

The trace of the extrinsic curvature can be found to be equal to

$$K = -\frac{f'}{2f^{1/2}} - \frac{D-2}{r}f^{1/2}.$$

The GHY term works out to be

$$I_{GHY}^{r=0} = \lim_{r \to 0} \frac{1}{8\pi G_N} \int d^{D-1}x\sqrt{h}\, K = 0, \tag{6.5}$$

where we have considered $D \geq 3$. *Thus the GHY term contribution arising from the singularity vanishes*!

- **The GHY piece from the null boundaries of the WdW patch**
  We will first deform the two null boundaries of the WdW patch described by the conditions,

$$t_{u/d} - T = \pm \int_r^\infty \frac{dx}{f(x)}$$

to a single codimension-1 timelike surface by introducing a null-to-timelike deformation parameter, ε as follows

$$(t - T)^2 - (1+\varepsilon)^2\, g(r)^2 = 0, \tag{6.6}$$

where for convenience we have defined, $g(r) = \int_r^\Lambda \frac{dx}{f(x)}$. This deformation simultaneously serves as a bulk IR regulator and the null-to-timelike deformation of the null boundaries of the WdW patch because the two regulators are related via the relation

$$\int_0^\infty \frac{dx}{f(x)} = (1+\varepsilon) \int_r^\Lambda \frac{dx}{f(x)}.$$

So $\varepsilon \approx \frac{2}{\pi}\frac{l}{\Lambda}$. At the end of the day we are going to set $\varepsilon = 0$ to recover the GHY contribution from the original null boundaries of the WdW patch. The induced metric on this timelike deformed hypersurface is

$$ds^2 = -2\varepsilon\frac{dr^2}{f(r)} + r^2 d\Omega_{D-2}^2 \,.$$

and the volume element on this timelike deformed hypersurface works out to be

$$d^{D-1}x\sqrt{-h} = d\Omega_{D-2}\, dr\, \frac{(2\varepsilon)^{1/2}\, r^{D-2}}{f^{1/2}}.$$

The unit outward normal to this hypersurface has components

$$n^t = -\frac{f^{-1/2}(t-T)}{\sqrt{g^2(1+\varepsilon)^4 - (t-T)^2}} \; , \qquad n^r = \frac{(1+\varepsilon)^2 f^{1/2} g}{\sqrt{g^2(1+\varepsilon)^4 - (t-T)^2}} \qquad n^\Omega = 0.$$

From these we compute the trace of the extrinsic curvature to be

$$K = \frac{1}{(2\varepsilon)^{1/2} f^{1/2}} \left[\frac{f'}{2} + \frac{D-2}{r} f \right].$$

Now we are ready to work out the GHY integral in the null limit $\varepsilon \to 0$:

$$\begin{aligned} I_{GHY}^{\partial W dW} &= \frac{1}{8\pi G_N} \int d^{D-1}x \sqrt{h} \; K \; , \\ &= \frac{\Omega_{D-2}}{16\pi G_N} \int_0^\Lambda dr \; r^{D-2} \left[\frac{f'}{f} + 2\frac{D-2}{r} \right]. \end{aligned}$$

To tame the IR divergences we had to cutoff the range of r-integration to Λ. We simplify the result a bit to the form,

$$I_{GHY}^{\partial W dW} = \frac{\Omega_{D-2}}{16\pi G_N} \int_0^\Lambda dr \; r^{D-2} \frac{f'}{f} + \frac{\Omega_{D-2}\Lambda^{D-2}}{8\pi G_N} \; . \tag{6.7}$$

- **Joint contributions from the edges along the intersection of $r=0$ and $\partial W dW$**

  The joints are formed by the intersection of boundary segments $r = 0$, and timelike deformed boundaries (6.6). The induced metric on the joints takes the simple form

  $$ds^2 = r^2 d\Omega_{D-2}^2.$$

  The components of the normals at $r = 0$ are

  $$n_1^r = -f^{1/2}(r) \; , \qquad\qquad n_1^{t,\Omega} = 0 \; .$$

  And on the regulating surface, the components takes the form

  $$n_2^r = \frac{f^{1/2}}{(2\varepsilon)^{1/2}} \; , \qquad n_2^t = \frac{f^{-1/2}}{(2\varepsilon)^{1/2}}, \qquad n_2^\Omega = 0 \; .$$

  Thus, the contribution from each joint is identical and total contribution is

  $$\begin{aligned} I_{LMPS} &= 2 \times \frac{1}{8\pi G_N} \int d^{D-2}x \; \sqrt{\gamma} \; \ln|n_1.n_2| \; , \\ &= \frac{\Omega_{D-2}}{4\pi G_N} \lim_{r \to 0} \left(r^{D-2} \ln \left| \frac{1}{(2\varepsilon)^{1/2}} \right| \right) = 0. \end{aligned} \tag{6.8}$$

  Note that we have to take the $r \to 0$ limit before we turn off the deformation ε.

The final action complexity for the negative mass Schwarzschild-AdS geometry is given by the sum of the contributions (6.4), (6.5), (6.7) and (6.8). An exact closed form expression for the action complexity cannot be obtained since the integrals cannot be performed analytically without making any further approximations. One could alternatively choose to evaluate this expression perturbatively, expanding powers of some small parameter such as μ/l^{D-3} or μ/Λ^{D-3}. Instead of making approximations, we evaluate the final action complexity exactly by performing the integrals numerically for a range of values of the mass parameter μ and the bulk IR cutoff Λ. For concreteness, the dimensionality of the spacetime has been chosen to be $D = 4$ and AdS radius is set to unity, $l = 1$. The characteristic features of the action complexity can be surmised from the numerical data provided the table of C_A below with the appropriate IR cutoffs and for various values of the mass parameter. The following interesting features are evident from the table that the action complexity.

μ	IR cutoff	$\frac{G_N \hbar}{\Omega_{D-2}} C_A^{SAdS}$	$\frac{G_N \hbar}{\Omega_{D-2}}(C_A^{SAdS} - C_A^{AdS})$
2×10^4	10^6	6.33×10^9	-1.32 $\times 10^{-4}$
2×10^5	10^6	6.33×10^9	-1.26 $\times 10^{-3}$
2×10^6	10^6	6.33×10^9	-1.26 $\times 10^{-2}$
2×10^6	10^8	6.33×10^{13}	0.0*
2×10^7	10^8	6.33×10^{13}	-2.34×10^{-2}
2×10^8	10^8	6.33×10^{13}	-2.34×10^{-2}

Table 6.1: Table for dependence upon mass and cut off for negative mass SAdS using CA. (* Is negative but the machine precision is not enough to resolve the small number.)

- Firstly, the action complexity has strong quadratic dependence upon the bulk IR cutoff. This is easily understood in light of the UV-IR correspondence in the AdS-CFT duality set up. The bulk IR divergences encode the UV divergences of the dual boundary conformal field theory. If the dual boundary theory is a local theory, an extensive quantity such as complexity would naturally be expected to have a leading quadratic divergence (or UV divergence scaling Λ^{D-2} for general D-dimensional bulk).

- Secondly, the action complexity display extremely weak dependence on the negative mass parameter μ, which is not surprising since the dependence on μ is via the dimensionless combination μ/Λ^{D-3} i.e. is heavily suppressed by powers of the large bulk IR cutoff. The fourth column in the table 6.1 displays the values of complexity after background *(pure-AdS) subtraction*. It is immediate that the difference between the action complexity of negative mass SAdS and the pure AdS geometry is orders of magnitude smaller than the pure AdS complexity and is more significantly negative.

- Third and perhaps the most couterintuitive observation is that the timelike singularity does not contribute to the complexity at all! In case of the usual (positive mass) Schwarzschild case, the action complexity does receive a nonvanishing and finite (nondiverging) contribution[2]. We interpret this feature to the first sign that complexity is not a tool or probe that is sensitive to the presence of timelike singularties in the bulk.

- Finally complexity expression does not reveal that the dual boundary theory is sick (unstable since does not admit a ground state). Perhaps the only indication is that the complexity of negative mass Schwarzschild-AdS is lower that pure AdS (which is dual to the ground state/vacuum in a stable CFT). For positive mass Schwarzschild-AdS geometry the complexity of the dual theory is larger than empty AdS geometry.

According to Gubser criterion [216], since the negative mass Schwarzschild AdS geometry cannot be obtained as the extremal limit of any regular black hole solution, it is an example of unresolvable singular geometry in a fully quantum theory of gravity (string theory) in the sense that it can never be obtained in the semiclassical gravity approximation in a fully quantum theory of gravity. However, at the first glance, the action complexity (shown in the third column of table 6.1) of this unphysical background does not show any obvious signs of such pathology - it is positive definite and scales extensively with dual boundary theory. The only feature which hints at the pathology is the complexity of this geometry being *lower than that of the empty AdS*. This naively indicate that it is easier to create the negative mass singular bulk background than the empty AdS, effectively hinting at some kind of instability of the underlying fundamental theory. Armed with this observation we are led to a possible criterion for

---

[2]In fact this is true for most spacelike singularities, naked or cloaked [212, 75].

a given singular aAdS geometry to be resolvable in full quantum gravity (CFT), namely it must have a holographic complexity higher than empty AdS. To complete the analysis we will apply the volume complexity prescription in the next section to affirm our conjecture motivated from the action complexity exercise.

6.1.2 Volume complexity for the negative mass Schwarzschild AdS

In this section, we will probe the complexity of negative mass SAdS using the CV prescription. To this end, we consider spacelike hypersurface $t = t(r)$. The induced metric on this spatial hypersurface given by

$$d\gamma^2 = \left(-f(r)t'^2(r) + \frac{1}{f(r)}\right)dr^2 + r^2 d\Omega_{D-2}^2 \ .$$

We need to extreimize the volume for the codimension-1 spacelike hypersurface anchored at some specific[3] boundary time, say T:

$$V(T) = \Omega_{D-2} \int_0^\infty dr\, r^{D-2} \sqrt{-f(r)t'^2(r) + \frac{1}{f(r)}} \ .$$

The variational problem yields the following Euler-Lagrange equation

$$2(D-2)f(r)^3 t'(r)^3 - 2f(r)\left((D-2)t'(r) + rt''(r)\right) + rf(r)^2 f'(r)t'(r)^3 - 3rf'(r)t'(r) = 0 \ .$$

Assuming the near boundary expansion of the form

$$t(r) = T + \frac{t_1}{r} + + \frac{t_2}{r^2} + \frac{t_3}{r^3} + \frac{t_4}{r^4} + ... \ ,$$

and plugging back into the Euler-Lagrange equation to solve perturbatively term by term yields us the solution $t(r) = T$. This solution seems plausible upon exploiting the time translation symmetry to choose the symmetrical solution $t = \text{constant}(= T)$. The maximal volume then turns out to be

$$V(T) = \Omega_{D-2} \int_0^\infty dr\, \frac{r^{D-2}}{\sqrt{f(r)}} \ ,$$

$$= \Omega_{D-2} \int_0^\infty dr\, \frac{r^{D-2}}{\sqrt{1 + \frac{r^2}{l^2} + \frac{\mu}{r^{D-3}}}} \ .$$

Evidently the bulk volume is an IR divergent quantity, and so we impose a bulk IR cutoff, Λ. The regulated volume complexity turns out to be

$$\mathcal{C}_V(T) = \frac{\Omega_{D-2}}{G_N l} \int_0^\Lambda dr\, \frac{r^{D-2}}{\sqrt{1 + \frac{r^2}{l^2} + \frac{\mu}{r^{D-3}}}} \ . \tag{6.9}$$

The integral can only be solved perturbatively in the mass parameter. However, for our purpose, the numerical evaluation of the integral is better suited to unravel the relevant characteristics. We, therefore, list the various values of complexity using complexity volume duality along with appropriate IR cutoffs after fixing the AdS radius to be unity. The following interesting features are evident from the table 6.2 that the volume complexity.

- First of all, just like action complexity, the volume complexity displays strong quadratic dependence upon the bulk IR cutoff. As alluded to before, this behavior is expected of any local field theory extensive quantity.

---

[3]Due to the lack of event horizons in this negative mass geometry one has a global timelike killing vector, ∂_t, and consequently the complexity is T-independent

μ	IR cutoff	$\frac{G_N}{\omega_{D-2}}C_V^{SAdS}$	$\frac{G_N}{\omega_{D-2}}(C_V^{SAdS} - C_V^{AdS})$
$2{\times}10^4$	10^6	$5. \times 10^{11}$	-3.73
$2{\times}10^5$	10^6	$5. \times 10^{11}$	-37.32
$2{\times}10^6$	10^6	$5. \times 10^{11}$	-373.23
$2{\times}10^6$	10^8	$5. \times 10^{15}$	-4
$2{\times}10^7$	10^8	$5. \times 10^{15}$	-37
$2{\times}10^8$	10^8	$5. \times 10^{15}$	-373

Table 6.2: Table for dependence upon mass and cut off for negative mass SAdS using CV

- Secondly, the volume complexity display extremely weak dependence on the negative mass parameter μ, the behaviour reminiscent of the action complexity. Recall that this is because the dependence on μ is heavily suppressed by powers of the large bulk IR cutoff. The fourth column in the table 6.1 displays the values of complexity after background subtraction. It can again be easily seen that the difference between the action complexity of negative mass SAdS and the pure AdS geometry is negative and is orders of magnitude smaller than the pure AdS complexity.

- Thirdly, the volume and the action complexity results agree modulo an overall factor. It has been pointed out elsewhere, the mismatch in the overall coefficient in the terms of action and volume complexity is not significant [74] and is also likely to arise due to ambiguity in the choice of the characteristic length scale in the definition of volume complexity.

- From the entries of the last column in table (6.2) one can see that the volume complexity registers a greater difference in the complexity of the negative mass SAdS from the empty AdS that is orders larger than accounted for by the action complexity. This is an artifact of working with $D = 4$ as shown in the perturbative analysis performed in Appendix D. The action complexity leading term has a prefactor $D-4$ while the volume complexity has no such prefactor. As a result the first nontrivial correction in action complexity is of subleading order compared to volume complexity. Disagreements in the subleading pieces of various prescriptions of holographic complexity has been noted widely in the literature for a large class of asymptotically AdS geometric - the underlyig intuition is that these disagreements represent a scheme dependence in their field theory definitions.

- And finally, just like in the previous case of the action complexity, we are led to interpret the overall negative value after background subtraction as the indication of the sickness of the boundary dual in sync with the Gubser criterion.

In the subsequent sections, after working with different concrete examples, we will try to supply more evidence for our conjecture whether the complexity criterion cited above is in concordance with the already established Gubser criterion as an alternative diagnostic for the curability of a singular semiclassical geometrical background in a QG theory.

6.2 Timelike Kasner-AdS spacetime

In this section, we will take a look at an anisotropic solution to the Einstein field equations that appears in effective holographic theories. Effective holographic theories arise in string theory as a result of taking a sequence of limits in which we turn off the stringy physics by setting $\alpha' \to 0$ and also the volume of the compactified dimensions is also taken to be zero. This solution is closely related to the more familiar Kasner singularity. However, in this case, the time direction is also allowed to scale anisotropically along with other transverse coordinates. In this work, we are only subjecting the (3+1) dimensional timelike

spacetime to treatment. The metric for a "*Wick rotated*" version of the AdS-Kasner geometry in Poincaré like conformal coordinates is [220]

$$ds^2 = \frac{l^2}{z^2} \left(\frac{dz^2}{f(z)} - f^\alpha(z) \, dt^2 + f^\beta(z) \, dx^2 + f^\gamma(z) \, dy^2 \right), \tag{6.10}$$

where l is the AdS radius, and $f(z) = 1 - \frac{z^3}{z_0^3}$. We will set $z_0 = 1$ for convenience. Here exponents α, β, γ are positive by convention and they satisfy the usual Kasner condition(s)

$$\alpha + \beta + \gamma = \alpha^2 + \beta^2 + \gamma^2 = 1.$$

This metric has singularities at $z = 0$ and $z = 1$. While $z = 0$ is the spatial infinity (nonsingular), $z = 1$ is a *naked* timelike singularity i.e. the metric cannot be continued beyond $0 \le z \le 1$. The geometry of the singularity at $z = 1$ can be more clearly seen by the IR geometry

$$ds^2 = -r^{2\alpha} dt^2 + dr^2 + r^{2\beta} dx^2 + r^{2\gamma} dy^2 \ .$$

The Penrose diagram of this geometry is provided in figure 6.2. The limit $\alpha = 1, \beta = \gamma = 0$ reproduces
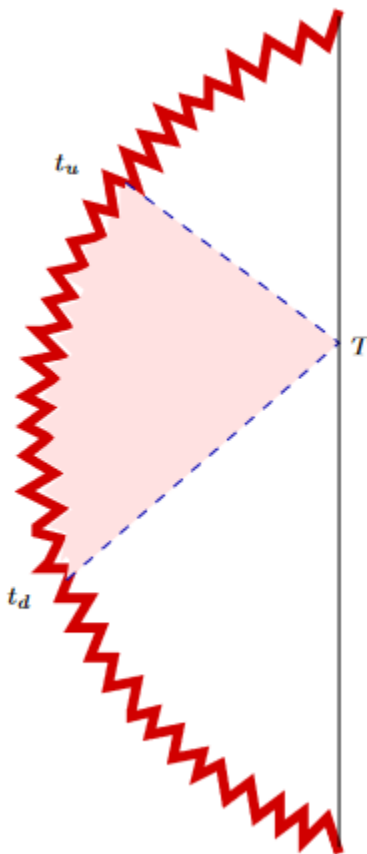

Figure 6.2: Penrose diagram for timelike Kasner AdS. The region shaded in pink is the WdW patch corresponding to boundary time T.

the (isotropic) black brane singularity at $z = 1$, so this metric represents the metric for an anisotropic black brane. By taking near boundary limit it is easy to see that geometry (6.10) connects the AdS at

the UV to the timelike Kasner singularity at the IR via RG flow. Despite the fact that the cloaked singularities in anisotropic spacetimes do not adhere to the Gubser criterion because they do not exist in pure gravity [221, 222] or in other words, cannot be obtained as the extremal limit of finite temperature black holes. However, there have been efforts to justify the existence of the anisotropic timelike Kasner singularity can be justified on other grounds, say for example using bulk causality constraints [223, 224, 225]. Therefore, if Gubser criterion is to be trusted, we anticipate that the holographic complexity of the timelike Kasner should display some pathological trait. Armed with this belief, we will first tackle the question of holographic complexity using the complexity action proposal and in the subsequent section, try to provide additional justification using the complexity volume prescription.

6.2.1 Action complexity for timelike singularity in Kasner spacetime

In this section, our aim is to compute the action complexity of the Kasner spacetime featuring naked timelike singularity. The first step towards achieving that is the determination of the WdW patch. Just like in the previous section, we follow the null rays emanating from the boundary point located at the fixed time T. The future (past) null boundaries of the WdW patch are given by the null surfaces,

$$
t_{u/d}(z) = t_* \pm \int_0^z \frac{dz'}{f^{\frac{1+\alpha}{2}}(z')}. \tag{6.11}
$$

where $t_{u/d}$ are respectively the upper/lower limits of the temporal integral. Following are the various contributions to the on-shell action for the timelike Kasner geometry computed over the WdW patch

- **The Einstein-Hilbert bulk contribution**
  Plugging the integrand $R - 2\lambda = -\frac{6}{l^2}$, the bulk volume contribution to the on-shell action evaluates to

$$
\begin{aligned}
I_{EH} &= \frac{1}{16\pi G_N} \int_{WdW} \sqrt{g}\,(R - 2\lambda)\ , \\
&= -\frac{3\,l^2\,V_{xy}}{4\pi G_N} \int_0^1 \frac{dz}{z^4} \int_0^z \frac{dz'}{f^{\frac{1+\alpha}{2}}(z')}\ .
\end{aligned} \tag{6.12}
$$

Evidently, the Einstein-Hilbert term is independent of the boundary time t_* and does not make a contribution to the time rate of change of complexity. It diverges as $z \to 0$ and we regulate this divergence by regulator prescription whereby we deform the null boundaries of the WdW patch to timelike, refer to the GHY term calculation in Sec. 6.2.1 for the details. The regulated EH term contribution to action complexity is,

$$
I_{EH} = -\frac{l^2}{8\pi\delta^2} - \frac{3\,l^2\,\Gamma\left(\frac{4}{3}\right)\sec\left(\frac{\pi\alpha}{2}\right)}{8\,z_0^2\,\Gamma\left(\frac{5}{6} - \frac{\alpha}{2}\right)\Gamma\left(\frac{\alpha-1}{2}\right)} + O(\delta)\ . \tag{6.13}
$$

Here we have restored z_0 in the final expression for dimensional consistency.

- **GHY term contribution from the singularity**

  The naked singularity at $z = 1$ supplies the timelike boundary to the WdW patch and its contribution is given by a suitable GHY term. The pull-back metric of the surface $z = constant$,

$$
ds^2 = \frac{L^2}{z^2}\left(-f^\alpha(z)\,dt^2 + f^\beta(z)\,dx^2 + f^\gamma(z)\,dy^2\right),
$$

  from which the volume element can be computed to be

$$
d^3x\,\sqrt{h} = l^3\,dt\,dx\,dy\,\frac{f^{\frac{1}{2}}(z)}{z^3}\ .
$$

The spacelike unit outward normal to this surface has only one non-zero component, $n^z = \frac{z f^{\frac{1}{2}}(z)}{L}$.
Therefore, the trace of the extrinsic curvature turns out to be

$$
\begin{aligned}
K &= \partial_z n^z + \Gamma^X_{Xz} n^z \ , \\
&= \frac{z f^{-\frac{1}{2}}(z) f'(z)}{2L} - \frac{3 f^{\frac{1}{2}}(z)}{L} \ .
\end{aligned}
$$

Thus, the GHY contribution to the action complexity turns out to be

$$
\begin{aligned}
I_{GHY1} &= \frac{1}{8\pi G_N} \sqrt{h} K \Big|_{z\to 1} \int dx\,dy \int_{t_d}^{t_u} dt \ , \\
&= -\frac{3l^2 V_{xy}}{8\pi G_N} \int_0^1 \frac{dz}{f^{\frac{1+\alpha}{2}}(z)} \ , \\
&= -\frac{3\,l^2\,\Gamma\left(\frac{4}{3}\right)\Gamma\left(\frac{1}{2} - \frac{\alpha}{2}\right)}{8\,\pi\,z_0^2\,\Gamma\left(\frac{5}{6} - \frac{\alpha}{2}\right)} + O(\delta) \ .
\end{aligned}
\tag{6.14}
$$

Here we have restored z_0 in the final result. Thus the contribution from the naked timelike singularity of the Kasner-AdS geometry is finite and negative definite for all α in the allowed range $0 < \alpha < 1$.

- **GHY term from the null boundaries of the WdW patch**

  The future and past null boundaries of the WdW patch in this case are given by (6.11). Just like in the previous section, we will deform the null boundaries of the WdW patch given by

  $$
  (t - T)^2 - g(z)^2 = 0 \qquad \text{where} \quad g(z) \equiv \int_0^z \frac{dz'}{f^{\frac{1+\alpha}{2}}(z')} \ ,
  \tag{6.15}
  $$

  to a single smooth timelike surface by means of a null-to-timelike regulator, ϵ

  $$
  (t - T)^2 - (1 + \epsilon)\left(\int_\delta^z \frac{dz'}{f^{\frac{1+\alpha}{2}}(z')}\right)^2 = 0 \ .
  \tag{6.16}
  $$

  and compute the GHY term for a usual timelike hypersurface. At the end we smoothly remove the deformation, i.e. make $\epsilon \to 0$, to recover the *total* null GHY term contribution from both future and past null boundaries in one stroke. The null-to-timelike deformation parameter and the IR regulator are related as

  $$
  \left(\int_0^1 \frac{dz'}{f^{\frac{1+\alpha}{2}}(z')}\right)^2 = (1 + \epsilon)\left(\int_\delta^z \frac{dz'}{f^{\frac{1+\alpha}{2}}(z')}\right)^2
  $$

  so that $\delta \approx \frac{g(1)}{2}\epsilon$. As we remarked earlier, this method is far simpler because there are no edges or corner contributions, unlike those one encounters while evaluating the surface contributions for null boundaries.

  The induced metric on this regulator surface is,

  $$
  ds^2 = \frac{l^2}{z^2}\left(-\epsilon\frac{dz^2}{f(z)} + f^\beta(z)\,dx^2 + f^\gamma(z)\,dy^2\right),
  $$

  the negative sign demonstrating that this is a timelike surface. The area element on this surface

  $$
  \sqrt{-\gamma}\,dx\,dy\,dz = \frac{l^3}{z^3}\sqrt{\epsilon}f^{-\alpha/2}\,dx\,dy\,dz.
  $$

The unit outward normal for this surface is

$$n^t = \frac{-z(t-T)f(z)^{-\alpha/2}}{l\sqrt{(\epsilon+1)^2 g(z)^2 - (t-T)^2}}, \quad n^z = \frac{-zg(z)f(z)^{\frac{1}{2}}}{l\sqrt{(\epsilon+1)^2 g(z)^2 - (t-T)^2}}, \quad n^{x,y} = 0,$$

Then the trace of the extrinsic curvature is,

$$K = \frac{3\sqrt{f(z)}}{l\sqrt{\epsilon}} - \frac{zf'(z)}{2l\sqrt{\epsilon}\sqrt{f(z)}} .$$

Combining all elements, the full GHY term for this outer boundary of the WdW patch is

$$\begin{aligned}
I_{GHY2} &= \frac{1}{8\pi G_N} \int d^3x \sqrt{-\gamma}\, K \\
&= \frac{l^2 V_{xy}}{8\pi G_N} \int_\delta^1 dz \left(\frac{3f(z)^{\frac{1-\alpha}{2}}}{z^3} - \frac{f'(z)}{2z^2 f(z)^{\frac{1+\alpha}{2}}} \right) \\
&= \frac{3l^2}{16\pi\delta^2} + \frac{l^2 \left(3\Gamma\left(\frac{4}{3}\right)\Gamma\left(\frac{1}{2} - \frac{\alpha}{2}\right) + 2\Gamma\left(-\frac{2}{3}\right)\Gamma\left(\frac{3}{2} - \frac{\alpha}{2}\right) \right)}{16\pi z_0^2 \Gamma\left(\frac{5}{6} - \frac{\alpha}{2}\right)} + O(\delta).
\end{aligned} \tag{6.17}$$

The finite piece is again finite for the allowed range of values of the Kasner exponent α, i.e. for $0 < \alpha < 1$.

- **Edge pieces**
  Here we compute the contribution from edges resulting from from the intersection/joint of the WdW boundary and the singularity. Although these joint terms were first worked out in [76], we followed the work [74], which very clearly and nicely tabulates these joint contributions to the action for various cases of joints. In our case we have the joint between two timelike surfaces. The action term for such a joint is

$$I_{LMPS} = \frac{1}{8\pi G_N} \int d^2x \sqrt{\eta}\, \ln|n_1.n_2| . \tag{6.18}$$

Where $\eta_{\mu\nu}$ is the induced metric on the joint and n_1, n_2 are the two timelike surfaces which intersect to produce the joint. In the present case these two timelike surfaces are given by the singularity, $z = 1$ and the WdW regulator surface (6.16). There are two joints, described by

$$z = 1, \quad t = T \pm \sqrt{1 + \epsilon}\, g(z) .$$

The induced metric on the joint is

$$ds^2 = \frac{L^2}{z^2} \left(f^\beta(z)\, dx^2 + f^\gamma(z)\, dy^2 \right),$$

from which we the jacobian can be computed to be

$$\sqrt{\eta}\, dx\, dy = \frac{L^2}{z^2} f^{\frac{1-\alpha}{2}}\, dx\, dy .$$

The unit normal on the $z = 1$ surface has non-vanishing component $n_1^z = \frac{zf^{\frac{1}{2}}(z)}{L}$ and for the null surface, the components are

$$n_2^z = -\frac{zf(z)^{1/2}}{L\sqrt{\epsilon}}, \qquad n_2^t = \frac{-zf(z)^{-\frac{\alpha}{2}}}{L\sqrt{\epsilon}}, \qquad n_2^{x,y} = 0.$$

It can be easily seen that

$$n_1.n_2 = \left.\frac{-z^2 f(z)}{L^2\sqrt{\epsilon}}\right|_{z=1} \to 0 \ ,$$

this expression vanishes at $z = 1$ and therefore its logarithm is divergent but due to the compensating jacobian vanishing faster than the logarithm, the integrand of the joint action is dominated by the vanishing jacobian and hence is zero. Thus, the joint term is

$$I_{LMPS} = -\frac{V_{xy}L^{\frac{3}{2}}}{8\pi G_N \epsilon}\left[\frac{L^2}{z^2}f(z)^{\frac{1-\alpha}{2}}\ln\left|\frac{-z^2 f(z)}{L^2\sqrt{\epsilon}}\right|\right]_{z=1} = 0 \ . \tag{6.19}$$

We now combine (6.13), (6.14), (6.17), and (6.19) and plug them back in (6.2) to obtain the following closed form expression for the action complexity of timelike Kasner-AdS spacetime

$$\mathcal{C}_A = \frac{l^2}{16\pi^2 G_N}\frac{V_{xy}}{\delta^2} - \frac{l^2}{32\pi\, G_N}\frac{V_{xy}}{z_0^2}\frac{(3-\alpha)\Gamma\left(\frac{1}{3}\right)\sec\left(\frac{\pi\alpha}{2}\right)}{\Gamma\left(\frac{5-3\alpha}{6}\right)\Gamma\left(\frac{\alpha+1}{2}\right)} \ . \tag{6.20}$$

The leading divergent piece corresponds to the pure AdS$_4$ contribution to the action complexity in the Poincaré patch [74] and the finite term comes from the deformation to Kasner-AdS. This result is not surprising because the bulk IR (boundary UV) divergence arises from the bulk IR region where the geometry is locally pure AdS$_4$ and the Kasner singularity makes an impact only in deep interior of the bulk (boundary IR). We note that the finite term is a monotonically decreasing function of the Kasner exponent α and and is negative definite, i.e. *timelike Kasner has lower action complexity than empty Poincaré AdS$_4$*. This trait is similar to that of negative mass Schwarzschild-AdS, which had lower complexity than global AdS.

Relationship to Gubser criterion: According to our formulated complexity criterion for allowable timelike singlarities in the last section, this timelike Kasner-AdS geometry is not allowed. This result is completely consistent with the Gubser criterion which too rules the existence of the timelike Kasner-AdS geometry since it cannot be obtained as the extremal limit of a black brane geometry [220]. Thus, this analysis hints that the action complexity criterion might be a suitable probe of allowable timelike singularities (independent of Gubser criterion). However, there is an alternative prescription, namely the volume complexity and it would be interesting to see whether the volume complexity prescription also leads to the same conclusion. With this in mind, we proceed in the upcoming subsection to compute the volume complexity of the field theory dual to the timelike Kasner-AdS spacetime.

6.2.2 Volume complexity of timelike Kasner-AdS

Consider the general codimension-one spatial slice anchored at the boundary time, T is obtained by treating $t = t(z)$. Then, the induced metric on the hypersurface becomes

$$ds^2 = \frac{L^2}{z^2}\left(\left(-f^\alpha t'^2 + \frac{1}{f}\right)dz^2 + f^\beta dx^2 + f^\gamma dy^2\right) \ .$$

Therefore, we will extremize the following volume

$$V = V_{xy}\int_0^1 dz\,\frac{L^3}{z^3}\sqrt{\left(-f^\alpha t'^2 + \frac{1}{f}\right)f^{1-\alpha}} \ . \tag{6.21}$$

The Euler-Lagrange equation imposing the condition of maximality upon the spatial volume is

$$2z\left(z^3 - 1\right)t''(z) + 3\left(\alpha z^3 + 2\right)t'(z) - 3\left(z^6 - 3z^3 + 2\right)\left(1 - z^3\right)^\alpha t'(z)^3 = 0 \ .$$

Assuming perturbative expansion about the boundary $z = 0$, t=T, and solving term by term leads us to the following constant time slice as the solution

$$t(z) = T \ .$$

This solution is obviously the maximum since any nonzero derivative t' in the volume functional (6.21) would lower the volume of the hypersurface. So the maximum volume is attained when $t' = 0$, i.e. $t = T$. According to the volume-complexity prescription, the volume complexity of the boundary state at time $t = T$ is

$$
\begin{aligned}
\mathcal{C}_V &= \frac{l^2 V_{xy}}{G_N} \int_\delta^1 dz \, \frac{1}{z^3 f(z)^{\frac{\alpha}{2}}} \ , \\
&= \frac{l^2}{2 \, G_N} \frac{V_{xy}}{\delta^2} - \frac{l^2}{2 \, G_N} \frac{V_{xy}}{z_0^2} \frac{\Gamma\left(\frac{1}{3}\right) \Gamma\left(\frac{2-\alpha}{2}\right)}{\Gamma\left(\frac{2-3\alpha}{6}\right)} + O(\delta) \ .
\end{aligned}
\tag{6.22}
$$

As expected, the volume complexity has a leading quadratic UV divergence that is characteristic of a local field theory with 2 spatial dimensions dual to the pure AdS$_{3+1}$ bulk. Here too this leading divergent piece is independent of the Kasner exponent(s). Volume complexity also has a finite piece, which is a monotonically increasing function on the Kasner exponent, α, again similar to the action complexity case. However, the finite pieces of the volume and action complexities are distinct (even after taking into account the mismatch of the leading quadratic divergent pieces). This, however, is not unexpected - the mismatch between the subleading terms in the volume and action complexity has been well documented in the literature [75, 132, 186]. Compared to the action-complexity result, where the finite piece was negative definite, here we obtain a finite piece that shows an change on sign from the negative to the positive values across $\alpha = 2/3$. If we adopt the criterion that a geometry can only be stable if its complexity is greater than or equal to empty AdS, then the range $2/3 < \alpha < 1$ represents allowed or stable timelike Kasner-AdS geometry. Therefore, the volume complexity results are in sync with what the Gubser criterion only for a somewhat restricted range of the Kasner coefficients, $\alpha < 2/3$.

After having seen the encouraging agreement between the complexity criterion and the Gubser criterion as regards to allowable naked timelike singularities, we attempt to seal the fate of our proposed complexity criterion as a valid probe for detecting the sick singular geometries by considering one more case of an asymptotically AdS geometry with a naked timelike singularity in the next section. The geometry, obtained as a solution to Einstein-Maxwell-Dilation system in asymptotically AdS, exhibits an interesting phase transition between the allowed phase and the disallowed phase as per the Gubser criterion. Our aim is twofold, firstly we hope to see the complexity too undergoing an analogous phase transition, from the sick geometrical phase to the allowed phase. And in due process, we also hope to settle the issue of whether complexity (and in particular which prescription) can be a suitable tool to probe the nature of geometries with naked timelike singularities - can it inform us which naked timelike singularities are allowed in the underlying theory or not.

6.3 Gubser criterion for an Einstein-dilaton system

We will begin this section by reviewing the Gubser criterion for the planar black holes arising in the Einstein-dilaton system. It is known that spacetime singularities in the IR may or may not be acceptable in terms of the AdS/CFT correspondence. Consider an Einstein-dilation system described by the action

$$I = \frac{1}{16\pi G_N} \int d^4x \sqrt{-g} \left[R - \frac{1}{2}(\partial_\mu \phi)^2 - V(\phi) \right] \ , \tag{6.23}$$

with a given potential $V(\phi)$. The IR geometry may contain a naked singularity. Gubser [216] proposed a criterion to distinguish acceptable and unacceptable singularities. The Gubser criterion has the following two statements:

(A) The potential of the scalar field is bounded from the above in the solution.

(B) The spacetime can be obtained as a limit of a regular black hole. This is a weaker form of the cosmic censorship principle.

The two statements are not exactly equivalent, but it was argued in [216] that statement (A) often implies statement (B). If statement (B) is satisfied, the singularity is good, i.e., acceptable.
The Einstein-scalar system with the following potential

$$V(\phi) = -\frac{2}{(1+\delta^2)^2 L^2}\left[\delta^2(3\delta^2 - 1)e^{-\phi/\delta} + 8\delta^2 e^{(\delta - 1/\delta)\phi/2} + (3 - \delta^2)e^{\delta\phi}\right], \tag{6.24}$$

enjoys an analytic solution, see (6.25). A nice feature of this potential is that the special values of the parameter $\delta = \frac{1}{\sqrt{3}}, 1, \sqrt{3}$, correspond to special cases in STU supergravity. The $\phi \to 0$ behavior is

$$V(\phi) = -6/L^2 - (1/L^2)\phi^2 + \dots,$$

where the first term is a cosmological constant. We assume $\delta > 0$ throughout.
This potential together with an exact solution of an Einstein-Maxwell-Scalar system was found in [226]. A nontrivial neutral limit of this solution gives an Einstein-dilaton system with naked spacetime singularities in the IR [227]. The solution of the metric and the scalar field is given by

$$ds^2 = f(r)(-dt^2 + d\vec{x}^2) + f^{-1}(r)dr^2, \tag{6.25}$$

$$f(r) = \frac{r^2}{L^2}\left(1 + \frac{Q}{r}\right)^{\frac{2}{1+\delta^2}}, \qquad \phi = -\frac{2\delta}{1+\delta^2}\ln\left(1 + \frac{Q}{r}\right).$$

The Kretschmann scalar for this metric is

$$R_{\mu\nu\rho\sigma}R^{\mu\nu\rho\sigma} = \frac{12((r + (r+Q)\delta^2)^4 + (r - Q\delta + (r+Q)\delta^2)^2(r + Q\delta + (r+Q)\delta^2)^2)}{L^4(1+\delta^2)^4(r+Q)^{\frac{4\delta^2}{1+\delta^2}}r^{\frac{4}{1+\delta^2}}}.$$

There is a curvature singularity at $r = 0$ and $r = -Q$. The region we are interested in is between the AdS boundary (UV) and the spacetime singularity (IR). The AdS boundary is at $r \to \infty$. When $Q > 0$, there is a spacetime singularity at $r = 0$ in the IR. When $Q < 0$, there is a spacetime singularity at $r = -Q$ in the IR.
Consider the $Q > 0$ case first. There is a spacetime singularity at $r = 0$. We will use the Gubser criterion to examine whether this singularity is acceptable, and show that the two statements give the same range of the parameter δ, except for the marginal case, $\delta = 1/\sqrt{3}$.
For statement (A), we plug the solution of ϕ in the potential, and obtain

$$V = -\frac{2\delta^2(3\delta^2 - 1)Q^2 + 12\delta^2(1+\delta^2)Qr + 6(1+\delta^2)^2 r^2}{L^2(1+\delta^2)^2(r+Q)^{\frac{2\delta^2}{1+\delta^2}}r^{\frac{2}{1+\delta^2}}}.$$

The divergence of the potential is at the IR, $r \to 0$. The $r \to 0$ behavior is

$$\lim_{r\to 0} V(\phi) \to \begin{cases} +\infty, & \delta < 1/\sqrt{3}, \\ -\infty, & \delta \geq 1/\sqrt{3}. \end{cases} \qquad (Q > 0)$$

According to statement (A), the singularity at $r = 0$ is acceptable if $\delta \geq 1/\sqrt{3}$.
For statement (B), we need to find a near-extremal geometry, which is at finite temperature and the horizon encloses the singularity. If such a geometry exists, the singularity is acceptable or resolvable.

The analytic solution of a finite temperature black hole in the above Einstein-dilaton system is not available. However, it is sufficient to examine the IR geometry. To obtain the IR geometry, we take the $r \to 0$ limit and keep the leading term. The potential is

$$V = -V_0 \, e^{-\phi/\delta} \ ,$$

where $V_0 = \frac{2\delta^2(3\delta^2-1)}{(1+\delta^2)^2 L^2}$. For this potential, the analytic solution as the IR geometry is

$$ds^2 = -f_0 r^{\frac{2\delta^2}{1+\delta^2}} dt^2 + \frac{dr^2}{g_0 r^{\frac{2\delta^2}{1+\delta^2}}} + f_0 r^{\frac{2\delta^2}{1+\delta^2}} d\vec{x}^2,$$

$$\phi = \ln\left(e^{\phi_0} r^{\frac{2\delta}{1+\delta^2}}\right) \ ,$$

where $f_0 = g_0 = Q^{\frac{2}{1+\delta^2}}/L^2$ and $e^{\phi_0} = Q^{\frac{-2\delta}{1+\delta^2}}$. This is a hyperscaling-violating geometry with the Lifshitz scaling $z = 1$. By adding a blackening factor, we obtain a near-extremal geometry given by

$$ds^2 = -f_0 r^{\frac{2\delta^2}{1+\delta^2}} \left[1 - \left(\frac{r_h}{r}\right)^\beta\right] dt^2 + \frac{dr^2}{g_0 r^{\frac{2\delta^2}{1+\delta^2}} \left[1 - \left(\frac{r_h}{r}\right)^\beta\right]} + f_0 r^{\frac{2\delta^2}{1+\delta^2}} d\vec{x}^2 \ , \qquad (6.26)$$

where r_h is the horizon radius and

$$\beta = \frac{3\delta^2 - 1}{1 + \delta^2} \ .$$

This is an exact solution to the Einstein-dilaton system with the potential (6.24). The range of r is $r_h < r < \infty$, so $r_h/r < 1$. If this solution makes sense for describing a black hole, we need $\beta > 0$, which gives

$$\delta > 1/\sqrt{3} \ .$$

Namely, $\delta \le 1/\sqrt{3}$ violates the Gubser criterion. If we ignore the marginal case $\delta = 1/\sqrt{3}$, the statements (A) and (B) are consistent.
When $\delta \ge 1$, the singularity at $r = 0$ is null. When $\delta < 1$, the singularity at $r = 0$ is timelike.
In the next and subsequent section, we present the details of the action complexity and volume complexity for the $Q > 0$ case for the hyperscaling violating black holes with timelike singularity in the IR.

6.3.1 Action complexity for Einstein-Scalar system

In this section, we tackle the problem of governing the holographic complexity of the Einstein-dilaton system using action complexity conjecture. As alluded to in the above section, as δ is dialed from below $\delta = 1/\sqrt{3}$ to the higher values, the naked timelike singularity turns from an unacceptable type to an acceptable type according to the Gubser criterion. If complexity is to be a reliable probe of timelike singularities, then both complexity prescriptions are expected to successfully capture this feature by showing some abrupt change (phase transition) in their behavior, and from the features of complexity for $\delta < 1/\sqrt{3}$ one should be able to formulate a complexity criterion for signalling unacceptable naked timelike singularities.
Einstein-dilation system is described by the gravitational action in (6.23). For the sake of calculational convenience, we treat each term of the potential individually (6.24) by writing, $V(\phi) = V_1(\phi) + V_2(\phi) + V_3(\phi)$ where

$$V(\phi) = \frac{2\delta^2\left(1 - 3\delta^2\right)}{\left(\delta^2 + 1\right)^2 L^2}\left(1 + \frac{Q}{r}\right)^{\frac{2}{\delta^2+1}} - \frac{16\delta^2}{\left(\delta^2 + 1\right)^2 L^2}\left(1 + \frac{Q}{r}\right)^{\frac{1-\delta^2}{\delta^2+1}} - \frac{2\left(3 - \delta^2\right)}{\left(\delta^2 + 1\right)^2 L^2}\left(1 + \frac{Q}{r}\right)^{-\frac{2\delta^2}{\delta^2+1}} \ .$$

The analytic solution to the above action is supplied by the geometry in (6.25), whose Ricci scalar can be computed to give

$$R = -\frac{6\left(2\left(\delta^2(Q+r)+r\right)^2 - \delta^2 Q^2\right)}{L^2\left(\delta^2+1\right)^2(Q+r)^2}\left(\frac{Q+r}{r}\right)^{\frac{2}{\delta^2+1}} .$$

As usual, the Wheeler-de Witt patch is obtained by following the evolution of light rays towards past and future, starting from the boundary at a given time and can be found to be bounded by the future (past) light-sheets

$$t_{\pm}(r) = t_* \mp \int_{\infty}^{r}\frac{dr'}{f(r')} .$$

We will first present the evaluation of the bulk action terms and in the subsequent subsections present the details of the higher codimension contributions. We split the on-shell bulk action into the sum of different contributions in the following manner

$$I_{bulk} = I_{EH} + I_{T(\phi)} - I_V .$$

Here the first two terms correspond to the Einstein-Hilbert term and scalar kinetic energy term, and the last three correspond to the potential terms for the scalar. All these contributions diverge as $r \to \infty$ and we regulate of the contributing integrals with the aid of the IR cutoff, Λ. Refer to Sec.6.3.3 for the details of the regularization procedure. We list the bulk contributions in the following

- **Einstein-Hilbert term:**

$$I_{EH} = \frac{1}{16\pi G_N}\int dx\,dy\int dr\sqrt{-g}\,R\left(\int_{t_-(r)}^{t_+(r)}dt\right),$$

$$= \frac{-6V_{xy}}{16\pi G_N\left(\delta^2+1\right)^2}\int_0^{\Lambda}dr\,r^2\left(\frac{Q+r}{r}\right)^{\frac{4}{\delta^2+1}}\frac{\left(2\left(\delta^2(Q+r)+r\right)^2 - \delta^2 Q^2\right)}{(Q+r)^2}\int_r^{\Lambda}\frac{dr'}{r'^2\left(1+\frac{Q}{r'}\right)^{\frac{2}{1+\delta^2}}},$$

$$= \frac{2V_{xy}}{16\pi G_N}\left(-\frac{2\Lambda^2}{L^2} - \frac{4\Lambda Q}{\left(\delta^2+1\right)L^2} + \frac{2\delta^2 Q^2\log\left(\frac{\Lambda}{Q}\right)}{\left(\delta^2+1\right)^2 L^2} + \frac{6\delta^2\left(\delta^2+1\right)\left(2\delta^2-1\right)\epsilon^{\frac{3\delta^2-1}{\delta^2+1}}Q^{\frac{3-\delta^2}{\delta^2+1}}}{\left(3\delta^2-1\right)\left(\delta^4-1\right)L^2} + (finite) + O(\Lambda^{-1}\right)$$

(6.27)

Where we mention the finite term separately for brevity to be

$$\frac{2Q^2}{\left(\delta^2+1\right)^2 L^2}\left[-2\delta^4 - \delta^2 + 4\left(1-3\delta^2\right)\delta^2\left(\psi^{(0)}\left(\frac{4\delta^2}{\delta^2+1}\right) + \gamma\right) + 6\left(2\delta^2-1\right)\delta^2 H_{2-\frac{4}{\delta^2+1}} + 12\delta^4 H_{\frac{2\delta^2}{\delta^2+1}}\right.$$

$$\left. + \left(\delta^2 - 12\delta^4\right)H_{1-\frac{2}{\delta^2+1}} - 1\right]$$

(6.28)

- **Kinetic term for the scalar field:**

$$I_{T(\phi)} = \frac{1}{16\pi G_N}\int dx\,dy\int dr\sqrt{-g}\left(-\frac{g^{rr}}{2}\left(\partial_r\phi\right)^2\left(\int_{t_-(r)}^{t_+(r)}dt\right)\right),$$

$$= \frac{-4V_{xy}\delta^2 Q^2}{16\pi G_N\left(\delta^2+1\right)^2}\int_0^{\Lambda}dr\left(1+\frac{Q}{r}\right)^{\frac{2(1-\delta^2)}{1+\delta^2}}\int_r^{\Lambda}\frac{dr'}{r'^2\left(1+\frac{Q}{r'}\right)^{\frac{2}{1+\delta^2}}},$$

(6.29)

$$= \frac{2V_{xy}}{16\pi G_N}\left(-\frac{2\delta^2 Q^2\log\left(\frac{\Lambda}{Q}\right)}{\left(\delta^2+1\right)^2 L^2} + \frac{2\delta^2\left(\delta^2+1\right)\epsilon^{\frac{3\delta^2-1}{\delta^2+1}}Q^{\frac{3-\delta^2}{\delta^2+1}}}{\left(3\delta^2-1\right)\left(1-\delta^4\right)L^2} + (finite) + O\left(\Lambda^{-1}\right)\right),$$

144

the finite term is

$$\frac{2\gamma\delta^2 Q^2}{(\delta^2+1)^2 L^2} + \frac{4\delta^2 Q^2 \psi^{(0)}\left(\frac{3\delta^2-1}{\delta^2+1}+1\right)}{(\delta^2+1)^2 L^2} - \frac{2\delta^2 Q^2 \psi^{(0)}\left(\frac{2\delta^2}{\delta^2+1}\right)}{(\delta^2+1)^2 L^2} \tag{6.30}$$

- **Scalar potential term in action:**

$$\begin{aligned}
I_{V(\phi)} &= \frac{1}{16\pi G_N}\int dx\,dy \int dr\sqrt{-g}\,V(\phi)\left(\int_{t_-(r)}^{t_+(r)} dt\right)\,, \\
&= \frac{2V_{xy}}{16\pi G_N}\int_0^\Lambda dr\,r^2\left(1+\frac{Q}{r}\right)^{\frac{2}{1+\delta^2}} V(\phi)\int_r^\Lambda \frac{dr'}{r'^2\left(1+\frac{Q}{r'}\right)^{\frac{2}{1+\delta^2}}}\,, \\
&= \frac{2V_{xy}}{16\pi G_N}\left(-\frac{\Lambda^2}{L^2} - \frac{2\Lambda Q}{(\delta^2+1)L^2} - \frac{2\delta^2 Q^{\frac{3-\delta^2}{\delta^2+1}}\epsilon^{\frac{3\delta^2-1}{\delta^2+1}}}{(\delta^2-1)L^2} + (finite) + O(\Lambda^{-1})\right)\,.
\end{aligned} \tag{6.31}$$

Where the finite term is

$$\frac{Q^2}{(\delta^2+1)^2 L^2}\Bigg[-2\delta^4 - \delta^2 + 4\left(1-3\delta^2\right)\delta^2\left(\psi^{(0)}\left(\frac{4\delta^2}{\delta^2+1}\right)+\gamma\right) + 4\left(3\delta^2-1\right)\delta^2 H_{2-\frac{4}{\delta^2+1}} + 12\delta^4 H_{\frac{2\delta^2}{\delta^2+1}}$$

$$-12\delta^4 H_{1-\frac{2}{\delta^2+1}} - 1\Bigg] \tag{6.32}$$

The integrals are divergent at the lower limit of integration, ε is the IR cutoff at the lower limit.

6.3.2 Complexity contribution from the singularity

The naked timelike singularity is located at $r=0$. The induced metric on fixed r surface is

$$ds^2 = -f(r)\,dt^2 + f(r)\left(dx^2+dy^2\right)\,,$$

while the unit outward normal to the WdW volume is $n = -f^{1/2}(r)\,\partial_r$. These lead to the induced metric determinant

$$\sqrt{-h} = f^{3/2}(r),$$

and the trace of the extrinsic curvature

$$K \equiv \nabla_L n^L = \partial_r n^r + \Gamma^L_{Lr} n^r = -\frac{3}{2}f'(r)f^{-1/2}(r).$$

The GHY term contribution from the singularity is

$$16\pi G_N\, I^0_{GHY} = \lim_{r\to 0} 2\int d^3x\,\sqrt{-h}\,K = -3V_{xy}\lim_{r\to 0}\left(t_u(r)-t_d(r)\right)\left(f'(r)f(r)\right)$$

Using the limiting forms as $r\to 0$,

$$f(r) \sim Q^{\frac{2}{1+\delta^2}} r^{\frac{2\delta^2}{1+\delta^2}}\,, \qquad t_u(r)-t_d(r) = \frac{(\delta^2+1)\left(\frac{Q}{r}\right)^{\frac{\delta^2-1}{\delta^2+1}}}{(\delta^2-1)Q}$$

we get,

$$16\pi G_N\, I^0_{GHY} = -3V_{xy}\frac{2\delta^2}{\delta^2-1}Q^{\frac{2}{1+\delta^2}}\left(\lim_{r\to 0} r^{\frac{2\delta^2}{1+\delta^2}}\right) = 0. \tag{6.33}$$

Thus the contribution to action complexity from the naked timelike singularity vanishes!

6.3.3 Contribution from the null boundary of the WdW patch

To calculate the contribution of the null boundaries towards the gravitational action, we again use a ploy of using the regulating surface that deforms the null surface

$$(t - T)^2 - \left(\int_r^\infty \frac{dr'}{f(r')} \right)^2 = 0 \ , \tag{6.34}$$

with the joints into a smooth timelike surface after the introduction of a regulator in the following manner

$$(t(r) - T)^2 - (1 + \epsilon)g(r)^2 = 0 \ , \qquad\qquad g(r) := \int_r^\Lambda \frac{dr}{f(r')} \ .$$

Here, ϵ is a null-to-timelike regulator which is related to the IR regulator, Λ through

$$\int_0^\infty \frac{dr}{f(r)} = \sqrt{1 + \epsilon} \int_0^\Lambda \frac{dr}{f(r)} \ ,$$

from which it follows that the deformation parameters are related by $\epsilon \approx \frac{2Q(1 - \delta^2)}{\Lambda(\delta^2 + 1)}$. The unit outward normal to this surface is given by,

$$n^t = \frac{-(t - T)}{f(r)^{1/2}\sqrt{(\epsilon + 1)^2 g(r)^2 - (t - T)^2}}, \qquad n^r = \frac{(\epsilon + 1)f(r)^{1/2} g(r)}{\sqrt{(\epsilon + 1)^2 g(r)^2 - (t - T)^2}}, \qquad n^{x,y} = 0 \ .$$

With these orthonormal components the trace of the extrinsic curvature becomes

$$K = \frac{3f'(r)}{2\sqrt{\epsilon}\sqrt{f(r)}}.$$

The pull-back metric on the regulating surface is

$$ds^2 = -\epsilon \frac{dr^2}{f(r)} + d\vec{x}^2 f(r),$$

which results in the following jacobian factor

$$\sqrt{-h}\, dr\, dx\, dy = \sqrt{\epsilon} f(r)^{1/2}\, dr\, dx\, dy.$$

Thus the integrand of the surface integral contribution to the on shell action from the null surfaces is

$$\sqrt{-h}K = \frac{3f'(r)}{2} \ .$$

Therefore, the boundary contribution is given by GHY boundary term

$$\begin{aligned} I_{GHY}^{null} &= \int_0^\Lambda dr \ \sqrt{-h} \ K \ , \\ &= \frac{3V_{xy}}{16\pi G_N} f(\Lambda) \ , \\ &= \frac{3V_{xy}}{16\pi G_N} \left[\frac{\Lambda^2}{L^2} + \frac{2}{1 + \delta^2} \frac{Q}{L} \frac{\Lambda}{L} + \frac{1 - \delta^2}{(1 + \delta^2)^2} \frac{Q^2}{L^2} \right]. \end{aligned}$$

The leading term is quadratically UV-divergent, which is notably Q, δ-independent. The subleading linearly UV-divergent piece and the finite piece both depend on Q, δ. The most important thing to note is that there is no abrupt change in either of the divergent or finite pieces when δ is dialled across the putative Gubser point $\delta = 1/\sqrt{3}$.

146

6.4 Analytical and numerical estimates of action contribution

In table (6.3) we show the numerical estimates of total action contribution for different values of cut off Λ, where it can be confirmed that the result roughly scales as $\sim \Lambda^2$ for the part of the geometry that is allowed as per the Gubser criterion and there is virtually no dependence on Q! The numerics also confirm that this term undergoes a dramatic change in behavior across the Gubser bound at $\delta = 1/\sqrt{3}$ where it virtually blows up to arbitrarily large negative values.

Q	δ	Λ	$\frac{G_N \hbar}{V_{xy}} C_A$	$\frac{G_N \hbar}{V_{xy}} (C_A - C_A^{AdS})$
10	0.1	10^6	-1.13×10^{230}	-1.13×10^{230}
10	0.4	10^6	-1.17×10^{110}	-1.17×10^{110}
10	0.5	10^6	-3.32×10^{51}	-3.32×10^{51}
10	0.6	10^6	2.47×10^{12}	3.63×10^{7}
10	0.9	10^6	2.47×10^{12}	2.73×10^{7}
10	0.1	10^{10}	-1.62×10^{226}	-1.62×10^{226}
10	0.4	10^{10}	-1.88×10^{108}	-1.88×10^{108}
10	0.5	10^{10}	-5.26×10^{50}	-5.26×10^{50}
10	0.6	10^{10}	2.47×10^{20}	3.63×10^{11}
10	0.9	10^{10}	2.47×10^{20}	2.73×10^{11}
1000	0.1	10^6	-9.40×10^{235}	-9.40×10^{235}
1000	0.4	10^6	-9.21×10^{114}	-9.21×10^{114}
1000	0.5	10^6	-8.34×10^{55}	-8.34×10^{55}
1000	0.6	10^6	2.47×10^{12}	3.62×10^{9}
1000	0.9	10^6	2.47×10^{12}	2.73×10^{9}
1000	0.1	10^{10}	-1.35×10^{232}	-1.35×10^{232}
1000	0.4	10^{10}	-1.48×10^{113}	-1.48×10^{113}
1000	0.5	10^{10}	-1.32×10^{55}	-1.32×10^{55}
1000	0.6	10^{10}	2.47×10^{20}	3.64×10^{13}
1000	0.9	10^{10}	2.47×10^{20}	2.73×10^{13}

Table 6.3: Table for dependence upon Q, δ and cut off Λ for the complexity of the Einstein-Scalar system.

The trend captured by the numerical estimates can also be seen by combining (6.27) (6.29), (6.31) and (6.3.3) where we obtain the following contribution towards the action complexity of the Einstein Scalar system

$$
I_{WdW} = \frac{V_{xy}}{8\pi G_N} \left[\frac{\Lambda^2}{2L^2} + \frac{\Lambda Q}{(\delta^2 + 1) L^2} + \frac{6\delta^2 \epsilon^{\frac{3\delta^2 - 1}{\delta^2 + 1}} Q^{\frac{3-\delta^2}{\delta^2 + 1}}}{(3\delta^2 - 1) L^2} + \frac{Q^2 \delta^2}{2(\delta^2 + 1)^2 L^2} \left((4\gamma - 4\gamma + 7)\delta^2 + 8\delta^4 \right. \right.
$$

$$
\left. \left. + 8\left(3\delta^2 - 1\right)\delta^2 \left(\psi^{(0)}\left(3 - \frac{4}{\delta^2 + 1}\right) - \psi^{(0)}\left(\frac{4\delta^2}{\delta^2 + 1}\right)\right) + 1 \right) + O\left(\frac{1}{\Lambda}\right) \right]
$$

It is immediate from (6.4) that the complexity of the geometry containing the timelike singularity arising from the Einstein Scalar system is positive in the range $\delta > 1/\sqrt{3}$. Moreover, in the same range of values of δ, the action complexity is greater than the complexity of the empty AdS spacetime which can be obtained by taking the $Q = 0$ in the above expression. And quite interestingly, this is the same range

of values where the geometry is in the allowed phase according to the Gubser criterion. In the complementary range, $\delta < 1/\sqrt{3}$ the action complexity criterion adheres to the Gubser criterion by furnishing the value of negative infinity thereby signaling that the phase the geometry is in, is disallowed. Therefore, we see that the action complexity successfully detects as the geometry transitions from the allowed phase to the disallowed phase across the Gubser point of $\delta = 1/\sqrt{3}$. It remains for us to see whether the volume complexity also follows the same trend and registers the agreement with the Gubser criterion by reproducing the same result as the action complexity in the next section.

6.4.1   Volume Complexity for the Einstein-Scalar system

It will be interesting to compute the volume complexity to see if it reproduces the same behavior as action complexity. Consider a codimension one spatial hypersurface specified by the condition $t = t(r), \forall x, y$. The pullback of (6.25) on this hypersurface is

$$ ds^2 = \left(\frac{1}{f(r)} - f(r)t'(r)^2 \right) dr^2 + f(r) \, d\boldsymbol{x}^2 \ . $$

The volume of the spacelike slice turns out to be

$$ V = V_{xy} \int_0^\infty dr \ f(r) \sqrt{ \frac{1}{f(r)} - f(r)t'^2(r) } \ . $$

Evidently the volume is maximized when the quantity inside the square root is maximized, i.e. $t'(r) = 0$. Thus the maximal volume spatial slice is the constant time slice, $t(r) = T$, where, T is the time value at which the spatial slice meets the spatial boundary (where the WDW patch is anchored).
Therefore, the maximal volume slice volume is

$$ V_{max} = V_{xy} \int_0^\infty dr \ \sqrt{f(r)} \ . $$

This integral is clearly UV divergent, so we introduce a UV (bulk IR) cutoff, Λ. Then,

$$ V_{max} = \frac{V_{xy}}{L} \int_0^\Lambda dr \ r \left(1 + \frac{Q}{r} \right)^{\frac{1}{1+\delta^2}} $$

$$ = \frac{V_{xy}}{L} \left[\frac{\Lambda^2}{2} + \frac{Q}{1+\delta^2}\Lambda - \frac{\delta^2 Q^2}{2(1+\delta^2)^2} \ln\Lambda - \frac{\delta^2 Q^2}{4(1+\delta^2)^2} \left(3 - 2H_{\frac{\delta^2}{1+\delta^2}} \right) + O(\Lambda^{-1}) \right] . $$

The volume complexity is,

$$ C_V \equiv \frac{V_{max}}{G_N \, L} = \frac{V_{xy}}{G_N} \left[\frac{\Lambda^2}{L^2} + \frac{Q/L}{1+\delta^2}\frac{\Lambda}{L} - \frac{\delta^2 Q^2/L^2}{2(1+\delta^2)^2} \ln\Lambda - \frac{\delta^2 Q^2/L^2}{4(1+\delta^2)^2} \left(3 - 2H_{\frac{\delta^2}{1+\delta^2}} \right) \right] . \tag{6.33} $$

From this expression we note the following features of volume complexity:

- The volume complexity has a leading quadratic UV-divergence, $\frac{V_{xy}}{G_N}\frac{\Lambda^2}{2L^2}$, as expected for an extensive quantity in a $2+1$-dimensional field theory dual and *manifestly positive*. There are subleading linear and log divergent pieces and a finite piece.

- The leading UV-divergent contribution is also *independent of Q* and is identical to a pure AdS volume complexity. The subleading piece is positive definite for positive Q, i.e. higher complexity than that of empty AdS.

- Numerical computations for some fixed large value of the UV cutoff Λ, say $\Lambda \sim 10^{10}$ in AdS units, and for several distinct values of $Q > 0$, the complexity is a monotonically decreasing function of δ, while $Q < 0$ the volume complexity is monotonically increasing function of δ. The results are displayed in Fig. 6.3.

- There is no contribution from the naked timelike singularity at $r = 0$ - since the volume crunches at the singularity! This is evident from the volume intgeral, which receives vanishing contribution at the lower limit $r = 0$.

- According to the Gubser criterion, for $\delta < \frac{1}{\sqrt{3}}$, the naked timelike singularity is not resolvable or allowable, in the sense that it cannot be resolved by embedding in string/M theory. However, as is evident from the C_V expression (6.4.1) or the C_V vs. δ plots in Fig. 6.3, the volume complexity does not seem to display any sudden change in pattern as we vary δ across the Gubser bound, $\delta = \frac{1}{\sqrt{3}}$ in all cases.

The results of this sections leads us to conclude that volume complexity, as opposed to action complexity, is not a sensitive probe of the nature of timelike singularities, i.e. whether they are resolvable (allowable) in a fundamental quantum theory (UV-completion) of gravity.
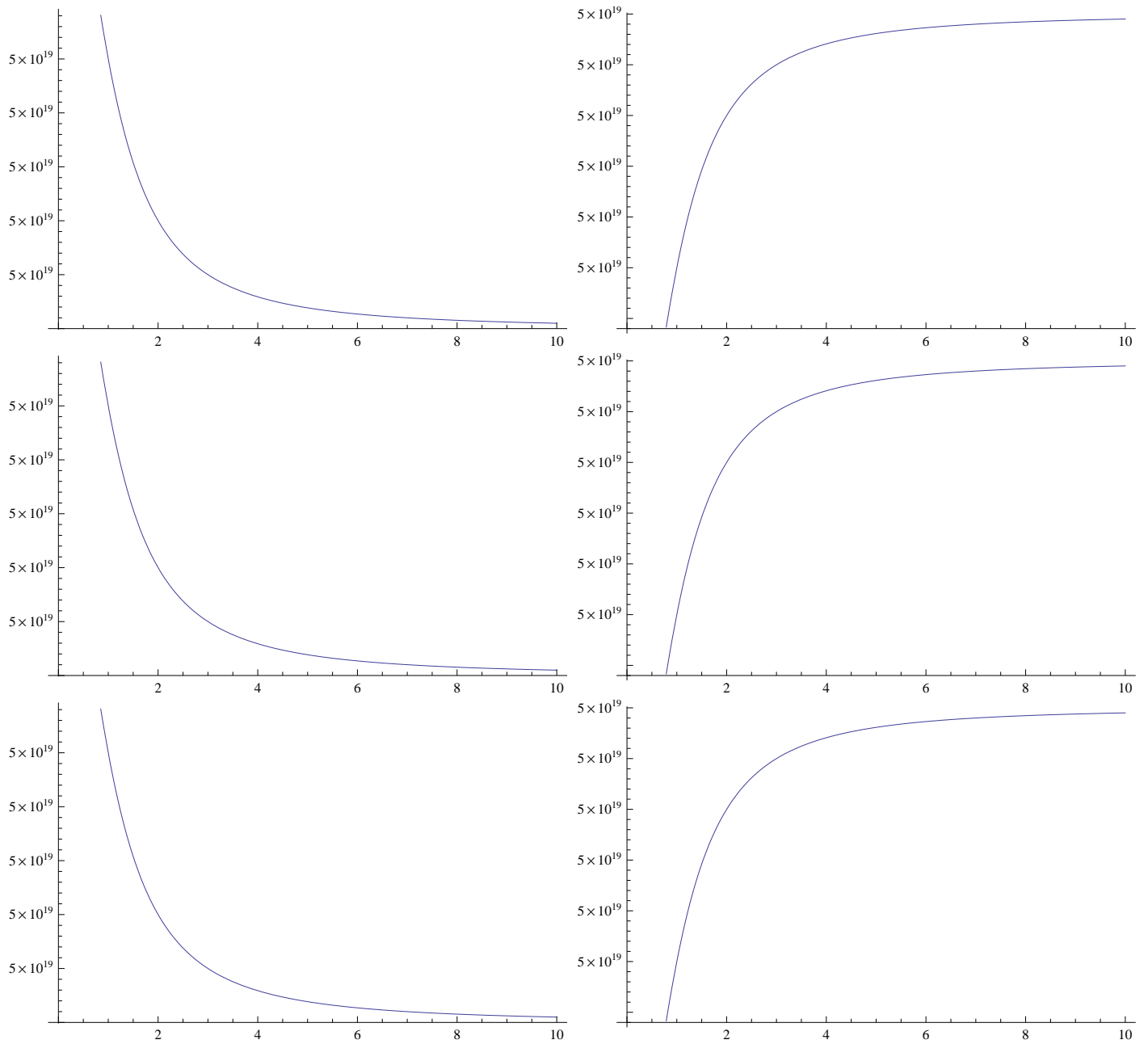
Figure 6.3: Volume (Complexity) plots as a function of the exponent, δ for different values of Q. The top row is $|Q| = 10$, middle row is $|Q| = 0.1$ and the bottom row is $|Q| = 1.0$. The left panel are for $Q > 0$, while the right panel is for $Q < 0$.

6.5 Conclusion & Outlook

The complexity has recently been added in the arsenal of holographic tools available to study quantum gravity [48, 49, 50] because of its anticipated role in addressing unresolved issues in Quantum Gravity when viewed in the light of Quantum Information Theory. However, its potential scope in closing crucial gaps in our understanding of quantum gravity compared to other entanglement measures, such as entanglement entropy, is still being investigated and explored. There are reasons to believe that complexity can shed light on the nature of gravitational singularities in general, a topic in which so far the holographic approach to quantum gravity has not been particularly fruitful. In this work, have tried to explore holographic complexity as a tool in probing naked timelike singularities, the status of which are not clear in traditional string theory approaches. In past works, the question of the existence of the naked timelike singularities, particularly in holographic contexts, has been attacked with the tool of Gubser criterion [216, 217], which constitutes a set of diagnostic conditions for allowing or disallowing a particular case of the singular geometries. With the anticipation that the physics of complexity will also supply a testing ground alongside the Gubser criterion, we probed the well-known sick geometry of negative mass Schwarzschild AdS black hole [219] using action complexity and volume complexity as a warm-up example. In its study, we found that although superficially both definitions of complexity provided us with what would naively appear as a physically acceptable result (a well-behaved positive complexity with the appropriate divergence structure), a closer inspection reveals the singular geometry was less complex than the empty AdS background! This led us to formulate a *complexity criterion*, namely that if the singular geometries have lower complexity compared to the empty AdS backgrounds, then they are not allowed a theory of quantum gravity. The insight behind this proposed criterion is that complexity represents a measure of the ease of creating a state (bulk geometry) from some specified reference state. And if a singular bulk geometry is less complex than empty AdS, then empty AdS will be susceptible to a quantum instability with the the singular geometry - the cost of creating a singular geometry is less than the cost of creating empty AdS space. This would be undesirable in a UV-complete theory of (AdS) quantum gravity where the vacuum state, i .e. a semiclassical smooth pure/empty AdS spacetime is stable and will have lowest holographic complexity among all allowable semiclassical geometries. Armed with this criterion, we went ahead in the next section to focus on an anisotropic geometry occurring in the effective holographic theories namely, timelike Kasner AdS spacetime [220]. According to Gubser criterion, this geometry is not a allowable singularity. Our the action complexity result clearly reveals that the complexity of this timelike Kasner-AdS spacetime is lesser than the empty (Poincaré) AdS and hence according to our formulated complexity criterion is not an allowable singular geometry in a quantum gravity theory. We find this agreement of the action complexity criterion and Gubser criterion as greatly encouraging. To confirm our findings, in the next section computed the volume complexity of the timelike Kasner which partly agreed with action complexity (and Gubser criterion) in a restricted range of the Kasner exponent, namely $\alpha < 2/3$. This feature could imply either that volume complexity is either not a reliable probe of timelike singularties, or the timelike Kasner AdS could be an isolated or anomalous example. In the hopes to settle this issue, in the next section, we explore asymptotically AdS timelike singularities which arise in the Einstein-Scalar system [226, 227] in holographic condensed matter studies. Such a smooth bulk background have been extensively investigated in the light of the Gubser criterion and is known to exhibit the transition from the disallowed to the allowed geometry as the relevant parameter, α is tuned. The final case study of the Einstein-Scalar system suggests a striking agreement with the Gubser criterion solidifying our faith in the action complexity criterion. The action complexity criterion is successfully able to identify the Gubser point thereby making our belief in its diagnostic ability stronger. On the other hand, the volume complexity is not able to register the transition of the geometry hinting that the volume complexity as a probe is not very suitable for investigation of the timelike naked singularities.

Based on the evidence gained from studying the various cases, we infer that the action complexity may furnish a reliable probe in the investigation of the sick geometries alongside the Gubser criterion. This

action complexity criterion is certainly operationally much easier to implement than Gubser criterion itself, since given a spacetime containing a (naked) timelike singularity, it is not immediately obvious whether that geometry can or cannot be realized as the extremal limit of some black-hole geometry - one just needs to compute the onshell action supported in the WdW patch and compare to the pure AdS! However in this work we have only scratched the surface as far as timelike singularities and their holographic complexity features are concerned, looking at three simple examples. To accept our action complexity criterion as a foolproof criterion to diagnose allowable (timelike) singularities we have to conduct an exhaustive survey of various other geometries with timelike singularities, beyond even the asymptotically AdS examples. We leave such an exhaustive study for future work(s).

Appendix A

Perturbative analysis of divergences arising at finite temperature

The general form of the total contribution coming from the integrals from the various regions of the WdW patch for the finite temperature case are typically of the following form

$$2 \int_{U_T}^{\frac{l_s}{\epsilon}} dU \, f(U, U_T, \epsilon) + \int_0^{U_T} dU g(U, U_T) \tag{A.0}$$

Where the first integral is contributed by both exterior regions and the last integral is for the Region II. We notice that from these integrals, only the first one contains the information about the asymptotic boundary region. We are hence forth interested in looking at only the first integral i.e. from the exterior region.

Since, the zero temperature solution is already known to us, we will treat the finite temperature as the perturbation to the zero temperature. Therefore, we are only interested in the terms which comes from the corrections to the zero temperature. To do this, we do a Taylor series expansion of the term of the interest and arrive at:

$$2 \int_{U_T}^{\frac{l_s}{\epsilon}} dU \, f(U, U_T, \epsilon) \simeq 2 \int_0^{\frac{l_s}{\epsilon}} dU \, f(U, 0, \epsilon) + 2 U_T \left(\frac{d}{dU_T} \int_{U_T}^{\frac{l_s}{\epsilon}} dU \, f(U, U_T, \epsilon) \right)_{U_T=0}$$

$$+ 2 U_T^2 \left(\frac{d2}{dU_T^2} \int_{U_T}^{\frac{l_s}{\epsilon}} dU \, f(U, U_T, \epsilon) \right)_{U_T=0}$$

The zeroth order result in temperature is known to us, therefore the higher order corrections are:

$$-2U_T \left[\left(f(U, U_T, \epsilon) \right)_{U=U_T} \right]_{U_T=0} + 2U_T \left[\left(\int_{U_T}^{\frac{l_s}{\epsilon}} dU \frac{df(U, U_T, \epsilon)}{dU_T} \right)_{U=U_T} \right]_{U_T=0} - U_T^2 \left[\frac{d}{dU_T} f(U_T, U_T, \epsilon) \right]_{U_T=0}$$

$$- U_T^2 \left[\left(\frac{d}{dU_T} f(U, U_T, \epsilon) \right)_{U=U_T} \right]_{U_T=0} + U_T^2 \left[\int_{U_T}^{l/\epsilon} dU \frac{d^2}{dU_T^2} f(U, U_T, \epsilon) \right]_{U_T=0}.$$

The Ricci scalar term & the dilaton kinetic term:
The Ricci scalar term in the supergravity action in region I contributes

$$S_R^I = \frac{L_x}{16\pi G_N} \int_{U_T}^{\frac{l_s}{\epsilon}} dU \int_{t_R + 2U_*(U)}^{t_R} dv \sqrt{-g} e^{-2(\Phi - \Phi_0)} R$$

$$= \frac{L_x k^{\frac{1}{2}}}{8\pi G_N} \int_{U_T}^{\frac{l_s}{\epsilon}} dU U \left(\frac{2U_T^2 k\lambda \left(2k\lambda U^2 - 5\right) + 8k\lambda U^2 - 6}{(k\lambda U^2 + 1)^2} \right) \left(\int_U^{\frac{l_s}{\epsilon}} dU' \frac{\sqrt{\lambda k U'^2 + 1}}{(U'^2 - U_T^2)} \right). \tag{A.1}$$

$$S_\Phi^I = \frac{4L_x}{16\pi\,G_N} \int_{U_T}^{\frac{l_s}{\epsilon}} dU \int_{T_R+2U_*(U)}^{T_R} dv\sqrt{-g}e^{-2(\Phi-\Phi_0)}g^{\mu\nu}\partial_\mu\Phi\partial_\nu\Phi$$

$$= \frac{L_x k^{\frac{5}{2}}\lambda^2}{2\pi\,G_N} \int_{U_T}^{\frac{l_s}{\epsilon}} dU \left(\frac{U^5}{(k\lambda U^2+1)^2} - \frac{U^3 U_T^2}{(k\lambda U^2+1)^2} \right) \left(\int_U^{\frac{l_s}{\epsilon}} dU' \frac{\sqrt{\lambda k U'^2+1}}{(U'^2-U_T^2)} \right)$$

The finite temperature correction to the sum of Ricci scalar and the dilaton kinetic term is

$$\frac{3k\sqrt{\lambda}\,U_T L_x}{2\pi G_N} \log\left(\frac{2\sqrt{k\lambda}l_s}{\epsilon} \right) - \frac{3k\sqrt{\lambda}L_x U_T^2}{2\pi G_N} \log\left(\frac{2\sqrt{k\lambda}l_s}{\epsilon} \right) \tag{A.1}$$

Where, the first order temperature correction comes from the Ricci term. At the level of second order correction, the Ricci and the dilaton kinetic contributions add up to give a logarithmic divergence.

The cosmological constant term:

The contribution to the onshell action from regions outside the horizons (region I, III) is

$$S_\Lambda^I = \frac{4L_x}{16\pi k l_s^2\,G_N} \int_{U_T}^{\frac{l_s}{\epsilon}} dU \int_{t_R+2U_*(U)}^{t_R} dv\sqrt{-g}e^{-2(\Phi-\Phi_0)}$$

$$= \frac{L_x k^{\frac{1}{2}}}{2\pi\,G_N} \int_{U_T}^{\frac{l_s}{\epsilon}} dU U \left(\int_U^{\frac{l_s}{\epsilon}} dU' \frac{\sqrt{\lambda k U'^2+1}}{(U'^2-U_T^2)} \right) \tag{A.2}$$

This term receives following asymptotic UV contribution from the finite temperature correction at $O(U_T^2)$

$$\simeq \frac{-2k\sqrt{\lambda}L_x U_T^2}{\pi G_N} \log\left(\frac{2\sqrt{k\lambda}l_s}{\epsilon} \right) - \frac{2k^2\lambda^{3/2}l_s^2 L_x U_T^2}{3\pi\epsilon^2 G_N} \tag{A.2}$$

The Kalb-Ramond term:

The contribution to action complexity from the Kalb-Ramond term in region I is given by:

$$S_H^I = -\frac{L_x}{12\times 16\pi\,G_N} \int_{U_T}^{\frac{l_s}{\epsilon}} dU \int_{t_R+2U_*(U)}^{t_R} dv\sqrt{-g}e^{-2(\Phi-\Phi_0)}H^2$$

$$= -\frac{L_x}{4\pi G_N\,k^{\frac{3}{2}}} \int_{U_T}^{l_s/\epsilon} \frac{dU}{U^3\,f^2} \left(\int_U^{\frac{l_s}{\epsilon}} dU' \frac{\sqrt{\lambda k U'^2+1}}{(U'^2-U_T^2)} \right) . \tag{A.3}$$

The finite temperature correction

$$\simeq \frac{U_T^2 k^{5/2}\sqrt{\lambda}l_s L_x}{\pi G_N} \log\left(\frac{2\sqrt{k\lambda}l_s}{\epsilon} \right) \tag{A.3}$$

So up to second order in U_T or finite temperature corrections there are no newer exotic type of divergences coming from the volume term of action complexity. The GHY term contribution (3.89) is already exact to order U_T^2 and the correction is manifestly log-divergent. So no newer exotic divergences arise from the GHY term(s) either. The plot of the complexity as a function of ϵ/β_H, displayed in figure 3.6. Qualitatively the action complexity at finite temperature exhibits the same behavior as that of the zero temperature case. More importantly, *no new divergences* arise compared to the zero temperature case perturbatively up to second order in finite temperature corrections.

Appendix B

Determining the 4 dimensional background from the σ-model action

The euclidean signature worldsheet (bosonic) sigma model action (ignoring the dilaton piece $\alpha' \Phi R$ at leading order in α') is,

$$I = \frac{1}{4\pi} \int d^2\sigma \sqrt{g} \left(g^{ab} G_{\mu\nu} + i\epsilon^{ab} B_{\mu\nu} \right) \partial_a X^\mu \partial_b X^\nu. \tag{B.0}$$

where we have set $\alpha' = 1$. Working in conformal gauge, i.e. with the worldsheet metric

$$g_{11} = g^{11} = g_{22} = g^{22} = 1, g_{12} = g_{21} = g^{12} = g^{21} = 0.$$

and the Levi-Civita tensor,

$$\epsilon_{12} = 1, \epsilon_{21} = -1, \epsilon_{11} = \epsilon_{22} = 0.$$
$$\Rightarrow \epsilon^{12} = 1, \epsilon^{21} = -1, \epsilon^{11} = \epsilon^{22} = 0.$$

Substituting these in (B), we get

$$I = \frac{1}{4\pi} \int d^2\sigma \left[G_{\mu\nu} \left(\partial_1 X^\mu \partial_1 X^\nu + \partial_2 X^\mu \partial_2 X^\nu \right) + i B_{\mu\nu} \left(\partial_1 X^\mu \partial_2 X^\nu - \partial_2 X^\mu \partial_1 X^\nu \right) \right]. \tag{B.0}$$

Switching to lightcone worldsheet coordinates, $z = \sigma^1 + i\sigma^2$ and $\bar{z} = \sigma^1 - i\sigma^2$, the sigma model action,

$$I = \frac{1}{2\pi} \int d^2z \left[\frac{G_{\mu\nu} + B_{\mu\nu}}{2} \partial X^\mu \bar{\partial} X^\nu + \frac{G_{\mu\nu} - B_{\mu\nu}}{2} \bar{\partial} X^\mu \partial X^\nu \right]$$

To compare this with Eq. (4.5) of [114] we have to use a 4-dimensional target space, i.e. X^μ's can be the four coordinates $\phi, y, \gamma, \bar{\gamma}$, whereby we readily read off,

$$G_{\phi\phi} = k, \quad G_{yy} = \frac{h}{f}, \tag{B.0}$$

and,

$$G_{\gamma\bar{\gamma}} - B_{\gamma\bar{\gamma}} = hk, \qquad G_{\gamma\bar{\gamma}} + B_{\gamma\bar{\gamma}} = 0,$$
$$G_{y\gamma} + B_{y\gamma} = 2\epsilon_+ h\sqrt{k}, \qquad G_{y\gamma} - B_{y\gamma} = 0,$$
$$G_{y\bar{\gamma}} - B_{y\bar{\gamma}} = 2\epsilon_- h\sqrt{k}, \qquad G_{y\bar{\gamma}} + B_{y\bar{\gamma}} = 0.$$

Solving these we obtain the 4 dimensional metric components,

$$G_{\bar{\gamma}\gamma} = G_{\gamma\bar{\gamma}} = \frac{hk}{2}, \qquad G_{y\gamma} = G_{\gamma y} = \epsilon_+ h\sqrt{k}, \qquad G_{\bar{\gamma}y} = G_{y\bar{\gamma}} = \epsilon_- h\sqrt{k}, \tag{B.-2}$$

or more conventionally the 4 dimensional line element.

$$ds_4^2 = k \, d\phi^2 + \frac{h}{f} dy^2 + hk \, d\gamma \, d\overline{\gamma} + 2\epsilon_+ h\sqrt{k} \, dy \, d\gamma + 2\epsilon_- h\sqrt{k} \, dy \, d\overline{\gamma}. \tag{B.-2}$$

This line element expression is exactly the same as in Eq. (4.9) of [105] with $\alpha' = 1$ and modulo the decoupled T^3 and S^3 directions. In $U, \gamma, \overline{\gamma}$ coordinates,

$$ds^2 = \frac{k}{U^2} dU^2 + \frac{h}{f} dy^2 + hk \, d\gamma \, d\overline{\gamma} + 2\epsilon_+ h\sqrt{k} \, dy \, d\gamma + 2\epsilon_- h\sqrt{k} \, dy \, d\overline{\gamma}, \tag{B.-2}$$

while the 4 dimensional B-field components,

$$B_{\gamma\overline{\gamma}} = -\frac{hk}{2}, \qquad B_{y\gamma} = -B_{\gamma y} = \epsilon_+ h\sqrt{k}, \qquad B_{y\overline{\gamma}} = -B_{\overline{\gamma} y} = -\epsilon_- h\sqrt{k}. \tag{B.-2}$$

or in component-basis form,

$$B = -\frac{hk}{2} \, d\gamma \wedge d\overline{\gamma} + \epsilon_+ h\sqrt{k} \, dy \wedge d\gamma - \epsilon_- h\sqrt{k} \, d\overline{\gamma} \wedge dy.$$

The 4 dimensional field strength, H is thus

$$H = dB = -\frac{h'k}{2} \, dU \wedge d\gamma \wedge d\overline{\gamma} + \epsilon_+ h'\sqrt{k} \, dU \wedge dy \wedge d\gamma - \epsilon_- h'\sqrt{k} \, dU \wedge dy \wedge d\overline{\gamma}. \tag{B.-2}$$

where $h' = \frac{dh}{dU}$. The components of the H 3-form field strength tensor,

$$H_{U\gamma\overline{\gamma}} = -\frac{h'k}{2}, \qquad H_{Uy\gamma} = \epsilon_+ h'\sqrt{k}, \qquad H_{Uy\overline{\gamma}} = -\epsilon_- h'\sqrt{k}. \tag{B.-2}$$

From these we compute that

$$-H^2 = \frac{6U^2 \, h'(U)^2}{k \, l_s^2 \, h(U)^2}. \tag{B.-2}$$

Here we have restored factors of l_s. The 4 dimensional volume element is,

$$\sqrt{G} d^4 x = \frac{hk^{3/2} l_s^3}{2U} dU \, d\gamma \, d\overline{\gamma} dy. \tag{B.-2}$$

Thus the 4 dimensional onshell Lagrangian contribution of the three form field strength H is,

$$\sqrt{G} \left(-\frac{1}{12} H^2 \right) = \frac{l_s \sqrt{k}}{4} \left(\frac{U h'^2}{h} \right). \tag{B.-2}$$

The vanishing of the worldsheet beta functions give the Dilaton, $e^{-2(\Phi_{(4)} - \Phi_0)} = kU^2 h^{-1}$, and thus the H term contribution to the 4-dimensional gravity action is,

$$\frac{1}{16\pi G_N^{(4)}} \int \sqrt{G} \, d^4 x \, e^{-2(\Phi_{(4)} - \Phi_0)} \left(-\frac{1}{12} H^2 \right) = \frac{1}{16\pi G_N} \left(\frac{l_s}{\sqrt{k}} \right) \int dU \, \frac{h^2}{U^3} \int d\gamma \, d\overline{\gamma} \, . \tag{B.-2}$$

Here we have already performed the y-integration: $\int dy = 2\pi R_y$, R_y being the radius of the y-circle. Here the 3 dimensional Newton's constant is defined as,

$$G_N = \frac{G^{(4)}}{2\pi R_y}. \tag{B.-2}$$

Next we switch to X and T defined by,

$$X = \frac{\sqrt{k}l_s}{2\sqrt{\epsilon_+\epsilon_-}}\left(\epsilon_+\gamma + \epsilon_-\overline{\gamma}\right),$$

$$T = \frac{\sqrt{k}l_s}{2\sqrt{\epsilon_+\epsilon_-}}\left(\epsilon_+\gamma - \epsilon_-\overline{\gamma}\right).$$

In such case we have

$$dX\,dT = \frac{kl_s^2}{2}d\gamma\,d\overline{\gamma}$$

and we have the H-field contribution (B),

$$\frac{1}{16\pi G_N^{(4)}}\int\sqrt{G}\,d^4x\,e^{-2\left(\Phi_{(4)}-\Phi_0\right)}\left(-\frac{1}{12}H^2\right) = \frac{1}{16\pi G_N}\left(\frac{l_s}{\sqrt{k}}\right)\int dU\,\frac{h^2}{U^3}\left(\frac{2\int dX\,dT}{kl_s^2}\right)$$

$$= \frac{L_x}{8\pi G_N l_s k^{3/2}}\int dU\,\frac{h^2}{U^3}\int dT.$$

B.1 Kaluza-Klein reduction on the y circle

Here we repeat the exercise of KK reduction of the y-circle to fill in some of the details, in particular, the KK reduced 3 dimensional Kalb-Ramond field and the associated KK one-form gauge field expressions were omitted in [114], as well as with the aim to check the equivalence of the 4 dimensional and the 3 dimensional (onshell) actions. The equivalence of the 4 dimensional and 3 dimensional actions guarantee that the action complexity remains the same before and after the KK reduction. For the KK reduction we closely follow Pope's review [?] but departing from its convention by setting

$$\alpha = 0, \beta = 1, \tag{B.-3}$$

and calling the KK scalar σ following [114]. This convention is advantageous because it implies,

$$\sqrt{-G}\,e^{-2\Phi^{(4)}} = \sqrt{-g}\,e^{-2\Phi}. \tag{B.-3}$$

The 4 dimensional metric in this convention is split up as,

$$ds_4^2 = ds_3^2 + e^{2\sigma}\left(dy + \mathcal{A}_\mu dx^\mu\right)^2$$

from which we can determine the 3 dimensional metric components, $g_{\mu\nu}$ and the gauge field components, $\mathcal{A}_\mu$

$$G_{yy} = e^{2\sigma},$$
$$G_{y\mu} = e^{2\sigma}\mathcal{A}_\mu,$$
$$G_{\mu\nu} = g_{\mu\nu} + e^{2\sigma}\mathcal{A}_\mu\mathcal{A}_\nu.$$

Using (B) and (B) we identify,

$$e^{2\sigma} = \frac{h}{f},$$

$$\mathcal{A}_\gamma = \epsilon_+ f\sqrt{k}, \qquad \mathcal{A}_{\overline{\gamma}} = \epsilon_- f\sqrt{k}, \qquad \mathcal{A}_\phi = 0,$$

$$g_{\phi\phi} = k, \quad g_{\gamma\gamma} = -\epsilon_+^2 hfk, \quad g_{\overline{\gamma}\overline{\gamma}} = -\epsilon_-^2 hfk, \quad g_{\gamma\overline{\gamma}} = \frac{hk}{2}\left(1 - 2\epsilon_+\epsilon_- f\right).$$

Thus the 3 dimensional line element is,

$$ds_3^2 = k \left[d\phi^2 - \epsilon_+^2 hf d\gamma^2 - \epsilon_-^2 hf d\overline{\gamma}^2 + h \left(1 - 2\epsilon_+\epsilon_- f \right) d\gamma d\overline{\gamma} \right]$$
$$= k \left(d\phi^2 + h \, d\gamma d\overline{\gamma} - fh \left(\epsilon_+ d\gamma + \epsilon_- d\overline{\gamma} \right)^2 \right)$$

For this 3 dimensional metric we note that,

$$\sqrt{-g} = \frac{k^{3/2}\sqrt{fh}}{2}. \tag{B.-4}$$

With this choice of α, β obviously, one needs to change the Dilaton, such that the action has same normalization for the Ricci and the c.c. term

$$\sqrt{-G}e^{-2\Phi^{(4)}} R^{(4)} = \sqrt{-g}e^{-2\Phi} \left(R + ... \right)$$

$$\sqrt{-G}e^{-2\Phi^{(4)}} \Lambda = \sqrt{-g}e^{-2\Phi} \Lambda$$

Acccording to (1.14) of Pope,

$$\sqrt{-G} = e^\sigma \sqrt{-g}.$$

and the unnumbered equation in the passage before (1.11),

$$\sqrt{-G} R^{(4)} = e^\sigma \sqrt{-g} R.$$

Thus we can consistently choose, $\Phi = \Phi^{(4)} - \frac{\sigma}{2}$ or,

$$e^{2\Phi} = g_s^2 e^{-2\phi} \sqrt{fh} = g_s^2 \frac{\sqrt{fh}}{kU^2}. \tag{B.-4}$$

This coincides with eq. (4.8) of [114].

B.1.1 KK reduction of the Kalb-Ramond field

Now we perform the KK reduction of the 4 dimensional three-form field strength, H to the 3 dimensional three-form field strength $\widetilde{H}$ and two-form field strength $\widetilde{F}$. But before we do that, we note that in 4 dimensions, the term in the action is,

$$\sqrt{-G}e^{-2\left(\Phi^{(4)} - \Phi_0\right)} \left(H^{(4)} \right)^2.$$

Under the current convention this term becomes,

$$\sqrt{-G}e^{-2\left(\Phi^{(4)} - \Phi_0\right)} \left(H^{(4)} \right)^2 = \left(e^\sigma \sqrt{-g} \right) \left(e^{-2(\Phi - \Phi_0)} e^{-\sigma} \right) \left(H^{(4)} \right)^2 = \sqrt{-g}e^{-2(\Phi - \Phi_0)} \left(H^{(4)} \right)^2.$$

Now, the first step in the KK reduction for the H^2 term as per the recipe of [?] is to split up the 4 dimensional NS-NS B-field potential (B) using Eq.(1.18) of [?] :

$$B = -\frac{hk}{2} \, d\gamma \wedge d\overline{\gamma} + \epsilon_+ h\sqrt{k} \, dy \wedge d\gamma - \epsilon_- h\sqrt{k} \, dy \wedge d\overline{\gamma}$$
$$= -\frac{hk}{2} \, d\gamma \wedge d\overline{\gamma} + \left(-\epsilon_+ h\sqrt{k} \, d\gamma + \epsilon_- h\sqrt{k} \, d\overline{\gamma} \right) \wedge dy$$
$$= A_{(2)} + A_{(1)} \wedge dy$$

where,

$$A_{(2)} = -\frac{hk}{2} \, d\gamma \wedge d\overline{\gamma}, \qquad A_{(1)} = -\epsilon_+ h\sqrt{k} \, d\gamma + \epsilon_- h\sqrt{k} \, d\overline{\gamma}. \tag{B.-4}$$

We have previously noted that from the Ricci sector,

$$\mathcal{A} = f\sqrt{k}\left(\epsilon_+\, d\gamma + \epsilon_-\, d\overline{\gamma}\right). \tag{B.-4}$$

Next step is to substitute (B.1.1), (??) in Eq. (1.21) of [?] to get the 3-dimensional field strengths, $\widetilde{H}$ and $\widetilde{F}$:

$$\widetilde{F} = dA_{(1)} = \sqrt{k}h'\left(-\epsilon_+ dU \wedge d\gamma + \epsilon_-\, dU \wedge d\overline{\gamma}\right). \tag{B.-4}$$

$$\widetilde{H} = dA_{(2)} - dA_{(1)} \wedge \mathcal{A} = -\frac{h'fk}{2h}\, dU \wedge d\gamma \wedge d\overline{\gamma} = -\frac{h'fk}{2h}\, \widetilde{\epsilon}.$$

where $\tilde{\epsilon}$ is the 3 dimensional Levi-Civita symbol (nontensor). In terms of components,

$$\widetilde{H}_{U\gamma\overline{\gamma}} = -\frac{h'fk}{2h}, \tag{B.-4}$$

and,

$$i\widetilde{F}_{\gamma\overline{\gamma}} = 0, \qquad i\widetilde{F}_{U\gamma} = -\epsilon_+\sqrt{k}h', \qquad i\widetilde{F}_{U\overline{\gamma}} = \epsilon_-\sqrt{k}h'. \tag{B.-4}$$

B.1.2 Matching the 4d action terms with the 3d action terms

The volume terms in the bulk action (4.87) are

$$S_{4D} = \frac{1}{16\pi G_N^{(4)}}\int d^4x\sqrt{-G}e^{-2(\Phi^{(4)}-\Phi_0^{(4)})}\left(R^{(4)} + 4G^{\mu\nu}\partial_\mu\Phi^{(4)}\partial_\nu\Phi^{(4)} - \frac{1}{12}H^2 - 4\Lambda\right). \tag{B.-3}$$

Here we demonstrate that this 4 dimensional action is equal to the following 3 dimensional action as a consistency check,

$$\begin{aligned}
S_{(3D)} = \frac{1}{16\pi G_N}\int d^3x\sqrt{-g}\; e^{-2(\Phi-\Phi_0)}\Big(&R - (\partial\sigma)^2 - 2\Box\sigma - \frac{1}{4}e^{2\sigma}\mathcal{F}^2 - 4\Lambda \\
&+ 4g^{\mu\nu}\partial_\mu\Phi\partial_\nu\Phi + 4g^{\mu\nu}\partial_\mu\Phi\partial_\nu\sigma \\
&-\frac{1}{12}\widetilde{H}^2 - \frac{1}{4}e^{-2\sigma}\widetilde{F}^2\Big).
\end{aligned}$$

One might wonder why are we keeping total derivative terms like $\Box\sigma$ in the 3 dimensional action upon KK reduction since they do not contribute to the equation of motion. The reason we have to keep these terms is that these total derivative terms *do not vanish on-shell* and in fact make non-trivial contributions to action complexity, including *introducing new surface (GHY) counterterms.* Similar phenomenon was first pointed out in [228].

By separately considering equality of blocks of terms in the actions, (B.1.2), (B.1.2), (B.1.2) and (B.1.2), in the following subsections and upon summing over both sides of those terms, we demonstrate the equality of the two actions (B.-3) and (B.1.2).

Matching the contributions of the Kalb-Ramond field sector before and after KK reduction

From (B.1.1) we obtain,

$$\begin{aligned}
-\widetilde{H}^2 &= H_{\lambda\mu\nu}H_{\rho\sigma\tau}g^{\lambda\rho}g^{\mu\sigma}g^{\nu\tau} \\
&= \left(-\frac{h'fk}{2h}\right)^2\underbrace{\widetilde{\epsilon}_{\lambda\mu\nu}\widetilde{\epsilon}_{\rho\sigma\tau}g^{\lambda\rho}g^{\mu\sigma}g^{\nu\tau}}_{=3!g^{-1}} \\
&= \left(\frac{h'fk}{2h}\right)^2\frac{3!}{g}.
\end{aligned}$$

and from (B.1.1) we get,

$$-\widetilde{F}^2 = i\widetilde{F}_{\mu\nu}i\widetilde{F}_{\rho\sigma}g^{\mu\rho}g^{\nu\sigma}$$
$$= \mathrm{tr}\left(\widetilde{F}g^{-1}\widetilde{F}g^{-1}\right)$$
$$= \frac{8h'^2U^2\epsilon_+\epsilon_-}{hk}.$$

So the RHS of (1.24) of [?] using eq. (1.23) works out in this case to be,

$$\sqrt{-g}e^{-2\Phi}\left(-\frac{1}{12}\widetilde{H}^2 - \frac{1}{4}e^{-2\sigma}\widetilde{F}^2\right) = e^{-2\Phi_{(4)}}\left(\left(\frac{h'fk}{2h}\right)^2\frac{e^\sigma}{2\sqrt{-g}} + \frac{2h'^2U^2\epsilon_+\epsilon_-}{hk}e^{-\sigma}\sqrt{-g}\right)$$

$$= e^{-2\Phi_{(4)}}\frac{h'^2k^2f^2}{4h^2}\frac{\sqrt{\frac{h}{f}}U}{k^{3/2}\sqrt{fh}} + \frac{2e^{-2\Phi_{(4)}}h'^2\epsilon_+\epsilon_-U^2}{hk}\left(\sqrt{\frac{f}{h}}\right)\left(\frac{k^{3/2}}{2U}\sqrt{fh}\right)$$

$$= \frac{e^{-2\Phi_{(4)}}h'^2f\sqrt{k}U}{4h^2} + \frac{e^{-2\Phi_{(4)}}h'^2f\sqrt{k}U\epsilon_+\epsilon_-}{h}$$

$$= e^{-2\Phi_{(4)}}\frac{h'^2f\sqrt{k}U}{4h^2}\underbrace{(1 + 4\epsilon_+\epsilon_-h)}_{=h/f}$$

$$= e^{-2\Phi_{(4)}}\underbrace{\frac{\sqrt{k}Uh'^2}{4h}}_{=-\sqrt{-G}H^2/12}$$

$$= -\sqrt{-G}e^{-2\Phi_{(4)}}\frac{H^2}{12}.$$

Thus we have just verified that the LHS and RHS of Eq. (1.24) of [?] are consistent for this special string background. From (B.1.2) of last section and integrating out the y-circle leads to the equivlanece of the H^2 term in 4d and to the $\widetilde{H}^2, \widetilde{F}^2$ terms in 3d,

$$S_H = \frac{1}{16\pi G_N^4}\int d^3x\, dy\sqrt{-G}e^{-2\left(\Phi_{(4)}-\Phi_0\right)}\left(-\frac{H^2}{12}\right) = \frac{1}{16\pi G_N}\int d^3x\sqrt{-g}e^{-2(\Phi-\Phi_0)}\left(-\frac{1}{12}\widetilde{H}^2 - \frac{1}{4}e^{-2\sigma}\widetilde{F}^2\right).$$

Plugging in the background fields and integrating over the (regularized) WdW patch, this contribution can be expressed as a nested integral,

$$S_H = \frac{L_X}{4\pi G_N k}\int \frac{dU}{U^3}h^2(U)\int_U^{\frac{l_s}{\epsilon}}\frac{dU'}{U'}\frac{1}{\sqrt{h(U')}}, \tag{B.-14}$$

where we have used, $\frac{h'}{h} = \frac{2h}{kU^3}$. $\mathcal{M}_3$ If we set $\epsilon_\pm = 0$, $h = f$, then the above contribution becomes,

$$S_H = -\frac{L_X}{4\pi G_N k}\int_0^{\frac{l_s}{\epsilon}}\frac{dU}{U^3}f^2(U)\int_U^{\frac{l_s}{\epsilon}}\frac{dU'}{U'}\frac{1}{\sqrt{f(U')}},$$

which is the exact same expression as Eq. (3.34) of our previous paper [132] on $\mathcal{M}_3$ complexity.

Matching the contributions of the Dilaton sector before and after KK reduction

Since $\Phi = \Phi(U)$, the Dilaton contribution to the 4d action simplifies to

$$S_\Phi = \frac{1}{16\pi G_N^{(4)}}\int_{WdW} d^4x\,\sqrt{-G}\,e^{-2\left(\Phi_{(4)}-\Phi_0\right)}\,4G^{UU}\,\partial_U\Phi_{(4)}\,\partial_U\Phi_{(4)}. \tag{B.-15}$$

In our conventions, $\sqrt{-G}\,e^{-2(\Phi_{(4)}-\Phi_0)} = \sqrt{-g}\,e^{-2(\Phi-\Phi_0)}$ and $G^{UU} = g^{UU}$ while $\Phi_{(4)} = \Phi + \frac{\sigma}{2}$. Substituting all this in the 4 dimensional action (B.1.2) and then integrating over the y-circle we get the desired 3d action,

$$
\begin{aligned}
S_\Phi &= \frac{1}{16\pi G_N^{(4)}} \int_{W\,dW} d^4x\,\sqrt{-G}\,e^{-2(\Phi_{(4)}-\Phi_0)}\,4G^{UU}\,\partial_U\Phi_{(4)}\,\partial_U\Phi_{(4)} \\
&= \frac{1}{16\pi G_N} \int_{W\,dW} d^3x\,e^{-2(\Phi-\Phi_0)}\,\sqrt{-g}\,g^{UU}\left(4\partial_U\Phi\,\partial_U\Phi + 4\partial_U\Phi\,\partial\sigma + (\partial_U\sigma)^2\right).
\end{aligned}
$$

As a nested integral this is,

$$
S_\Phi = \frac{\lambda'^2 k^3 L_X}{2\pi G_N} \int_0^{\frac{l_s}{\epsilon}} dU\,\frac{U^5}{(1+\lambda'\,kU^2)^2} \int_U^{\frac{l_s}{\epsilon}} \frac{dU'}{U'\sqrt{h(U')}}.
$$

Again we can explicitly check that setting $\epsilon_\pm = 0$, i.e. $\lambda' = \lambda, h = f$ reproduces the $\mathcal{M}_3$ dilaton action-complexity contribution Eq. (3.28) of our previous paper [132].

Matching the contributions of the Cosmological constant term before and after KK reduction

Next consider the contribution to the action from the cosmological constant term. Here we will see again for this term the 3 and 4 dimensional calculations match exactly. Our convention for the change of metric and Dilaton under KK reduction (B.1) implies,

$$
\sqrt{-G}\,e^{-2(\Phi^{(4)}-\Phi_0)} = \sqrt{-g}\,e^{-2(\Phi-\Phi_0)}
$$

and hence we get the desired match between cc terms in the the 4 dimensional and 3 dimensional actions:

$$
S_\Lambda = \frac{1}{16\pi G_N^{(4)}} \int \sqrt{-G}e^{-2(\Phi^{(4)}-\Phi_0)}\,(-4\Lambda) = \frac{1}{16\pi G_N} \int d^3x\sqrt{-g}e^{-2(\Phi-\Phi_0)}\,(-4\Lambda). \tag{B.-16}
$$

Here we have again integrated out the y-circle in going from the LHS to the RHS and set the 3d Newton's constant $G_N = G_N^4/2\pi R_y$. In the static coordinates we get

$$
\sqrt{-g} = \frac{\sqrt{k}l_s}{U}f,
$$

and recall that in 3 dimensions the dilaton factor is

$$
e^{-2(\Phi-\Phi_0)} = \frac{kU^2}{\sqrt{fh}}.
$$

Finally using,

$$
\Lambda = -\frac{1}{kl_s^2}
$$

we get the 3 dimesional cosmological term contribution as a nested integral

$$
S_\Lambda = \frac{L_X k}{2\pi G_N} \int_0^{\frac{l_s}{\epsilon}} dU\,U \int_U^{\frac{l_s}{\epsilon}} \frac{dU'}{U'\sqrt{h(U')}}.
$$

$\mathcal{M}_3$ limit check: Again setting $\epsilon_\pm = 0$ and $h = f$ we get,

$$
S_\Lambda = \frac{L_X k}{2\pi G_N} \int_0^{\frac{l_s}{\epsilon}} dU\,U \int_U^{\frac{l_s}{\epsilon}} \frac{dU'}{U'\sqrt{f(U')}},
$$

which is the same as Eq. (3.31) of our previous [132] paper.

Matching the contributions of the Ricci scalar sector before and after KK reduction

Finally consider the Ricci scalar term In 4 dimensions. Upon KK reduction this term gets split up into action term contributions from the 3 dimensional Ricci scalar, the KK-scalar, σ and the KK gauge field, $\mathcal{A}$. To this end recall Equation (1.14) of Chris Pope's remarkable review [?]. In our convention, i.e. $\beta = 1, \alpha = 0$, and for our case, $D = 3$, it reduces to

$$R^{(4)} = R^{(3)} - 2\left(\partial\sigma\right)^2 - 2\Box\sigma - \frac{1}{4}e^{2\sigma}\mathcal{F}^2. \tag{B.-16}$$

For the string background under consideration the Ricci scalar is,

$$R^{(4)} = \frac{-6 + 8\lambda' \, k \, U^2}{k \, l_s^2 \, \left(1 + \lambda' \, k \, U^2\right)^2}, \tag{B.-16}$$

and the dilaton is given by,

$$\Phi^{(4)} = \Phi_0^{(4)} + \frac{1}{2}\log\left(\frac{h(U)}{k \, U^2}\right). \tag{B.-16}$$

On the other hand, for the 3 dimensional background, the Ricci scalar works out to be

$$R = \frac{8\lambda k^3 \left(\lambda^2 + 8\epsilon_+^2\epsilon_-^2 - 6\lambda\epsilon_+\epsilon_-\right)U^6 - 2k^2\left(-5\lambda^2 + 16\epsilon_+^2\epsilon_-^2 + 20\lambda\epsilon_+\epsilon_-\right)U^4 + 4k(2\epsilon_+\epsilon_- - \lambda)U^2 - 6}{k\left(\lambda kU^2 + 1\right)^2\left((\lambda - 4\epsilon_+\epsilon_-)kU^2 + 1\right)^2} \tag{B.-16}$$

while the 3 dimensional dilaton factor is,

$$e^{-2(\Phi - \Phi_0)} = \sqrt{\lambda kU^2 + 1}\sqrt{(\lambda - 4\epsilon_+\epsilon_-)\,kU^2 + 1}, \tag{B.-16}$$

the KK-gauge field strength contribution,

$$\mathcal{F}^2 = \frac{64kU^4\epsilon_+^2\epsilon_-^2}{\left(\lambda kU^2 + 1\right)^4}, \tag{B.-16}$$

and the KK scalar σ contributions,

$$\left(\partial\sigma\right)^2 = \frac{16kU^4\epsilon_+^2\epsilon_-^2}{\left(\lambda kU^2 + 1\right)^2\left((\lambda - 4\epsilon_+\epsilon_-)kU^2 + 1\right)^2} \tag{B.-15}$$

$$\Box\sigma = \frac{8U^2\epsilon_+\epsilon_-\left(k^2\lambda U^4(4\epsilon_+\epsilon_- - \lambda) + kU^2(\lambda - 2\epsilon_+\epsilon_-) + 2\right)}{\left(\lambda kU^2 + 1\right)^2\left((\lambda - 4\epsilon_+\epsilon_-)\,kU^2 + 1\right)^2} \tag{B.-14}$$

From (B.1.2)-(B.-14) one can explicity verify (B.1.2). Now that we have checked (B.1.2), it is easy to verify (in light of (B.1)) that,

$$S_R = \frac{1}{16\pi G_N^{(4)}}\int d^4x\sqrt{-G}\, e^{-2(\Phi^4 - \Phi_0)}R^{(4)} = \frac{1}{16\pi G_N}\int d^3x\sqrt{-g}\, e^{-2(\Phi - \Phi_0)}\left(R^{(3)} - 2\left(\partial\sigma\right)^2 - 2\Box\sigma - \frac{1}{4}e^{2\sigma}\mathcal{F}^2\right) \tag{B.-14}$$

after integrating out the y-circle. Restricting the integral over the 3 dimensional WdW patch, this contribution can be expressed as the nested integral,

$$S_R = \frac{k\, L_X}{4\pi G_N}\int_0^{\frac{l_s}{\epsilon}} dU\, U\, \frac{-3 + 4\lambda' kU^2}{\left(1 + \lambda' kU^2\right)^2}\int_U^{\frac{l_s}{\epsilon}}\frac{dU'}{U\sqrt{h(U')}}. \tag{B.-14}$$

$\mathcal{M}_3$ limit check: On setting $\epsilon_\pm = 0$ and $h = f, \lambda' = \lambda$, we get,

$$S_R = \frac{k\, L_X}{4\pi G_N}\int_0^{\frac{l_s}{\epsilon}} dU\, U\, \frac{-3 + 4\lambda kU^2}{\left(1 + \lambda kU^2\right)^2}\int_U^{\frac{l_s}{\epsilon}}\frac{dU'}{U\sqrt{f(U')}}$$

which is the same as Eq. (3.25) of our previous [132] paper.

Full nonperturbative result for the Ricci sector:

$$
S_R = \frac{L_X}{4\pi G_N \sqrt{\lambda'}} \left[-\frac{\pi^2}{6} - \frac{7}{2\sqrt{1+\frac{\epsilon^2}{\lambda' k l_S^2}}} + \frac{7}{2}\sqrt{\frac{\epsilon^2}{\lambda' k l_s^2}+1} - \frac{7\frac{\epsilon^2}{\lambda' k l_s^2}}{2\sqrt{1+\frac{\epsilon^2}{\lambda' k l_S^2}}} - 2\sqrt{1+\frac{\epsilon^2}{\lambda' k l_S^2}}\ln\left(1+\frac{\lambda' k l_s^2}{\epsilon^2}\right) \right.
$$

$$
-\frac{7}{2}\sinh^{-1}\left(\frac{\sqrt{\lambda' k}\, l_s}{\epsilon}\right) + 4\ln\left(\sqrt{1+\frac{\lambda' k\, l_s^2}{\epsilon^2}}+\frac{\sqrt{\lambda' k}\, l_s}{\epsilon}\right) + 2\ln\left(1+\frac{\lambda' k\, l_s^2}{\epsilon^2}\right)\sinh^{-1}\left(\frac{\sqrt{\lambda' k}\, l_s}{\epsilon}\right)
$$

$$
+2\left(\sinh^{-1}\left(\frac{\sqrt{\lambda' k}\, l_s}{\epsilon}\right)\right)^2 - 4\ln\left(1+\left(\sqrt{1+\frac{\lambda' k\, l_s^2}{\epsilon^2}}+\frac{\sqrt{\lambda' k}\, l_s}{\epsilon}\right)^2\right)\sinh^{-1}\left(\frac{\sqrt{\lambda' k}\, l_s}{\epsilon}\right)
$$

$$
\left. -2\mathrm{Li}_2\left(-\left(\sqrt{1+\frac{\lambda' k\, l_s^2}{\epsilon^2}}+\frac{\sqrt{\lambda' k}\, l_s}{\epsilon}\right)^2\right)\right].
$$

B.2 GHY type surface terms in 3 dimensions

Since the 3 dimensional action has the a second derivative term from the KK scalar σ, one will need a boundary term to cancel its variation. Here we work out that term,

$$
-\frac{1}{8\pi G_N}\int_M \sqrt{-g}\, e^{-2(\Phi-\Phi_0)}\Box\left(\delta\sigma\right) = -\frac{1}{8\pi G_N}\int_M \sqrt{-g}\nabla^\mu\left[e^{-2(\Phi-\Phi_0)}\nabla_\mu\left(\delta\sigma\right)\right] + \frac{1}{8\pi G_N}\int \sqrt{-g}\nabla^\mu e^{-2(\Phi-\Phi_0)}\nabla_\mu\left(\delta\sigma\right)
$$

$$
= -\frac{1}{8\pi G_N}\int_{\partial M}\sqrt{-\gamma}\, n^\mu\left[e^{-2(\Phi-\Phi_0)}\delta\left(\nabla_\mu\sigma\right)\right] - \dots
$$

$$
= -\frac{1}{8\pi G_N}\int_{\partial M}\delta\left(\sqrt{-\gamma}\, n^\mu e^{-2(\Phi-\Phi_0)}\nabla_\mu\sigma\right) - \dots.
$$

This first term can be canceled if we add the surface counter term,

$$
I_{GHY;\sigma} = \frac{1}{8\pi G_N}\int_{\partial M}\sqrt{-\gamma}\, e^{-2(\Phi-\Phi_0)}\, n^\mu\partial_\mu\sigma.
$$

In addition we also have the usual GHY term for the string frame metric variation to be well defined,

$$
I_{GHY;g} = \frac{1}{8\pi G_N}\int_{\partial M}\sqrt{-\gamma}e^{-2(\Phi-\Phi_0)}K.
$$

Thus the full *GHY* term is,

$$
I_{GHY} = \frac{1}{8\pi G_N}\int_{\partial M}\sqrt{-\gamma}e^{-2(\Phi-\Phi_0)}\left(K + n^\mu\partial_\mu\sigma\right). \tag{B.-17}
$$

B.3 Holographic Entanglement Entropy

The holographic entanglement entropy of WCFT dual to null warped AdS_3 (following the prescription for nontrivail dilaton turned on in the bulk [126]) is,

$$
S_A = \frac{1}{4G_N}\int e^{-2(\Phi(U)-\Phi_\infty)}dx\sqrt{\gamma}
$$

$$
= \frac{1}{4G_N}\int_{U_0}^{\frac{l_s}{\epsilon}} dx\sqrt{\frac{kl_s^2}{U^2}\frac{(U^4(1-kU^2\epsilon_-^2)(U^2-V^2-k\epsilon_-^2(U^4-U_0^4))}{U_0^2 l_s^2(1-kU_0^2\epsilon_-^2)}+kU^2(1-kU^2\epsilon_-^2)}
$$

After simplifying and replacing dx as $\frac{dU}{U'}$ the equation for our metric becomes,

$$S_A = \frac{1}{4G_N} \sqrt{k} l_s \int_{U_0}^{\frac{l_s}{\epsilon}} dU \frac{\sqrt{1 - kU^2\epsilon_-^2}}{\sqrt{U^2 - U_0^2 - k\epsilon_-^2(U^4 - U_0^4)}}$$

For, Warped AdS, after expanding the integrand in equation B.3 in a Taylor series with respect to ϵ_-, we get the entanglement entropy to be,

$$S_A = \frac{\sqrt{k} l_s}{4G_N}\left(1 + \frac{6kl_s^2}{L^2}\epsilon_-^2\right) \ln\left(\frac{L}{\epsilon}\right) + O(\epsilon_-^4)$$

Here, we have used Eq. (4.80) to replace U_0 as a function of L. Also, we can see that, putting warping parameter, $\epsilon_- \to 0$ gets us the result back for pure AdS which is, $S_A = \frac{\sqrt{k} l_s}{4G_N} \ln\left(\frac{L}{\epsilon}\right)$. This is also can be seen in [140] from the comparison of equation (3.23) and (3.27).

Through numerical integration of eqn B.3, we have found the nature of the Holographic Entanglement Entropy as a function of L for Warped AdS_3. We have used parametric plot here and used eqn 4.85 for the expression of L.
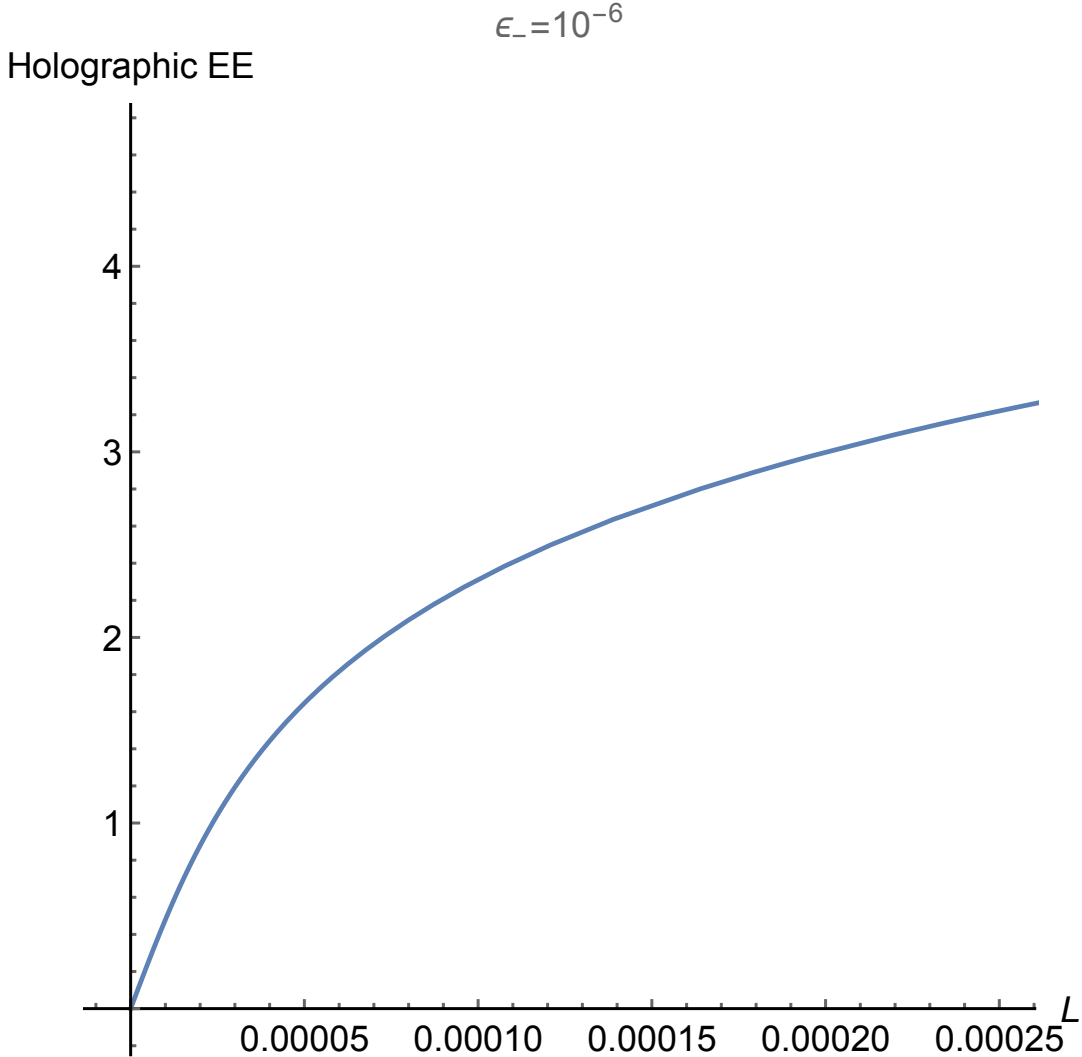

Figure B.1: Holographic Entanglement Entropy vs L plot. The values used here are following, $k = 10^4$, $l_s = 0.01$ and $\epsilon = 10^{-5}$

Here again, we used the value of the warping factor as, $\epsilon_- = 10^{-6}$ for the same reason mentioned at the end of Sec. 4.5.2.

One curious fact to note is that the holographic entanglement entropy doesn't display any on-locality in terms of the UV divergences appearing - for any value of the warping the only type of UV divergence appearing is the log divergence, much akin to a local field theory like CFT_2. This is polar opposite of the pattern of UV divergences appearing in subregion volume complexity (all orders of UV divergences appear there). The fact that the entanglement entropy of a $WCFT_2$, a highly nonlocal and Lorentz boost violating theory, but has the exact same UV divergence structure as that of the entanglement entropy of a local CFT_2 has been noted in earlier works [140, 141].

Appendix C

Review of timelike WAdS$_3$

Our starting point is the black string metric, equation (4.10) of [174]

$$ds'^2 = l^2 \left(\frac{(1 + \lambda^2 A^2)}{4(r^2 - A^2 B^2)} dr^2 + A^2 dv^2 + (B^2(1 + \lambda^2 A^2) - \lambda^2 r^2) du^2 + 2r dudv \right) ,$$

where, the non-compact event horizon is located at $r_h = AB$. We will rewrite the above metric in order to arrive at timelike WAdS$_3$ metric. To this end let's separately write the λ independent unwarped part of the metric as

$$ds_0^2 = \frac{dr^2}{4(r^2 - A^2 B^2)} + A^2 dv^2 + B^2 du^2 + 2r \, dudv$$

where we have taken $l = 1$. If we further perform the following set of coordinate changes and parameter redefinitions,

$$du = dx + dt, \quad dv = dx - dt, \quad r = \frac{1}{2}\left(\rho^2 - \frac{a^2 + b^2}{2}\right),$$

$$A = \frac{a + b}{2}, \quad B = \frac{a - b}{2}.$$

then the black string metric (C) turns into

$$ds_0^2 = \frac{d\rho^2 \rho^2}{(\rho^2 - a^2)(\rho^2 - b^2)} - \frac{(\rho^2 - a^2)(\rho^2 - b^2)}{\rho^2} dt^2 + \rho^2 \left(dx - \frac{ab}{\rho^2} dt \right)^2 .$$

This is evidently the metric of BTZ spacetime in disguise with horizons at a and b. In this setup, A is related to the level of Kac-Moody algebra. As we can see that in order to obtain a black hole free background by making horizon disappear simply amounts to taking $a = 0 = b$ (i.e. vanishing Kac-Moody level). This choice simplifies the metric to the form

$$ds_0^2 = \frac{dr^2}{4r^2} + 2 r \, dudv ,$$

thus we recover the pure AdS_3 metric

$$ds_0^2 = \frac{d\rho^2}{\rho^2} + (-dt^2 + dx^2)\rho^2,$$

which we immediately recognise to be the metric of the Poincare patch of the AdS_3. After taking $\rho \to \frac{1}{z}$, further simplifies the metric to

$$ds_0^2 = \frac{dz^2 - dt^2 + dx^2}{z^2} .$$

Let's turn our attention towards the warped part of the metric . After plugging in $A = 0 = B$ in (C) and carrying out the exact same transformations as above, leads us to the warped portion of the metric

$$ds_\lambda^2 = -\lambda^2 \frac{(dt + dx)^2}{4z^4} \ .$$

Hence, the required timelike $WAdS_3$ metric we work with in section (6.1) takes the following form

$$ds^2 = \frac{dz^2 - dt^2 + dx^2}{z^2} - \lambda^2 \frac{(dt + dx)^2}{4z^4} \ .$$

Appendix D

Perturbative analysis for negative mass SAdS complexity

Here we perform an analytic computation of the action and volume complexity for the negative mass AdS-Schwarzschild black hole by performing a perturbation to first two orders in the parameter μ/Λ^{D-3}. Our aim is to confirm, at least to leading order in perturbation theory, the numerical results that the negative mass Schwarzschild-AdS geometry has a lower complexity than empty AdS.

Action Complexity: The Einstein-Hilbert term (6.4) works out to be,

$$I_{EH} = I_{EH}^0 + \mu \Lambda^3 \frac{(D-1)\,\Omega_{D-2}}{4\,\pi\,G_N\,l^2} \int_0^1 dy\, y^{D-2} \int_y^1 \frac{dz}{z^{D-3}(1+(z\Lambda/l)^2)^2}.$$

The nested integral can be evaluated for arbitrary D,

$$I_{EH} = I_{EH}^0 + \frac{\Omega_{D-2}}{16\,\pi\,G_N}\pi\,\mu\,l - \frac{\Omega_{D-2}}{4\,\pi\,G_N}\frac{\mu\,l}{\Lambda} + O(l^2/\Lambda^2). \tag{D.0}$$

Thus this EH term complexity contribution is larger than the empty AdS EH term complexity contribution. The GHY-term arising from the null boundaries of the WdW patch (6.7), to first two orders, works out to be

$$I_{GHY}^{\partial WdW} = I_{GHY}^{0\,\partial WdW} - \frac{\Omega_{D-2}\,\mu\,\Lambda}{16\pi G_N}\int_0^1 dy\,\frac{((D-3)+(D-1)y^2/a^2)}{(1+y^2/a^2)^2}$$

where $a = l/\Lambda$. This integral can be computed exactly for arbitrary D and we get,

$$I_{GHY}^{\partial WdW} = I_{GHY}^{0\,\partial WdW} - \frac{\Omega_{D-2}}{16\pi G_N}\frac{(D-2)\,\pi\,\mu\,l}{2} + \frac{\Omega_{D-2}}{16\pi G_N}\frac{(D-1)\,\mu\,l}{\Lambda} + O(l^2/\Lambda^2) \tag{D.0}$$

Thus to subsubleading order in μ/Λ^{D-3}, the action-complexity for the negative mass Schwarzschild-AdS geometry is is evidently lower than empty AdS complexity,

$$\mathcal{C}_A = \mathcal{C}_A^{AdS} - \frac{\Omega_{D-2}}{16\pi G_N}\frac{(D-4)\,\mu\,l}{2} + \frac{(D-5)\,\Omega_{D-2}}{16\pi G_N}\frac{\mu\,l^2}{\Lambda} + O(l^2/\Lambda^2). \tag{D.0}$$

Note that $\mathcal{C}_A^{AdS} \sim O\left((\Lambda/l)^{D-2}\right)$, so the linear order term in μ is suppressed by a factor of $\mu\,l/\Lambda^{D-2}$. For the special case of $D = 4$, the linear (leading) order in l/Λ difference vanishes, however the negative mass SAdS still receives a negative contribution from the subleading term and has a lower complexity than empty AdS$_4$.

Volume complexity: The volume complexity expression (6.9) to linear order in μ is,

$$\mathcal{C}_V = \mathcal{C}_V^0 - \frac{\mu\,\Omega_{D-2}}{2\,G_N\,l}\int_0^\Lambda dr\,\frac{r}{\left(1+\frac{r^2}{l^2}\right)^{3/2}} = \mathcal{C}_V^0(T) - \frac{\Omega_{D-2}\,\mu\,l}{2\,G_N} + O\left(l^2/\Lambda^2\right).$$

Evidently this is lesser that empty AdS complexity, $\mathcal{C}_V^0 \sim \Lambda^2$.

Bibliography

[1] Stephen William Hawking. Particle creation by black holes. *Communications in Mathematical Physics*, 43:199–220, 1975.

[2] Jacob David Bekenstein. Black holes and the second law. *Lettere al Nuovo Cimento (1971-1985)*, 4:737–740, 1972.

[3] Gerard 't Hooft. Dimensional reduction in quantum gravity. *Conf. Proc. C*, 930308:284–296, 1993.

[4] Leonard Susskind. The World as a hologram. *J. Math. Phys.*, 36:6377–6396, 1995.

[5] Juan Martin Maldacena. The Large N limit of superconformal field theories and supergravity. *Int. J. Theor. Phys.*, 38:1113–1133, 1999.

[6] S.S. Gubser, Igor R. Klebanov, and Alexander M. Polyakov. Gauge theory correlators from non-critical string theory. *Phys. Lett. B*, 428:105–114, 1998.

[7] Edward Witten. Anti-de Sitter space and holography. *Adv. Theor. Math. Phys.*, 2:253–291, 1998.

[8] Ofer Aharony, Steven S. Gubser, Juan Martin Maldacena, Hirosi Ooguri, and Yaron Oz. Large N field theories, string theory and gravity. *Phys. Rept.*, 323:183–386, 2000.

[9] Nissan Itzhaki, Juan Martin Maldacena, Jacob Sonnenschein, and Shimon Yankielowicz. Supergravity and the large N limit of theories with sixteen supercharges. *Phys. Rev. D*, 58:046004, 1998.

[10] S. W. Hawking and G. F. R. Ellis. *The Large Scale Structure of Space-Time.* Cambridge Monographs on Mathematical Physics. Cambridge University Press, 2 2011.

[11] M. Nakahara. *Geometry, topology and physics.* 2003.

[12] Joseph Polchinski. Scale and Conformal Invariance in Quantum Field Theory. *Nucl. Phys. B*, 303:226–236, 1988.

[13] P. Di Francesco, P. Mathieu, and D. Senechal. *Conformal Field Theory.* Graduate Texts in Contemporary Physics. Springer-Verlag, New York, 1997.

[14] Peter Breitenlohner and Daniel Z. Freedman. Stability in Gauged Extended Supergravity. *Annals Phys.*, 144:249, 1982.

[15] Tom Banks, Michael R. Douglas, Gary T. Horowitz, and Emil J. Martinec. AdS dynamics from conformal field theory. 8 1998.

[16] Daniel Harlow and Douglas Stanford. Operator Dictionaries and Wave Functions in AdS/CFT and dS/CFT. 4 2011.

[17] Mark Van Raamsdonk. Building up spacetime with quantum entanglement. *Gen. Rel. Grav.*, 42:2323–2329, 2010.

[18] David D. Blanco, Horacio Casini, Ling-Yan Hung, and Robert C. Myers. Relative Entropy and Holography. *JHEP*, 08:060, 2013.

[19] Nima Lashkari, Michael B. McDermott, and Mark Van Raamsdonk. Gravitational dynamics from entanglement 'thermodynamics'. *JHEP*, 04:195, 2014.

[20] Shinsei Ryu and Tadashi Takayanagi. Holographic derivation of entanglement entropy from AdS/CFT. *Phys. Rev. Lett.*, 96:181602, 2006.

[21] Veronika E. Hubeny, Mukund Rangamani, and Tadashi Takayanagi. A Covariant holographic entanglement entropy proposal. *JHEP*, 07:062, 2007.

[22] Thomas Hartman. Entanglement Entropy at Large Central Charge. 3 2013.

[23] Thomas Faulkner. The Entanglement Renyi Entropies of Disjoint Intervals in AdS/CFT. 3 2013.

[24] Aitor Lewkowycz and Juan Maldacena. Generalized gravitational entropy. *JHEP*, 08:090, 2013.

[25] Thomas Faulkner, Aitor Lewkowycz, and Juan Maldacena. Quantum corrections to holographic entanglement entropy. *JHEP*, 11:074, 2013.

[26] Geoff Penington, Stephen H. Shenker, Douglas Stanford, and Zhenbin Yang. Replica wormholes and the black hole interior. *JHEP*, 03:205, 2022.

[27] Ahmed Almheiri, Thomas Hartman, Juan Maldacena, Edgar Shaghoulian, and Amirhossein Tajdini. Replica Wormholes and the Entropy of Hawking Radiation. *JHEP*, 05:013, 2020.

[28] Juan Martin Maldacena. Eternal black holes in anti-de Sitter. *JHEP*, 04:021, 2003.

[29] Mark Van Raamsdonk. Comments on quantum gravity and entanglement. 7 2009.

[30] Juan Maldacena and Leonard Susskind. Cool horizons for entangled black holes. *Fortsch. Phys.*, 61:781–811, 2013.

[31] Brian Swingle. Entanglement Renormalization and Holography. *Phys. Rev. D*, 86:065007, 2012.

[32] Brian Swingle. Constructing holographic spacetimes using entanglement renormalization. 9 2012.

[33] G. Vidal. Entanglement Renormalization. *Phys. Rev. Lett.*, 99(22):220405, 2007.

[34] G. Vidal. Class of Quantum Many-Body States That Can Be Efficiently Simulated. *Phys. Rev. Lett.*, 101:110501, 2008.

[35] Netta Engelhardt and Aron C. Wall. Quantum Extremal Surfaces: Holographic Entanglement Entropy beyond the Classical Regime. *JHEP*, 01:073, 2015.

[36] Chris Akers and Geoff Penington. Leading order corrections to the quantum extremal surface prescription. *JHEP*, 04:062, 2021.

[37] Jordan Cotler, Patrick Hayden, Geoffrey Penington, Grant Salton, Brian Swingle, and Michael Walter. Entanglement Wedge Reconstruction via Universal Recovery Channels. *Phys. Rev. X*, 9(3):031011, 2019.

[38] Geoffrey Penington. Entanglement Wedge Reconstruction and the Information Paradox. *JHEP*, 09:002, 2020.

[39] Ahmed Almheiri, Netta Engelhardt, Donald Marolf, and Henry Maxfield. The entropy of bulk quantum fields and the entanglement wedge of an evaporating black hole. *JHEP*, 12:063, 2019.

[40] Bartlomiej Czech, Joanna L. Karczmarek, Fernando Nogueira, and Mark Van Raamsdonk. The Gravity Dual of a Density Matrix. *Class. Quant. Grav.*, 29:155009, 2012.

[41] Matthew Headrick, Veronika E. Hubeny, Albion Lawrence, and Mukund Rangamani. Causality & holographic entanglement entropy. *JHEP*, 12:162, 2014.

[42] Aron C. Wall. Maximin Surfaces, and the Strong Subadditivity of the Covariant Holographic Entanglement Entropy. *Class. Quant. Grav.*, 31(22):225007, 2014.

[43] Xi Dong, Daniel Harlow, and Aron C. Wall. Reconstruction of Bulk Operators within the Entanglement Wedge in Gauge-Gravity Duality. *Phys. Rev. Lett.*, 117(2):021601, 2016.

[44] Ahmed Almheiri, Xi Dong, and Daniel Harlow. Bulk Locality and Quantum Error Correction in AdS/CFT. *JHEP*, 04:163, 2015.

[45] Mark Van Raamsdonk. Lectures on Gravity and Entanglement. In *Theoretical Advanced Study Institute in Elementary Particle Physics: New Frontiers in Fields and Strings*, pages 297–351, 2017.

[46] Leonard Susskind. Entanglement is not enough. *Fortsch. Phys.*, 64:49–71, 2016.

[47] Douglas Stanford and Leonard Susskind. Complexity and Shock Wave Geometries. *Phys. Rev. D*, 90(12):126007, 2014.

[48] Leonard Susskind. Computational Complexity and Black Hole Horizons. *Fortsch. Phys.*, 64:24–43, 2016. [Addendum: Fortsch.Phys. 64, 44–48 (2016)].

[49] Adam R. Brown, Daniel A. Roberts, Leonard Susskind, Brian Swingle, and Ying Zhao. Holographic Complexity Equals Bulk Action? *Phys. Rev. Lett.*, 116(19):191301, 2016.

[50] Adam R. Brown, Daniel A. Roberts, Leonard Susskind, Brian Swingle, and Ying Zhao. Complexity, action, and black holes. *Phys. Rev. D*, 93(8):086006, 2016.

[51] Ro Jefferson and Robert C. Myers. Circuit complexity in quantum field theory. *JHEP*, 10:107, 2017.

[52] Shira Chapman, Michal P. Heller, Hugo Marrochio, and Fernando Pastawski. Toward a Definition of Complexity for Quantum Field Theory States. *Phys. Rev. Lett.*, 120(12):121602, 2018.

[53] Rifath Khan, Chethan Krishnan, and Sanchita Sharma. Circuit Complexity in Fermionic Field Theory. *Phys. Rev. D*, 98(12):126001, 2018.

[54] Run-Qiu Yang, Yu-Sen An, Chao Niu, Cheng-Yong Zhang, and Keun-Young Kim. Principles and symmetries of complexity in quantum field theory. *Eur. Phys. J. C*, 79(2):109, 2019.

[55] J. Molina-Vilaplana and A. Del Campo. Complexity Functionals and Complexity Growth Limits in Continuous MERA Circuits. *JHEP*, 08:012, 2018.

[56] Lucas Hackl and Robert C. Myers. Circuit complexity for free fermions. *JHEP*, 07:139, 2018.

[57] Arpan Bhattacharyya, Pawel Caputa, Sumit R. Das, Nilay Kundu, Masamichi Miyaji, and Tadashi Takayanagi. Path-Integral Complexity for Perturbed CFTs. *JHEP*, 07:086, 2018.

[58] Minyong Guo, Juan Hernandez, Robert C. Myers, and Shan-Ming Ruan. Circuit Complexity for Coherent States. *JHEP*, 10:011, 2018.

[59] Arpan Bhattacharyya, Arvind Shekar, and Aninda Sinha. Circuit complexity in interacting QFTs and RG flows. *JHEP*, 10:140, 2018.

[60] Run-Qiu Yang, Yu-Sen An, Chao Niu, Cheng-Yong Zhang, and Keun-Young Kim. More on complexity of operators in quantum field theory. *JHEP*, 03:161, 2019.

[61] Hugo A. Camargo, Michal P. Heller, Ro Jefferson, and Johannes Knaute. Path integral optimization as circuit complexity. *Phys. Rev. Lett.*, 123(1):011601, 2019.

[62] Vijay Balasubramanian, Matthew Decross, Arjun Kar, and Onkar Parrikar. Quantum Complexity of Time Evolution with Chaotic Hamiltonians. *JHEP*, 01:134, 2020.

[63] Arpan Bhattacharyya, Pratik Nandy, and Aninda Sinha. Renormalized Circuit Complexity. *Phys. Rev. Lett.*, 124(10):101602, 2020.

[64] Johanna Erdmenger, Marius Gerbershagen, and Anna-Lena Weigel. Complexity measures from geometric actions on Virasoro and Kac-Moody orbits. *JHEP*, 11:003, 2020.

[65] Pablo Bueno, Javier M. Magan, and C.S. Shahbazi. Complexity measures in QFT and constrained geometric actions. 8 2019.

[66] Bowen Chen, Bartlomiej Czech, and Zi-zhi Wang. Cutoff Dependence and Complexity of the CFT$_2$ Ground State. 4 2020.

[67] Mario Flory and Michal P. Heller. Complexity and Conformal Field Theory. 5 2020.

[68] Mario Flory and Michal P. Heller. Conformal field theory complexity from Euler-Arnold equations. 7 2020.

[69] Richard P. Feynman. Simulating physics with computers. *Int. J. Theor. Phys.*, 21:467–488, 1982.

[70] Adam R. Brown and Leonard Susskind. Second law of quantum complexity. *Phys. Rev. D*, 97(8):086015, 2018.

[71] Michael A. Nielsen. A geometric approach to quantum circuit lower bounds. *arXiv e-prints*, pages quant–ph/0502070, February 2005.

[72] Michael A. Nielsen, Mark R. Dowling, Mile Gu, and Andrew C. Doherty. Quantum Computation as Geometry. *Science*, 311(5764):1133–1135, February 2006.

[73] Dean Carmi, Robert C. Myers, and Pratik Rath. Comments on Holographic Complexity. *JHEP*, 03:118, 2017.

[74] Alan Reynolds and Simon F. Ross. Divergences in Holographic Complexity. *Class. Quant. Grav.*, 34(10):105004, 2017.

[75] Stefano Bolognesi, Eliezer Rabinovici, and Shubho R. Roy. On Some Universal Features of the Holographic Quantum Complexity of Bulk Singularities. *JHEP*, 06:016, 2018.

[76] Luis Lehner, Robert C. Myers, Eric Poisson, and Rafael D. Sorkin. Gravitational action with null boundaries. *Phys. Rev. D*, 94(8):084046, 2016.

[77] Krishnamohan Parattu, Sumanta Chakraborty, Bibhas Ranjan Majhi, and T. Padmanabhan. A Boundary Term for the Gravitational Action with Null Boundaries. *Gen. Rel. Grav.*, 48(7):94, 2016.

[78] Josiah Couch, Willy Fischler, and Phuc H. Nguyen. Noether charge, black hole volume, and complexity. *JHEP*, 03:119, 2017.

[79] Alexandre Belin, Robert C. Myers, Shan-Ming Ruan, Gábor Sárosi, and Antony J. Speranza. Does Complexity Equal Anything? *Phys. Rev. Lett.*, 128(8):081602, 2022.

[80] Alexandre Belin, Robert C. Myers, Shan-Ming Ruan, Gábor Sárosi, and Antony J. Speranza. Complexity Equals Anything II. 10 2022.

[81] Pawel Caputa and Javier M. Magan. Quantum Computation as Gravity. *Phys. Rev. Lett.*, 122(23):231302, 2019.

[82] Roman Orus. A Practical Introduction to Tensor Networks: Matrix Product States and Projected Entangled Pair States. *Annals Phys.*, 349:117–158, 2014.

[83] Thomas Hartman and Juan Maldacena. Time Evolution of Entanglement Entropy from Black Hole Interiors. *JHEP*, 05:014, 2013.

[84] Hong Liu and S. Josephine Suh. Entanglement Tsunami: Universal Scaling in Holographic Thermalization. *Phys. Rev. Lett.*, 112:011601, 2014.

[85] Masahiro Nozaki, Shinsei Ryu, and Tadashi Takayanagi. Holographic Geometry of Entanglement Renormalization in Quantum Field Theories. *JHEP*, 10:193, 2012.

[86] Xiao-Liang Qi. Exact holographic mapping and emergent space-time geometry. 9 2013.

[87] Fernando Pastawski, Beni Yoshida, Daniel Harlow, and John Preskill. Holographic quantum error-correcting codes: Toy models for the bulk/boundary correspondence. *JHEP*, 06:149, 2015.

[88] Ning Bao, ChunJun Cao, Sean M. Carroll, Aidan Chatwin-Davies, Nicholas Hunter-Jones, Jason Pollack, and Grant N. Remmen. Consistency conditions for an AdS multiscale entanglement renormalization ansatz correspondence. *Phys. Rev. D*, 91(12):125036, 2015.

[89] Bartlomiej Czech, Lampros Lamprou, Samuel McCandlish, and James Sully. Integral Geometry and Holography. *JHEP*, 10:175, 2015.

[90] Jutho Haegeman, Tobias J. Osborne, Henri Verschelde, and Frank Verstraete. Entanglement Renormalization for Quantum Fields in Real Space. *Phys. Rev. Lett.*, 110(10):100402, 2013.

[91] Masamichi Miyaji, Tokiro Numasawa, Noburo Shiba, Tadashi Takayanagi, and Kento Watanabe. Continuous Multiscale Entanglement Renormalization Ansatz as Holographic Surface-State Correspondence. *Phys. Rev. Lett.*, 115(17):171602, 2015.

[92] Pawel Caputa, Nilay Kundu, Masamichi Miyaji, Tadashi Takayanagi, and Kento Watanabe. Liouville Action as Path-Integral Complexity: From Continuous Tensor Networks to AdS/CFT. *JHEP*, 11:097, 2017.

[93] Masamichi Miyaji, Tadashi Takayanagi, and Kento Watanabe. From path integrals to tensor networks for the AdS/CFT correspondence. *Phys. Rev. D*, 95(6):066004, 2017.

[94] Masamichi Miyaji, Tokiro Numasawa, Noburo Shiba, Tadashi Takayanagi, and Kento Watanabe. Distance between Quantum States and Gauge-Gravity Duality. *Phys. Rev. Lett.*, 115(26):261602, 2015.

[95] Mario Flory. A complexity/fidelity susceptibility g-theorem for AdS$_3$/BCFT$_2$. *JHEP*, 06:131, 2017.

[96] Masamichi Miyaji. Butterflies from Information Metric. *JHEP*, 09:002, 2016.

[97] Ofer Aharony, Micha Berkooz, David Kutasov, and Nathan Seiberg. Linear dilatons, NS five-branes and holography. *JHEP*, 10:004, 1998.

[98] D. Kutasov. Introduction to little string theory. *ICTP Lect. Notes Ser.*, 7:165–209, 2002.

[99] F.A. Smirnov and A.B. Zamolodchikov. On space of integrable quantum field theories. *Nucl. Phys. B*, 915:363–383, 2017.

[100] Andrea Cavaglià, Stefano Negro, István M. Szécsényi, and Roberto Tateo. $T\bar{T}$-deformed 2D Quantum Field Theories. *JHEP*, 10:112, 2016.

[101] Amit Giveon, Nissan Itzhaki, and David Kutasov. $T\bar{T}$ and LST. *JHEP*, 07:122, 2017.

[102] Meseret Asrat, Amit Giveon, Nissan Itzhaki, and David Kutasov. Holography Beyond AdS. *Nucl. Phys. B*, 932:241–253, 2018.

[103] Soumangsu Chakraborty, Amit Giveon, Nissan Itzhaki, and David Kutasov. Entanglement beyond AdS. *Nucl. Phys. B*, 935:290–309, 2018.

[104] Soumangsu Chakraborty. Wilson loop in a $T\bar{T}$ like deformed CFT$_2$. *Nucl. Phys. B*, 938:605–620, 2019.

[105] Soumangsu Chakraborty and Akikazu Hashimoto. Thermodynamics of $T\bar{T}$, $J\bar{T}$, $T\bar{J}$ deformed conformal field theories. *JHEP*, 07:188, 2020.

[106] Soumangsu Chakraborty and Akikazu Hashimoto. Entanglement Entropy for $T\bar{T}$, $J\bar{T}$, $T\bar{J}$ deformed holographic CFT. 10 2020.

[107] Soumangsu Chakraborty. $\frac{SL(2,\mathbb{R}) \times U(1)}{U(1)}$ CFT, NS5+F1 system and single trace $T\bar{T}$. 12 2020.

[108] Amin Akhavan, Mohsen Alishahiha, Ali Naseh, and Hamed Zolfi. Complexity and Behind the Horizon Cut Off. *JHEP*, 12:090, 2018.

[109] Ghadir Jafari, Ali Naseh, and Hamed Zolfi. Path Integral Optimization for $T\bar{T}$ Deformation. *Phys. Rev. D*, 101(2):026007, 2020.

[110] Hao Geng. $T\bar{T}$ Deformation and the Complexity=Volume Conjecture. *Fortsch. Phys.*, 68(7):2000036, 2020.

[111] Juan Martin Maldacena and Hirosi Ooguri. Strings in AdS(3) and SL(2,R) WZW model 1.: The Spectrum. *J. Math. Phys.*, 42:2929–2960, 2001.

[112] Nathan Seiberg and Edward Witten. The D1 / D5 system and singular CFT. *JHEP*, 04:017, 1999.

[113] David Kutasov and Nathan Seiberg. More comments on string theory on AdS(3). *JHEP*, 04:008, 1999.

[114] Soumangsu Chakraborty, Amit Giveon, and David Kutasov. $T\bar{T}$, $J\bar{T}$, $T\bar{J}$ and String Theory. *J. Phys. A*, 52(38):384003, 2019.

[115] Soumangsu Chakraborty, Amit Giveon, and David Kutasov. $J\bar{T}$ deformed CFT$_2$ and string theory. *JHEP*, 10:057, 2018.

[116] Stefan Forste. A Truly marginal deformation of SL(2, R) in a null direction. *Phys. Lett. B*, 338:36–39, 1994.

[117] Dan Israel, Costas Kounnas, and Marios P. Petropoulos. Superstrings on NS5 backgrounds, deformed AdS(3) and holography. *JHEP*, 10:028, 2003.

[118] A. Giveon, D. Kutasov, E. Rabinovici, and A. Sever. Phases of quantum gravity in AdS(3) and linear dilaton backgrounds. *Nucl. Phys. B*, 719:3–34, 2005.

[119] Soumangsu Chakraborty, Amit Giveon, and David Kutasov. $T\bar{T}$, black holes and negative strings. *JHEP*, 09:057, 2020.

[120] Ofer Aharony, Amit Giveon, and David Kutasov. LSZ in LST. *Nucl. Phys. B*, 691:3–78, 2004.

[121] Luis Apolo, Stephane Detournay, and Wei Song. TsT, $T\bar{T}$ and black strings. *JHEP*, 06:109, 2020.

[122] Amit Giveon, Nissan Itzhaki, and David Kutasov. A solvable irrelevant deformation of AdS$_3$/CFT$_2$. *JHEP*, 12:155, 2017.

[123] Gaston Giribet. $T\bar{T}$-deformations, AdS/CFT and correlation functions. *JHEP*, 02:114, 2018.

[124] Soumangsu Chakraborty, Amit Giveon, and David Kutasov. Strings in irrelevant deformations of AdS$_3$/CFT$_2$. *JHEP*, 11:057, 2020.

[125] Jeremias Aguilera-Damia, Louise M. Anderson, and Evan Coleman. A substrate for brane shells from $T\bar{T}$. 12 2020.

[126] Igor R. Klebanov, David Kutasov, and Arvind Murugan. Entanglement as a probe of confinement. *Nucl. Phys. B*, 796:274–293, 2008.

[127] Jose L.F. Barbon and Carlos A. Fuertes. Holographic entanglement entropy probes (non)locality. *JHEP*, 04:096, 2008.

[128] Meseret Asrat. Entropic c–functions in $T\bar{T}, J\bar{T}, T\bar{J}$ deformations. *Nucl. Phys. B*, 960:115186, 2020.

[129] Meseret Asrat and Jonah Kudler-Flam. $T\bar{T}$, the entanglement wedge cross section, and the breakdown of the split property. *Phys. Rev. D*, 102(4):045009, 2020.

[130] Monica Guica. An integrable Lorentz-breaking deformation of two-dimensional CFTs. *SciPost Phys.*, 5(5):048, 2018.

[131] Luis Apolo and Wei Song. Strings on warped AdS$_3$ via T$\bar{\text{J}}$ deformations. *JHEP*, 10:165, 2018.

[132] Soumangsu Chakraborty, Gaurav Katoch, and Shubho R. Roy. Holographic complexity of LST and single trace $T\bar{T}$. *JHEP*, 03:275, 2021.

[133] Mohsen Alishahiha. Holographic Complexity. *Phys. Rev. D*, 92(12):126009, 2015.

[134] Omer Ben-Ami and Dean Carmi. On Volumes of Subregions in Holography and Complexity. *JHEP*, 11:129, 2016.

[135] Joanna L. Karczmarek and Charles Rabideau. Holographic entanglement entropy in nonlocal theories. *JHEP*, 10:078, 2013.

[136] Shiraz Minwalla and Nathan Seiberg. Comments on the IIA (NS)five-brane. *JHEP*, 06:007, 1999.

[137] Stephane Detournay, Thomas Hartman, and Diego M. Hofman. Warped Conformal Field Theory. *Phys. Rev. D*, 86:124018, 2012.

[138] Diego M. Hofman and Blaise Rollier. Warped Conformal Field Theory as Lower Spin Gravity. *Nucl. Phys. B*, 897:1–38, 2015.

[139] Dionysios Anninos, Joshua Samani, and Edgar Shaghoulian. Warped Entanglement Entropy. *JHEP*, 02:118, 2014.

[140] Alejandra Castro, Diego M. Hofman, and Nabil Iqbal. Entanglement Entropy in Warped Conformal Field Theories. *JHEP*, 02:033, 2016.

[141] Luca Basanisi and Shankhadeep Chakrabortty. Holographic Entanglement Entropy in NMG. *JHEP*, 09:144, 2016.

[142] Abdulrahim Al Balushi, Robie A. Hennigar, Hari K. Kunduri, and Robert B. Mann. Holographic complexity of rotating black holes. *JHEP*, 05:226, 2021.

[143] Alice Bernamonti, Francesco Bigazzi, Davide Billo, Lapo Faggi, and Federico Galli. Holographic and QFT complexity with angular momentum. *JHEP*, 11:037, 2021.

[144] Luis Apolo and Wei Song. TsT, black holes, and $T\overline{T} + J\overline{T} + T\overline{J}$. *JHEP*, 04:177, 2022.

[145] Alex Hamilton, Daniel N. Kabat, Gilad Lifschytz, and David A. Lowe. Local bulk operators in AdS/CFT: A Boundary view of horizons and locality. *Phys. Rev. D*, 73:086003, 2006.

[146] Alex Hamilton, Daniel N. Kabat, Gilad Lifschytz, and David A. Lowe. Holographic representation of local bulk operators. *Phys. Rev. D*, 74:066009, 2006.

[147] Alex Hamilton, Daniel N. Kabat, Gilad Lifschytz, and David A. Lowe. Local bulk operators in AdS/CFT: A Holographic description of the black hole interior. *Phys. Rev. D*, 75:106001, 2007. [Erratum: Phys.Rev.D 75, 129902 (2007)].

[148] Diego M. Hofman and Andrew Strominger. Chiral Scale and Conformal Invariance in 2D Quantum Field Theory. *Phys. Rev. Lett.*, 107:161601, 2011.

[149] Dionysios Anninos, Wei Li, Megha Padi, Wei Song, and Andrew Strominger. Warped AdS(3) Black Holes. *JHEP*, 03:130, 2009.

[150] Wei Song and Jianfei Xu. Correlation Functions of Warped CFT. *JHEP*, 04:067, 2018.

[151] Geoffrey Compère, Wei Song, and Andrew Strominger. Chiral Liouville Gravity. *JHEP*, 05:154, 2013.

[152] Kristan Jensen. Locality and anomalies in warped conformal field theory. *JHEP*, 12:111, 2017.

[153] Alejandra Castro, Diego M. Hofman, and Gábor Sárosi. Warped Weyl fermion partition functions. *JHEP*, 11:129, 2015.

[154] Pankaj Chaturvedi, Yingfei Gu, Wei Song, and Boyang Yu. A note on the complex SYK model and warped CFTs. *JHEP*, 12:101, 2018.

[155] Richard A. Davison, Wenbo Fu, Antoine Georges, Yingfei Gu, Kristan Jensen, and Subir Sachdev. Thermoelectric transport in disordered metals without quasiparticles: The Sachdev-Ye-Kitaev models and holography. *Phys. Rev. B*, 95(15):155131, 2017.

[156] Bin Chen, Peng-xiang Hao, and Yan-jun Liu. Supersymmetric Warped Conformal Field Theory. *Phys. Rev. D*, 102(6):065016, 2020.

[157] Luis Apolo and Wei Song. Bootstrapping holographic warped CFTs or: how I learned to stop worrying and tolerate negative norms. *JHEP*, 07:112, 2018.

[158] Wei Song and Jianfei Xu. Structure Constants from Modularity in Warped CFT. *JHEP*, 10:211, 2019.

[159] I. Vuorio. TOPOLOGICALLY MASSIVE PLANAR UNIVERSE. *Phys. Lett. B*, 163:91–95, 1985.

[160] R. Percacci, P. Sodano, and I. Vuorio. Topologically Massive Planar Universes With Constant Twist. *Annals Phys.*, 176:344, 1987.

[161] Miguel E. Ortiz. Homogeneous Space-times With Isotropy in (2+1)-dimensions as Solutions to Topologically Massive Gravity. *Class. Quant. Grav.*, 7:1835–1840, 1990.

[162] Y. Nutku. Exact solutions of topologically massive gravity with a cosmological constant. *Class. Quant. Grav.*, 10:2657–2661, 1993.

[163] Metin Gürses. Perfect Fluid Sources in 2+1 Dimensions. *Class. Quant. Grav.*, 11(10):2585, 1994.

[164] Dionysios Anninos. Hopfing and Puffing Warped Anti-de Sitter Space. *JHEP*, 09:075, 2009.

[165] Geoffrey Compere, Stephane Detournay, and Mauricio Romo. Supersymmetric Godel and warped black holes in string theory. *Phys. Rev. D*, 78:104030, 2008.

[166] Stephane Detournay, Domenico Orlando, P. Marios Petropoulos, and Philippe Spindel. Three-dimensional black holes from deformed anti-de Sitter. *JHEP*, 07:072, 2005.

[167] Dan Israel, Costas Kounnas, Domenico Orlando, and P. Marios Petropoulos. Electric/magnetic deformations of S**3 and AdS(3), and geometric cosets. *Fortsch. Phys.*, 53:73–104, 2005.

[168] Geoffrey Compere and Stephane Detournay. Centrally extended symmetry algebra of asymptotically Godel spacetimes. *JHEP*, 03:098, 2007.

[169] Geoffrey Compere and Stephane Detournay. Semi-classical central charge in topologically massive gravity. *Class. Quant. Grav.*, 26:012001, 2009. [Erratum: Class.Quant.Grav. 26, 139801 (2009)].

[170] M. Blagojevic and B. Cvetkovic. Canonical structure of topologically massive gravity with a cosmological constant. *JHEP*, 05:073, 2009.

[171] Geoffrey Compere and Stephane Detournay. Boundary conditions for spacelike and timelike warped AdS_3 spaces in topologically massive gravity. *JHEP*, 08:092, 2009.

[172] Marc Henneaux, Cristian Martinez, and Ricardo Troncoso. Asymptotically warped anti-de Sitter spacetimes in topologically massive gravity. *Phys. Rev. D*, 84:124016, 2011.

[173] Mukund Rangamani and Tadashi Takayanagi. *Holographic Entanglement Entropy*, volume 931. Springer, 2017.

[174] Wei Song, Qiang Wen, and Jianfei Xu. Modifications to Holographic Entanglement Entropy in Warped CFT. *JHEP*, 02:067, 2017.

[175] Bin Chen, Peng-Xiang Hao, and Wei Song. Rényi mutual information in holographic warped CFTs. *JHEP*, 10:037, 2019.

[176] Luis Apolo, Song He, Wei Song, Jianfei Xu, and Junjie Zheng. Entanglement and chaos in warped conformal field theories. *JHEP*, 04:009, 2019.

[177] Stéphane Detournay, Daniel Grumiller, Max Riegler, and Quentin Vandermiers. Uniformization of Entanglement Entropy in Holographic Warped Conformal Field Theories. 6 2020.

[178] Ro Jefferson and Robert C. Myers. Circuit complexity in quantum field theory. *JHEP*, 10:107, 2017.

[179] Tibra Ali, Arpan Bhattacharyya, S. Shajidul Haque, Eugene H. Kim, and Nathan Moynihan. Time Evolution of Complexity: A Critique of Three Methods. *JHEP*, 04:087, 2019.

[180] Javier M. Magán. Black holes, complexity and quantum chaos. *JHEP*, 09:043, 2018.

[181] Johanna Erdmenger, Mario Flory, Marius Gerbershagen, Michal P. Heller, and Anna-Lena Weigel. Exact Gravity Duals for Simple Quantum Circuits. 12 2021.

[182] Nicolas Chagnet, Shira Chapman, Jan de Boer, and Claire Zukowski. Complexity for Conformal Field Theories in General Dimensions. *Phys. Rev. Lett.*, 128(5):051601, 2022.

[183] Robert de Mello Koch, Minkyoo Kim, and Hendrik J. R. Van Zyl. Complexity from spinning primaries. *JHEP*, 12:030, 2021.

[184] Shira Chapman and Giuseppe Policastro. Quantum Computational Complexity – From Quantum Information to Black Holes and Back. 10 2021.

[185] Arpan Bhattacharyya. Circuit complexity and (some of) its applications. *Int. J. Mod. Phys. E*, 30(07):2130005, 2021.

[186] Gaurav Katoch, Swejyoti Mitra, and Shubho R. Roy. Holographic complexity of LST and single trace $T\overline{T}$, $J\overline{T}$ and $T\overline{J}$ deformations. *JHEP*, 10:143, 2022.

[187] Mahdis Ghodrati. Complexity and emergence of warped AdS$_3$ space-time from chiral Liouville action. *JHEP*, 02:052, 2020.

[188] Mahdis Ghodrati. Complexity growth in massive gravity theories, the effects of chirality, and more. *Phys. Rev. D*, 96(10):106020, 2017.

[189] Roberto Auzzi, Stefano Baiguera, Matteo Grassi, Giuseppe Nardelli, and Nicolò Zenoni. Complexity and action for warped AdS black holes. *JHEP*, 09:013, 2018.

[190] Roberto Auzzi, Stefano Baiguera, Arpita Mitra, Giuseppe Nardelli, and Nicolò Zenoni. Subsystem complexity in warped AdS. *JHEP*, 09:114, 2019.

[191] Ankit Aggarwal, Luca Ciambelli, Stéphane Detournay, and Antoine Somerhausen. Boundary Conditions for Warped AdS$_3$ in Quadratic Ensemble. 12 2021.

[192] Anatoly Dymarsky and Michael Smolkin. Krylov complexity in conformal field theory. *Phys. Rev. D*, 104(8):L081702, 2021.

[193] Roger Penrose. Gravitational collapse and space-time singularities. *Phys. Rev. Lett.*, 14:57–59, 1965.

[194] S. W. Hawking and R. Penrose. The Singularities of gravitational collapse and cosmology. *Proc. Roy. Soc. Lond. A*, 314:529–548, 1970.

[195] John McGreevy and Eva Silverstein. The Tachyon at the end of the universe. *JHEP*, 08:090, 2005.

[196] Andrew Strominger. Massless black holes and conifolds in string theory. *Nucl. Phys. B*, 451:96–108, 1995.

[197] Atish Dabholkar, Renata Kallosh, and Alexander Maloney. A Stringy cloak for a classical singularity. *JHEP*, 12:059, 2004.

[198] G Horowitz. Introduction to singularity resolution. KITP Miniprogram: The Quantum Nature of Spacetime Singularities (January 8-26, 2007), 2007.

[199] Hong Liu, Gregory W. Moore, and Nathan Seiberg. Strings in a time dependent orbifold. *JHEP*, 06:045, 2002.

[200] Hong Liu, Gregory W. Moore, and Nathan Seiberg. Strings in time dependent orbifolds. *JHEP*, 10:031, 2002.

[201] Lorenzo Cornalba and Miguel S. Costa. A New cosmological scenario in string theory. *Phys. Rev. D*, 66:066001, 2002.

[202] L. Cornalba, M. S. Costa, and C. Kounnas. A Resolution of the cosmological singularity with orientifolds. *Nucl. Phys. B*, 637:378–394, 2002.

[203] Lorenzo Cornalba and Miguel S. Costa. Time dependent orbifolds and string cosmology. *Fortsch. Phys.*, 52:145–199, 2004.

[204] Eva Silverstein. Singularities and closed string tachyons. In *23rd Solvay Conference in Physics: The Quantum Structure of Space and Time*, pages 70–81, 2 2006.

[205] Ashoke Sen. Rolling tachyon. *JHEP*, 04:048, 2002.

[206] Ben Craps, Savdeep Sethi, and Erik P. Verlinde. A Matrix big bang. *JHEP*, 10:005, 2005.

[207] Sumit R. Das, Jeremy Michelson, K. Narayan, and Sandip P. Trivedi. Time dependent cosmologies and their duals. *Phys. Rev. D*, 74:026002, 2006.

[208] Sumit R. Das, Jeremy Michelson, K. Narayan, and Sandip P. Trivedi. Cosmologies with Null Singularities and their Gauge Theory Duals. *Phys. Rev. D*, 75:026002, 2007.

[209] Adel Awad, Sumit R. Das, Suresh Nampuri, K. Narayan, and Sandip P. Trivedi. Gauge Theories with Time Dependent Couplings and their Cosmological Duals. *Phys. Rev. D*, 79:046004, 2009.

[210] Chethan Krishnan and Shubho Roy. Desingularization of the Milne Universe. *Phys. Lett. B*, 734:92–95, 2014.

[211] Benjamin Burrington, Leopoldo A. Pando Zayas, and Nicholas Rombes. On Resolutions of Cosmological Singularities in Higher-Spin Gravity. *Int. J. Mod. Phys. D*, 28(15):1950168, 2019.

[212] Jose L. F. Barbon and Eliezer Rabinovici. Holographic complexity and spacetime singularities. *JHEP*, 01:084, 2016.

[213] Ahmed Almheiri, Donald Marolf, Joseph Polchinski, and James Sully. Black Holes: Complementarity or Firewalls? *JHEP*, 02:062, 2013.

[214] Clifford V. Johnson, Amanda W. Peet, and Joseph Polchinski. Gauge theory and the excision of repulson singularities. *Phys. Rev. D*, 61:086001, 2000.

[215] Satoshi Yamaguchi. Enhancon and resolution of singularity. In *Meeting of Frontier of Cosmology and Gravitation*, 8 2001.

[216] Steven S. Gubser. Curvature singularities: The Good, the bad, and the naked. *Adv. Theor. Math. Phys.*, 4:679–745, 2000.

[217] U. Gursoy, E. Kiritsis, L. Mazzanti, and F. Nitti. Holography and Thermodynamics of 5D Dilaton-gravity. *JHEP*, 05:033, 2009.

[218] Arpan Bhattacharyya, Gaurav Katoch, and Shubho R. Roy. Complexity of warped conformal field theory. 2 2022.

[219] Gary T. Horowitz and Robert C. Myers. The value of singularities. *Gen. Rel. Grav.*, 27:915–919, 1995.

[220] Jie Ren. Asymptotically AdS spacetimes with a timelike Kasner singularity. *JHEP*, 07:112, 2016.

[221] Norihiro Iizuka and Kengo Maeda. Study of Anisotropic Black Branes in Asymptotically anti-de Sitter. *JHEP*, 07:129, 2012.

[222] Paolo Glorioso. Classification of certain asymptotically AdS space-times with Ricci-flat boundary. *JHEP*, 12:126, 2016.

[223] Matthew Kleban, John McGreevy, and Scott D. Thomas. Implications of bulk causality for holography in AdS. *JHEP*, 03:006, 2004.

[224] Dongsu Bak, Michael Gutperle, Shinji Hirano, and Nobuyoshi Ohta. Dilatonic repulsons and confinement via the AdS / CFT correspondence. *Phys. Rev. D*, 70:086004, 2004.

[225] Sijie Gao and Robert M. Wald. Theorems on gravitational time delay and related issues. *Class. Quant. Grav.*, 17:4999–5008, 2000.

[226] Chang Jun Gao and Shuang Nan Zhang. Dilaton black holes in de Sitter or Anti-de Sitter universe. *Phys. Rev. D*, 70:124019, 2004.

[227] Jie Ren. Phase transitions of hyperbolic black holes in anti-de Sitter space. 10 2019.

[228] Kanato Goto, Hugo Marrochio, Robert C. Myers, Leonel Queimada, and Beni Yoshida. Holographic Complexity Equals Which Action? *JHEP*, 02:160, 2019.